

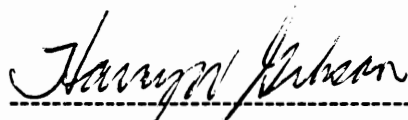
# MOLECULAR NECKLACES: POLYESTER ROTAXANES

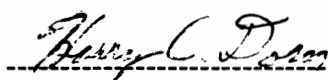
by  
Shu Liu

A dissertation submitted to the Faculty of the  
Virginia Polytechnic Institute and State University  
in partial fulfillment of the requirements for the degree of

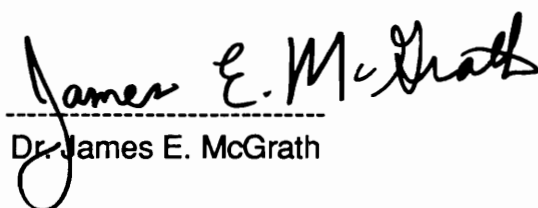
**Doctor of Philosophy**  
in Chemistry

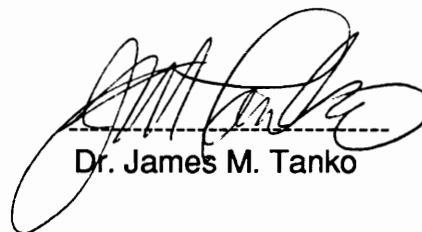
APPROVED:

  
-----  
Dr. Harry W. Gibson, chairman

  
-----  
Dr. Harry C. Dorn

  
-----  
Dr. Hervé Marand

  
-----  
Dr. James E. McGrath

  
-----  
Dr. James M. Tanko

January 1995  
Blacksburg, Virginia

# **MOLECULAR NECKLACES: POLYESTER ROTAXANES**

by

Shu Liu

Dr. Harry W. Gibson, Chairman

Department of Chemistry

(ABSTRACT)

Polyrotaxanes consisting of 30-60 membered aliphatic crown ether macrocycles whose cavities are pierced by polysebacate chains were synthesized by several polymerization approaches including transesterification polymerization, the acid chloride method, and interfacial polymerization.

The polyrotaxanes were purified by multiple reprecipitations into good solvents for the crown ethers. In some cases the threaded macrocycles are constrained onto polymer chains by the incorporation of monofunctional blocking groups at polymer chain ends, or by the copolymerization of a difunctional blocking group with other monomers.

The compositions and the physical properties of the polyrotaxanes were determined by a variety of characterization techniques including NMR, UV, VPO, GPC, DSC, TGA, and intrinsic viscosity measurements. Significant amounts, up to 51 mass %, of the macrocyclic components were incorporated. Because of incorporation of flexible and polar macrocycles, polyrotaxanes

display special behavior in solution and in the solid state. In solution the linear components of polyrotaxanes are stiffened by the threaded macrocycles, resulting in increased hydrodynamic volumes. The solubilities of linear polymers in polar solvents are enhanced by the incorporated crown ethers. The glass transitions are also affected by the crown ether component. Due to the movement of the macrocycles along the backbone, the macrocycles are able to aggregate and crystallize without dethreading from the polysebacate backbones.

The threading and dethreading processes were systematically studied in the diol/diacid chloride system. Due to the hydrogen bonding between the cyclic and linear species, the macrocycle contents of unblocked polyrotaxanes are significantly affected by the feed ratio of macrocycle to linear monomers up to a value of 2 but are independent of reaction time and the length of diol monomers. The macrocycle content of polyrotaxanes increases non-linearly with the size of the macrocycles, presumably due to changes in the fraction of threadable conformations of the macrocycles. Although some macrocycles near the unblocked polymer chain ends are apparently susceptible to the dethreading from polymer chains, most of the macrocycles are prevented on reasonable time scales, e.g., months in solution, from the dethreading by the entanglement of cyclic and linear species.

*In the Memory of My Father*

## ACKNOWLEDGMENTS

I would like to express a very special gratitude to Dr. Harry W. Gibson for his guidance, encouragement, patience, and support. I learned from him not only chemistry but most importantly the professional pride, the diligence, and the strict work attitude. These characters will influence my whole life in the future.

I wish to extend sincere appreciation to Dr. Hervé Marand, Dr. James M. Tanko, Dr. James E. McGrath, and Dr. Harry C. Dorn for serving on my committee and for valuable suggestions and encouragement.

I would like to thank my friends in Dr. Gibson's group, Dr. Devdatt Nagvekar, Mingfei Chen, Darin Dotson, Sang-Hun Lee, Lance Wang, Donghang Xie, and Jim Yang, for their discussions and friendships.

I want to thank my parents for their endless love. I also want to thank my uncle, Zenglian Lin, for his generous support.

Finally, my wholehearted thanks go to my wife, Gusui. Without her love and sacrifice, I surely would not have succeeded.

## TABLE OF CONTENTS

<b>Chapter I. Polymer Architectures</b>	1
I. Topologies of Polymers	1
II. Polymers with Supramolecular Topologies	6
References	11
<b>Chapter II. Literature Review: Polyrotaxanes</b>	13
I. Monorotaxanes and Monocatenanes	13
II. Oligomeric Rotaxanes	23
III. Polymeric Rotaxanes	27
IV. Polyester Rotaxanes	32
References	39
<b>Chapter III. Objectives</b>	45
<b>Chapter IV. Macrocycles: Aliphatic crown Ethers</b>	48
Results and Discussion	51
I. Hexa(ethylene glycol)	51
II. Oligo(ethylene glycol) Ditosylates	53
III. Syntheses of Crown Ethers	54
A. Length of Starting Materials	55
B. Temperature	55
C. Synthetic Procedures	55
IV. Purification of Crown Ethers	56

Conclusions	60
Experimental	61
References	70
<b>Chapter V. Monofunctional Blocking Groups</b>	<b>94</b>
Results and Discussion	96
Conclusions	102
Experimental	103
References	107
<b>Chapter VI. Knots for Molecular Strings of Beads:</b>	
<b>Difunctional Blocking Groups</b>	<b>119</b>
Results and Discussion	120
I. Difunctional Blocking Groups for Step Growth Polymerization	120
A. $\alpha,\alpha,\omega,\omega$ -Tetraaryl- $\alpha,\omega$ -difunctional Blocking Groups	120
B. Diethyl Di( <i>p</i> - <i>t</i> -butylbenzyl)malonate	125
II. A Difunctional Blocking Group for Chain Growth Polymerization	126
Conclusions	128
Experimental	129
References	138
<b>Chapter VII. Polyester Rotaxanes</b>	
<b>(Transesterification Method)</b>	<b>156</b>
Results and Discussion	158
I. Synthesis and Purification	161

A. Model Polymers	161
B. Polyester Rotaxanes	163
II. Proof of Structures	166
III. Molecular Weight Determinations	170
A. Gel Permeation Chromatography (GPC)	170
B. NMR Spectroscopy	172
C. Ultraviolet Spectroscopy	173
D. Vapor Pressure Osmometry	174
E. Gel Permeation Chromatography with Viscosity Detection and Universal Calibration ("Absolute GPC")	175
F. End Blocking Efficiency	176
G. Effect of Rotaxane Structure on Hydrodynamic Volume	177
IV. Threading Efficiencies of Macrocycles: Effects of Ring Size and Backbone structure	178
V. Solubility Properties of Polyrotaxanes	181
VI. Thermal Transitions, Solution Properties of Polyrotaxanes	183
A. Poly(triethyleneoxy Sebacate) Systems	183
B. Poly(butylene Sebacate) Systems	185
VII. Thermo-Oxidative Stability of Polyrotaxanes	187
Conclusions	188
Experimental	189
References	197



<b>Chapter VIII. Polyester Rotaxanes</b>	
<b>(Acid Chloride Method)</b>	230
Results and discussion	230
I. Solution Polymerization	230
A. Optimization of Reaction Conditions in Model Studies	230
B. Studies of Threading Processes in Polyrotaxane	
Syntheses	233
C. Molecular Strings of Beads with Knots	249
D. Dethreading experiments	250
E. Thermal Properties of Polyrotaxanes	252
F. Metal Complexation of Crown Ether Components	
of Polyrotaxanes	257
II. Interfacial Polymerization	259
Conclusions	263
Experimental	265
References	273
<b>Chapter IX. Overall Conclusions and Future Work</b>	319
I. Overall Conclusions	319
II. Future Work	320
A. Study of the Threading Equilibria	321
B. Quantitative Determination of Metal Complexation of	
Polyrotaxanes	323
C. Study of the Solution Behavior of Polyrotaxanes	324

D. Study of the Topological Properties of Polyrotaxanes	325
E. Syntheses of Polyrotaxanes by Interfacial Polymerization	326
<b>References</b>	<b>327</b>
<b>Vita</b>	<b>330</b>

## LIST OF TABLES

### CHAPTER IV

Table 1. The yields of 42-crown-14 82

Table 2. Melting points of crown ethers 83

### CHAPTER VII

Table 1. Reprecipitation results for polysebacate rotaxanes 203

Table 2. Molecular weights of polysebacates and corresponding  
polyrotaxanes 204

Table 3. Solubility of polysebacates and corresponding polyrotaxanes 206

Table 4. Thermal properties of model polymers and polyrotaxanes 207

### CHAPTER VIII

Table 1. Optimization for the synthesis of poly(decamethylene  
sebacate) 282

Table 2. Errors of determination of m/n value from sampling of  
poly[(decamethylene sebacate)-rotaxa-(42-crown-14)] 283

Table 3. Errors of determination of m/n value from measuring of  
poly[(decamethylene sebacate)-rotaxa-(42-crown-14)] 283

Table 4. The effect of macrocycle size on the threading of 1,10-  
decanediol by crown ethers 284

Table 5. The effect of feed ratio on the threading of 1,10-  
decanediol by 42-crown-14 284

Table 6. The effect of the diol length on the threading of HO(CH <sub>2</sub> ) <sub>x</sub> OH by 42-crown-14	285
Table 7. The effect of prethreading time on the threading of 1,10- decanediol by 42-crown-14	285
Table 8. Prethreading of 42-crown-14 by sebacoyl chloride and by 1,10-decanediol	286
Table 9. The effect of temperature on the threading of 1,10- decanediol by 42-crown-14	286
Table 10. Intrinsic viscosities of the model polymer <b>9</b> and the polyrotaxane <b>14</b> as functions of solvents	287
Table 11. Dethreading experiments of 42-crown-14 from poly[(decamethylene sebacate)-rotaxa-(42-crown-14)]	288
Table 12. Thermal properties of model polymer and polyrotaxanes	289
Table 13. Metal complexation tests of crown ethers, poly(decamethylene sebacate), and poly(decamethylene sebacate) rotaxanes	290

## LIST OF FIGURES

### CHAPTER I

Figure 1. Polymer topologies	2
Figure 2. Interpenetrating polymer network	6
Figure 3. Some subclasses of polycatenanes	8
Figure 4. Polyrotaxane structures	9

### CHAPTER II

Figure 1. Harrison's approach by acid catalyzed equilibration	15
Figure 2. Schill's chemical conversion approach	17
Figure 3. Functional structure and molecular dimensions of cyclodextrins	19
Figure 4. Synthesis of a rotaxane comprised of a dicobalt (III) diamine complex and cyclodextrins	20
Figure 5. Zilkha's approach for syntheses of oligomeric and polymeric rotaxanes	24

### CHAPTER IV

Figure 1. FTIR spectrum of hexa(ethylene glycol) on KBr plate	84
Figure 2. 270 MHz $^1\text{H}$ NMR spectrum of hexa(ethylene glycol) in $\text{CDCl}_3$	85
Figure 3. 270 MHz $^1\text{H}$ NMR spectrum of tri(ethylene glycol) ditosylate in $\text{CDCl}_3$	86
Figure 4. 270 MHz $^1\text{H}$ NMR spectrum of tetra(ethylene glycol)	

ditosylate in CDCl <sub>3</sub>	87
Figure 5. 400 MHz <sup>1</sup> H NMR spectrum of crude 42C14 in DMSO-d <sub>6</sub> at 20 °C showing a signal due to OH	88
Figure 6. 400 <sup>1</sup> H NMR spectrum of crude 42C14 in CDCl <sub>3</sub> at 20 °C showing signals due to terminal vinyl ether protons and other impurities	89
Figure 7. 400 MHz <sup>1</sup> H NMR spectrum of pure 42C14 in DMSO-d <sub>6</sub> at 20 °C showing lack of OH signal	90
Figure 8. 400 MHz <sup>1</sup> H NMR spectrum of pure 42C14 in CDCl <sub>3</sub> at 20 °C showing lack of terminal vinyl ether protons and other impurity signals	91
Figure 9. DSC trace for crude 42C14	92
Figure 10. DSC trace for pure 42C14	93

## CHAPTER V

Figure 1. 270 MHz <sup>1</sup> H NMR spectrum of ethyl <i>p-t</i> -butylbenzoate in CDCl <sub>3</sub>	113
Figure 2. 270 MHz <sup>1</sup> H NMR spectrum of tris( <i>p-t</i> -butylphenyl)methanol in CDCl <sub>3</sub>	114
Figure 3. FTIR spectrum of tris( <i>p-t</i> -butylphenyl)( <i>p'</i> -hydroxyphenyl)-methane on KBr plate	115
Figure 4. 270 MHz <sup>1</sup> H NMR spectrum of tris( <i>p-t</i> -butylphenyl)-( <i>p'</i> -hydroxyphenyl)methane in CDCl <sub>3</sub>	116
Figure 5. FTIR spectrum of mono- <i>p</i> -[tris( <i>p-t</i> -butylphenyl)methyl]phenyl ether of di(ethylene glycol) on KBr plate	117

Figure 6. 270 MHz  $^1\text{H}$  NMR spectrum of mono-*p*-[tris(*p*'-*t*-butylphenyl)-methyl]phenyl ether of di(ethylene glycol) in  $\text{CDCl}_3$  118

## CHAPTER VI

Figure 1. 400 MHz  $^1\text{H}$  NMR spectrum of 1,10-bis(*p*-dicarbethoxyphenoxy)decane in  $\text{CDCl}_3$  145

Figure 2. 270 MHz  $^1\text{H}$  NMR spectrum of 1,10-bis{*p*-[di(*p*'-*t*-butylphenyl)hydroxymethyl]phenoxy}decane in  $\text{CDCl}_3$  146

Figure 3. 400 MHz  $^1\text{H}$  NMR spectrum of 1,4-bis[di(*p*-*t*-butylphenyl)hydroxymethyl]benzene in  $\text{CDCl}_3$  147

Figure 4. 400 MHz  $^1\text{H}$  NMR spectrum of 1,1,6,6-tetra(*p*-*t*-butylphenyl)-1,6-hexanediol in  $\text{CDCl}_3$  148

Figure 5. 270 MHz  $^1\text{H}$  NMR spectrum of 1,10-bis{*p*-[di(*p*'-*t*-butylphenyl)-(*p*"-hydroxyphenyl)methyl]phenoxy}decane in  $\text{CDCl}_3$  149

Figure 6. 270 MHz  $^1\text{H}$  NMR spectrum of 1,1,6,6-tetra(*p*-*t*-butylphenyl)-hexane in  $\text{CDCl}_3$  150

Figure 7. 400 MHz  $^1\text{H}$  NMR spectrum of 1,10-bis{*p*-[di(*p*'-*t*-butylphenyl)-[*p*"-2-(2'-hydroxyethoxy)ethoxy]phenylmethyl]phenoxy}-decane in  $\text{CDCl}_3$  151

Figure 8. 270 MHz  $^1\text{H}$  NMR spectrum of diethyl di(*p*-*t*-butylbenzyl)-malonate in  $\text{CDCl}_3$  152

Figure 9. 400 MHz  $^1\text{H}$  NMR spectrum of 1,1-di(*p*-*t*-butylphenyl)ethanol in  $\text{CDCl}_3$  153

Figure 10. 400 MHz  $^1\text{H}$  NMR spectrum of 1,1-di(*p*-*t*-butylphenyl)ethene in  $\text{CDCl}_3$  154

## CHAPTER VII

- Figure 1. 270 MHz  $^1\text{H}$  NMR spectrum of poly(triethyleneoxy sebacate) in  $\text{CDCl}_3$  208
- Figure 2. 100 MHz  $^{13}\text{C}$  NMR spectrum of poly(triethyleneoxy sebacate) in  $\text{CDCl}_3$  209
- Figure 3. 400 MHz  $^1\text{H}$  NMR spectrum of a) poly(butylene sebacate) and b) poly[(butylene sebacate)-rotaxa-(42-crown-14)] in  $\text{CDCl}_3$  210
- Figure 4. 100 MHz  $^{13}\text{C}$  NMR spectrum of poly(butylene sebacate) in  $\text{CDCl}_3$  211
- Figure 5. 400 MHz  $^1\text{H}$  NMR spectrum of poly[(triethyleneoxy sebacate)-rotaxa-(60-crown-20)] in  $\text{CDCl}_3$  212
- Figure 6. 100 MHz  $^{13}\text{C}$  NMR spectrum of poly[(triethyleneoxy sebacate)-rotaxa-(60-crown-20)] in  $\text{CDCl}_3$  213
- Figure 7. 100 MHz  $^{13}\text{C}$  NMR spectrum of poly[(butylene sebacate)-rotaxa-(42-crown-14)] in  $\text{CDCl}_3$  214
- Figure 8. GPC traces for a) poly(butylene sebacate); b) a physical mixture of poly(butylene sebacate) and 42-crown 14; c) 42-crown-14 and d) poly[(butylene sebacate)-rotaxa-(42-crown-14)] in  $\text{CHCl}_3$  at 30 °C 215
- Figure 9. GPC traces for a) poly(butylene sebacate); b) a physical mixture of poly(butylene sebacate) and 60-crown-20; c) 60-crown-20 and d) poly[(butylene sebacate)-rotaxa-(60-crown-20)] in  $\text{CHCl}_3$  at 30 °C. 216



Figure 10. Calibration curve for UV measurement of mono- <i>p</i> -[tris( <i>p</i> '- <i>t</i> -butylphenyl)-methyl]phenyl ether of di(ethylene glycol) in CHCl <sub>3</sub>	217
Figure 11. Plots of $\Delta V$ vs. concentration <i>c</i> (g/L) for polystyrene standards	218
Figure 12. Calibration curve for VPO measurements	219
Figure 13. Plots of $\Delta V$ vs. concentration <i>c</i> (g/L) for polyesters and polyrotaxanes	220
Figure 14. Cyclic ratio ( <i>m/n</i> ) and mass percent cyclic in polyrotaxanes as a function of crown ether ring size	221
Figure 15. DSC traces for poly(triethyleneoxy sebacate)	222
Figure 16. DSC trace for poly[(triethyleneoxy sebacate)-rotaxa-(30-crown-10)]	223
Figure 17. DSC traces for poly[(triethyleneoxy sebacate)-rotaxa-(60-crown-20)]	224
Figure 18. DSC traces for 60-crown-20	225
Figure 19. DSC traces for poly(butylene sebacate)	226
Figure 20. DSC traces for poly[(butylene sebacate)-rotaxa-(42-crown-14)]	227
Figure 21. DSC traces for 42-crown-14	228
Figure 22. DSC traces for poly[(butylene sebacate)-rotaxa-(60-crown-20)]	229

## CHAPTER VIII

Figure 1. 400 MHz <sup>1</sup> H NMR spectrum of poly(decamethylene sebacate) in CDCl <sub>3</sub>	291
--	-----

Figure 2. 100 MHz $^{13}\text{C}$ NMR spectrum of poly(decamethylene sebacate) in $\text{CDCl}_3$	292
Figure 3. GPC traces for a) poly(decamethylene sebacate); b) a physical mixture of poly(decamethylene sebacate) and 42-crown-14; c) 42-crown-14 and d) poly[(decamethylene sebacate)-rotaxa-(42-crown-14)] in $\text{CHCl}_3$	293
Figure 4. 400 MHz $^1\text{H}$ NMR spectrum of poly[(decamethylene sebacate)-rotaxa-(42-crown-14)] in $\text{CDCl}_3$	294
Figure 5. m/n value of poly(decamethylene sebacate) rotaxanes vs. ring size of the crown ether	295
Figure 6. Log of the rotaxane yield as a function of ring size of the macrocycle	296
Figure 7. Log of the equilibrium constant, K, for threading of cyclic poly(dimethylsiloxane)s by linear poly(dimethylsiloxane) of $M_n$ 18 kg/mol vs. ring size of the cyclic species	297
Figure 8. 100 MHz $^{13}\text{C}$ NMR spectrum of poly[(decamethylene sebacate)-rotaxa-(42-crown-14)] in $\text{CDCl}_3$	298
Figure 9. m/n value and mass percent cyclic in poly[(decamethylene sebacate)-rotaxa-(42-crown-14)] as a function of the mole ratio of 42-crown-14 to 1,10-decanediol	299
Figure 10. m/n value of polysebacate rotaxanes and mass percent 42-crown-14 as a function of length, y, of alkylene diols	300
Figure 11. 400 MHz $^1\text{H}$ NMR spectrum of poly[(hexamethylene sebacate)-rotaxa-(42-crown-14)] in $\text{CDCl}_3$	301

Figure 12. 100 MHz $^{13}\text{C}$ NMR spectrum of poly[(hexamethylene sebacate)-rotaxa-(42-crown-14)] in $\text{CDCl}_3$	302
Figure 13. GPC traces for polyrotaxanes <b>10-16</b>	303
Figure 14. 270 MHz $^1\text{H}$ NMR spectrum of Poly[{decamethylene sebacate}-co-1,10-bis{ <i>p</i> -[di( <i>p</i> '- <i>t</i> -butylphenyl)-4-phenylmethyl]phenoxy}decamethylene sebacate]-rotaxa-(42-crown-14)] in $\text{CDCl}_3$	304
Figure 15. m/n value of poly[(decamethylene sebacate)-rotaxa-(42-crown-14)] as a function of dethreading time	305
Figure 16. DSC traces for poly(decamethylene sebacate)	306
Figure 17. DSC traces for poly[(decamethylene sebacate)-rotaxa-(30-crown-10)]	307
Figure 18. DSC traces for poly[(decamethylene sebacate)-rotaxa-(36-crown-12)]	308
Figure 19. DSC traces for 36-crown-12	309
Figure 20. DSC traces for poly[(decamethylene sebacate)-rotaxa-(42-crown-14)]	310
Figure 21. DSC traces for poly[(decamethylene sebacate)-rotaxa-(48-crown-16)]	311
Figure 22. DSC traces for 48-crown-16	312
Figure 23. DSC traces for poly[(decamethylene sebacate)-rotaxa-(60-crown-20)]	313
Figure 24. DSC traces for poly[(butylene sebacate)-rotaxa-(42-crown-14)]	314
Figure 25. DSC trace for poly[(hexamethylene sebacate)-rotaxa-	

	(42-crown-14)]	315
Figure 26.	DSC trace for Poly[decamethylene sebacate-co-1,10-bis( <i>p</i> -[di( <i>p</i> '- <i>t</i> -butylphenyl)-4-phenylmethyl]phenoxy)-decamethylene sebacate]-rotaxa-(42-crown-14)]	316
Figure 27.	400 MHz <sup>1</sup> H NMR spectrum of poly[(bisphenol A sebacate)-rotaxa-(42-crown-14)] in CDCl <sub>3</sub>	317
Figure 28.	DSC traces for poly[(bisphenol A sebacate)-rotaxa-(42-crown-14)]	318

# CHAPTER I

## POLYMER ARCHITECTURES

Polymers are large molecules made up of a large number of low molar mass base units which are connected by primary bonds (Greek *poly meros* = many parts). Since German chemists developed a synthetic "methyl" rubber to replace the natural rubbers in 1917, the requirements of replacing traditional materials, such as wood, metals, ceramics, and natural fibers by synthetic polymers have increased dramatically. This development requires a fundamental understanding of relations of structure-property which can be examined under two broad aspects. (a). The chemical level which is concerned with structural information, including the order in which the specific atoms are connected; the type of covalent bonds; and the three dimensional arrangements around rigid centers. For some chemical systems this level is not sufficient. (b). The architectural level which deals with the properties being invariant for various structures consistent with the chemical level. Topological isomerism in chemistry refers to differences in the way in which molecules are imbedded as a whole in three dimensional space.

### I. TOPOLOGIES OF POLYMERS

Molecular chemistry, the chemistry of the covalent bond, deals with the natural rules governing the structures, properties, and conversions of molecules. In the molecular chemistry point of view, polymers can be classified by their molecular

topology as cyclic, linear, branched and network polymers (1), as depicted in Figure 1:

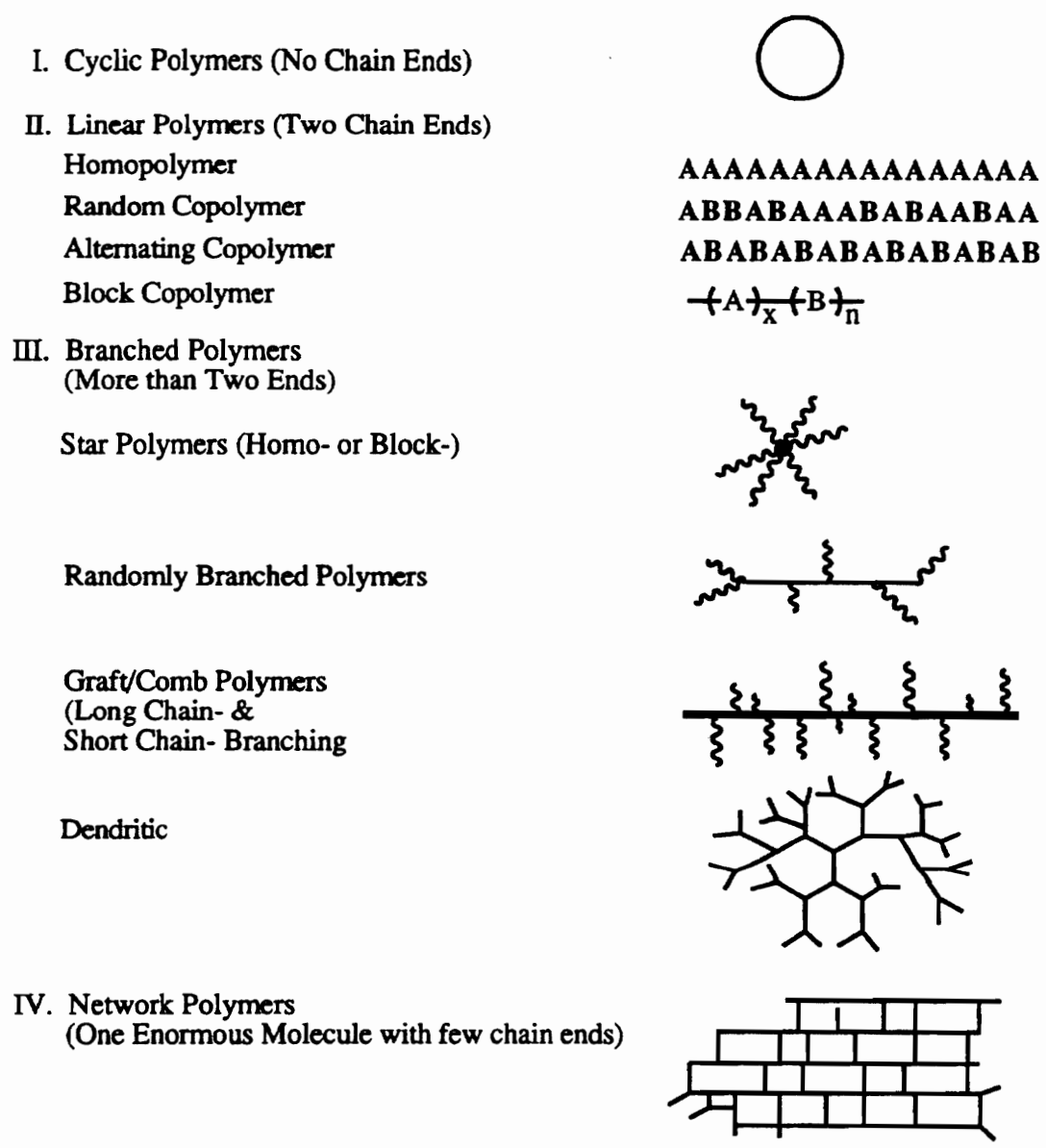


Figure 1. Polymer topologies

Cyclic polymers have no chain ends. They represent the extreme case in the whole spectrum of polymer topology. Because of their non-chain-end structure, cyclic polymers display special dilute solution, diffusional and rheological properties such as lower hydrodynamic volumes, lower melt viscosity, and higher glass transition temperatures than linear polymers [2,3].

A linear polymer has two chain ends and has no branching other than the pendant groups associated with the monomers. If the polymer is prepared from a single monomer, the product is referred to as a homopolymer. The intermolecular interactions of homopolymers determines their physical behavior in the solid state. If two or more monomers are copolymerized, several arrangements are possible in the polymer structure. If the structural units alternate in a linear fashion, the product is called an alternating copolymer. Usually the properties of an alternating copolymer are a combination of the properties of the two monomers along with structural regularity. If the distribution of structural units are random, the polymer is called a random copolymer whose properties are an average of the properties of monomers. A third arrangement is where homopolymers jointed end-to-end. Such an arrangement is referred to as a block copolymer. Block copolymers frequently exhibit phase separation which typically gives rise to a dispersed phase consisting of one block type in a continuous matrix consisting of the second block type [4]. In many applications, the dispersed phase consists of hard domains which are crystalline or glassy and amorphous, and the matrix is soft and rubber-like. A block copolymer can act as an emulsifier for a system of two immiscible homopolymers [5]. Block polymers exhibiting phase separation show

two transitions where the modulus changes markedly over a narrow temperature range. Elasticity is a general property of block copolymers containing a combination of incompatible hard and soft blocks. The hard blocks in the domains serve as tie-points, or thermolabile crosslinking sites [6]. These physical crosslinks are reversible.

Long-chain branched polymers, including star-shaped, comb-like, and randomly branched polymers, are a class of polymers between the linear polymers and polymer networks. The properties of the polymers are influenced by their overall dimensions and long-chain branching. The presence of long-chain branched molecules causes different properties compared to a pure linear polymers such as narrow molecular weight distribution [7], smaller radius of gyration [8], and different properties in solid state governed by the overall dimensions of polymer chains.

Dendrimers are monodispersed macromolecules with radially symmetric branching. Dendrimers consist of three architectural components: a core; interior layers (generations) attached to the core; and an exterior of terminal functionality connected to the outmost generation. Due to their special architectures, dendrimers show interesting properties such as controllable size, compartmentalization, solubilization, preorientation, and cage location [9].

Graft polymers are macromolecules with a 'backbone' of one polymeric species attached to which are one or more side chains of another polymeric species. Graft polymers may have comblike or random graft structures. Because of



thermodynamic incompatibility of the backbone and side chain, most graft polymers show microphase separation behavior in solid state (4, 10). These polymers exhibit many unique thermal and mechanical properties including thermoplastic elasticity. Generally property differences between linear and branched polymers apply to graft copolymers.

Crosslinked polymers are insoluble and infusible three-dimensional networks in which polymer chains are joined together. Crosslinked polymers exhibit many special properties compared to linear and branched polymers. Improvement of physical properties by cross-linking are most significant. For example, modulus increases with degree of crosslinking. Crosslinked polymers behave like soft elastic solids at elevated temperature [11]. Other special behavior include improved creep, compression set, and stress relaxation; lower thermal expansion and heat capacity; higher heat distortion temperature, tensile strength and refractive index. Glass transition temperature increases as crosslink density increases [12].

An economic way to meet the needs for new materials is to make polymer blends, the mixtures of at least two polymers or copolymers, including homologous, miscible, immiscible, and compatible polymers [13]. From the economic point of view, this approach has many advantages over others such as extending engineering resin performance by diluting it with a low cost polymers; developing materials with expected properties; forming a high performance blend from synergistically interacting polymers, etc. However, The development of polymer blends is limited by the fact that many polymers are

immisible to each other and the microphase separation occurs in immisible blends, resulting in poor elongation and impact-strength properties.

## II. POLYMERS WITH SUPRAMOLECULAR TOPOLOGIES

In contrast to molecular chemistry, supramolecular chemistry, the chemistry beyond molecules, is concerned with the organized entities of high complexity resulting from the association of at least two chemical species by intermolecular (noncovalent) interactions [14].

Interpenetrating polymer networks (IPN) are a combination of at least two polymers in a network which are synthesized in juxtaposition (Figure 2) [15].

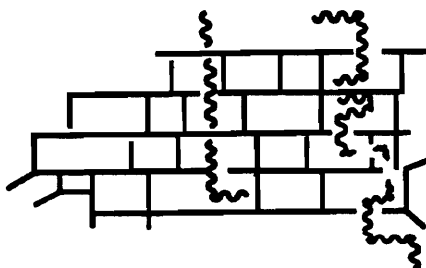


Figure 2. Interpenetrating polymer network

For IPN, if mixing takes place at the early stage of the polymerization and the polymerization proceeds simultaneously with crosslinking, phase separation may be controlled. Therefore, polymer mixtures with limited phase separation

can be produced via interpenetration polymerization. IPN are a special example of topological isomerism of polymers [16]. Some permanent entanglements between two crosslinked polymers are inevitable in any intimate mixture of crosslinked polymers.

Polycatenanes are extended interlocking ring systems without covalent bonds between the rings. The term “catenane” comes from the Latin word *catene* meaning chains. However, since Frisch et al. first suggested the existence and possible syntheses of polycatenanes in 1953 [17], no pure polycatenanes have been isolated and characterized. Some subclasses of polycatenanes are shown in Figure 3.

Polyrotaxanes are supramolecular assemblies consisting of linear molecules onto which are threaded cyclic species (Figure 4). The term ‘rotaxane’ is derived from the Latin words for wheel and axle [18]. Bulky groups are attached to the linear molecules, either at the ends or in the middle of the chain, to prevent diffusion loss of the molecules, dethreading. If there exist strongly attractive forces between cyclic and linear species, blocking groups may not be necessary. Polyrotaxanes can be classified as main chain and side chain polyrotaxanes, depending on the differences in the location of the covalent and physical linkages. Polyrotaxanes can also be divided into two types, homopolyrotaxanes and heteropolyrotaxanes, based on the chemical structures of cyclic and linear species. Homopolyrotaxanes consist of chemically equivalent macrocycles and polymer chains. Heteropolyrotaxanes are comprised of chemically different cyclic and linear components.

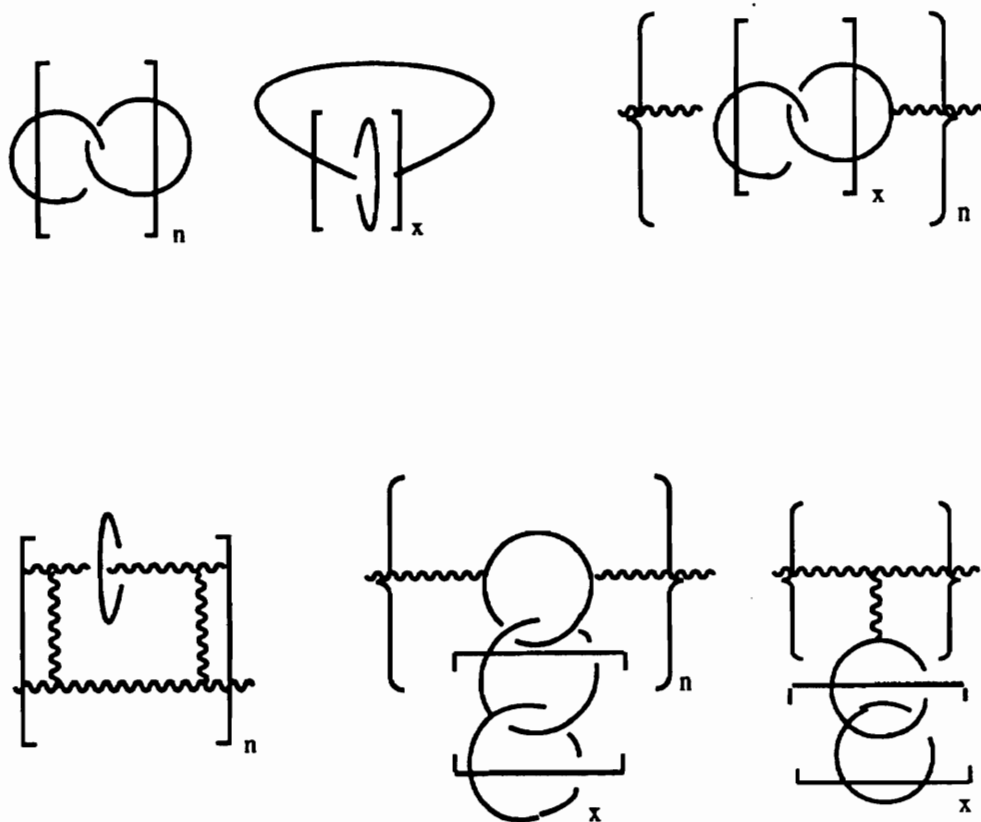


Figure 3. Some subclasses of polycatenanes

Similarly to conventional copolymers and polymer blends, a wide range of physical properties can result from judicious combination of cyclic and linear components of polyrotaxanes. If the macrocycles and linear polymer chains are compatible, the crystallinity of polyrotaxanes can be changed by adjusting the macrocycle contents in polymers. The toughness of the polymers can be

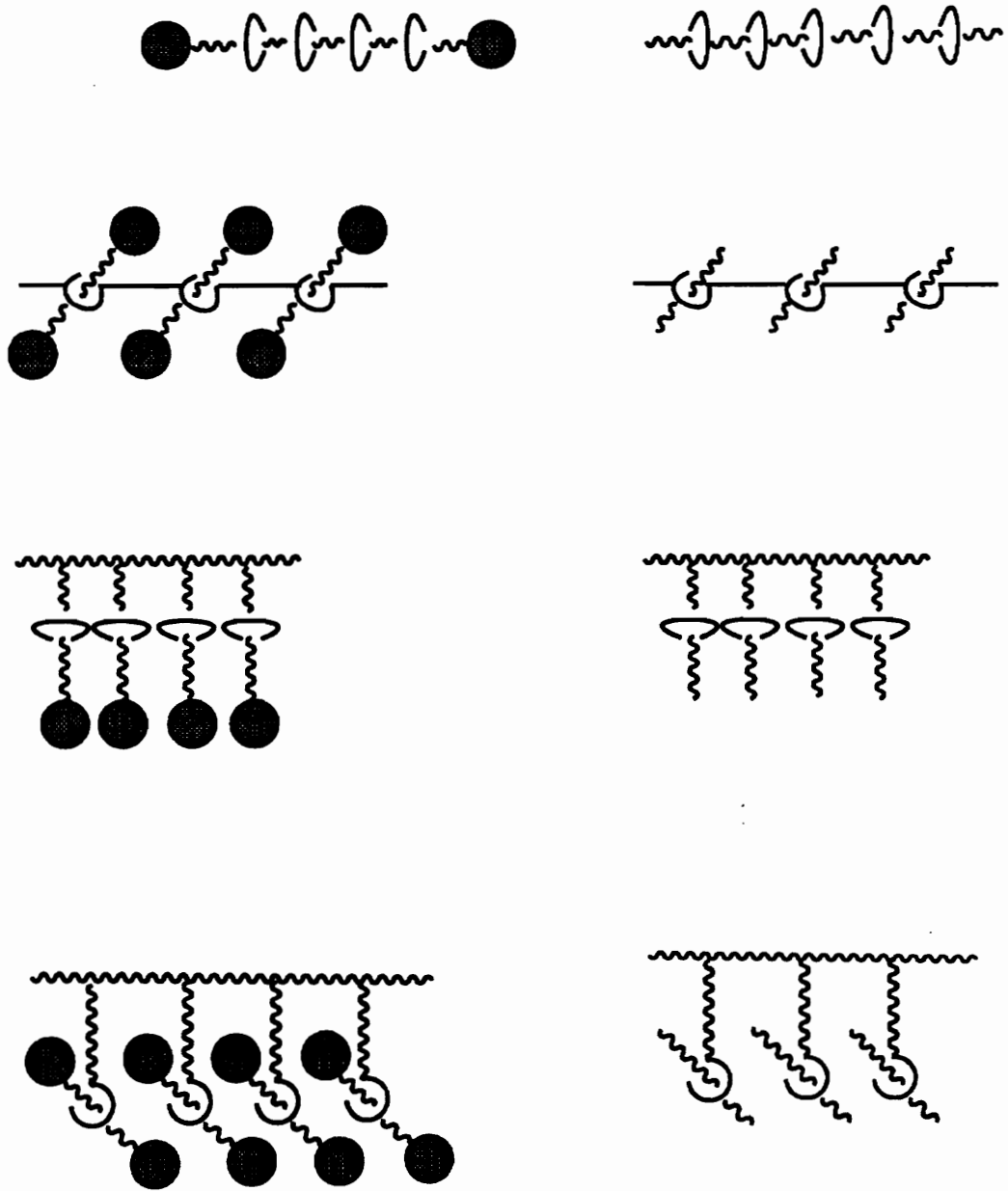


Figure 4. Polyrotaxane structures

increased by introducing intermolecular interaction between the macrocycles and chains. If cyclic and linear species are not compatible, the macrocycles could move along the chain and both cyclic and linear species can aggregate and crystallize independently, resulting in microphase separation. The solubility and processibility of high performance polymers could be modified by threading low melting and highly soluble macrocycles onto the polymer chains.

Furthermore, polyrotaxanes are expected to have distinguishing features compared to conventional copolymers and polymer blends, due to the physical barriers to dethreading of macrocycles and due to the freedom of macrocycles to move laterally, translationally, and circumferentially relative to the linear unit that penetrates them. Hence, macrocycle distribution could be changed by changing configuration and conformation of polymer chains.

## REFERENCES

1. Gibson, H.W.; Bheda, M. C.; Engen, P. T. *Prog. Polym. Sci.* **1994**, *19*, 843.
2. Semylen, J.A., ed.; *Cyclic Polymers*, Elsevier Applied Science; New York, **1986**.
3. McKenna, G. B.; Hosteltter, B. J.; Hadjichristidis, N.; Fetters, L. J.; Plazek, D. J. *Macromolecules*, **1989**, *22*, 1834.
4. Noshay, , A.; McGrath, J. E.; *Block Copolymers: Overview and Critical Survey*. Academic Press, Inc., New York, **1977**.
5. Inous, T.; Soen, T.; Hashimoto, T.; Kawai, H. *Macromolecules*, **1970**, *3*, 87.
6. Bonart, R.; Morbitzer, L.; Rinke, H.; *Kolloid-Z.* **1970**, *240*, 807.
7. Schaefgen, J. R.; Flory, P. J. *J. Am. Chem. Soc.* **1948**, *70*, 2709.
8. Zimm, B. M.; Stockmayer, W. M. *J. Chem. Phys.* **1949**, *17*, 1301.
9. Tomalia, D. A.; Hedstrand, D. M.; Wilson, L. R. *Encycl. Polym. Sci. Eng.*, Wiley, New York, **1990**, index vol., pp. 46-92; Newkome, G. R.; Moorefield, C. N.; Baker, G. R.; Behera, R. K.; Escamillia, G. H.; Saunders, M. J. *angew. Chem., Int. Ed. Engl.*, **1992**, *31*, 917; Xu, Z.; Moore, J. S. *Angew. Chem. Int. Ed. Engl.*, **1993**, *32*, 1354; Gitsov, I.; Frechet, J. M. J. *Macromolecules*, **1993**, *26*, 6536.
10. Sperling, L. H. ed., *Recent Advances in Polymer Blends, Grafts, and Blocks*, Plenum Press, New York, **1974**.
11. Ferry, J. D. *Viscoelastic Properties of Polymers*, John Wiley & Sons, Inc., New York, **1970**, pp431-465.

12. Loshack, S. J. *J. Polym. Sci.* **1955**, *15*, 391; Chompff, A. J. *Polymer Networks - Structure and Mechanical Properties*, Plenum Press, New York, **1971**, pp. 145-190; Fox, T. G.; Loshack, L. *J. Polym. Sci.* **1955**, *15*, 371.
13. Utracki, L. A. *Polymer Alloys and Blends, Thermodynamics and rheology*. Hanser Publishers, New York, **1990**.
14. Lehn, J.-M. *Angew Chem. Int. Ed. Engl.* **1990**, *29*, 1304; Lehn, J.-H. *Angew. . Chem. Int. Ed. Engl.* **1988**, *27*, 89.
15. Klempner, D.; Sperling, L. H.; Utracki, L. A. *Interpenetrating Polymer Networks. Advances in Chemistry Series, 239*. Am. Chem. Soc., Washington, DC **1994**.
16. Frish, H. L.; Wasserman, E. *J. Am. Chem. Soc.* **1961**, *83*, 3789; Frisch, H. L.; Klempner, D. *Adv. Macromol. Chem.* **1970**, *2*, 149.
17. Frish, H. L.; Martin, I.; Mark, H. *Monatsh.*, **1953**, *84*, 250.
18. Schill, G.; Zöllenkopf, H. *Nachr. Chem. Techn.*, **1967**, *79*, 149; Schill, G.; Zöllenkopf, H. *Ann. Chem.* **1969**, *721*, 53.



## CHAPTER II

### LITERATURE REVIEW: POLYROTAXANES

#### I. MONOROTAXANES AND MONOCATENANES

Willstatter was the first person who suggested the existence and possible syntheses of catenanes and rotaxanes [1]. However, this brilliant suggestion had not caused extensive interest for about a half century until Frisch et al. discussed polycatenanes in 1953 [2]. The studies on this ring-ring or ring-chain interlocking topology were accelerated by the increasing demands for new materials. Generally speaking, there are three approaches, the statistical threading, the chemical conversion, and the template approach, for the syntheses of catenanes and their precursors, rotaxanes.

##### A. The Statistical Approach

The interlocking of a ring with a linear molecule may be accomplished by the penetration of the chain into the cavity of the macrocycle. If there are no strong attractive interactions between the ring and the chain, the threading is of a statistical nature. A rotaxane is formed if the linear molecule is end-capped by a bulky unit to generate a molecular "dumb-bell". A catenane is prepared if two ends of the chain connect to each other to form a second ring.

Wasserman first reported the synthesis of a catenane by an acyloin ring closure of diethyl tetatricontanedioate in the presence of a deuterated macrocycle [3]. He proved the catenane structure by oxidatively splitting the acyloin macrocycle, obtaining the deuterated macrocycle and the tetratricontanedioic acid.

Harrison and Harrison synthesized this “dumb-bell” molecule in solution and gave it a name “hooplane” [4]. Later they improved the statistical method by use of a polymeric support [5]. They introduced the hemisuccinate ester of 2-hydroxycyclooctacosanone to Merrifield’s peptide resin. The resin-bound macrocycle was then rinsed 70 times sequentially by the solutions of 1,10-decanediol and then triphenylmethyl (trityl) chloride. After they isolated the rotaxane from byproducts and polymer resins, they supported the rotaxane structure by the cleavage of the rotaxane with boron trifluoride etherate, generating 1,10-decanediol, triphenylmethanol, and the acyloin macrocycle.

In a later paper, Harrison utilized two methods to generate rotaxanes [6]. The first method was the approach of acid catalyzed equilibration, consisting of the reversible cleavage of the blocking groups of rotaxanes (Figure 1). He mixed a mixture of 14- to 42-membered cycloalkanes with 1,10-bis(triphenylmethoxy)-decane at 120 °C followed by the addition of trichloroacetic acid which acted as a catalyst for the blocking group detachment. A mixture of rotaxanes with different rings was isolated by chromatography. The mixture was hydrolyzed and 23- to 29-membered macrocycles were obtained. This experiment demonstrated: (1) that a 23-membered ring size is necessary for the threading of the ring by a methylene chains; (2) that macrocycles with 29 or more atoms can slip over the

triphenylmethyl blocking group; and (3) that the relative yield of the rotaxane increases with increasing ring size.

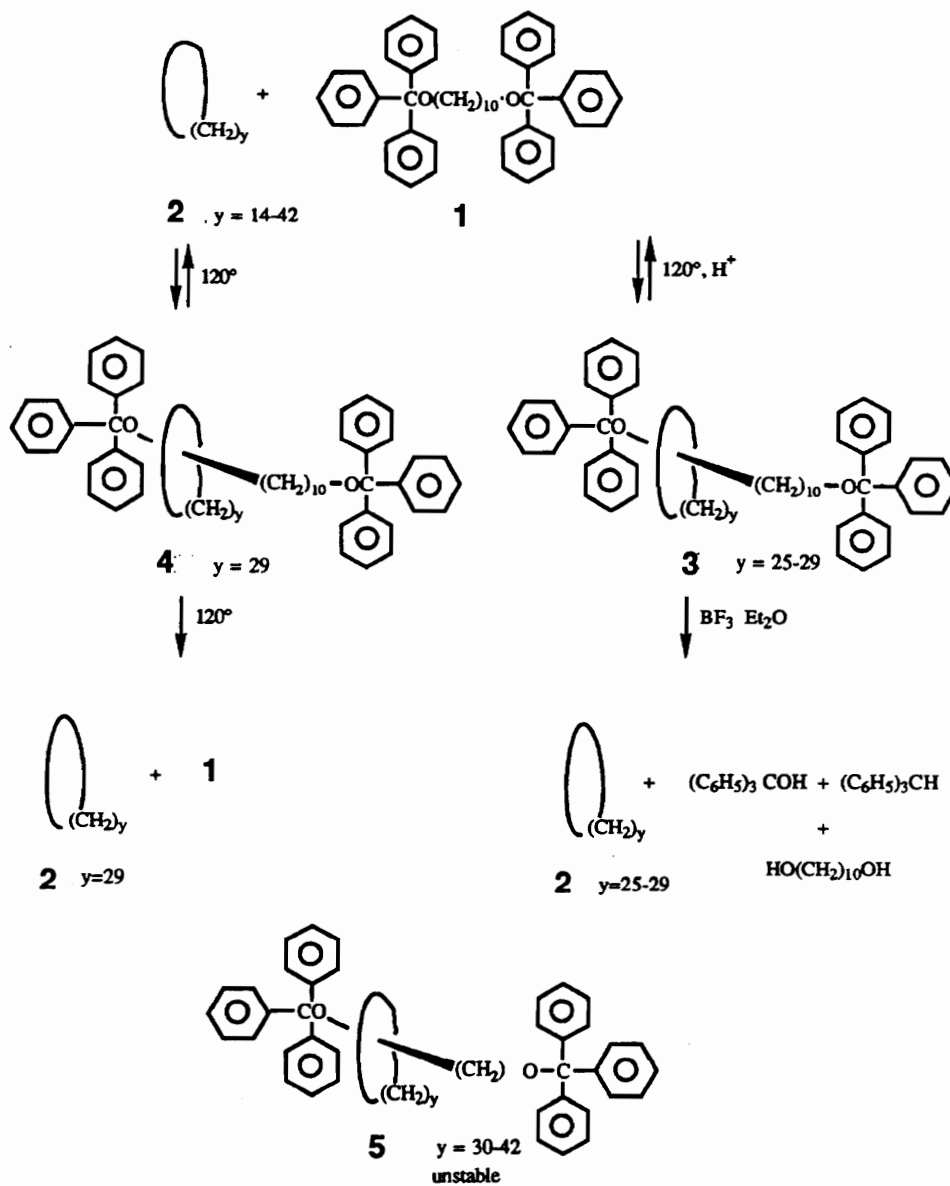


Figure 1. Harrison's approach of acid catalyzed equilibration

The second method was a thermal variation whose procedure is same as the first one except there is no catalyst for the bulky end group cleavage. A rotaxane based on the 29 membered macrocycle was generated, due to the fact that the macrocycles with large enough ring size can slip over the triphenylmethyl bulky end group to form a rotaxanes if enough thermal energy is provided. This experiment showed that 14- to 28-membered macrocycles can not slip over the blocking group to afford rotaxanes, while threaded 30- to 42-membered rings can dethread, passing over the blocking group.

Harrison continued to test the blocking effectiveness of a larger bulky end group, tri(4-*t*-butylphenyl)methanol, using both the acid catalyzed equilibration approach and the thermal variation approach [7]. From the acid catalyzed equilibration experiments he concluded that the yields of rotaxanes increase monotonically with increasing ring size. The thermal variation experiments, however, did not generate any stable rotaxanes. When Harrison tested blocking effectiveness of the dicyclohexylmethyl group using the thermal variation approach, only a rotaxane based on the 28 membered macrocycle was obtained.

Schill et al. studied the effects of ring size on the rotaxane yield and blocking effectiveness of the triphenylmethyl moiety, using both acid catalyzed equilibration and thermal variation approaches, that is, equilibrating individual pure cycloalkane macrocycles of 21 to 29 carbons with bis(triphenylmethylthio)dodecane, either thermally or in the presence of *p*-toluenesulfonic acid [7]. They found that yields of rotaxanes increased with increasing ring size and a minimum ring size of 21 atoms is necessary for the

threading to occur. By varying the length of the linear molecules in the thermal variation experiments in which the 29 membered cycloalkane was used, they found that the yields of rotaxanes increased with the chain length.

## B. Chemical Conversion

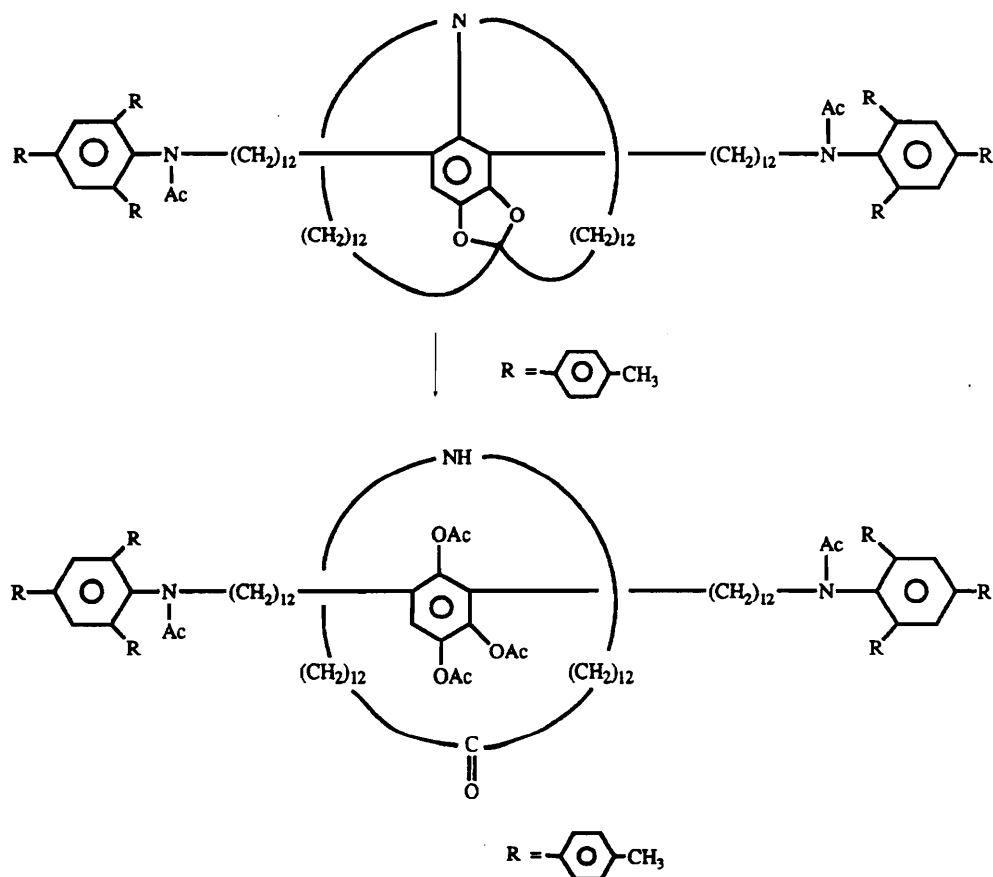


Figure 2. Schill's chemical conversion approach

Schill and Luttringhaus first developed the chemical conversion method to synthesize rotaxanes and catenanes [8]. This method started from covalent connection of a chain and a ring, resulting in prerotaxane/catenane structures. A

rotaxane was formed after bulky groups were attached to the ends of the linear molecule and after the covalent bonds between the ring and chain were broken. A catenane was produced by the ring closure of the linear molecule and the disconnection of the two interlocked rings. Using this approach Schill and Luttringhaus synthesized a catenane containing 4,5-dimethoxyisophthalaldehyde as a central core [8]. Schill and his coworkers also produced prerotaxanes in which a macrocycle was covalently connected to a phenyl ring of a linear molecule. The prerotaxanes were then converted to rotaxanes by the cleavage of the linkage between the ring and the chain (Figure 2) [9].

### C. The Template Approach

The third method for the catenane and rotaxane syntheses is the template approach which involves strong attractive interactions between a macrocycle and a linear molecule.

The ring-ring or ring-chain interlocking systems can be formed by using transition metals to link two molecules which have electron donating groups acting as ligands. Sauvage et al. produced catenanes by forming a complex of  $\text{Cu}^+$  and 1,10-phenanthroline [10]. Using the same chemistry Wu et al. [11] and Sauvage et al. [12] prepared rotaxanes in which both chains and rings contained phenanthroline groups.

Cyclodextrins (CD) are host molecules which can form complexes with guest molecules (Figure 3). These doughnut-shaped molecules have six primary

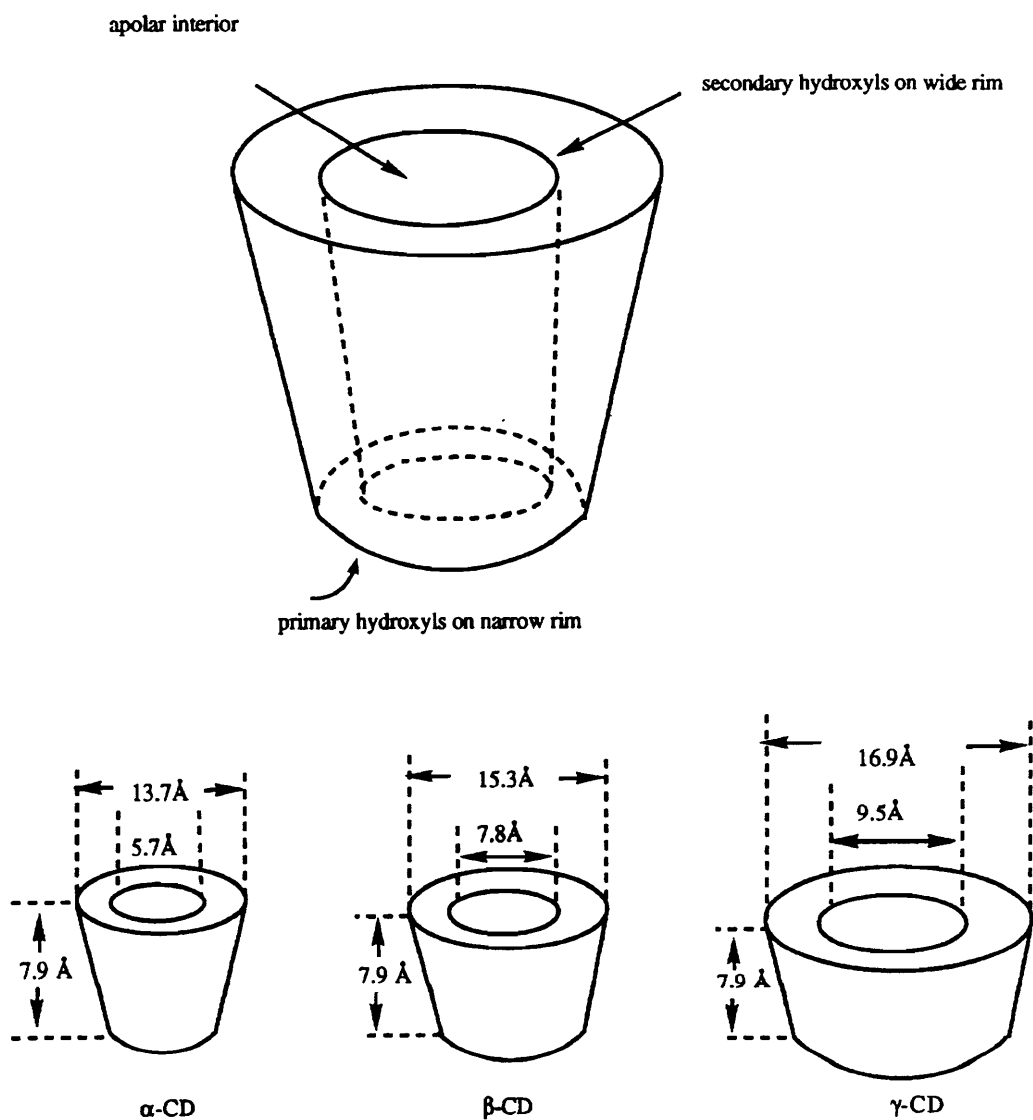


Figure 3. Functional structure and molecular dimensions of cyclodextrins

hydroxyl groups from the 6-position of the glucose residues at the narrow end of the torus, and the twelve secondary hydroxyl groups from the 2- and 3-positions

on the wide rim of the torus. On the inside of the cavity there is a ring of CH groups, a ring of glycosidic oxygens, and a further ring of CH groups, resulting in a hydrophobic ether-like interior while the external faces are hydrophilic. Rotaxanes have been produced in relatively good yields by using cyclodextrins as macrocycles. Ogino prepared rotaxanes comprised of a dicobalt (III) diamine complex and cyclodextrins (Figure 4) [13]. He studied the effect of the length of aliphatic diamines on the rotaxane yields and found that the yield reached a maximum when the n value, the number of methylenes in the diamine, equaled 12.

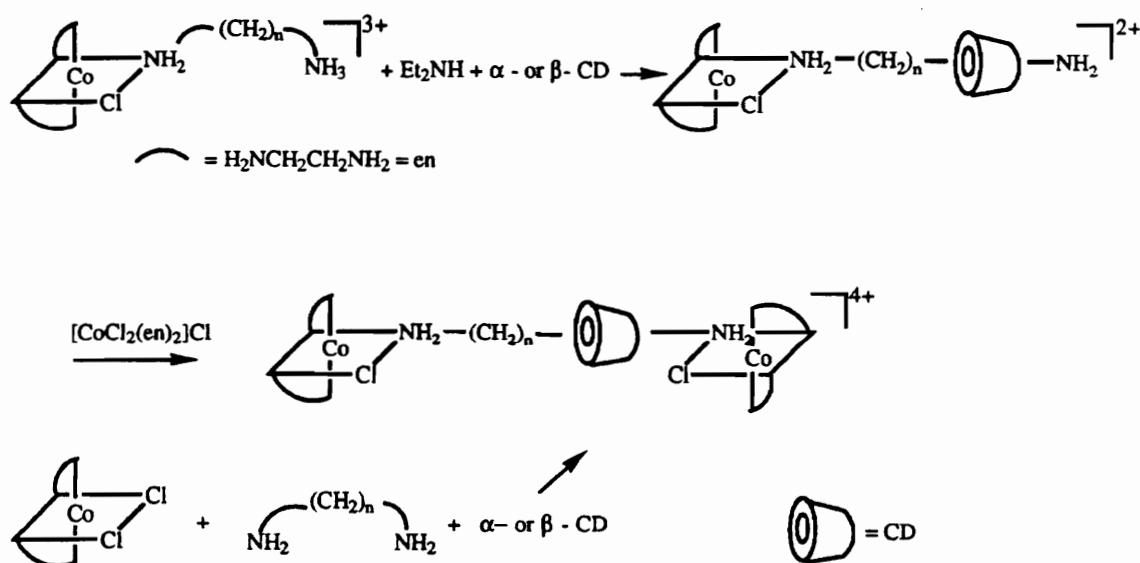


Figure 4. Synthesis of a rotaxane comprised of a dicobalt (III) diamine complex and cyclodextrins

Wylie and Macartney made the [2]rotaxane-metal complexes with  $\alpha$ -CD by mixing  $\alpha$ -CD, 1,1'-( $\alpha,\omega$ -alkanediyl)-bis(4,4'-bipyridinium) bromide and  $\text{Na}_3[\text{Fe}(\text{CN})_5\text{NH}_3] \cdot 3\text{H}_2\text{O}$  [14]. Similarly, Wenz et al. produced rotaxanes

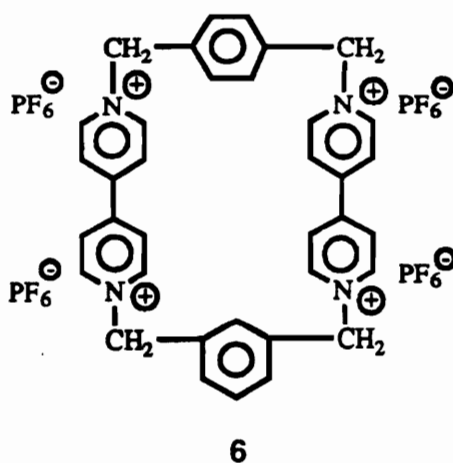


consisting of a linear component of bipyridinium, an O-derivatized  $\beta$ -CD, and bulky end groups [15].

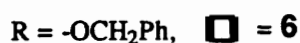
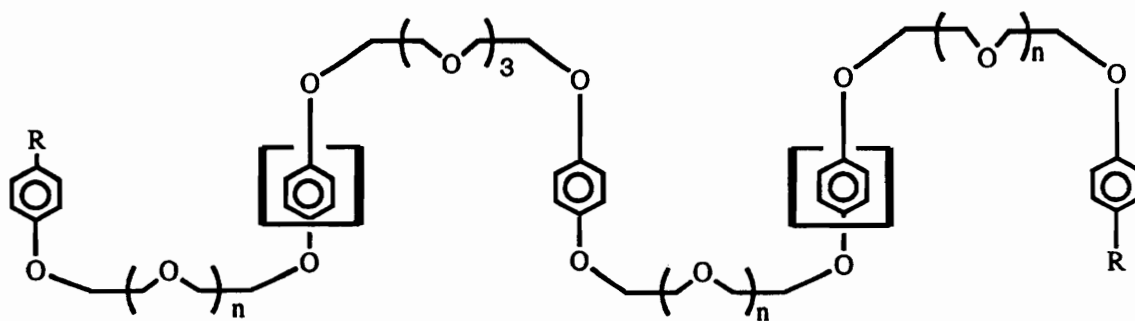
Stoddart et al. prepared [diquat]<sup>2+</sup>(N, N'-dimethyl-2,2'-bipyridyl) or [paraquat]<sup>2+</sup>(N,N'-dimethyl-4,4'-bipyridyl)-dibenzo crown ether rotaxanes, utilizing the fact that pyridinium rings of [diquat]<sup>2+</sup> and [paraquat]<sup>2+</sup> can form 1:1 complexes with the aromatic crown ethers [16]. Stoddart et al. also synthesized bis(cycloparaquat-28-N<sub>4</sub>)<sup>+</sup>(BP-28-N<sub>4</sub><sup>+4</sup> : 4PF<sub>6</sub><sup>-</sup>), **6**, a macrocycle containing two [paraquat]<sup>2+</sup> moieties jointed by two p-xylene units. This macrocycle formed stable complexes with hydroquinone and catechol ethers, due to special interactions such as  $\pi/\pi$  stacking, charge transfer, and electrostatic interactions [17]. They reported syntheses of [2]catenanes by interlocking these di[paraquat]<sup>2+</sup> macrocycles with dibenzo crown ethers [18], and a [3]catenane by interlocking a large di[paraquat]<sup>2+</sup> macrocycle with two dibenzo crown ethers [19]. The [2]catenanes consisting a bipyridium macrocycle and tetrabenzo crown ethers behaved like molecule shuttles. The bipyridium macrocycle moved around the four hydroquinol units (stations) while it moves circumferentially [20].

Stoddart et al. extended these approaches to synthesize a chiral bis([2]catenane) [21]; a catenane in which the gold surface was a part of a dibenzo crown ether [22]; catenanes consisting of dibenzo crown ethers and bis(bipyridinium) macrocycles derived from an azobenzene [23]; and catenanes comprised of a bis(bipyridinium) macrocycle and a cyclic compound of strapped porphyrins [24].

Stoddart and coworkers also applied the chemistry of the donor:acceptor complex to the formation of rotaxanes. These rotaxanes are interlocking systems of a bipyridium macrocycle, **6**, and a linear molecule containing 2-4 hydroquinone moieties [16, 25]. **7** is one of these rotaxanes. These rotaxanes were also “molecular shuttles”. However, when the rotaxane possesses two bipyridium macrocycles and five hydroquinol units in its linear chain, the macrocycles were immobile at low temperatures.



Stoddart et al. also produced a “pseudo-rotaxane”, a rotaxane without bulky end groups, using 1,5-bis[2-(hydroxyethoxy)ethoxy]naphthalene. Dethreading was observed only when the electron transfer from the excited state of anthracene-9-carboxylic acid to the bipyridium macrocycle occurred [26]. Later they reported syntheses of rotaxanes containing a dibenzo crown ether, a bipyridium linear molecule and triarylmethyl end blocking groups [27]. The rapid movement of the dibenzo crown ether between bipyridium “stations” was observed by NMR spectroscopy.



7

## II. OLIGOMERIC ROTAXANES

### A. Statistical Threading

Zilkha and coworkers reported the preparations of rotaxanes by mixing dibenzo crown ethers with oligo(ethylene glycol)s. The resultant oligorotaxanes were polymerized with naphthalene-1,5-diisocyanate to constrain the threaded macrocycles (Figure 4) [28]. They demonstrated that high threading could be achieved by use of an excess of the macrocycle relative to the linear chains; large macrocycles; long chains; and high concentrations. The percent threading of large rings by linear chains reached a maximum when the number of atoms in linear species was ca 42. They rationalized this result by the decrease of chain end concentration with increasing chain length.

Zilkha et al. also investigated the effect of temperature on the threading process. They did not observe significant changes of the percent threading in the

temperature range from 100-207 °C. Therefore, the enthalpy of the threading was believed to be zero and  $\ln K = \Delta S/R$ , where K is the equilibrium constant of the threading.

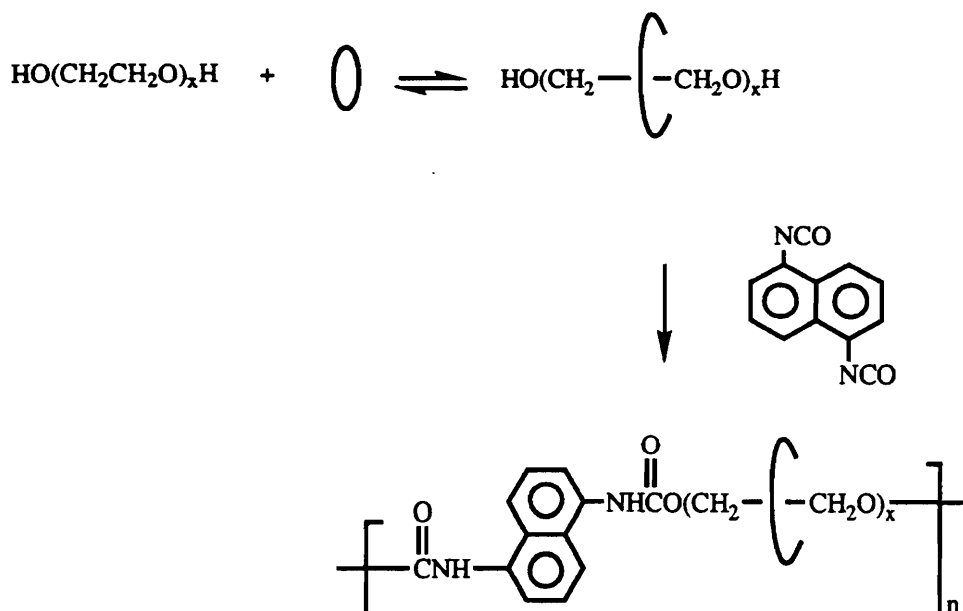


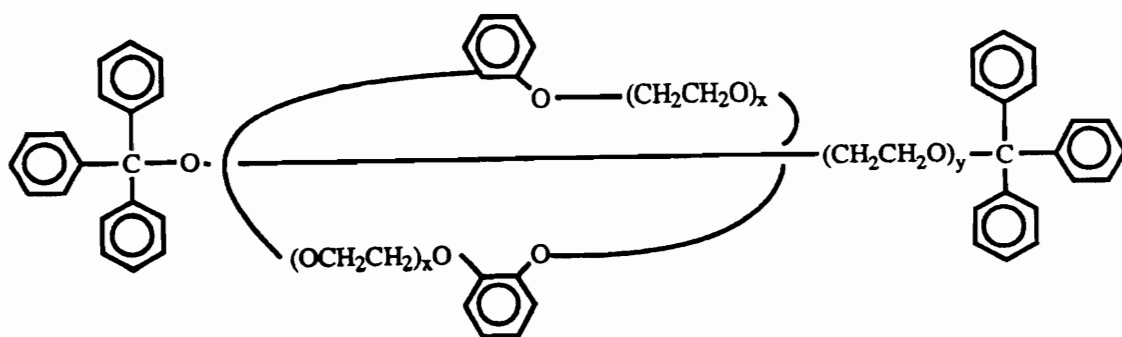
Figure 5. Zilkha's approach for synthesis of oligomeric and polymeric rotaxanes

Based on above results Zilkha et al. deduced an equation for the number of threadings:

$$N = K[m_c m_g (1 - e^{-n c/m_g} \cdot n_c n_g^{\beta \theta})] / V \quad (1)$$

Where  $N$  = number of penetrations  
 $m_c, m_g$  = number of moles of rings and chains, respectively

- $n_c, n_g$  = number of atoms in a cycle and a chain, respectively
- $\beta$  = constant characterizing the degree of curling-up of chain molecules, which affects the threading and dethreading of rings
- $\theta$  = penetration angle, depending on the ring radius ( $r$ ) and chain diameter ( $d$ ) and determined as  $\cos\theta = d/2r$
- $V$  = total volume



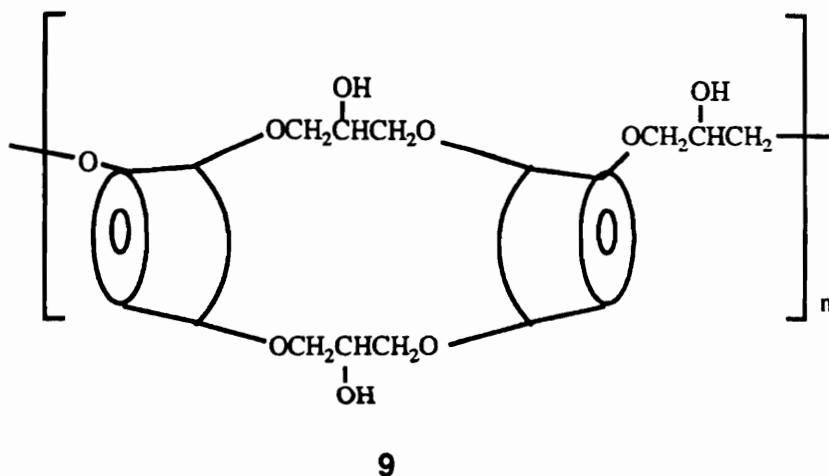
8

Zilkha and his colleagues prepared rotaxane **8** whose colligative molecular weight was intermediate between those of the linear chain and the macrocycle [28, 29]. They attributed this special colligative property of the rotaxane to the independent movement of cyclic and linear species. The dethreading rate of macrocycles from rotaxane **8** was significantly affected by solvents. The dethreading rate constant in diglyme or in neat system was two times higher than in xylene, presumably due to weak dipole-dipole interaction between linear and cyclic component and xylene. Because of strong hydrogen bonding interactions

between 2-octanol and cyclic and linear components of the rotaxane, the dethreading rate in the alcohol was much higher compared to neat systems.

## B. Template Threading

Harada and Kamachi reported the preparations of rotaxanes by forming complexes of oligo(ethylene glycol)s with  $\alpha$ -cyclodextrin (CD) [30]. The molar ratios of ethyleneoxy repeat unit to  $\alpha$ -CD were always two and the complexes showed "channel-type" arrangements. They also prepared similar rotaxanes endcapped by 2,4-dinitroaniline [31]. The  $\alpha$ -CD molecules in the rotaxanes showed an alternating head-to head, tail-to tail arrangement. A molecular tube **9** was believed to be formed by linking all three hydroxyl groups of the  $\alpha$ -CD units together.



Harada and Kamachi produced oligo(propylene glycol) rotaxanes using  $\beta$ -CD and  $\gamma$ -CD as macrocycles [32]. The rotaxane yields increased with increasing amount of linear chains and reached a maximum at 1000 molecular weight of

poly(propylene glycol). Syntheses of oligo(isobutylenes)- $\beta$ -CD rotaxanes and oligo(isobutylenes)- $\gamma$ -CD rotaxanes were also reported [33].

### III. POLYMERIC ROTAXANES

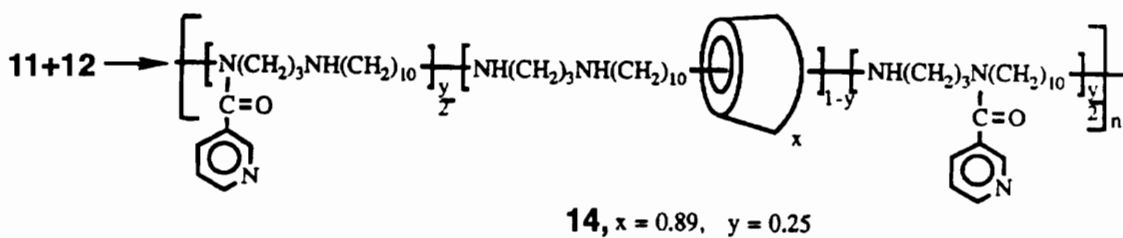
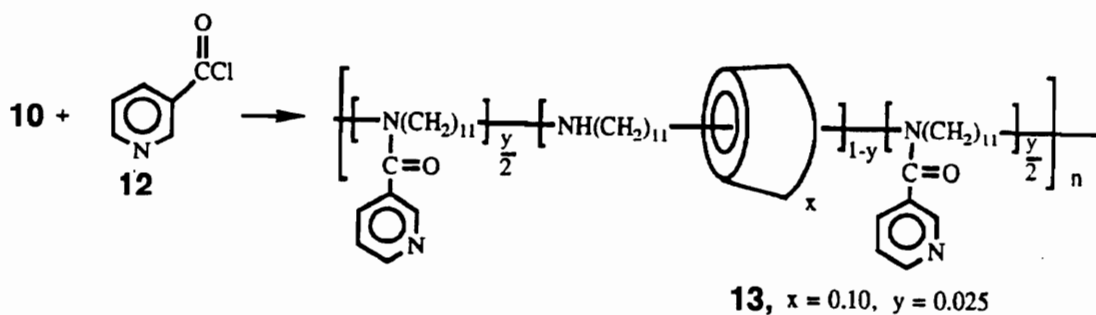
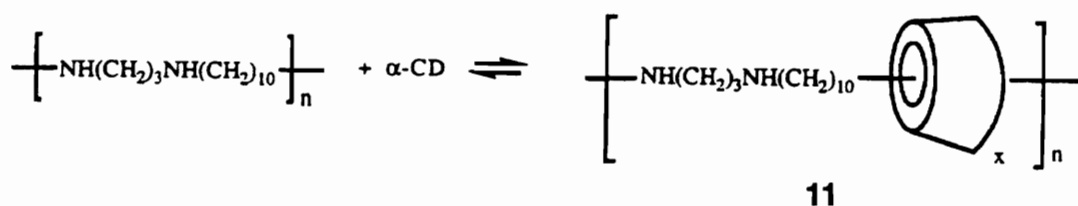
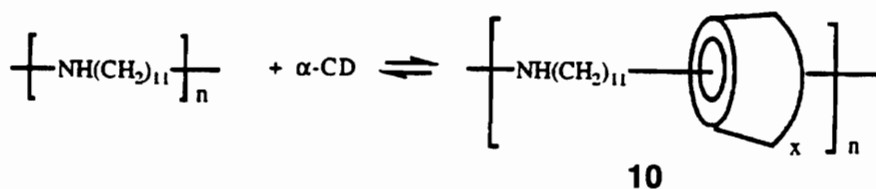
Agam et al. attempted to prepare polymeric rotaxanes by polymerization of oligo(ethylene glycol)-crown ether rotaxanes with naphthalene-1,5-diisocyanate [28]. However, the polyrotaxanes were not isolated.

Ogata and coworkers reported that polyamide- $\beta$ -cyclodextrin rotaxanes were synthesized via interfacial polymerization or solution polymerization [34]. However, molecular weights of the polyrotaxanes were apparently low.

Maciejewski reported the synthesis of poly(vinylidene chloride)-rotaxa-( $\beta$ -cyclodextrin) via radiation polymerization [35]. The polyrotaxane had high macrocycle content and high molecular weight. Maciejewski et al. [36] also prepared this polyrotaxane via free radical polymerization [36]. While the ratio of the polyrotaxane to homopolymer increased with increasing temperature, the macrocycle content in the polyrotaxane reached a maximum at 90-100 °C. Unfortunately, molecular weight of the polyrotaxane was low.

Lipatova and coworkers synthesized polyrotaxanes comprised of cyclic urethanes and linear polystyrenes [37]. The polystyrene rotaxanes were prepared by thermal polymerization of styrene in the presence of swollen cyclic urethanes which had been complexed with ZnCl<sub>2</sub>. The highly ordered

aggregates of the complexes of  $ZnCl_2$  with cyclic urethanes favored the ring incorporation onto polystyrene chains.



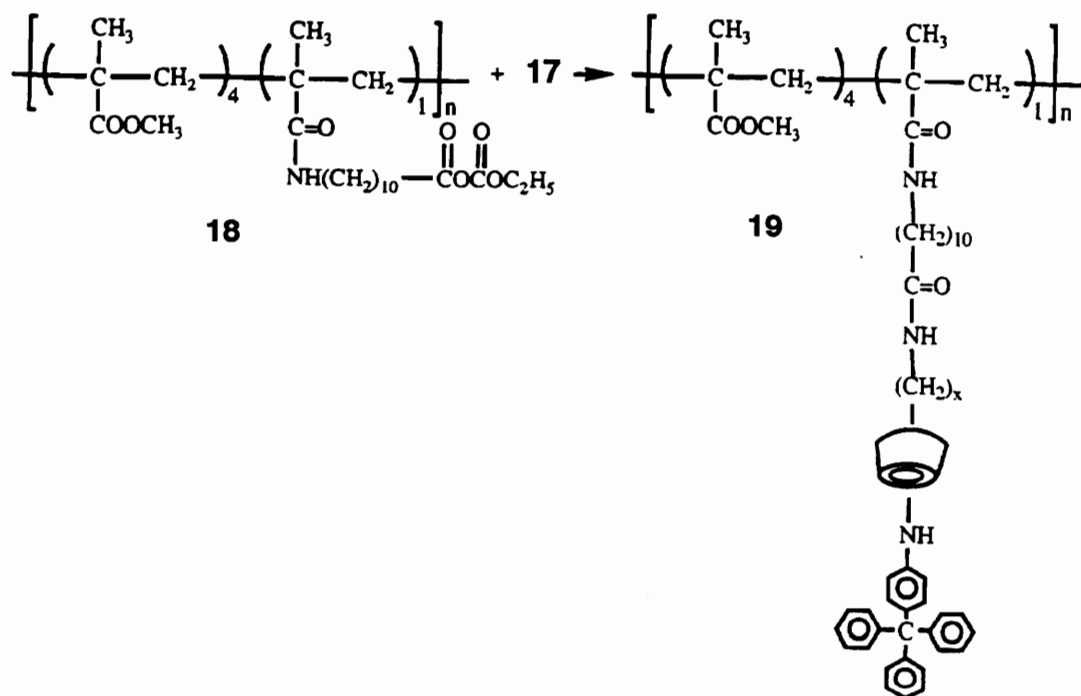
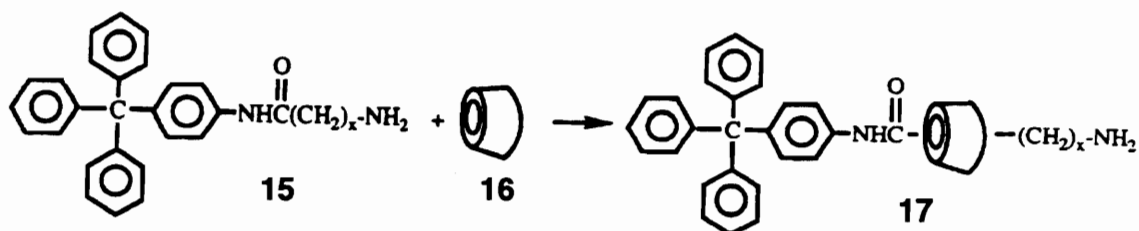
Syntheses of poly[(iminoundecamethylene)-rotaxa-( $\alpha$ -CD)], **10**, and poly[(iminotri



methylene-imino-decamethylene)-rotaxa-( $\alpha$ -CD)], **11**, were reported by Wenz and Keller [38]. Treatment of the polyrotaxanes with nicotinyl chloride, **12**, led to polyrotaxanes with blocking groups along the polymer backbones (**13**, **14**). Polyrotaxanes had high molecular weights and high macrocycle contents.

Born and Ritter reported syntheses of side chain polyrotaxanes, graft polymers whose side chains were rotaxanes [39]. The syntheses were initiated by the preparation of amino amides by introducing a tetraphenyl blocking group to one end of aliphatic diamines (**15**). Forming complexes of these amino amides with 2,6-dimethyl- $\beta$ -cyclodextrin, **16**, generated "semirotaxanes" (**17**). Reactions of these "semirotaxanes" with a poly(methyl methacrylate) copolymer bearing anhydride terminated pendant groups (**18**) led to side chain polyrotaxanes (**19**). These side chain polyrotaxanes displayed a better solubility in ether and reduced viscosity at low concentrations compared to model polymers.

Gibson and coworkers synthesized poly(urethane rotaxanes) from tetra(ethylene glycol), bis(*p*-isocyanatophenyl)methane (MDI) and 36-60 membered aliphatic crown ethers [40]. Up to 63 weight percent crown ethers were incorporated onto polyurethane chains. The macrocycle contents of polyrotaxanes increased with the size of the crown ethers and with molar feed ratio of macrocycle to the glycol monomer. The relation of glass transition temperature and macrocycle content of polyrotaxanes followed the Fox equation. The solubility of the polyrotaxanes in polar solvents increased with respect to the model polymer. Polyurethane rotaxanes with high macrocycle content are soluble in water at room temperature but exhibit lower critical solution temperatures upon heating.



Polyamide-crown ether rotaxanes were produced by Gibson and coworkers [41]. The glass transition temperatures and transition enthalpies of polyrotaxanes increased with aging time at room temperature. This was rationalized by the fact that the hydrogen bonding between crown ethers and amide linkages was replaced by more stable amide-amide hydrogen bonding.

Gibson et al. reported synthesis of polyrotaxanes comprised of bis(*p*-phenylene)-34-crown-10 macrocycle and polyurethane backbone containing bispyridinium moieties, either by the polymerization in the presence of the crown ether or by the template directed threading of a preformed polyurethane into the cavity of the macrocycle[42].

Polystyrene based polyrotaxanes were produced by Gibson and coworkers via both free radical polymerization and anionic polymerization [41]. An azo compound containing triarylalkyl moieties was used as both a free radical initiator and an end blocking group. The polystyrene rotaxanes exhibit two glass transition temperatures, corresponding to those of the macrocycle and the linear backbone. In spite of the intimate physical connection of the components, phase mixing does not seem to occur. In polar solvents, the polyrotaxanes form micelles with a polystyrene core and a crown ether shell. The presence of crystalline domains of the macrocycles of polyrotaxanes was detected using DSC; the linear macromolecular backbones are amorphous. The melting points are slightly depressed compared to crown ethers themselves.

Gibson and coworkers also prepared polyacrylonitrile based rotaxanes via free radical polymerization [43]. While polyacrylonitrile itself is soluble only in dipolar aprotic solvents like DMF and NMP, the corresponding polyrotaxanes are soluble in methanol. In DSC measurements the independent crystallization of threaded macrocycles was also observed.

Gibson and coworkers also reported the synthesis of polyazomethine-crown ether rotaxanes [44]. The solubilities of the polymers in organic solvents were improved compared to the model polymers. Incorporation of the macrocycle reduced the melting temperature by 100 °C and promoted the development of a new liquid-crystalline phase.

#### IV. POLYESTER ROTAXANES

##### A. Polyesters

Polyesters are organic polymers characterized by the possession of carboxylate ester groups in the repeat units of their main chains. Although the first studies on the synthesis of polyesters date back to the last century [45], it was only in the late 1920s that Carother undertook an extensive study of this subject. Beginning with polyesters he laid the foundations of step polymerization chemistry and the relationships among molecular structure, molar mass, and polymer properties [46]. However, it was only after Whinfield prepared poly(ethylene terephthalate) (PET) [47] that polyesters started to find their applications. For example, PET is widely used for fibers, films, and beverage bottles. Poly(1,4-butylene terephthalate) (PBT) is a good plastic molding material. Poly( $\epsilon$ -caprolactone) (PCL) is able to form compatible blends with a large number of other polymers. Some thermoplastic polyesters are completely biodegradable and are very useful when the environmental effects are of primary importance [48]. Polyarylates are excellent engineering materials because they display high heat distortion temperatures and good mechanical properties. Copolyesters containing aromatic

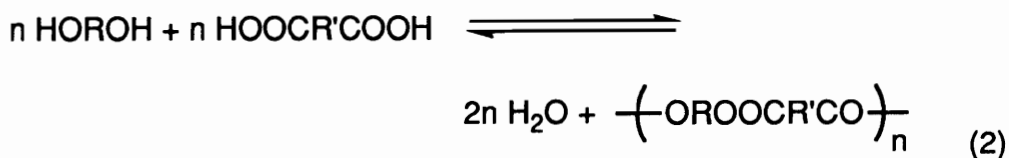
blocks separated by flexible linkages may have thermotropic liquid-crystalline character [49]. Random copolyesters prepared from aliphatic diols and mixtures of aliphatic and aromatic dicarboxylic acids act as hot-melt adhesives [50], while segmented block copolymers have found applications as thermoplastic elastomers [51].

The linear homopolymeric polyesters are two types: A-B polymers derived from hydroxycarboxylic acids or their carboxylic derivatives by self-esterification; and A-A-B-B polymers derived from the interaction of diols with dicarboxylic acids or their derivatives. Most polyesters are prepared by step growth polymerization. High molecular weight can be achieved by using pure starting monomers; controlling the precise stoichiometry (in the case of AA/BB type polymerization); and reducing side reactions by choosing appropriate reaction conditions.

Most polyesters can be synthesized by the following polymerization approaches. While almost all the methods are suitable for preparation of both A-A-B-B and A-B type polymers, the reactions will be expressed stoichiometrically in equations representing the formation of A-A-B-B type polyesters:

a. Direct Esterification

The simplest method of polyester synthesis consists in heating a hydroxycarboxylic acid, or a mixture of a glycol with a dicarboxylic acid:

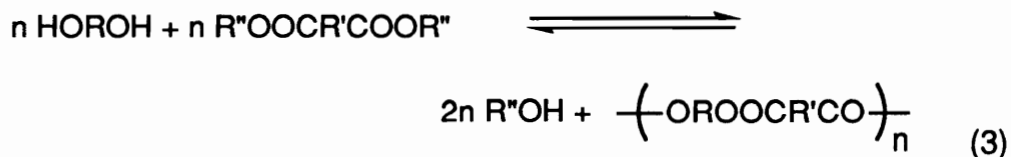


These are equilibrium reactions. The molecular weight of a polymer is determined by the removal of water from the reactions. It is usual to use an excess of glycol for syntheses of A-A-B-B type polymers both to compensate for physical loss and to provide hydroxyl-terminated macromolecules at whose chain ends further polymerization can be promoted by interchain transesterifications. The polycondensation can be driven to the right by removal of the liberated diol from the reaction, especially by working under reduced pressure.

The direct esterification is most suitable for the preparation of polyesters from glycols containing primary or secondary hydroxyl groups. It is not applicable to tertiary hydroxyl diols, which are prone to dehydration, or phenols, which are not reactive enough to be esterified directly. Some side reactions such as decarboxylation of carboxyl end groups; oxidation of terminal hydroxyl groups; and thermal fission of chain ester groups occurs under high-temperature reaction conditions.

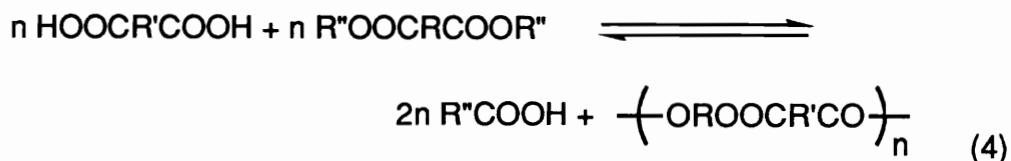
#### b. Transesterification

This approach differs from the direct esterification procedure in that the dicarboxylic acids are replaced by their dialkyl and diaryl esters:



Virtually all polyesters that can be prepared by direct esterification methods can be equally well, and often advantageously, prepared in this way. Advantages of this approach include: (a) that many diesters can be more readily refined than corresponding dicarboxylic acids; (b) that condensation of diesters with bisphenols proceeds more readily than carboxylic acids; and (c) diesters are normally lower melting and more miscible with other reagents than their acids.

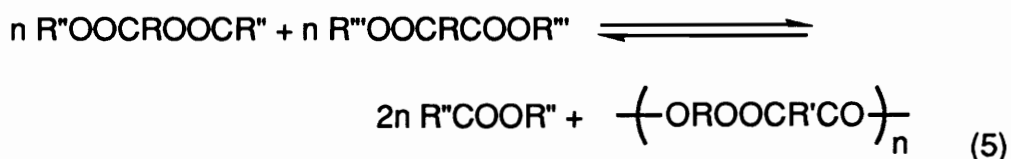
#### c. Acidolysis



The counterpart to transesterification approach lies in acidolysis method, where dicarboxylic acids are reacted with simple diesters of diols or where simple esters of hydroxy-acids are used. This approach is particularly useful for preparation of polyarylates of aliphatic and ring containing dicarboxylic acids.

#### d. Ester-ester Exchange

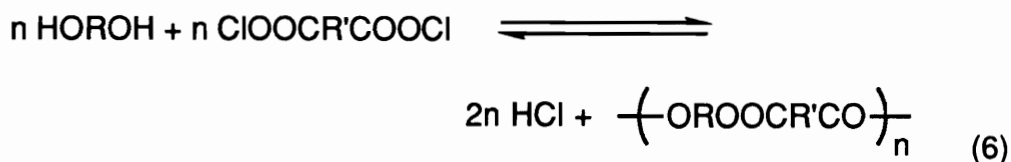
Some polyesters can also be prepared by ester-ester exchange reactions in which the eliminated species is itself an ester:



However, for many polyesters such reactions are too slow to be of practical value.

#### e. Acid Chloride Method

This method involves the direct reaction of diols with diacid chlorides:



The reactions can be performed either at high or low temperature, though the low temperature method is the most widely used. Under mild conditions, due to the high reactivity of acid chloride groups, these reactions are generally called “non-equilibrium” polyesterifications. At high temperatures, however, side reactions can seriously limit the attainment of high molecular weight. Therefore, water-free conditions should be maintained because traces of moisture hydrolyze the acid chlorides. The hydrogen chloride generated from the reactions should be removed since it hydrolyzes both diacid chloride monomers and ester groups of polymers. For all these reasons the reaction is preferably carried out at low temperature in solution or by interfacial polymerization.



Interfacial polymerization is usually performed in water and water-immiscible organic solvents [52] but has also been carried out using two immiscible organic solvents [53]. Briefly, the whole reaction may be conducted in an organic medium by combining the two reactants in the presence of a tertiary base such as pyridine or dimethylaniline, or the absorption of hydrogen chloride may be effected by the use of aqueous sodium hydroxide, the organic reactants being used alone or preferably with a water-immiscible solvent. The reaction of aqueous alkaline solutions of dihydric phenols (for which the reaction is particularly suitable) with the solutions of diacyl chlorides in organic solvents is assisted by vigorous stirring, which breaks up the water-immiscible phase into fine droplets at whose surface condensation occurs at normal temperatures with extreme rapidity. The dispersion process can be promoted by the addition of traces of ionic surfactants, yielding polyesters of very high molecular weight more easily than any other condensation methods. Because of its avoidance of high temperatures, this method of polyesterification is applicable to substances which would not survive the more extreme conditions of all the other reactions.

## B. Polyester Rotaxanes

The first polyrotaxane synthesized in 1987 in Gibson's group was poly(decamethylene sebacate)-rotaxa-(30-crown-10) from sebacoyl chloride and 1,10-decanediol using 30-crown-10 as a solvent [41, 54]. For example, with 3.42 moles of crown per mole of diol, a polyrotaxane with 16 wt % of crown ether was obtained. Mark-Houwink constants,  $K$  and  $a$ , of the linear polymer changed

dramatically because of the incorporation of the crown ether:  $K$  was changed by two orders of magnitude and  $a$  was almost doubled.

Poly(triethyleneoxy sebacate) crown ether rotaxanes and poly(butylene sebacate) crown ether rotaxanes were also made by transesterification in the presence of the crown ethers [41, 55]. All the polyrotaxanes prepared were partially soluble in methanol, while the parent polyester itself were completely insoluble in methanol. Examination of the polarized optical micrographs taken during isothermal crystallization of the poly(butylene sebacate), the crown ether, the polyrotaxane, and the polyester-crown ether blend demonstrated the phase-separated nature of the polyester/crown ether blends and provided some evidence for the effect of threading on the spherulitic morphology for the rotaxane than for the parent homopolymer. The isothermal spherulitic growth rate of the polyester component of the polyrotaxane was about one order magnitude slower than that of the pure polyester at the same temperature. This was due to the diffusion of macrocycle prior to the folding of the linear backbone. Differential scanning calorimetry and wide angle X-ray diffraction demonstrated that the overall degrees of crystallinity of the crown ether and the polyester were lower in the polyrotaxane than in the pure components. Melting studies and small-angle X-ray scattering suggested that the lamellar poly(butylene sebacate) crystals were thinner in the polyrotaxane than in the pure polyester for the same crystallization temperature and the average spacing between polyester lamellae was larger in the polyrotaxane than in the pure polyester, due to the residing of the crown ether macrocycles threaded by non-crystallized sections of polyester chains in the interlamellar region of the poly(butylene sebacate) crystals.

## REFERENCES

1. See footnote in Frisch, H. L. Wasserman, E. *J. Am. Chem. Soc.*, **1961**, *83*, 3789.
2. Frisch, H. L.; Martin, I.; Mark, H. *Monatsh*, **1953**, *84*, 250.
3. (a). Wasserman, E. *J. Am. Chem. Soc.*, **1960**, *82*, 4433; (b). Wasserman, E. *Sci. American*, **1962**, *207* (5), 94.
4. Harrison, I. T.; Harrison, S. *J. Am. Chem. Soc.*, **1967**, *89*, 5723.
5. Harrison, I. T. *J. Chem. Soc. Chem. Comm.*, **1972**, 231.
6. Harrison, I. T. *J. Chem. Soc. Perk. Trans. 1* **1974**, 301.
7. Schill, G.; Beckmann, W., Schweickert, N.; Fritz, H. *Chem. Ber.*, **1986**, *119*, 2647.
8. Schill, G.; Luttringhaus, A. *Angew. Chem. Int. Ed. Engl.*, **1964**, *3*, 546.
9. (a). Schill, G.; Zollenkopf, H. *Nachr. Chem. Technol.*, **1967**, *79*, 149; (b). Schill, G.; Zollenkopf, H. *Ann. Chem.*, **1969**, *721*, 53; (c). Schill, C.; Beckmann W.; Vetter, W. *Chem. Ber.*, **1980**, *113*, 941.
10. (a). Sauvage, J. P.; Dietrich-Buchecker, C. O. *Tetrahedron Lett.*, **1983**, *24*, 5095; (b). Dietrich-Buchecker, C. O.; Fronimberer, B.; Ler, I.; Sauvage, J.-P.; Vögtle, F. *Angew. Chem. Int. Ed. Engl.*, **1993**, *32*, 1434.
11. Wu, C.; Lecavalier, P. R.; Shen, Y. X.; Gibson, H. W. *Chem. Mater.*, **1991**, *3*, 569.
12. (a). Chambron, J.-C.; Heitz, V.; Sauvage, J.-P. *J. Chem. Soc., Chem. Commun.*, **1992**, 1131; (b). Chambron, J.-C.; Harriman, A., Heitz, V.; Sauvage, J.-P. *J. Am. Chem. Soc.*, **1993**, *115*, 7419.

13. (a). Ogino, H. *J. Am. Chem. Soc.*, **1981**, *103*, 1303; (b). Ogino, H.; Ohata, K. *Inorg. Chem.*, **1984**, *23*, 3312; (c). Ogino, H. *New J. Chem.*, **1993**, *17*, 683.
14. Wylie, R.; Macartney, D. *J. Am. Chem. Soc.*, **1992**, *114*, 3136.
15. (a). Wenz, G.; Bey, E.; Schmidt, L. *Angew. Chem. Int. Ed. Engl.*, **1992**, *31*, 783; (b). Wenz, G.; Wolf, F.; Wagner, M.; Kubik, S. *New J. Chem.*, **1993**, *17*, 729.
16. (a). Allwood, B. L.; Spencer, N.; Shahriari-Zavareh, H.; Stoddart, J. F.; Williams, D. J. *J. Chem. Soc., Chem. Commun.*, **1987**, 1058; (b). Allwood, B. L.; Spencer, N.; Shahriari-Zavareh, H.; Stoddart, J. F.; Williams, D. J. *J. Chem. Soc., Chem. Commun.*, **1987**, 1064; (c). Ashton, P. R.; Slawin, A. M. Z.; Spencer, N.; Stoddart, J. F. and Williams, D. J. *J. Chem. Soc., Chem. Commun.*, **1987**, 1066; (d). Allwood, B. L.; Spencer, N.; Shahriari-Zavareh, H.; Stoddart, J. F.; Williams, D. J. *J. Chem. Soc., Chem. Commun.*, **1987**, 1061; (e). Ortholand, J. -Y.; Slawin, A. M. Z.; Spencer, W.; Stoddart, J. F.; Williams, D. J. *Angew. Chem. Int. Ed. Engl.*, **1989**, *28*, 1394; (f). Anelli, P.-L.; Ashton, P. R.; Ballardini, R.; Balzani, V.; Delgado, M.; Gandolphi, M. T.; Goodnow, T. T.; Kaifer, A. E.; Philp, D.; Pietraszkiewicz, M.; Prodi, L.; Reddington M. V.; Slawin, A. M. Z.; Spencer, N.; Stoddart, J. F.; Vicent, C.; Williams, D. J. *J. Am. Chem. Soc.*, **1992**, *114*, 193.
17. Ashton, P. R.; Odell, B.; Reddington, M. V.; Slawin, A. M. Z.; Stoddart, J. F.; Williams, D. J. *Angew. Chem. Int. Ed. Engl.*, **1988**, *27*, 1550.

18. Ashton, P. R.; Goodnow, T. T.; Kaifer, A. E.; Reddington, M. V.; Slawin, A. M. Z.; Spencer, N.; Stoddart, J. F.; Vincent, C.; Williams, D. J. *Angew. Chem. Int. Ed. Engl.* **1989**, *28*, 1396.
19. Ashton, P. R.; Brown, C. L.; Chrystal, E. J. T.; Goodnow, T. T.; Kaifer, A. E.; Parry, K. P.; Slawin, A. M. Z.; Spencer, N.; Stoddart, J. F.; Vincent, C.; Williams, D. J. *Angew. Chem. Int. Ed. Engl.*, **1991**, *30*, 1039.
20. Ashton, P. R.; Brown, C. L.; Chrystal, E. J. T.; Goodnow, T. T.; Kaifer, A. E.; Parry, K. P.; Pietraszkiewicz, M.; Spencer, N.; Stoddart, J. F. *Angew. Chem. Int. Ed. Engl.*, **1991**, *30*, 1042.
21. Ashton, P. R.; Reder, A. S.; Spencer, N.; Stoddart, J. F. *J. Am. Chem. Soc.*, **1993**, *115*, 5286.
22. Lu, T.; Zhang, L.; Gokel, G. W.; Kaifer, A. E. *J. Am. Chem. Soc.*, **1993**, *115*, 2542.
23. Vogtle, F.; Muller, M.; Muller, U.; Bauer, M.; Rissanen, K. *Angew. Chem. Int. Ed. Engl.*, **1993**, *32*, 1295.
24. Gunter, M. J.; Johnston, M. R. *J. Chem. Soc., Chem. Commun.*, **1992**, 1163.
25. Ashton, P. R.; Groguz, M.; Slawin, A. M. Z.; Spencer, N.; Stoddart, J. F.; Williams, D. J. *Tetrahedron Letters*, **1991**, *32*, 6235.
26. Ballardini, R.; Balzani, V.; Gandolphi, M. T.; Prodi, L.; Venturi, M.; Philp, D.; Ricketts, H. G.; Stoddart, J. F. *Angew. Chem., Int. Ed. Engl.*, **1993**, *32*, 1301.
27. (a) Ashton, P. R.; Philp, D.; Spencer, N.; Stoddart, J. F. *J. Chem. Soc., Chem. Commun.*, **1992**, 1124; (b) Ashton, P. R.; Belohradsky, M.; Philp,

- D.; Spencer, N.; Stoddart, J. F. *J. Chem. Soc., Chem. Commun.*, **1993**, 1274.
28. Agam, G.; Gravier, D.; Zilkha, A. *J. Am. Chem. Soc.*, **1976**, *98*, 5206.
29. Agam, G.; Zilkha, A. *J. Am. Chem. Soc.*, **1976**, *98*, 5214.
30. (a). Harada, A.; Kamachi, M. *Macromolecules*, **1990**, *23*, 2821; (b). Harada, H.; Li, J.; Kamachi, M. *Macromolecules*, **1993**, *26*, 5698.
31. (a). Harada, A.; Li, J.; Kamachi, M. *Nature*, **356**, 325 (1992); (b). Harada, A.; Li, J.; Kamachi, M. *Nature*, **1993**, *364*, 516.
32. Harada, A.; Kamachi, M. *J. Chem. Soc., Chem. Commun.*, **1990**, 1322.
33. Harada, A.; Li, J.; Suzuki, S.; Kamachi, M. *Macromolecules*, **1993**, *26*, 5267.
34. Ogata, N.; Sanui, K.; Wada, J. *J. Polym. Sci., Polym. Lett. Ed.*, **1975**, *14*, 459.
35. Maciejewski, M. *J. Macromol. Sci.-Chem.*, **1979**, *A13*, 77.
36. Maciejewski, M.; Gwizdowski, A.; Peczak, P.; Pietrzak, A. *J. Macromol. Sci.-Chem.*, **1979**, *A13*, 87.
37. Lipatova, T. E.; Kosyanchuk, L. F.; Gomza, Y. P.; Shilov, V. V.; Lipatov, Y. S. *Dokl. Akad. Nauk SSSR (Engl. Tr.)*, **1982**, *263*, 140.
38. Wenz, G.; Keller, B. *Angew. Chem. Int. Ed. Engl.*, **1992**, *31*, 197.
39. Born, M.; Ritter, H. *Makromol. Chem., Rapid Commun.* **1991**, *12*, 471.
40. Shen, Y. X.; Xie, D.; Gibson, H. W. *J. Am. Chem. Soc.*, **1994**, *116*, 537.
41. Gibson, H. W.; Marand, H. *Adv. Mater.*, **1993**, *5*, 11.
42. Shen, Y. X.; Engen, P. T.; Berg, M. A. G.; Merola, J. S.; Gibson, H. W. *Macromolecules*, **1992**, *25*, 2786.
43. Gibson, H. W.; Engen, P. T. *New J. Chem.*, **1993**, *17*, 723.

44. Sze, J. Y.; Gibson, H. W. *Polym. Prepr. Am. Chem. Soc. Div. Polym. Chem.*, **1992**, *33(2)*, 331.
45. Goodman, I.; Rhys, J. A. *Polyesters*, Vol. 1, American Elsevier Publishing Company Inc., New York, **1965**, pp 4-20.
46. Mark, H.; Whitby, G. S., eds., *Collected Papers of Wallace Hume Carothers on High Polymeric Substances*, Interscience Publishers, Inc., New York, **1994**.
47. Whinfield, J. R. *Nature (London)*, **1946**, 158, 930.
48. Marchessault, R. H. *CHEMTECH*, **1984**, 542.
49. Kwolek, S. L.; Morgan, P. W.; Schaeffgen, J. R. in *Encyclopedia of Polymer Science and Engineering*, ed. Kroschwitz, J. I., Wiley, New York, **1987**, Vol. 9, pp 1-61.
50. Temin, S. C. in *Encyclopedia of Polymer Science and Engineering*, ed. Kroschwitz, J. I., Wiley, New York, **1985**, Vol. 1, pp 572.
51. Holden, G. in *Encyclopedia of Polymer Science and Engineering*, ed. Kroschwitz, J. I., Wiley, New York, **1985**, Vol. 5, pp 426-429.
52. Morgan, P. W. *Polym. Rev.*, **1965**, 10.
53. Morgan, P. W. in *Encyclopedia of Polymer Science and Engineering*, ed. Kroschwitz, J. I., Wiley, New York, **1984**, Vol. 8, pp 231.
54. (a). Gibson, H. W.; Engen, P. T.; Lecavalier, P. R. *Polym Prepr. Am. Chem. Soc. Div. Polym. Chem.*, **1988**, *29 (1)*, 248; (b). Lecavalier, P. R.; Engen, P. T.; Shen, Y. X.; Joardar, S.; Ward, T. C.; Gibson, H. W. *Polym Prepr. Am. Chem. Soc. Div. Polym. Chem.*, **1989**, *30 (1)*, 189.
55. (a). Wu, C.; Bheda, M. C.; Lim, C.; Shen, Y. X.; Sze, J.; Gibson, H. W. *Polymer Commun.*, **1991**, *32*, 204; (b). Marand, H.; Prasad, A.; Wu, C.;

Bheda, M. C.; Gibson, H. W. *Polym. Prepr. Am. Chem. Soc. Div. Polym. Chem.*, **1991**, *32* (3), 639.



## **CHAPTER III**

### **OBJECTIVES**

The overall objective of my research is to explore and exploit the novel topographic and topological features of polyester rotaxanes. Therefore, I have chosen crown ethers as the macrocycles whose different chemical structure from aliphatic polyesters will result in distinguishing properties of polyrotaxanes compared to the linear macromolecules.

The following objectives relate to synthetic aspects: a) explore the most efficient method to produce polyrotaxanes with high macrocycle content and high molecular weight by comparing the results of transesterification polymerization, the acid chloride method, and interfacial polymerization. b) investigate three methods in terms of constraint of macrocycles onto polymer backbones: not using any blocking groups, using monofunctional blocking groups to end-capped polymer chains, and copolymerizing difunctional blocking groups into polymer chains. Synthesis of polyrotaxanes without blocking groups allows me to learn whether macrocycles can be constrained merely by the entanglement of linear and cyclic species. Questions to be answered related to use of monofunctional blocking groups are end-capping efficiency and influence of monofunctional blocking groups on molecular weight. Finally, the complete constraint of macrocycles can be achieved by synthesizing polyrotaxanes with bulky spacers along polymer backbones. c) study the effects of some variables on the threading. Parameters of interest are the size of the macrocycles, the length of linear species, the molar ratio of macrocycle to linear monomers,

threading time, and temperature. These investigations could lead to mathematical models for the thermodynamics and kinetics of the threading of cyclic species by linear ones.

I wanted to produce polyrotaxanes in sufficient quantity to carry out traditional characterization experiments in solution and bulk solid states in order to: a) address the issue whether polyrotaxanes obey the universal calibration by comparison of the absolute molecular weight determined by gel permeation chromatography (GPC) with a differential viscosity detector with that determined by vapor pressure osmometry (VPO). b) study the influence of macrocycles on the chain stiffness and hydrodynamic volumes by the comparison of the molecular weight determined by VPO with that determined by GPC with polystyrene standards. Viscosities as a function of solvent and temperature also relate to this issue. c) compare the solubility of polyrotaxanes in polar organic solvents with that of linear polymers. d) investigate the special thermal properties of the polyrotaxanes in terms of transition temperatures and stability by differential scanning calorimetry (DSC) and thermogravimetric analysis (TGA).

## **CHAPTER VI**

### **MACROCYCLES: ALIPHATIC CROWN ETHERS**

Macrocycles for the syntheses of polyrotaxanes should meet the following requirements: (1) they are large enough to be threaded by polymer chains; (2) they are chemically different from most commercial polymers such as polyesters, polystyrenes, polyurethanes, polyamides, etc.; (3) they do not possess functional groups that might interfere with the polymerization of monomers; (4) they can coordinate with monomers and/or polymers; (5) their melting points are 30 °C or more below the polymerization temperature so that they are in melt state during the polymerization; (6) they are able to dissolve monomers and are soluble in or miscible with many cosolvents; and (7) they are thermally stable under the reaction conditions.

Cyclodextrins, dibenzo-crown ethers and their analogous macrocycles, and aliphatic crown ethers are three main kinds of macrocycles used in polyrotaxane syntheses [1]. Cyclodextrins, also known as Schardinger dextrins and cycloamyloses, are a family of cyclic oligosaccharides obtained from starch by enzymatic degradation. Cyclodextrins are host molecules which have the ability to form stable complexes with a variety of organic and inorganic guest molecules by inclusion within the hydrophobic cavity. Cyclodextrins have been used as macrocycles for the syntheses of rotaxanes and polyrotaxanes via template method [2-13]. However, cyclodextrins are not suitable for most step growth polymerizations because their hydroxyl groups can interfere with polymerizations.

Dibenzo crown ethers and analogous macrocycles can form 1:1 complexes with paraquat molecules due to electrostatic and charge transfer interactions with the electron rich aromatic ether units in the crown ethers. A variety of rotaxanes and polyrotaxanes were prepared by the complex formations [14-19]. However, use of the dibenzo crown ethers in the statistical threading was not successful presumably because the rapid rotation of p-phenylene rings effectively closed the cavity of the ring, a process called the "saloon door mechanism" [20].

On the other hand, large (>24-membered) aliphatic crown ethers are ideally suited for the syntheses of polyrotaxanes via the statistical threading strategy because they meet all the requirements listed above. These crown ethers have been successfully used as macrocycles in many rotaxane and polyrotaxane syntheses [21].

The syntheses of cyclic polyethers, crown ethers, date from 1967 when Pedesen first reported the preparation of crown ethers, including dibenzo-18-crown-6, 18-crown-6, and other crown ethers [22-25]. The research activities about modification of crown ether macrocycles were stimulated by the fact that crown ethers can form complexes with many inorganic and organic substances [26, 27]. The selectivity of the complexation is determined by the structure of crown ethers such as ring size, nature of heteroatoms as well as aliphatic chains between two heteroatoms, etc.

Crown ethers are usually synthesized via Williamson reactions involving  $S_N2$  nucleophilic substitution reactions. The ring closures are accompanied by the

formation of linear oligomeric or polymeric molecules. In order to maximize the ring formation and minimize the chain production, strategies such as the high dilution principle [28], the cesium effect [29], and the gauche effect [30] are normally utilized. However, not all of these methods are suitable for large scale productions. The high dilution method, for example, is very expensive because it requires large amount of solvents.

There are three approaches for the syntheses of crown ether macrocycles, as depicted by Scheme 1-3:

- a. Single molecular ring closure. This is a self-cyclization process of an oligo(ethylene glycol) with a leaving group at one end.
- b. Two molecule combination. This is the “one plus one” method involving the two nucleophilic substitution reactions of an oligo(ethylene glycol) molecule with an oligo(ethylene glycol) molecule having two end leaving groups.
- c. Four molecule combination involving four replacement reactions of two oligo(ethylene glycol) molecules with two oligo(ethylene glycol) molecules having two end leaving groups.

While a variety of small crown ethers have been synthesized using approaches a and b [27, 31], preparation of large (>27 atoms) crown ethers using these two methods is not easy because it requires preparation of pure oligo(ethylene glycol)s with more than six oxyethylene units. Unfortunately, purification

becomes difficult as the molecular weight of oligo(ethylene glycol) increases. For example, syntheses of 12 to 30 membered aliphatic crown ethers using approach a were reported by Vitali and Masci [32]. They synthesized nona(ethylene glycol) and deca(ethylene glycol) from low molecular weight oligo(ethylene glycol)s. The long chain glycols were purified by vacuum distillation followed by recrystallization in low yields with purity less than 98.5 %. They also prepared crown ethers with ring sizes larger than 36 atoms by the cyclooligomerization of small oligo(ethylene glycol)s in low yields and poor purity.

Chenevert reported the syntheses of large crown ethers by the condensation of one oligo(ethylene glycol) molecule with one oligo(ethylene glycol) ditosylate molecule, that is, using approach b [33]. The yields of the macrocycles were affected by the metal hydrides used. For example, the yields of 27 to 35 membered crown ethers using NaH were higher compared to using KH. This approach, however, is difficult for the preparation of large crowns because it also requires the syntheses of pure oligo(ethylene glycol)s. This method is expensive too since macrocycles were purified by column chromatography.

Approach c, the method of four molecule combination, was developed to synthesize large ( $\geq 27$  membered) crown ethers [34]. Since this method used commercially available low molecular weight oligo(ethylene glycol)s and oligo(ethylene glycol) ditosylates as starting materials, preparations of pure high molecular oligo(ethylene glycol)s were avoided. In the reactions side open chain poly(ethylene glycol)s were also produced and small rings were undoubtedly formed by condensations of 1 equiv of glycol with 1 equiv of ditosylate (approach

b). A simple protocol was developed to isolate and purify the larger crown ethers without expensive chromatographic purification.

## RESULTS AND DISCUSSION

Approach c was adopted to produce 42-60 membered crown ethers. In a typical reaction, two oligo(ethylene glycol) molecules were allowed to react with two oligo(ethylene glycol) ditosylate molecules to form a large crown ether. Therefore, the preparation and purification of high molecular weight oligo(ethylene glycol)s were not necessary.

### I. Hexa(ethylene glycol)

While commercially available and cheap glycols containing up to four ethyleneoxy units were used as starting materials to prepare rings comprised of up to 48 atoms, synthesis of 60-crown-20 required use of hexa(ethylene glycol) which is readily available but expensive. However, it can be synthesized from cheap tetra(ethylene glycol) and can be easily purified by vacuum distillation.

Okahara et al. synthesized hexa(ethylene glycol) by a Williamson-type condensation reaction of tri(ethylene glycol) with tri(ethylene glycol) monotosylate [35]. Tri(ethylene glycol) monotosylate was produced *in situ* by the reaction of tri(ethylene glycol) with tosyl chloride. However, the actual yield was very low (10-33 %) [34].

Hexa(ethylene glycol) can also be prepared by the conversion of tetra(ethylene glycol) to tetra(ethylene glycol) dichloride followed by the reaction of the dichloride with ethylene glycolate [23]. the yield of this method is also low (25-35 %).

A new method for the synthesis of hexa(ethylene glycol) was reported by Bartsch and coworkers in 1989 (Scheme 4) [36]. We adopted this method because of its high reported yield (80 %). In the reaction, an excess of 2-tetrahydropyranyl protected 2-chloroethanol was mixed with tetra(ethylene glycol). This organic phase was stirred with 50 % aqueous sodium hydroxide at 65 °C for 3 days. Tetrabutylammonium hydrogen sulfate was used as a phase transfer catalyst. After the reaction, unreacted THP protected chloroethanol was removed by vacuum distillation. The product was then deprotected by HCl and hexa(ethylene glycol) was purified by vacuum distillation (52 %).

The structure of hexa(ethylene glycol) was supported by its boiling point, FTIR spectrum and <sup>1</sup>H NMR spectrum. The boiling point was similar to the reported value (37). It was higher than the starting material tetra(ethylene glycol) due to its higher molecular weight. The FTIR spectrum (Figure 1) showed a strong signal for the aliphatic C-O-C stretch at 1112 cm<sup>-1</sup>. The absence of C-Cl stretch signals indicated the total removal of ethylene glycol monochloride. Methylene protons α to hydroxyl groups in the <sup>1</sup>H NMR spectrum (Figure 2) appeared at 3.77 δ; the 16 middle methylene protons occurred at 3.66 δ as a singlet; signals



of the four methylene protons  $\beta$  to hydroxyl groups appeared at 3.60  $\delta$  as a triplet; and the OH protons showed a triplet at 3.47  $\delta$ .

## II. Oligo(ethylene glycol) Ditosylates

Oligo(ethylene glycol) ditosylates were prepared by the reaction of oligo(ethylene glycol)s with *p*-toluenesulfonyl chloride in tetrahydrofuran (THF) at 0°C, using sodium hydroxide as a base (Scheme 5). Ouchi et al. reported the preparation of oligo(ethylene glycol) ditosylates using this method in a 2 h reaction [38]. However, our studies showed that longer reaction time (> 10 h) was needed to complete the reaction [34]. Under these conditions oligo(ethylene glycol) ditosylates were obtained in yields of over 90 %. The nature of the ditosylates depends on the mass percent of benzene ring with respect to the ethyleneoxy units. Tetra(ethylene glycol) ditosylate is an oil. It was purified by extractions and washings to remove salts and unreacted starting materials. Tri(ethylene glycol) ditosylate is a crystalline solid and was easily purified by recrystallizations.

All the oligo(ethylene glycol) ditosylates synthesized gave satisfactory characterization results. In case of tri(ethylene glycol) ditosylate, for example, the melting point matched the reported value [38]. The FTIR spectrum showed the C-H stretch of the methyl group at 2960  $\text{cm}^{-1}$ ; the  $\text{SO}_2$  antisymmetric stretch at 1344  $\text{cm}^{-1}$  and the  $\text{SO}_2$  symmetric stretch at 1176  $\text{cm}^{-1}$ ; the C-H out-of-plane deformation of *para*-disubstituted benzene at 829  $\text{cm}^{-1}$ . No hydroxyl signals were observed. The six methyl protons in the  $^1\text{H}$  NMR spectrum (Figure 3) appeared at 2.44  $\delta$  as a singlet; the four middle methylene protons appeared at

3.52  $\delta$  as a singlet; the four methylene protons  $\beta$  to tosylate units occurred at 3.65  $\delta$  as a triplet; the four methylene protons  $\alpha$  to tosylate units appeared as a triplet at 4.13  $\delta$ ; and the eight aromatic protons occurred at 7.34 and 7.78  $\delta$  as two doublets. Tetra(ethylene glycol) ditosylate also showed satisfactory  $^1\text{H}$  NMR spectral data (Figure 4).

### III. Syntheses of Crown Ethers

Large aliphatic crown ethers with 30-60 membered sized were synthesized on a large scale by the reaction of oligo(ethylene glycol)s with oligo(ethylene glycol) ditosylates in THF, using NaH as a base, at modest (0.67 M) dilution (Scheme 6). Two crown ethers were generated from each reaction. A small crown (**3**) was formed by the reaction of one oligo(ethylene glycol) molecule with one oligo(ethylene glycol) ditosylate molecule involving two  $\text{S}_{\text{N}}2$  processes. A large crown ether (**4**) was obtained by the reaction of 2 oligo(ethylene glycol) molecules with 2 oligo(ethylene glycol) ditosylate molecules involving four  $\text{S}_{\text{N}}2$  reactions.

Several reactions competed with each other in the syntheses of crown ethers such as formation of linear diols and ditosylates; formation of small rings; and formation of large crowns. In order to increase the yields of large crown ethers, some variables were studied:

## A. Length of Starting Materials

It was found that use of short ditosylates and long glycols favored large ring formations. Alternate arrangement using short glycols and long ditosylates decreased yields of large crown ethers [34]. This phenomenon was also observed by Ouchi et al. [38].

## B. Temperature

The relative yields of the two crown ethers were affected by temperature. Lower temperature favored the formation of small crowns. This is probably due to the shorter end-to-end distance and resultant higher collision probability. On the other hand, higher temperature favored the formation of large rings. For example, the yield of 42-crown-14 (**4**,  $a + b = 7$ ) was 22 % at 25 °C [34] and was 48 % at 67 °C.

## C. Synthetic Procedures

Three synthetic procedures were employed. In procedure A (Scheme 7) the dialkoxide was prepared by the reaction of the oligo(ethylene glycol) with excess NaH. After the system had been diluted the oligo(ethylene glycol) ditosylate was added dropwise. Because of its dilute condition during the addition of the ditosylate, this method favored the formation of macrocycles with respect to the competitive formation of linear species. Small crown ethers, however, were formed in a relatively large amount in this method.

In procedure B (Scheme 8) the oligo(ethylene glycol) reacted with an excess of NaH to form the dialkoxide followed by the slow addition of 0.5 equiv of the oligo(ethylene glycol) ditosylate to form a long chain dialkoxide *in situ*. After several hours of reaction the solution was diluted and another 0.5 equiv of the oligo(ethylene glycol) ditosylate was added [34]. This method helped the assembly of the two diol molecules and two ditosylate molecules to give a large macrocycle. However, linear chains were easily formed due to the concentrated condition during the addition of the first half of the ditosylate.

In procedure C (Scheme 9) the monoalkoxide was prepared *in situ* by the reaction of the oligo(ethylene glycol) with 0.6 equiv of NaH followed by the slow addition of 0.5 equiv of oligo(ethylene glycol) ditosylate to form a long chain diol. Because of the monodeprotonation of the oligo(ethylene glycol) molecules, the amount of linear poly(ethylene glycol) generated was presumably reduced. The diol was then treated with an excess of NaH to form a dialkoxide. The solution was then highly diluted and another 0.5 equiv of ditosylate was added. This procedure combined the advantages of procedure A and B. Therefore, it gave the highest yields of large macrocycles as shown in Table 1.

#### IV. Purification of crown ethers

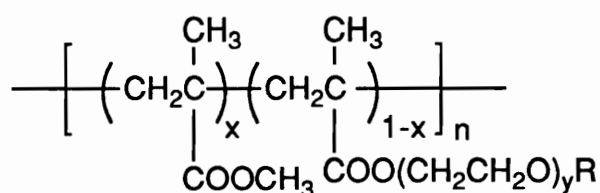
The isolation and purification of crown ethers are very difficult because the crude products are mixtures of rings with different sizes, chains with different lengths, and catenanes. In the  $^1\text{H}$  NMR spectrum of crude 42-crown-14 using dry  $\text{DMSO-}d_6$  as a solvent the hydroxyl groups of oligo(ethylene glycol)s showed a triplet at

4.57  $\delta$  [39] as shown in Figure 5. In the  $^1\text{H}$  NMR spectrum of crude 42-crown-14 using  $\text{CDCl}_3$  as a solvent (Figure 6) vinyl ether end groups in linear species gave three signals (doublets of doublets) at 3.97, 4.18, and 6.50  $\delta$  [40]. The vinyl ethers were generated by E2 elimination from the tosylates. Figure 6 also shows impurity signals at ca. 3.70 and 3.85  $\delta$ .

The linear glycols must be removed because they upset the stoichiometry of polymerization in polyrotaxane syntheses. However, these impurities can not be removed by vacuum distillation because crown ethers decompose at the distillation temperature of the diols. Column chromatography is also not practical not only because it is expensive but also because the polarities of the cyclic and linear poly(ethylene oxide) are so close.

An alternative purification procedure was employed to isolate and purify the crown ethers. Crude products were first filtered through short silica gel columns. The products were then treated with poly(methacryloyl chloride). The glycols were removed by their reaction with poly(methacryloyl chloride). After the reaction the solution was precipitated into methanol which is a good solvent for crown ethers but a non-solvent for poly(methacryloyl chloride). The glycols and methanol reacted with poly(methacryloyl chloride). In order to get good precipitation of the resultant polyester **5** from methanol the polymer should be high molecular weight and low mass percent of poly(ethylene glycol) ester segments (low 1-x). Hydrolysis of acid chloride groups of poly(methacryloyl chloride) also has an impact on its precipitation. Therefore, the methacryloyl chloride monomer was vacuum distilled. The solvents for the polymerization and

the reaction of the polymer with crude crown ethers were carefully dried. A large excess of the polymer (polymer : crown ether = 2 : 1 in grams) was used to reduce the 1-x value in the resultant polymer **5**. Freshly prepared poly(methacryloyl chloride) was used immediately after the polymerization to avoid the hydrolysis of acid chloride groups. After the polymer **5** had been removed, the crown ether was filtered again through a short silica gel column. The open chain impurities were totally removed by this method.



**5**

The next problem was to isolate large crown ethers (**4**) from the small crown ethers (**3**). For the pair of 42-crown-14 (**4**, a + b = 7) and 21-crown-7 (**3**, a + b = 7) 42-crown-14 was easily separated from 21-crown-7 by crystallization from acetone because the large crown was a crystalline solid while small crown was an oil. The pair 48-crown-16 (**4**, a + b = 8) and 24-crown-8 (**3**, a + b = 8) was also separated by crystallization from acetone in the same way. However, 60-crown-20 (**4**, a + b = 10) can not be easily separated from 30-crown-10 (**3**, a + b = 10) generated in the same reaction by crystallization from acetone because both crowns are crystalline solids. Fortunately, 30-crown-10 is soluble in hot hexane while 60-crown-20 is not. Thus, the mixture was extracted with hot hexane to remove 30-crown-10. 60-crown-20 was then further purified by the crystallization from acetone.

The improved purification protocol enabled us to obtain very pure crown ethers. As shown in Table 2 melting points of crown ethers are up to 26 °C higher than any previously reported. All the purified crown ethers showed a single peak in the  $^1\text{H}$  NMR spectra. After the purification the hydroxyl signals at 4.57  $\delta$  in 42-crown-14 in  $\text{DMSO-d}_6$  solution disappeared (Figure 7). There were no vinyl ether signals at 3.97, 4.18, and 6.50  $\delta$  or other impurity signals in  $\text{CDCl}_3$ , as shown in Figure 8.

The high purity of the crown ethers was also demonstrated by DSC measurements. Figure 9 is the DSC trace of 42-crown-14 purified by simple recrystallization. The shoulder on the melting peak demonstrated the existence of impurities. After purification using the improved method the 42-crown-14 sample showed a single symmetric melting peak in its DSC diagram (Figure 10).

## CONCLUSIONS

Large aliphatic crown ethers have been synthesized in large scales from low molecular weight oligo(ethylene glycol)s and oligo(ethylene glycol) ditosylates by the reaction of two glycol molecules with two glycol ditosylate molecules. The starting materials were commercially available or preparable in good yields from the inexpensive lower homologs. This method avoids the use of high molecular weight oligo(ethylene glycol)s which are difficult to purify by conventional purification methods. The large macrocycles were obtained in high yields if short ditosylates and long glycol were used. High reaction temperature favors formation of large crown ethers. A multiple step procedure involving preparation of monoalkoxide and then the long chain glycol in situ was developed. Using this method large crown ethers were obtained in yields up to 55 %.

The crown ethers were isolated and purified by a new purification method involving treatment of the crude products with poly(methacryloyl chloride), extraction, crystallization, and filtration. The purities of crown ethers were judged by the melting point measurements, NMR and DSC analyses.



## EXPERIMENTAL

**General.** Melting points were taken in capillary tubes and have been corrected. TGA data were obtained using DuPont TGA 951 and Perkin-Elmer TGA-7 instruments at a scan rate of 10 °C/min. DSC data were obtained using DuPont DSC 912 and Perkin-Elmer DSC-2 instruments at a scan rate of 10 °C/min. Proton and carbon NMR spectra were obtained on a Varian 400-MHz spectrometer using deuterated chloroform solutions with tetramethylsilane as an internal standard, unless otherwise noted; chemical shifts are in ppm. FTIR spectra, reported in  $\text{cm}^{-1}$ , were obtained on a Nicolet MX-1 instrument using KBr pellets unless otherwise noted. Elemental analyses were provided by Atlantic Microlab, Inc., Norcross, GA; samples were vacuum dried above the melting point for at least 18 h and protected from the atmosphere.

Ethylene glycol (99 %), di(ethylene glycol) (99 %), tri(ethylene glycol) (99 %), tetra(ethylene glycol) (99 %), tri(ethylene glycol) dichloride (99 %), were purchased and used without further purification. Sodium hydride (60 %) in mineral oil was purchased and washed with n-hexane before use. p-Toluene-sulfonyl chloride (98 %) was purchased and recrystallized from n-hexane. Tetrahydrofuran was distilled from Na/benzophenone and used immediately.

### THP protected 2-chloroethanol

3,4-Dihydro-2 H-pyran (381.6 g, 4.54 mol) was added to a 4 L beaker cooled in an ice bath and stirred with a magnetic stirring. After the liquid in the beaker was

cooled to 5 °C, 2-chloroethanol (356.2 g, 4.42 mol) and concentrated HCl (7 drops) were added. The mixture was stirred in the ice bath for 3.25 h. at room temperature. The product was then distilled at 43 °C under a vacuum of 0.35 mmHg (reported:  $63 \pm 2$  °C/1-2 mmHg [24]). A pure liquid (611.8 g, 84 %) was obtained. FTIR: 2945, 2873, 1456, 1142, 1133, 1126, 1080, 974, 968, 816, 756, 665.

### **Hexa(ethylene glycol)**

Tetra(ethylene glycol) (180.7g, 0.92 mol), THP protected chloroethanol (611.8 g, 3.72 mol), and tetrabutylammonium hydrogen sulfate ( 18.9 g, 54.0 mmol) were mixed at room temperature in a 5 L, 3-necked flask equipped with a condenser, and a mechanical stirrer. Aqueous NaOH solution (50%, 1 L, 19.3 mol) was then added dropwise to this mixture. The mixture became semisolid upon the addition of the basic solution. Water (100 mL) was then added to dissolve the semisolid. After it had been heated to 60 °C and stirred for 6.5 days, the mixture was cooled to room temperature. The solid salt was filtered and discarded after it had been washed with methylene chloride (200 mL). The aqueous phase was separated from the organic phase (agout 700 mL) with a separation funnel. The aqueous phase was then concentrated by rotary evaporation. Some solid (approximately 600 g) precipitated out when the concentrated aqueous phase was cooled to room temperature. The solid was removed by filtration and discarded after it had been washed with methylene chloride ( 3 x 120 mL). A yellow oil was obtained from the combined methylene chloride phase after rotary evaporation. The oil was then added to organic phase. THP protected 2-chloroethanol (174 mL) was

distilled out of the organic phase under a vacuum of 1.8 mm Hg at 45-49° C. A mixture of methanol and methylene chloride (1:1, 1.2 L) was then added, followed by addition of concentrated HCl (55 mL) to deprotect the hexa(ethylene glycol). The solution was then neutralized by sodium bicarbonate. After the solid was filtered and washed with methylene chloride, the solvent was removed by rotary evaporator. The salt was filtered and washed with methylene chloride. All methylene chloride washes were combined with the organic phase. After complete removal of the solvent, crude pale yellow hexa(ethylene glycol) was distilled under a vacuum of 0.005 mm Hg at 183-204 °C. The pale yellow product was then vacuum distilled again at 192-200 °C/0.07 Torr (Lit. [41] 216 °C/1-2 Torr). A colorless transparent product (135.2 g, 52 %) was obtained. IR: 3354, 2879, 1455, 1356, 1244, 1112, 941, 882. <sup>1</sup>H NMR: 3.72 (m, 4 H, -CH<sub>2</sub>OH), 3.67 (s, 16 H, CH<sub>2</sub>), 3.62 (t, J = 4.5 Hz, -CH<sub>2</sub>CH<sub>2</sub>OH), 3.10 (br s, 2H, -OH).

### **Tri(ethylene glycol) Ditosylate**

To a 5-L, 3-necked flask, NaOH (64.0 g, 1.60 mol) and water (600 mL) were added. The flask was placed in an ice bath. Tri(ethylene glycol) (80.1 g, 0.533 mol) in THF (200 mL) was added and the mixture was mechanically stirred for 30 min. Tosyl chloride (254 g, 1.33 mol) in THF (600 mL) was added dropwise. The mixture was stirred for 48 hours. After the reaction, the two phases were separated with a separation funnel. The residual product left in the water phase was extracted with methylene chloride (2 x 300 mL). All the organic phases were combined and rotary evaporated down to a white solid which was recrystallized two times in acetone. White crystals (176 g, 92 %), mp 79.5-80.7 °C (Lit. [38])

80.5-81.5), were obtained. IR: no -OH peak.  $^1\text{H}$  NMR: 2.44 (s, 6 H, -CH<sub>3</sub>), 3.52 (s, 4H, -OCH<sub>2</sub>CH<sub>2</sub>O-), 3.65 (t, J = 4.7 Hz, 4H, -CH<sub>2</sub>CH<sub>2</sub>OTs), 4.14 (t, J = 4.7 Hz, CH<sub>2</sub>OTs), 7.34 (d, J = 8.2 Hz, 4H, arom.), 7.78 (d, J = 8.2 Hz, 4H, arom.).

### **Tetra(ethylene glycol) ditosylate**

To a 5-L, 3-necked flask, NaOH (213 g, 5.32 mol) and water (1 L) were added. The flask was placed in an ice bath. Tetra(ethylene glycol) (314 g, 1.60 mol) in THF (800 mL) was added and the mixture was mechanically stirred for 30 min. Tosyl chloride (700 g, 3.60 mol) in THF (1 L) was added dropwise. The mixture was stirred for 48 hours. After the reaction the crude product was poured into 10% HCl (1500 mL) at 0 °C. The solution was then extracted with toluene (3 x 1500 mL). The combined organic phase was washed with water (2 x 3 L), dilute aqueous K<sub>2</sub>CO<sub>3</sub> solution (0.5 wt %, 1.3 L), and then water (2 L) and dried over Na<sub>2</sub>SO<sub>4</sub>. After removal of all the solvents by rotary evaporation the pale yellow oil was extracted with hot hexane to remove excess tosyl chloride. The product (780 g, 97 %) was obtained. IR: no hydroxyl peaks.  $^1\text{H}$  NMR: 2.45 (s, 6 H, -CH<sub>3</sub>), 3.55 (m, 8 H, -OCH<sub>2</sub>CH<sub>2</sub>OCH<sub>2</sub>CH<sub>2</sub>O-), 3.68 (t, J = 4.7 Hz, 4H, TsOCH<sub>2</sub>CH<sub>2</sub>-), 4.15 (t, J = 4.7 Hz, 4 H, TsOCH<sub>2</sub>-), 7.35 (d, J = 8.2 Hz, 4H, arom.), 7.80 (d, J = 8.2 Hz, 4H, arom.).

**Poly(methacryloyl chloride) (6).** In a 250 mL one-necked flask equipped with a condenser, nitrogen inlet, and magnetic stirrer were dissolved distilled methacryloyl chloride (30.0 g, 0.287 mol) and azobis(isobutyronitrile) (AIBN), 0.47 g, 2.87 mmol, in dried (Na) toluene (100 mL). The solution was stirred at 90

°C under nitrogen for 20 h. After the solution had been cooled to room temperature, it was precipitated into dried (4 A molecular sieves) n-hexane (1 L). The polymer (18.9, 63 %) was filtered and then was transferred into the flask to purify crude crown ethers.

### **Crown Ethers, Procedure A**

#### **42-Crown-14 (4, a + b = 7) and 21-crown-7 (3, a + b = 7)**

NaH (60 %, 40.0 g, 1.00 mol) was washed with n-hexane (2 x 60 mL) and transferred into a 5-L 3-necked flask with dry THF (500 mL) under nitrogen. Tetra(ethylene glycol) (63.5g, 0.327 mol) in THF (500 mL) was added slowly and the mixture was mechanically stirred for 2 hours. Tri(ethylene glycol) ditosylate (144.7 g, 0.316 mol) in THF (2 L) was added dropwise. The system was further diluted to a total volume of 4 L. The mixture was refluxed for 48 hours. Water (10 mL) was added to destroy the unreacted NaH. Bubbles were observed upon the addition of water. The precipitates were filtered and discarded and THF was removed by rotary evaporation. A reddish-purple oil (100 g) was obtained which solidified in 30 min. The solid was recrystallized in acetone 3 times. A white crystalline solid (47.1 g, 48 %) was obtained, mp 54.7-55.4 °C (Lit. [33] 28.5-31.0 °C). IR : 2898, 1470, 1363, 1343, 1284, 1244, 1111, 965, 839, 666. <sup>1</sup>H NMR: 3.647 (s).

21-crown-7 was not isolated from the mother liquor.

### **Purification Using Poly(methacryloyl chloride): 42C14**

To a 500 mL three-necked flask equipped with nitrogen inlet, a condenser, and magnetic stirrer were added 42C14, mp 52.5-54.9 °C (recrystallized from acetone 3x, 25.0 g, 40.5 mmol), freshly prepared poly(methacryloyl chloride) (50.0 g, 479 mmol of acid chloride), pyridine (1.5 mL, 18.5 mmol), and freshly distilled, dry THF (250 mL). The mixture was stirred at room temperature for 20 h and precipitated into methanol (500 mL). The precipitated polymer was removed by filtration. A yellow oil was obtained after all the solvents had been removed by rotary evaporation. The product was dissolved in CH<sub>2</sub>Cl<sub>2</sub> (500 mL), was passed through a short silica column (1 x 3.1 cm), and was recrystallized in acetone. A colorless solid (20.64 g, recovery 83 %), mp 54.9-57.4 °C (Lit. [33] 28.5-31.0 °C), was obtained after vacuum drying. IR: same as 42C14 (above). <sup>1</sup>H NMR: 3.647 (s). Anal. Calcd for C<sub>28</sub>H<sub>56</sub>O<sub>14</sub>: C, 54.53; H, 9.15. Found: C, 54.36; H, 9.10. Calcd for C<sub>28</sub>H<sub>58</sub>O<sub>15</sub> [H(OCH<sub>2</sub>CH<sub>2</sub>)<sub>14</sub>OH]: C, 52.98; H, 9.21.

### **60-crown-20 (4, a + b = 10) and 30-crown-10 (3, a + b = 10)**

Dry THF ( 2.5 L), and NaH (80%, 45.9 g, 1.53 mol) which was washed with hexane ( 3 x 25 mL) were added under nitrogen to a 5 L, 3 necked flask equipped with a condenser, and a mechanical stirrer. After the suspension was stirred for 20 min., hexa(ethylene glycol) (84.7 g, 0.3 mol) was added dropwise for 2 h. A lot of grey salt formed upon the addition of hexa(ethylene glycol). After the system had been heated to reflux and diluted to approximately 3.5 L, tetra(ethylene glycol) ditosylate (154.8 g, 0.308 mol) in THF (500 mL) was added

dropwise over a period of 16 h. The solution in the flask turned brown upon the addition of the ditosylate. The reaction mixture was then stirred under reflux for 48 h. After the system had been cooled to room temperature, water (100 mL) was added to destroy excess NaH. The salt was filtered and discarded. A brown oil (133 g) was obtained after the removal of THF by rotary evaporation. The proton NMR spectrum of the crude product indicated three compounds, namely 30C10 ( $\delta = 3.67$ ), 60C20 ( $\delta = 3.64$ ), and a very small amount of presumed catenane ( $\delta = 3.65$ ). 30C10 was separated from the mixture by washing the mixture with hot hexane (7 x 200 mL). Powdery 60C20 (15.5 g, 12 %) was obtained after recrystallizations from acetone at 0 °C, mp 56.2-56.6 °C (Lit. [33] 46.0-50.5). IR: same as 42C14 (above).  $^1\text{H}$  NMR: 3.646 (s).  $^{13}\text{C}$  NMR: 70.67.

The 30C10 fraction was purified by recrystallization from hexane at 4 °C, affording white crystals (14.3 g, 12 %), mp 46.3-48.1 °C ( Lit. [32] 35.5-36.8 °C). IR: same as 42C14.  $^1\text{H}$  NMR: 3.671 (s).

## Procedure C

### 48-Crown-16 (4, a + b = 8)

NaH (60%, 2.40 g, 0.060 mol) was washed with n-hexane (2 x 25 mL) and transferred into a 1-L 3-necked flask with fresh THF (80 mL) under nitrogen. Tetra(ethylene glycol) (9.71 g, 0.050 mol) in THF (40 mL) was added while the solution was mechanically stirred, bubbles were observed. After the mixture was refluxed for 0.5 h, tetra(ethylene glycol) ditosylate (12.56 g, 0.025 mol) in THF

(40 mL) was added dropwise over a period of 15 min. The mixture was refluxed for 2 h. After the system had been cooled down to room temperature, NaH (60%, 5.60 g, 0.14 mol) washed with n-hexane (2 x 40 mL) in THF (40 mL) was added. The mixture was refluxed for 0.5 h. The system was then diluted to 800 mL with THF. Tetra(ethylene glycol) ditosylate (12.57 g, 0.025 mol) in THF (50 mL) was added dropwise and the mixture was refluxed for 12 h. Water (25 mL) was added to destroy the unreacted NaH. Bubbles were observed upon the addition of water. The precipitates were removed by filtration. A reddish oil (14.6 g) was obtained after THF had been removed by the rotary evaporation. The product was recrystallized in acetone two times. A brown solid (7.06 g, 40%) was obtained, mp 52.5-53.9 °C (Lit. [32] 49.5-50.5 °C); <sup>1</sup>H NMR : 3.646 (s).

#### **42-Crown-14 (a + b = 7)**

NaH (60%, 12.0 g, 0.30 mol) was washed with n-hexane (2 x 50 mL) and transferred into a 5 L 3-necked flask with fresh THF (400 mL) under nitrogen. Tetra(ethylene glycol) (49.05 g, 0.250 mol) in THF (200 mL) was added while the solution was mechanically stirred, bubbles were observed. After the mixture was refluxed for 0.5 h, tri(ethylene glycol) ditosylate (57.95 g, 0.1250 mol) in THF (200 mL) was added dropwise over 15 min. The mixture was refluxed for 2 h. After the system had been cooled down to room temperature, TLC showed that no ditosylate was left. NaH [60%, 24.0 g, 0.60 mol, washed with n-hexane (2 x 50 mL)] in THF (200 mL) was added. The mixture was refluxed for 0.5 h. The system was then diluted to 3.6 L with THF. Tri(ethylene glycol) ditosylate (57.95 g, 0.1250 mol) in THF (400 mL) was added dropwise over 23 h. and the mixture



was refluxed for 17 h. Water (5 mL) was added to destroy the unreacted NaH. Bubbles were observed upon the addition of water. The precipitates were removed by filtration. A yellow oil was obtained after THF had been removed by rotary evaporation. After recrystallization in acetone four times, a white solid (42.6 g, 55.2 %) was obtained.

## REFERENCES

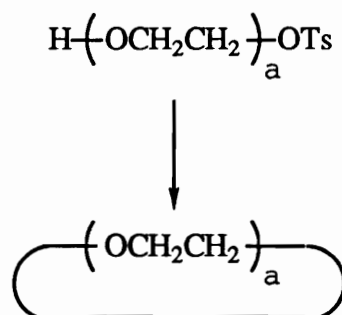
1. Gibson, H. W.; Bheda, C. M.; Engen, P. T. *Prog in Polym Sci.* **1994**, *79*, 843.
2. (a). Ogino, H. *J. Am. Chem. Soc.*, **1981**, *103*, 1303; (b). Ogino, H.; Ohata, K. *Inorg. Chem.*, **1984**, *23*, 3312; (c). Ogino, H. *New J. Chem.*, **1993**, *17*, 683.
3. Wylie, R.; Macartney, D. J. *Am. Chem. Soc.*, **1992**, *114*, 3136.
4. (a). Wenz, G.; Bey, E.; Schmidt, L. *Angew. Chem. Int. Ed. Engl.*, **1992**, *31*, 783; (b). Wenz, G.; Wolf, F.; Wagner, M.; Kubik, S. *New J. Chem.*, **1993**, *17*, 729.
5. (a). Harada, A.; Kamachi, M. *Macromolecules*, **1990**, *23*, 2821; (b). Harada, H.; Li, J.; Kamachi, M. *Macromolecules*, **1993**, *26*, 5698.
6. (a). Harada, A.; Li, J.; Kamachi, M. *Nature*, **356**, 325 (1992); (b). Harada, A.; Li, J.; Kamachi, M. *Nature*, **1993**, *364*, 516.
7. Harada, A.; Kamachi, M. *J. Chem. Soc., Chem. Commun.*, **1990**, 1322.
8. Harada, A.; Li, J.; Suzuki, S.; Kamachi, M. *Macromolecules*, **1993**, *26*, 5267.
9. Ogata, N.; Sanui, K.; Wada, J. *J. Polym. Sci., Polym. Lett. Ed.*, **1975**, *14*, 459.
10. Maciejewski, M. *J. Macromol. Sci.-Chem.*, **1979**, *A13*, 77.
11. Maciejewski, M.; Gwizdowski, A.; Peczak, P.; Pietrzak, A. *J. Macromol. Sci.-Chem.*, **1979**, *A13*, 87.
12. Wenz, G.; Keller, B. *Angew. Chem. Int. Ed. Engl.*, **1992**, *31*, 197.
13. Born, M.; Ritter, H. *Makromol. Chem., Rapid Commun.* **1991**, *12*, 471.

14. (a). Allwood, B. L.; Spencer, N.; Shahriari-Zavareh, H.; Stoddart, J. F.; Williams, D. J. *J. Chem. Soc., Chem. Commun.*, **1987**, 1058; (b). Allwood, B. L.; Spencer, N.; Shahriari-Zavareh, H.; Stoddart, J. F.; Williams, D. J. *J. Chem. Soc., Chem. Commun.*, **1987**, 1064; (c). Ashton, P. R.; Slawin, A. M. Z.; Spencer, N.; Stoddart, J. F. and Williams, D. J. *J. Chem. Soc., Chem. Commun.*, **1987**, 1066; (d). Allwood, B. L.; Spencer, N.; Shahriari-Zavareh, H.; Stoddart, J. F.; Williams, D. J. *J. Chem. Soc., Chem. Commun.*, **1987**, 1061; (e). Ortholand, J. -Y.; Slawin, A. M. Z.; Spencer, W.; Stoddart, J. F.; Williams, D. J. *Angew. Chem. Int. Ed. Engl.*, **1989**, *28*, 1394; (f). Anelli, P.-L.; Ashton, P. R.; Ballardini, R.; Balzani, V.; Delgado, M.; Gandolphi, M. T.; Goodnow, T. T.; Kaifer, A. E.; Philp, D.; Pietraszkiewicz, M.; Prodi, L.; Reddington M. V.; Slawin, A. M. Z.; Spencer, N.; Stoddart, J. F.; Vicent, C.; Williams, D. J. *J. Am. Chem. Soc.*, **1992**, *114*, 193.
15. Ashton, P. R.; Grognoz, M.; Slawin, A. M. Z.; Spencer, N.; Stoddart, J. F.; Williams, D. J. *Tetrahedron Letters*, **1991**, *32*, 6235.
16. Ballardini, R.; Balzani, V.; Gandolphi, M. T.; Prodi, L.; Venturi, M.; Philp D.; Ricketts, H. G.; Stoddart, J. F. *Angew. Chem., Int. Ed. Engl.*, **1993**, *32*, 1301.
17. (a). Ashton, P. R.; Philp, D.; Spencer, N.; Stoddart, J. F. *J. Chem. Soc., Chem. Commun.*, **1992**, 1124; (b). Ashton, P. R.; Belohradsky, M.; Philp, D.; Spencer, N.; Stoddart, J. F. *J. Chem. Soc., Chem. Commun.*, **1993**, 1274.
18. Agam, G.; Gravier, D.; Zilkha, A. *J. Am. Chem. Soc.*, **1976**, *98*, 5206.
19. Agam, G.; Zilkha, A. *J. Am. Chem. Soc.*, **1976**, *98*, 5214.

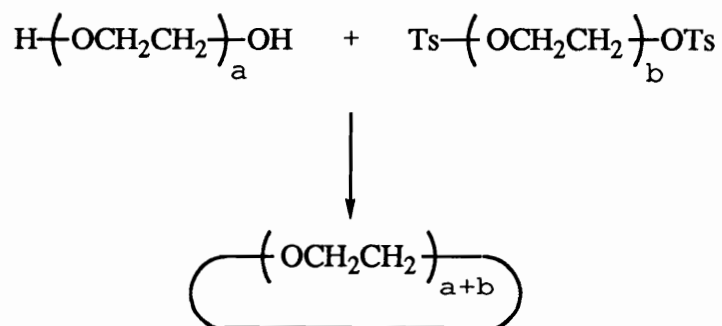
20. Gibson, H. W.; Liu, S.; Lecavalier, P.; Wu, C.; Shen, Y. X. *J Am. Chem. Soc.*, **1995**, *117*, in press.
21. Wu, C.; Bheda, M., Lim, C.; Shen, Y. X.; Sze, J.; Gibson, H. W. *Polym. Commun.* **1991**, *32*, 204. Gibson H. W.; Bheda, M.; Engen, P. T.; Shen, Y. X.; Sze, J.; Wu, C.; Joardar, S.; Ward, T. C.; Lecavalier, P. R. *Makromol Chem., Macromol Symp.* **1991**, *42/43*, 395. Wu, C.; Lecavalier, P. R; Shen, Y. X.; Gibson, H. W. *Chem. Materials* **1991**, *3*, 569. Gibson, H.W.; Engen, P. T.; Shen, Y. X.; Sze, J.; Lim, C.; Bheda, M.; Wu, C. *Makromol Chem., Macromol Symp.* **1992**, *54/55*, 519. Shen, Y. X.; Gibson, H. W. *Macromolecules* **1992**, *25*, 2058. Shen, Y. X.; Engen P. T.; Berg, M. A. G.; Merola, J. S.; Gibson, H. W. *Macromolecules*, **1992**, *25*, 2786. Delaviz, Y.; Gibson, H. W. *Macromolecules* **1992**, *25*, 18. Delaviz, Y.; Gibson, H. W. *Macromolecules* **1992**, *25*, 4859. Sze, J. Y.; Gibson, H. W. *Polymer Prepr. Am. Chem., Soc. Div. Polym. Chem.* **1992**, *33* (2), 331. Gibson, H. W.; Marand, H. *Adv. Mater.* **1993**, *5*, 11. Gibson, H. W.; Engen, P. T. *New J. Chem.* **1993**, *17*, 723. Shen, Y. X.; Xie, D.; Gibson, H. W. *J. Am. Chem. Soc.* **1994**, *116*, 537.
22. Pedersen, C. J. *J. Am. Chem. Soc.* **1967**, *89*, 2495.
23. Pedersen, C. J. *J. Am. Chem. Soc.* **1967**, *89*, 7017.
24. Pedersen, C. J. *Org. Synth.* **1972**, *52*, 66.
25. Pedersen, C. J. *J. Am. Chem. Soc.* **1970**, *92*, 391.
26. *Crown Ethers and Analogues*; Patai, S., Rappoport, Z., Eds.; Wiley: New York, **1989**. *Crown Ethers and Analogous Compounds*; Hiraoka, M., Ed.; Elsevier: New York, **1992**. *Macrocyclic Chemistry*; Dietrich, B., Viout, P., Lehn, J. M., Eds.; VCH Publishers: New York, **1993**.

27. Franke, J.; Vögtle, F. *Top Curr. Chem.* **1986**, *132*, 135. Diederich, F. *Angew. Chem., Int. Ed. Engl.* **1988**, *27*, 363. *Cation Binding by Macrocycles*; Inoue, Y. L, Gokel, G. W., Eds.; Wiley: New York, **1990**. Izatt, R. M.; Bradshaw, J. S.; Pawlak, K.; Bruening, B L.; Taret, B. J. *Chem. Rev.* **1992**, *92*, 1261.
28. Knops, P.; Sendhoff, N.; Mekelburger, H.-B.; Vögtle, F. *Topics Curr. Chem.* **1992**, *161*, 3.
29. Laidier, D. A. Stoddart, J. F. *Synthesis of Crown Ether and Analogues*. In *The Chemistry of Functional Groups; Patai, S., Ed.*; Wiley: New York, **1980**; Suppl. E, Part 1.
30. Baker, W.; Mac-Omie, J. F. W.; Ollis, W. D. *J. Chem. Soc.* **1951**, 200.
31. Walba, D. M.; Richards, B M.; Haltiwanger, B C. *J. Am. Chem. Soc.* **1982**, *104*, 3219. Waih D. M; Homan, T. C.; Richards, B M.; Haltiwanger, B C. *New J. Chem.* **1993**, *17*, 661.
32. Vitali, C. A.; Masci, B. *Tetrahedron* **1989**, *45*, 2201.
33. Chenevert, R.; D'Astous, L. J. *Heterocycl Chem.* **1986**, *23*, 1785.
34. Gibson, H. W.; Bheda, M. C.; Engen, P.; Shen, Y. X.; Sze, J.; Zhang, H.; Gibson, M. D.; Delaviz, Y.; Lee, S-H.; Liu, S.; Wang, L.; Nagvekar, D.; Rancourt, J.; Taylor, L. *J. Org. Chem.* **1994**, *59*, 2186.
35. Nakatauji, N.; Kameda, N.; Okahara, O. *Synthesis* **1987**, 280.
36. Bartsch, R. A.; Cason, C. V.; Czech, B. P. *J. Org. Chem.* **1989**, *54*, 857.
37. Cornforth, I. W.; Morgan, E. D.; Potts, K. T.; Rees, D. J. *Tetrahedron* **1973**, *29*, 1659.
38. Ouchi, M.; Inoue, Y.; Kanzaki, T.; Hakusbi, T. *J. Org. Chem.* **1984**, *49*, 1408.

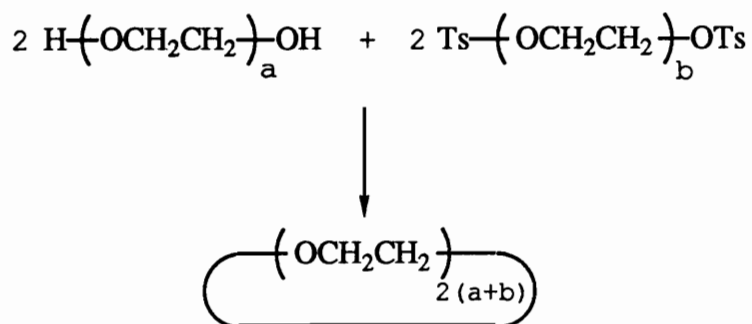
39. (a). Dust, J. M.; Fang, J. M. *Macromolecules* **1990**, *23*, 3742. (b). Kinugasa, S.; Takatsu, A.; Nakanishi, H.; Nakahara, H.; Hattori, S. *Macromolecules* **1992**, *25*, 4848.
40. This spectrum was provided by Mr. Sang-Hun Lee.
41. Cornforth, I. W.; Morgan, E. D.; Potts, K. T.; Rees, D. J. *Tetrahedron* **1973**, *29*, 1659.



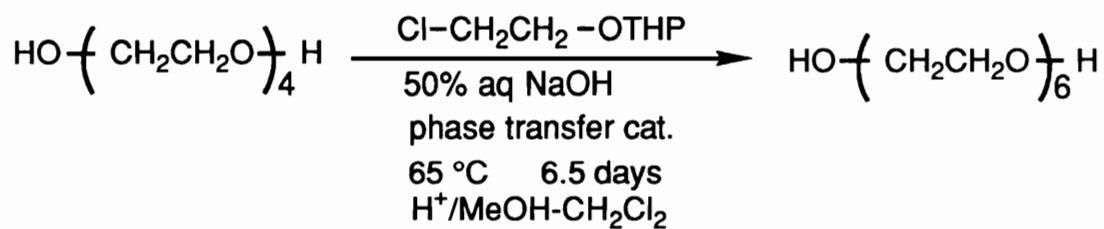
Scheme 1. Single molecular ring closure



Scheme 2. Two molecule combination

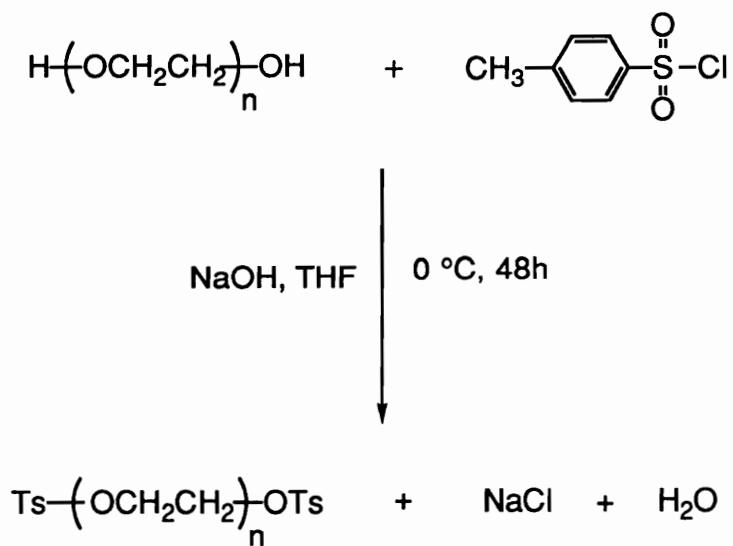


Scheme 3. Four molecule combination



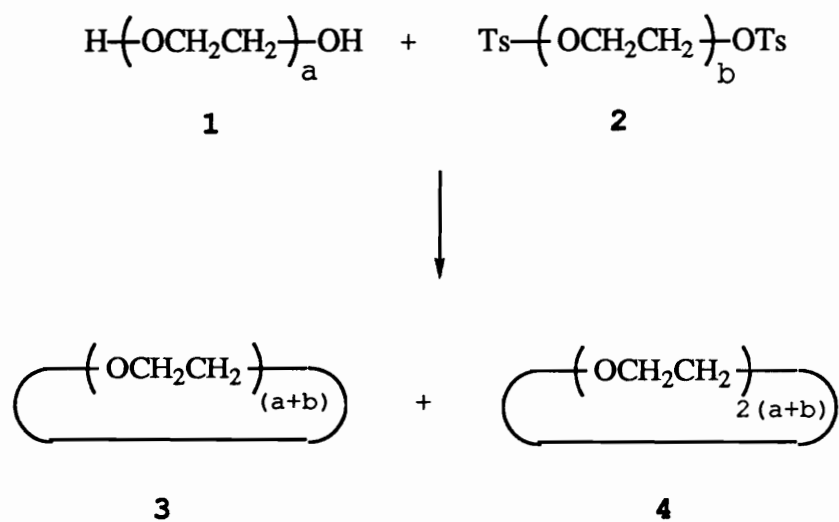
Scheme 4. Synthesis of hexa(ethylene glycol)



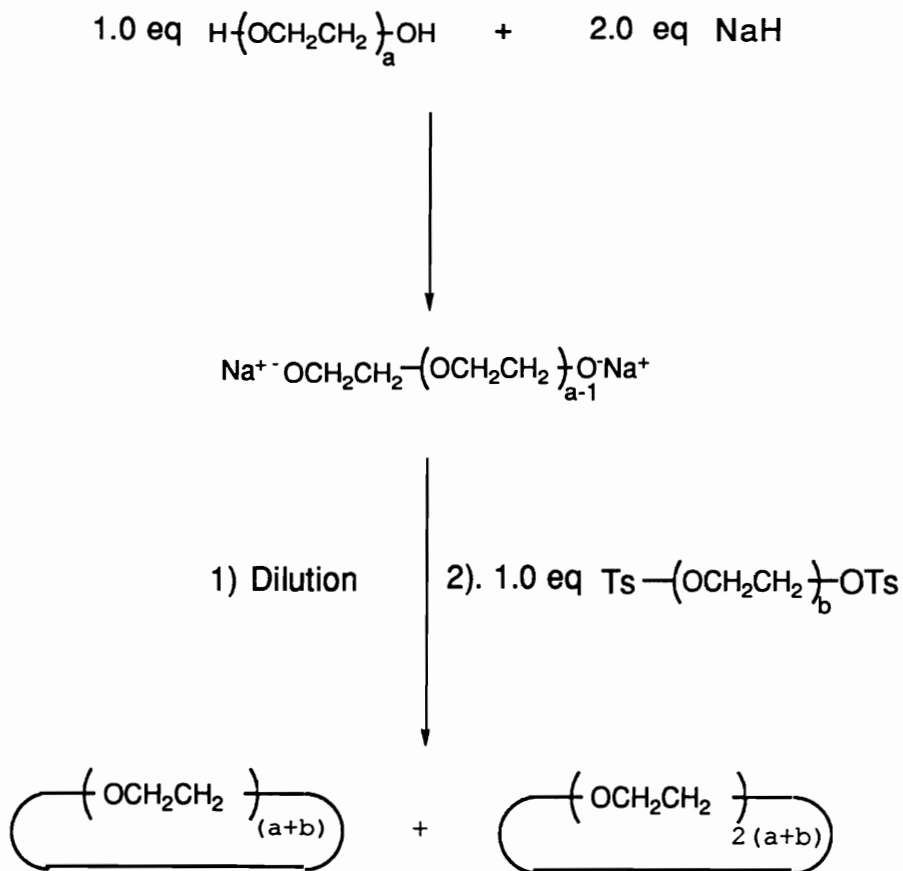


Where:  $n = 3, 4$

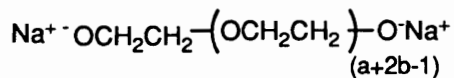
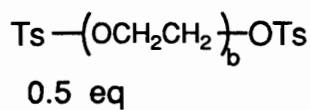
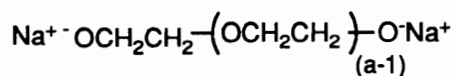
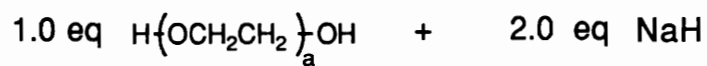
Scheme 5. Syntheses of oligo(ethylene glycol) ditosylates



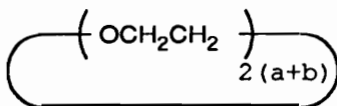
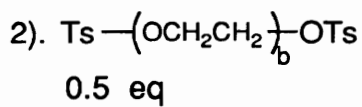
Scheme 6. Syntheses of large aliphatic crown ethers



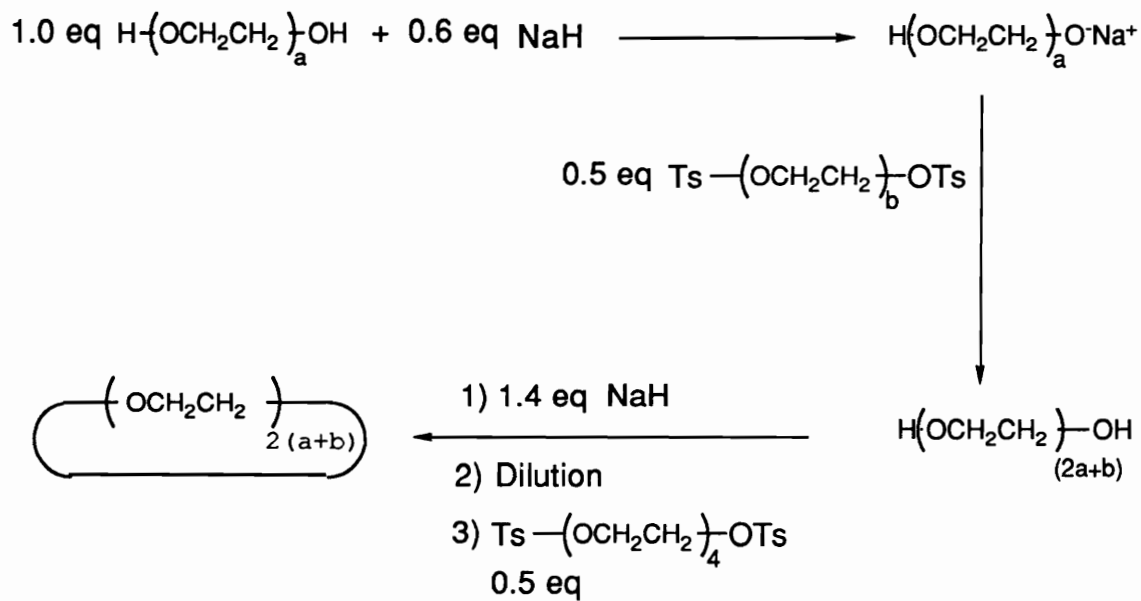
Scheme 7. Procedure A



1) Dilution



Scheme 8. Procedure B



Scheme 9. Procedure C

Table 1. The yields of 42-crown -14<sup>a</sup>

procedure	yield (%)
A <sup>b</sup>	48
B <sup>c</sup>	52 <sup>c</sup>
C <sup>d</sup>	55

- a. In refluxing THF using NaH as base. Diol concentration = 0.67 mol/L.
- b. 1.0 Equiv oligo(ethylene glycol) ditosylate was added into the THF solution of 1.0 equiv dialkoxide prepared from the oligo(ethylene glycol).
- c. 0.5 Equiv of oligo(ethylene glycol) ditosylate was added into the THF solution of 1.0 equiv dialkoxide prepared from the oligo(ethylene glycol). After several hours of reaction another 0.5 equiv ditosylate was added (from ref 34).
- d. 0.5 Equiv of oligo(ethylene glycol) ditosylate was added into the THF solution of 1.0 equiv monoalkoxide prepared *in situ* from the reaction of 1.0 equiv oligo(ethylene glycol) with 0.6 equiv NaH. After the addition of an excess of NaH, another 0.5 equiv of the ditosylate was added.

Table 2. Melting points of crown ethers

crown ether	mp (°C) <sup>a</sup>	reported mp (°C)	reference
30C10	46.3-48.1	35.5-36.8	32
42C14	54.9-57.4	28.5-31.0	33
48C16	52.5-53.9	49.5-50.5	32
60C20	56.2-56.6	46.0-50.5	33

a. Measured by capillary Mel-Temp II of Laboratory Devices.

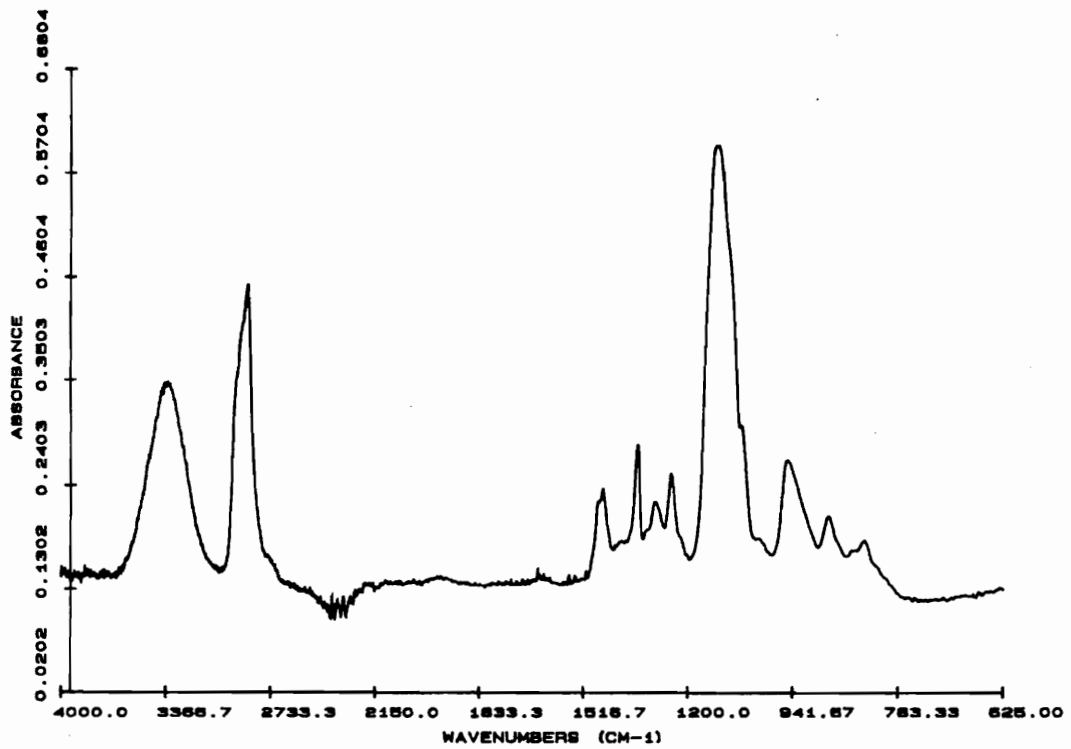
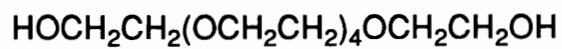


Figure 1. FTIR spectrum of hexa(ethylene glycol) on KBr plate





a      b    c    d

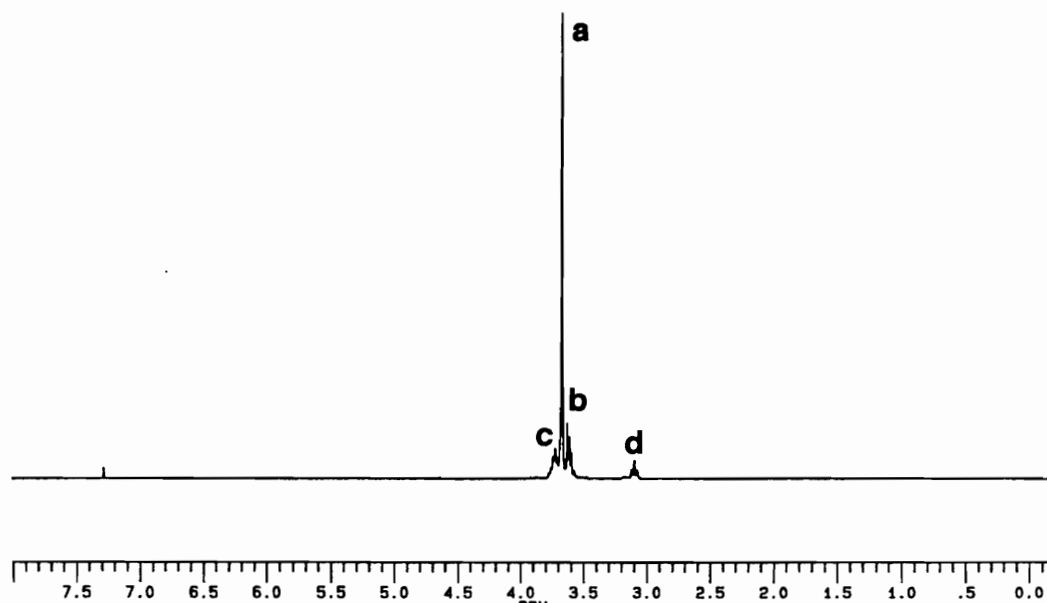


Figure 2. 270 MHz  $^1\text{H}$  NMR spectrum of hexa(ethylene glycol) in  $\text{CDCl}_3$ . The signal at 7.26 ppm is due to  $\text{CDCl}_3$ .

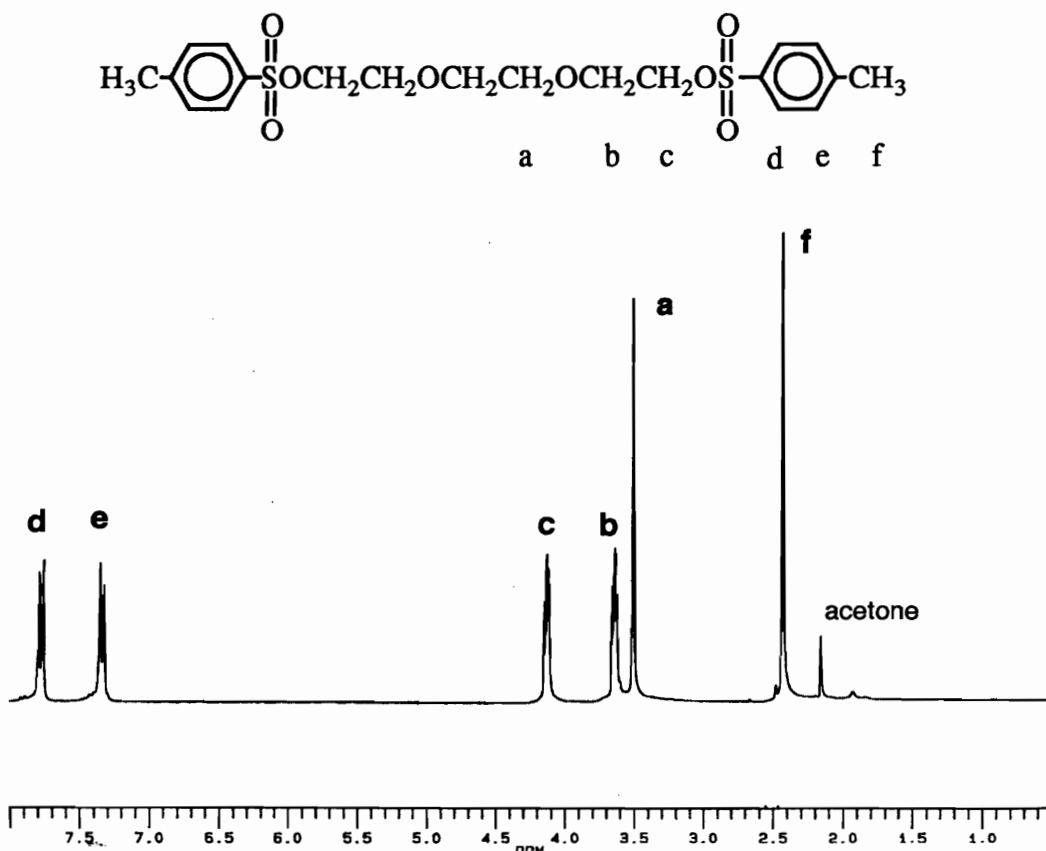


Figure 3. 270 MHz <sup>1</sup>H NMR spectrum of tri(ethylene glycol) ditosylate in CDCl<sub>3</sub>.

The signal at 7.26 ppm is due to CDCl<sub>3</sub>.

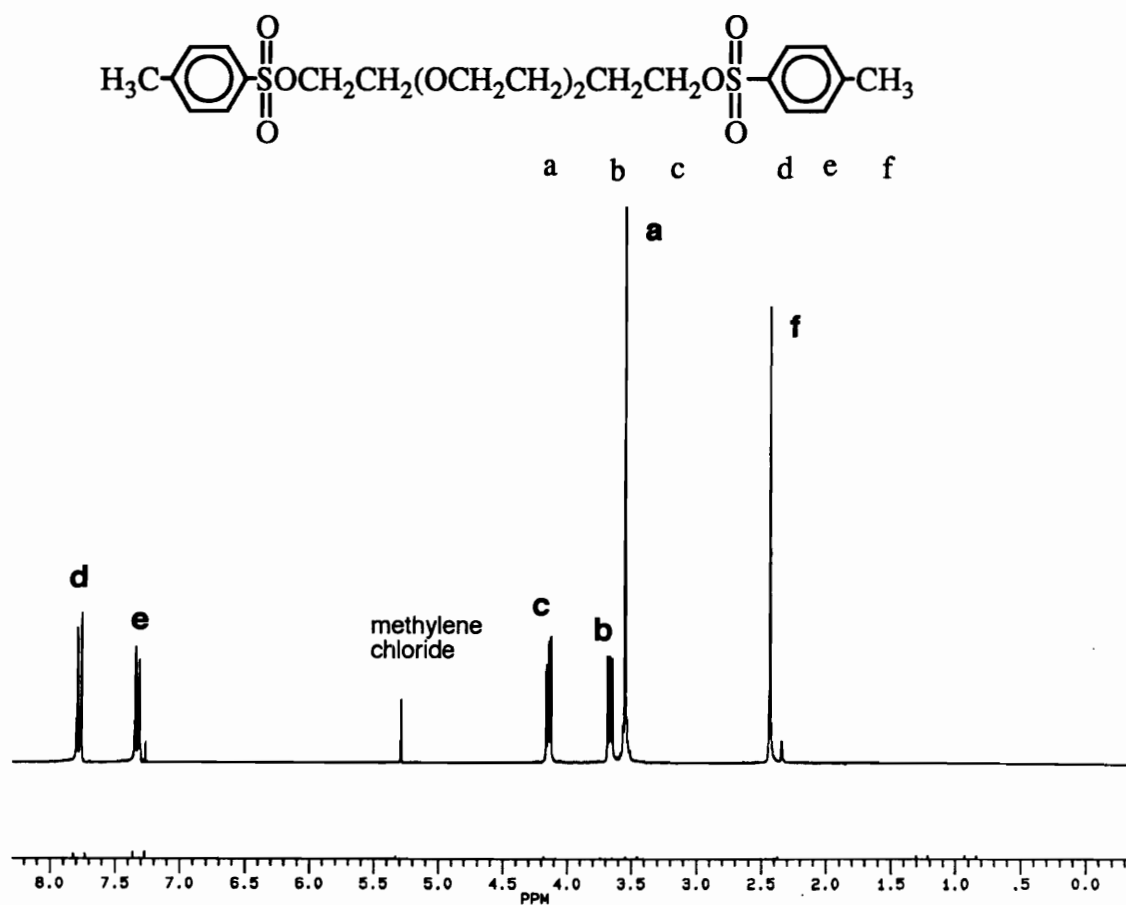


Figure 4. 270 MHz <sup>1</sup>H NMR spectrum of tetra(ethylene glycol) ditosylate in CDCl<sub>3</sub>. The signal at 7.26 ppm is due to CDCl<sub>3</sub>.

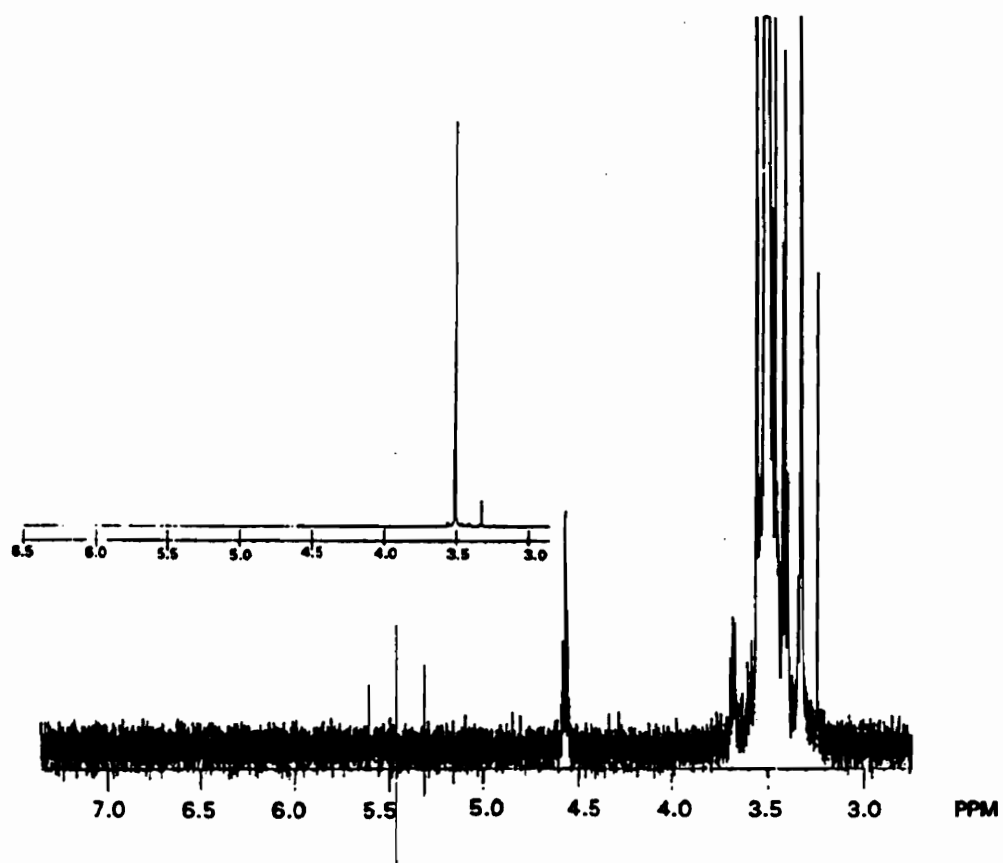


Figure 5. 400 MHz <sup>1</sup>H NMR spectrum of crude 42C14 in DMSO-d<sub>6</sub> at 20 °C showing a signal (4.57 ppm) due to OH. The signal at 3.68 is a <sup>13</sup>C satellite observed because of vertical expansion; the corresponding high-field signal is obscured by HOD. Note in the unexpanded spectrum that the overall impurity level is low.

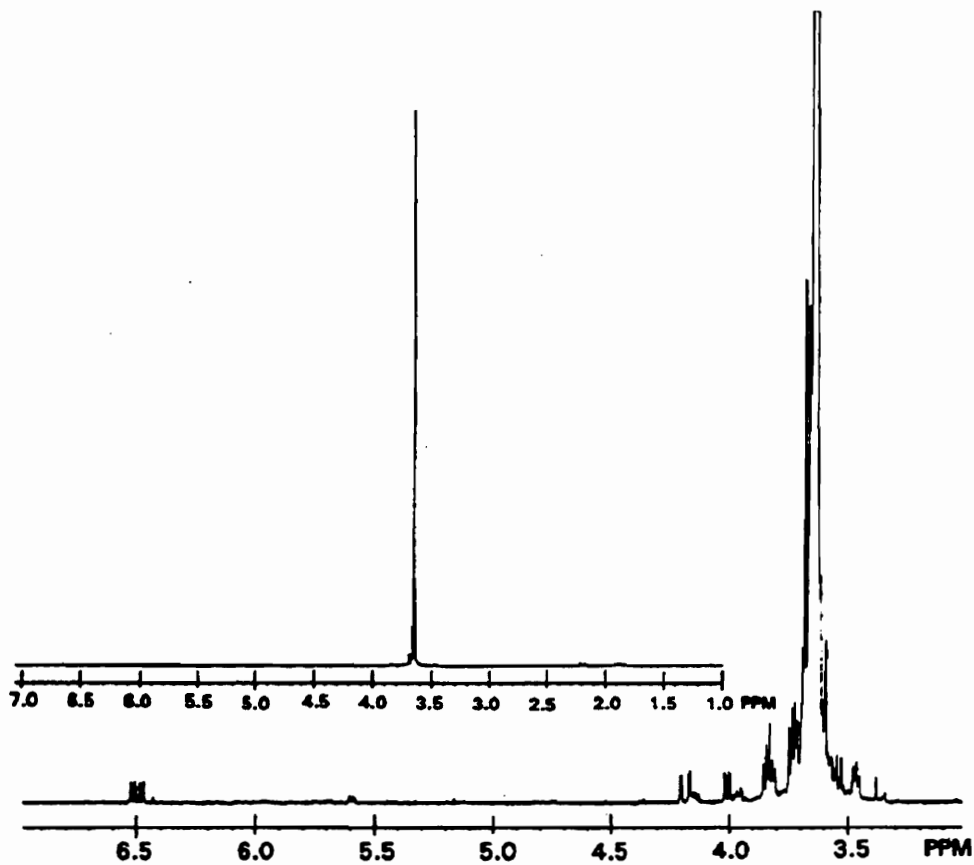


Figure 6. 400  $^1\text{H}$  NMR spectrum of crude 42C14 in chloroform-d at 20  $^\circ\text{C}$  showing signals due to terminal vinyl ether protons (3.97, 4.18, 6.50 ppm) and other impurities (3.66-3.76, 3.83-3.86 ppm). Note the expanded vertical scale which exaggerates the proportions of these impurity signals. The signals at 3.48 and 3.82 ppm are  $^{13}\text{C}$  satellites. Note in the unexpanded spectrum that the overall impurity level is low (from ref 34).

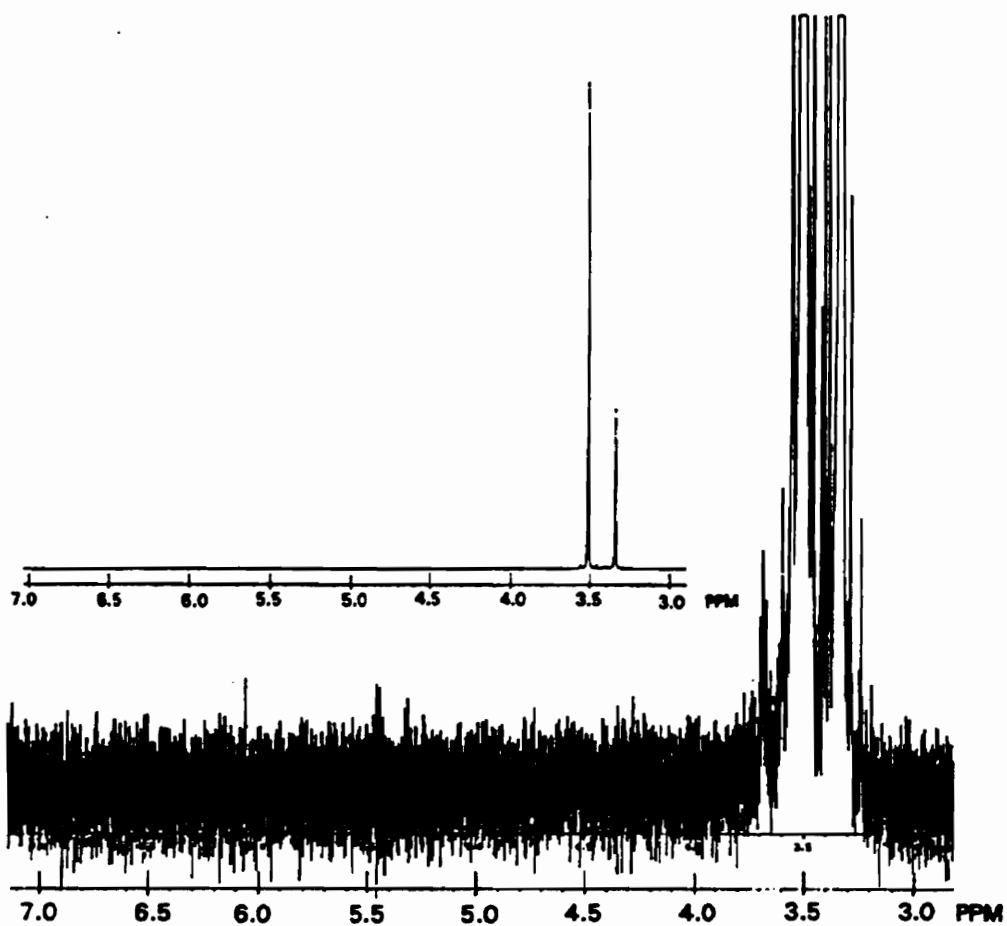


Figure 7. 400 MHz  $^1\text{H}$  NMR spectrum of pure 42C14 in  $\text{DMSO-d}_6$  at 20  $^\circ\text{C}$  showing lack of OH signal (4.57 ppm) even on a greatly expanded vertical scale. The signal at 3.35 is due to  $\text{H}_2\text{O}$ .

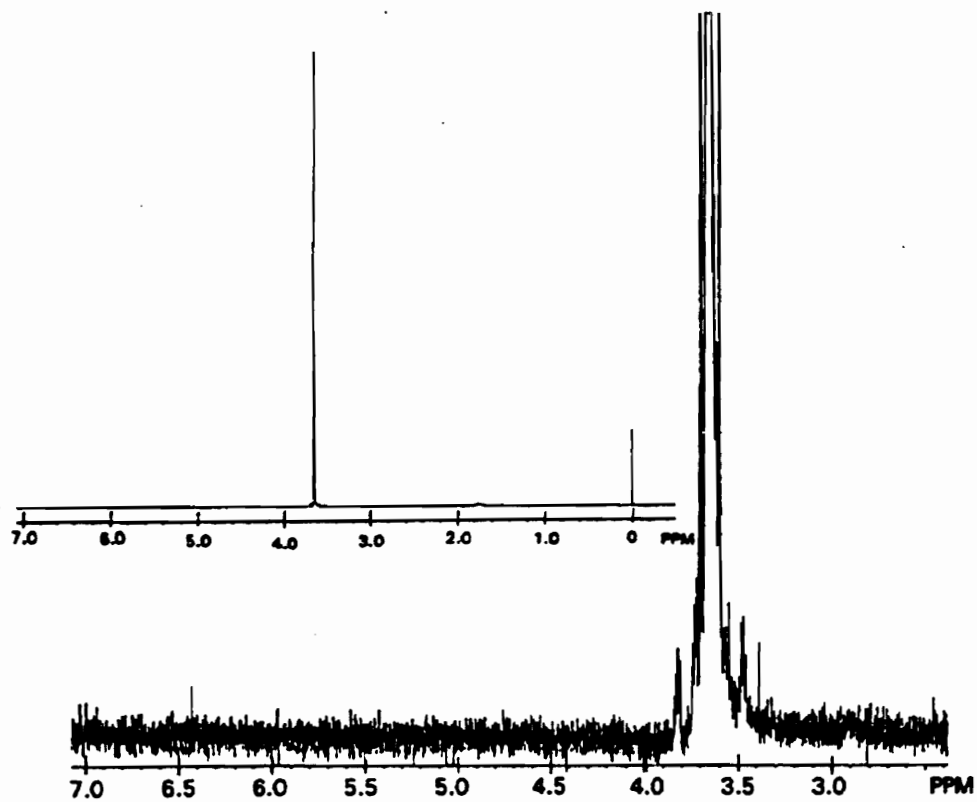


Figure 8. 400 MHz  $^1\text{H}$  NMR spectrum of pure 42C14 in  $\text{CDCl}_3$  at 20 °C showing lack of terminal vinyl ether protons and other impurity signals even on a greatly expanded vertical scale; the signals at 3.48 and 3.82 are  $^{13}\text{C}$  satellites, observed due to the vertical expansion.

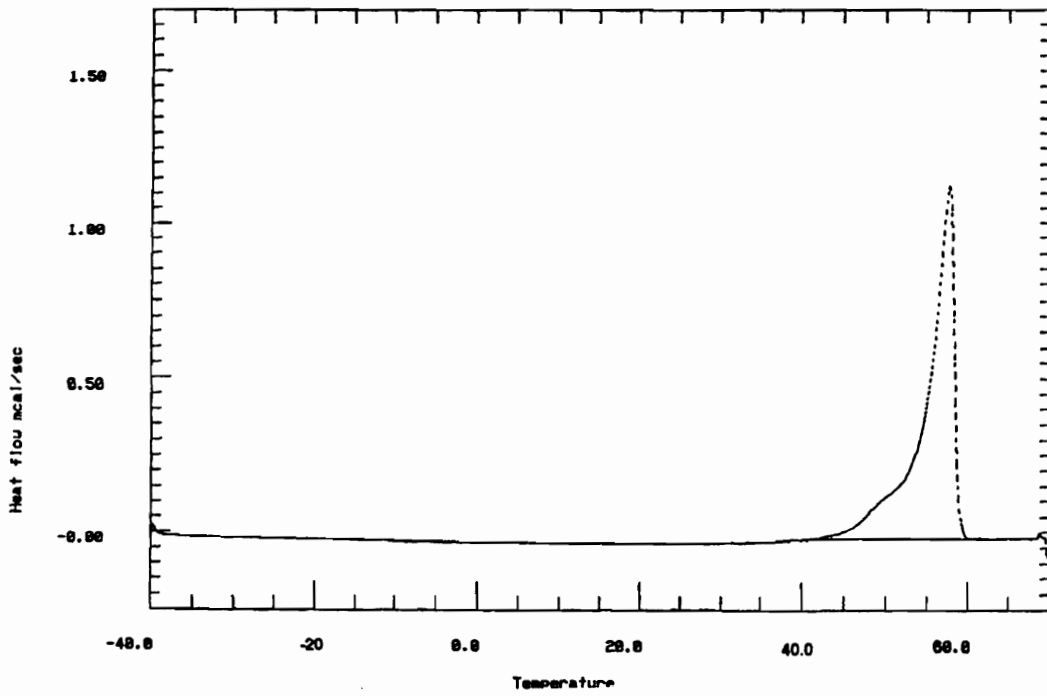


Figure 9. DSC trace for crude 42C14, second heating scan; 10 °C/min.



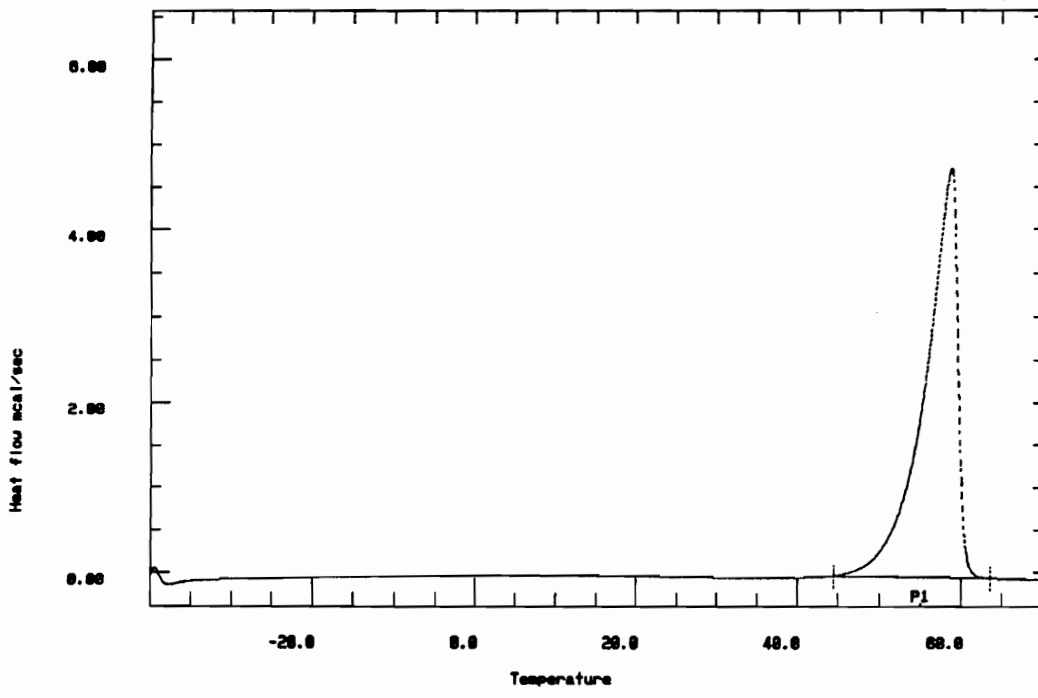


Figure 10. DSC trace of pure 42C14, second heating scan; 10 °C/min.

## CHAPTER V

### MONOFUNCTIONAL BLOCKING GROUPS

Monofunctional blocking groups are bulky compounds incorporated at the chain ends of polyrotaxane backbones to prevent macrocycles from dethreading [1]. The blocking groups should meet several requirements: (1) they have to be big enough to block threaded macrocycles. The size of a blocking group can be determined by a CPK molecular model or computer simulation; (2) they have suitable functional blocking groups which are highly reactive toward the monomers of polyrotaxanes. Therefore, halo, phenolic, alcoholic, carboxylic and amino blocking groups can be used in a wide variety of step growth polymerizations; (3) they should be soluble in reaction solvents which may be either a melted macrocycle or a mixture of macrocycle and another solvent.

Harrison prepared “dumb-bell” molecules by end-capping 1,10-decanediol with di(cyclohexyl)acetyl chloride or triphenylmethyl chloride and by end-capping 1,10-decanedichloride with tris(*p-t*-butylphenyl)methanol. He then synthesized rotaxanes using two approaches [2]. The first approach was the reversible cleavage of the blocking groups of the “dumb-bell” molecules catalyzed by trichloroacetic acid, in the presence of cycloalkanes with ring sizes of 14 to 42 atoms. A mixture of rotaxanes was obtained. The mixture was then hydrolyzed and threaded macrocycles were isolated. The second approach was the thermal variation, involving mixing the “dumb-bell” molecules with cycloalkanes at high temperature. Under this conditions the large rings received enough energy to incorporate onto “dumb-bell” molecules, passing over the blocking groups. The

results of these two methods demonstrated that the di(cyclohexyl)acetate group could constrain the macrocycles comprised of less than 28 atoms. The triphenylmethyl group could block 30-membered cycloalkanes, while tris(*p-t*-butylphenyl)methyl groups could constrain rings consisting of up to 42 atoms.

Schill et al. studied the blocking capacity of the triphenylmethyl moiety, using both the acid catalyzed equilibration method and the thermal variation approach [3]. They equilibrated individual pure cycloalkanes of 21 to 29 methylene units with 1,12-bis(triphenylmethylthio)dodecane, either thermally or in the presence of an acid catalyst. They found that 29-membered macrocycles could be constrained by the triphenylmethyl blocking group.

Based on Harrison's results we focused on the syntheses of the largest monofunctional blocking groups, tris(*p-t*-butylphenyl)methyl compounds. These compounds were chosen because they meet the requirements for blocking groups [4]. They exert a large steric influence capable of blocking macrocycles comprised of up to 42 atoms. They have functional groups reactive toward the end groups of linear species. Therefore, they can end-cap polymer chains prepared via step growth polymerization. They are soluble in melts of large aliphatic crown ethers which are macrocycles for our polyrotaxanes.

## RESULTS AND DISCUSSIONS

Although Harrison used tris(*p-t*-butylphenyl)methanol in his syntheses of rotaxanes [2], he did not report how to prepare this blocking group. Marvel and coworkers first reported the synthesis of this compound [5]. They studied the effects of substituents on the dissociation of phenyl rings of arylophanes. They prepared tris(*p-t*-butylphenyl)methanol and di(*p-t*-butylphenyl)phenylmethanol via the reactions of ethyl benzoate or ethyl *p-t*-butylbenzoate with *p-t*-butylphenylmagnesium bromide. Tris(*p-t*-butylphenyl)methanol was obtained in about 45 % yield as a crystalline solid with melting point of 212-213 °C. Di(*p-t*-butylphenyl)phenylmethanol was not purified. The arylmethanols were then converted to the corresponding arylmethyl chlorides. Coupling of two arylmethyl chloride molecules gave arylophanes [5].

Stoddart et al. reported the preparation of tris(*p-t*-butylphenyl)methanol via Grignard reaction of diethyl carbonate with *p-t*-butylphenylmagnesium bromide [6]. However, they did not report a detailed synthetic procedure.

Based on Marvel's principle that a bulky triaryl group can be built up by Grignard reaction of a bromobenzene derivative and a benzoate ester [5], we synthesized phenolic and alcoholic monofunctional blocking groups containing the tris(*p-t*-butylphenyl)methyl moiety. The synthetic route is shown in Scheme 1.

Our syntheses started from the reaction of ethyl *p-t*-butylbenzoate with the Grignard reagent derived from *p*-bromo-*t*-butylbenzene. The starting material,

ethyl *p-t*-butylbenzoate (**1**) was prepared in 91 % yield from direct esterification of *p-t*-butylbenzoic acid and ethanol, using HCl as a catalyst. Figure 1 is the  $^1\text{H}$  NMR spectrum of **1**. The Grignard reagent **2** was prepared *in situ* by the reaction of *p*-bromo-*t*-butylbenzene with magnesium in refluxing THF. Usually preparation of Grignard reagent generates a large amount of heat which needs to be removed by a water bath [7]. Our reaction, however, was under reflux condition because of the low reactivity of the aryl bromide toward magnesium. Ethyl ether, a common solvent for the preparation of Grignard reagents [7], was not suitable for this reaction, probably due to its low refluxing temperature. Iodine is a normal catalyst for the formation of Grignard reagents [7]. However, use of iodine was avoided because it also catalyzes a Gomberg-Bachmann reaction, resulting in a side product, 1,1,2,2-tetrakis(*p-t*-butylphenyl)-1,2-dihydroxyethane [4, 8].

The mechanism of the reaction is shown in Scheme 2. First, the Grignard reagent attacks the carbonyl group of the ester **1**, resulting in di(*p-t*-butylphenyl)ketone. The Grignard reagent then attacks the carbonyl group of the diaryl ketone, generating the magnesium salt of tris(*p-t*-butylphenyl)methanol. Hydrolysis of the methoxide gives tris(*p-t*-butylphenyl)methanol (**3**).

The structure of **3** was supported by melting point measurement, FTIR and  $^1\text{H}$  NMR spectra. The melting point was same as the reported value [4]. The FTIR spectrum shows the O-H stretch at  $3576\text{ cm}^{-1}$ . In the  $^1\text{H}$  NMR spectrum (Figure 2) the signal for 27 *t*-butyl protons appears at  $1.30\ \delta$ ; the hydroxyl proton occurs

at 2.71  $\delta$ ; signals of the 12 aromatic protons appear at 7.18  $\delta$  (doublet) and 7.31  $\delta$  (doublet).

Tris(*p-t*-butylphenyl)methanol (**3**) can not be directly used as a blocking group because the steric hindrance reduces its reactivity and also the resultant trityl ether type compounds are hydrolytically unstable. Although Harrison utilized this instability in his syntheses of rotaxanes via the approach of acid catalyzed equilibration [2], his rotaxanes were unstable compounds. Schill et al. circumvented the problem by reaction of the anion of triphenylmethane with a suitable electrophile [3]. The anion was formed *in situ* by the reaction of *n*-butyllithium with triphenylmethane.

In order to obtain stable polyrotaxanes it is necessary to have the functional blocking group remote from the region of steric hindrance. Using the principle proposed by Schill [3], a method involving carboanion chemistry was developed as shown in Scheme 3 [4]. First, tris(*p-t*-butylphenyl)methanol (**3**) is reduced to tris(*p-t*-butylphenyl)methane (**4**) by formic acid in toluene. This is essentially a quantitative reaction. The product was easily separated and purified. Tris(*p-t*-butylphenyl)methane (**4**) is converted to triarylmethyl carbanion **5** with *n*-butyllithium. The carbanion **5** then reacts with tetrahydropyran-protected (THP-protected) 3-chloropropanol to form chain extended THP-protected alcohol **6**. **6** is then subjected to deprotection with HCl to produce hydroxyl-terminated blocking group **7**.

This method has two drawbacks. First, the synthetic route involves several steps. Second, the reaction of the triarylmethyl carbanion and THP-protected 3-chloropropanol is not high yielding except in the presence of toxic HMPA [4].

The second approach for incorporation of a spacer between the triarylmethyl moiety and the functional group is a carbocationic process, as shown in Scheme 4 [4]. This method is based on the literature report by Mikroyannidis [9]. He prepared bis(*p*-hydroxyphenyl)diphenylmethane via the reaction of dichlorodiphenylmethane with phenol without any catalyst. This is a Friedel-Crafts alkylation reaction. In Scheme 4 tris(*p*-*t*-butylphenyl)methyl chloride (**8**) was synthesized by the reaction of tris(*p*-*t*-butylphenyl)methanol (**3**) with acetyl chloride, using the procedure suggested by Marvel et al.[5]. Tris(*p*-*t*-butylphenyl)methyl chloride (**8**) was then reacted with excess neat phenol at 100 °C to produce tris(*p*-*t*-butylphenyl)(4-hydroxyphenyl)methane (**9**). Stoddart and coworkers reported the synthesis of **9** from **8** in 95 % yield [6]. They prepared **8** from **3** using thionyl chloride in 69 % yield [6].

Alternatively, direct reaction of tris(*p*-*t*-butylphenyl)methanol (**3**) with phenol can be carried out with HCl as a catalyst to produce phenolic blocking group **9** in a good yield [3]. Obviously, this method is superior to the above one because of its shorter synthetic route. Therefore, it was adopted to synthesize **9**. This reaction is an aromatic electrophilic substitution reaction and the mechanism is shown in Scheme 5. First, **3** is protonated by HCl and loses a water molecule to form a triarylmethyl carbocation which is stabilized by three conjugated aryl groups. The triarylmethyl carbocation is then attacked by the para-position of phenol to form

**9.** After the reaction the excess phenol was removed by washing with aqueous NaOH solution. It was easily purified by crystallization since the symmetry is largely increased by the introduction of a fourth phenyl ring.

The phenolic blocking group **9** give satisfactory characterization results. Its melting point is 85 °C higher than starting material **3** because of its higher symmetry. The FTIR spectrum (Figure 3) shows a phenolic O-H out-of-plane deformation at 704 cm<sup>-1</sup>. In the <sup>1</sup>H NMR spectrum (Figure 4) the signal of 27 t-butyl protons appears at 1.30 δ; two aromatic protons appear at 6.72 δ; two at 7.03 δ; twelve at 7.08 and 7.22 δ.

The phenolic blocking group **9** made cationically is itself useful. It can be used in the synthesis of polyester rotaxanes via the acid chloride method. However, it is not reactive toward diester monomers in transesterification polymerization. Therefore, we also wished to have an alkanol terminated blocking group. This was done by elaboration of the phenol **9** by a Williamson reaction as shown in Scheme 1.

The conversion of phenol **9** to the alcohol **10** can be done by the reaction of phenol **9** with an excess of THP-protected di(ethylene glycol) monochloride in 1-butanol, using KOH as a base to deprotonate the phenol. After the deprotection with HCl the alcoholic blocking group **10** was obtained [5]. Although the reported yield was high [4], this method is not best because it involves protection and deprotection of the hydroxyl proton of di(ethylene glycol) monochloride.



A new one step method was adopted which avoids the protection of di(ethylene glycol) monochloride. In this reaction **9** was allowed to react with an excess of di(ethylene glycol) monochloride in 1-butanol, using  $K_2CO_3$  as a base. Since  $K_2CO_3$  can only deprotonate the phenol but not the alcohol, protection of alcohol **9** becomes unnecessary.

The purification of **10** was straightforward. After the product had been washed with water, the only impurity left was excess di(ethylene glycol) monochloride. It was removed by the crystallization of **10** in acetone.

The structure of **10** was proved by the characterization results. The FTIR spectrum (Figure 5) shows the aliphatic ether C-O-C stretch at  $1070\text{ cm}^{-1}$ . In the  $^1\text{H}$  NMR spectrum (Figure 6) the signal of 27 t-butyl protons appears at 1.30 ppm as a singlet; protons of ethylene oxide units occur at 3.69, 3.76, 3.87, and 4.11 ppm; aromatic protons appear at 6.79, 7.08, and 7.23 ppm.

The melting point of **10** is  $81\text{ }^\circ\text{C}$  lower than its precursor, phenol **9**. This is because the flexible ethylene oxide reduces its symmetry and rigidity. Therefore, the melting point and solubility of an alcoholic blocking group can be adjusted by proper choice of the length and nature of chains. This adjustment may be necessary for different polymerization conditions.

## CONCLUSIONS

Tris(*p-t*-butylphenyl)methanol (**3**) was synthesized via Grignard reaction of ethyl *p-t*-butylbenzoate with the Grignard reagent derived from *p*-bromo-*t*-butylbenzene. The reaction of **3** with an excess of phenol under acidic condition generated tris(*p-t*-butylphenyl)(*p*-hydroxyphenyl)methane (**9**), a phenolic blocking group. **9** was converted to a hydroxyl terminated blocking group **10** by its reaction with an excess of di(ethylene glycol) monochloride, using K<sub>2</sub>CO<sub>3</sub> as a base. These functionalized triarylmethyl derivatives **9** and **10** are able to end-cap polymer backbones of polyrotaxanes to constrain rings comprised of up to 42 atoms. They can also be used as end blocking units in rotaxane syntheses.

## EXPERIMENTAL

**Measurements.** Melting points were taken in capillary tubes and have been corrected. Proton NMR spectra, reported in ppm, were obtained on 270 or 400 MHz spectrometers using chloroform solutions with tetramethylsilane as an internal standard. The following abbreviations have been used in describing the NMR spectra: s (singlet), d (doublet), t (triplet), q (quartet), p (pentet), and m (multiplet). The values of coupling constants (J) were reported in Hz. FTIR spectra, reported in  $\text{cm}^{-1}$ , were obtained using KBr pellets unless otherwise noted.

**Starting Materials.** THF was dried over Na/benzenophenone and distilled just before use. The other chemicals were used without purification as obtained from commercial sources.

### **Ethyl *p*-*t*-butylbenzoate (1)**

*p*-*t*-Butylbenzoic acid (100 g, 560 mmol), ethanol (500 mL, 8.70 mol), and 98% sulfuric acid (50 mL, 900 mmol) were added in a 1-L, 1-necked flask equipped with a condenser and a magnetic stirrer. The mixture was stirred for 36 hours at reflux. After it had been cooled to room temperature, the mixture was poured into ice water (500 mL) and neutralized with NaOH (ca. 22 g). The mixture was then extracted with ethyl acetate (2 x 500 mL). The combined organic phase was washed with water and ethyl acetate was removed by rotary evaporation. A liquid product (111 g, 91 %) was obtained. IR: 2966, 2956, 1720, 1610, 1409, 1366, 1313, 1277, 1188, 1116, 1102, 1021, 775, 708.  $^1\text{H-NMR}$ : 1.35 (s, 9 H, t-

butyl), 1.40 (t, J = 7, 3 H, -CH<sub>3</sub>), 4.40 (q, J = 7, 2 H, -CH<sub>2</sub>-), 7.45 (d, J = 11, 2 H, arom.), 8.00 (d, J = 11, 2 H, arom.).

### **Tris(*p*-*t*-butylphenyl)methanol (3)**

To an oven-dried 500-mL 3-necked flask equipped with a condenser, magnetic stirring, a dropping funnel, and nitrogen system, magnesium turnings (7.39 g, 304 mmol) were added with dry (Na/benzophenone) THF (85 mL). *p*-Bromo-*t*-butylbenzene (43.2 g, 203 mmol) in dry THF (65 mL) was added dropwise over 2 hours. The mixture was then stirred for another 2 hours with gentle heating. Ethyl *p*-*t*-butylbenzoate (1) (20.9 g, 101 mmol) in dry THF (85 mL) was added dropwise over 2 hours. The mixture was stirred for 17 hours at reflux. The solution was cooled to room temperature and neutralized with 10 % HCl. After the remaining magnesium had been removed by filtration, THF was removed by rotary evaporation. The crude product was recrystallized in acetone 5 times to afford a white solid (26.6 g, 62 %), mp 216.5 - 217.7 °C (Lit. [4] mp 214.6 - 215.8 °C). IR: 3575, 3085, 3053, 3024, 2975, 2900, 2865, 1507, 1461, 1302, 1163. <sup>1</sup>H NMR: 1.31 (s, 27 H, *t*-butyl), 7.19 (d, J = 11, 6 H, arom.), 7.33 (d, J = 11, 6 H, arom.).

### **Tris(*p*-*t*-butylphenyl)(*p*'-hydroxyphenyl)methane (9)**

Tris(*p*-*t*-butylphenyl)methanol (13.0 g, 30.3 mmol) was dissolved in phenol (50 g) by warming in a 250-mL 1-necked flask equipped with a condenser and nitrogen system. HCl (36%, 1 mL) was added as a catalyst. A deep reddish blue color

was observed immediately. The mixture was refluxed for 24 hours. After the solution was cooled to room temperature, the product was extracted with toluene (3 x 150 mL). The combined organic phase was washed with aqueous NaOH solution (20 g/L, 3 x 250 mL), and with water (3 x 250 mL), and dried with Na<sub>2</sub>SO<sub>4</sub>. A white solid (12.3 g, 80 %) was obtained after it was decolorized with activated carbon and the solvent was rotary evaporated. The solid was boiled in n-hexane for 30 minutes, filtered, dried under vacuum and weighed (11.2 g, 73 %), mp 301.8-302.8°C (Lit. [4] mp 304.0 - 305.8 °C). IR: 3307, 3031, 2958, 1607, 1508, 1475, 1402, 1363, 1271, 1238, 1178, 1106, 1020, 822, 704. <sup>1</sup>H NMR: 1.30 (s, 27 H, t-butyl), 4.72 (s, 1 H, -OH), 6.70 (d, J = 11, 2 H, arom.), 7.05-7.25 (m, 14 H, arom.).

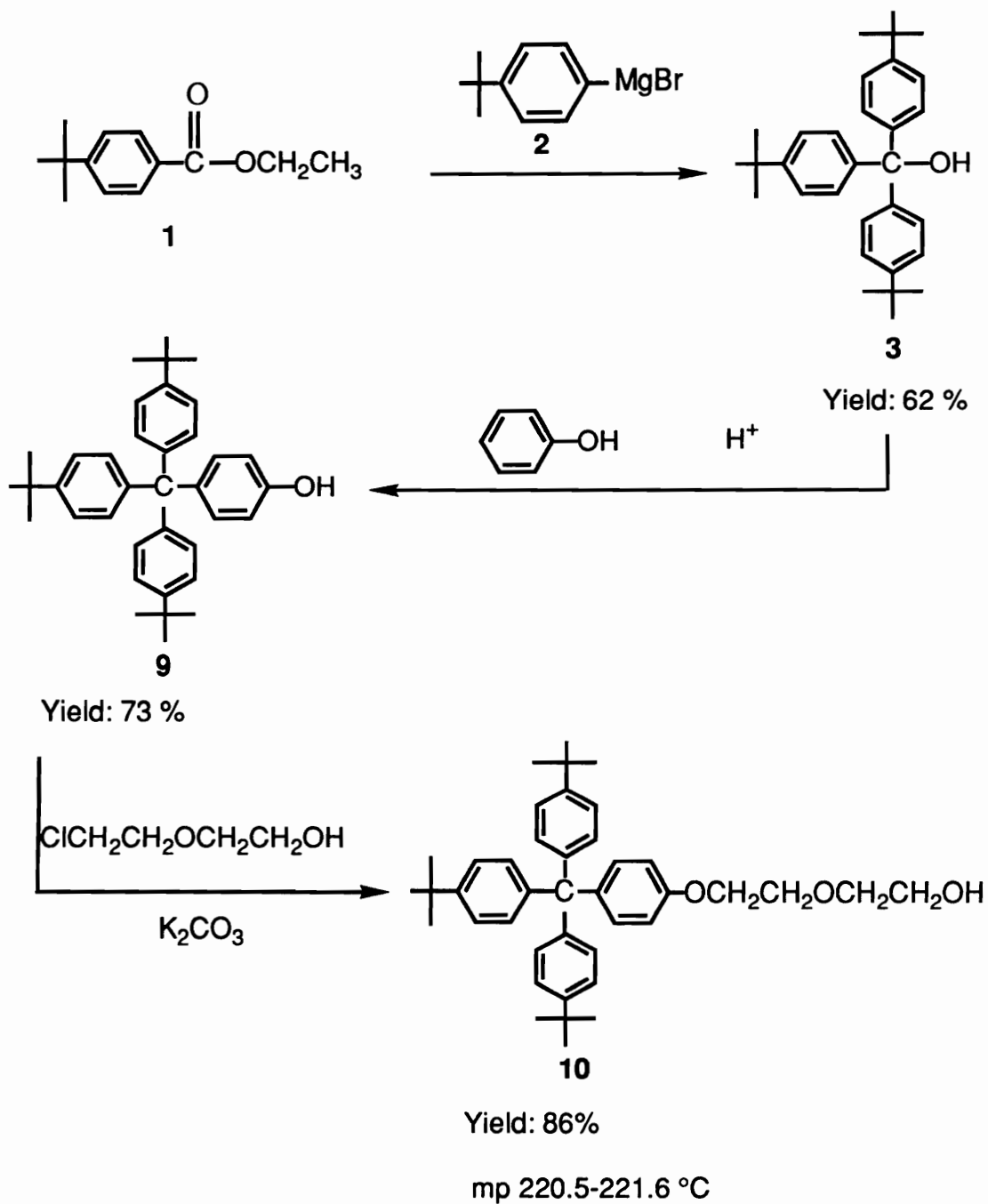
### **Mono-*p*-[tris(*p*'-*t*-butylphenyl)methyl]phenyl Ether of Di(ethylene glycol) (10)**

Tris(*p*-*t*-butylphenyl)(*p*'-hydroxyphenyl)methane (9) (10.1 g, 20.0 mmol) was dissolved in 1-butanol (200 mL) by heating in a 500-mL 1-necked flask equipped with a condenser, magnetic stirring and nitrogen inlet. K<sub>2</sub>CO<sub>3</sub> (27.6 g, 200 mmol) in water (70 mL) was added and the mixture was refluxed for 12 h. 2-(2'-Chloroethoxy)ethanol (24.9 g, 200 mmol) in 1-butanol (40 mL) was added. The solution was refluxed for 5 days. After the solution had been cooled to room temperature, salts were removed by filtration. A solid was obtained after 1-butanol was removed by rotary evaporation. The solid was then dissolved in methylene chloride (300 mL), washed with water (3 x 200 mL), and dried with Na<sub>2</sub>SO<sub>4</sub>. A white solid (15.3 g) was obtained after the removal of the solvent.

The solid was recrystallized in acetone three times to afford white crystals (11.9 g, 86 %), mp 220.5 -221.6 °C (Lit. [4] 218.3 -218.6 °C). IR: 3455, 2965, 2868, 1611, 1508, 1463, 1360, 1250, 1186, 1135, 1064, 1018, 819, 709, 580. <sup>1</sup>H NMR: 1.30 (s, 27 H, CH<sub>3</sub>), 3.69 (t, J = 5, 2 H, CH<sub>2</sub>CH<sub>2</sub>OH), 3.76 (m, 2 H, CH<sub>2</sub>OH), 3.87 (t, J = 5, 2 H, CH<sub>2</sub>CH<sub>2</sub>OCH<sub>2</sub>CH<sub>2</sub>OH), 4.11 (t, J = 5, 2 H, ArOCH<sub>2</sub>-), 6.79 (d, J = 11, 2 H, arom closest to OH), 7.08 (m, 6 H, arom), 7.23 (m, 6H, arom).

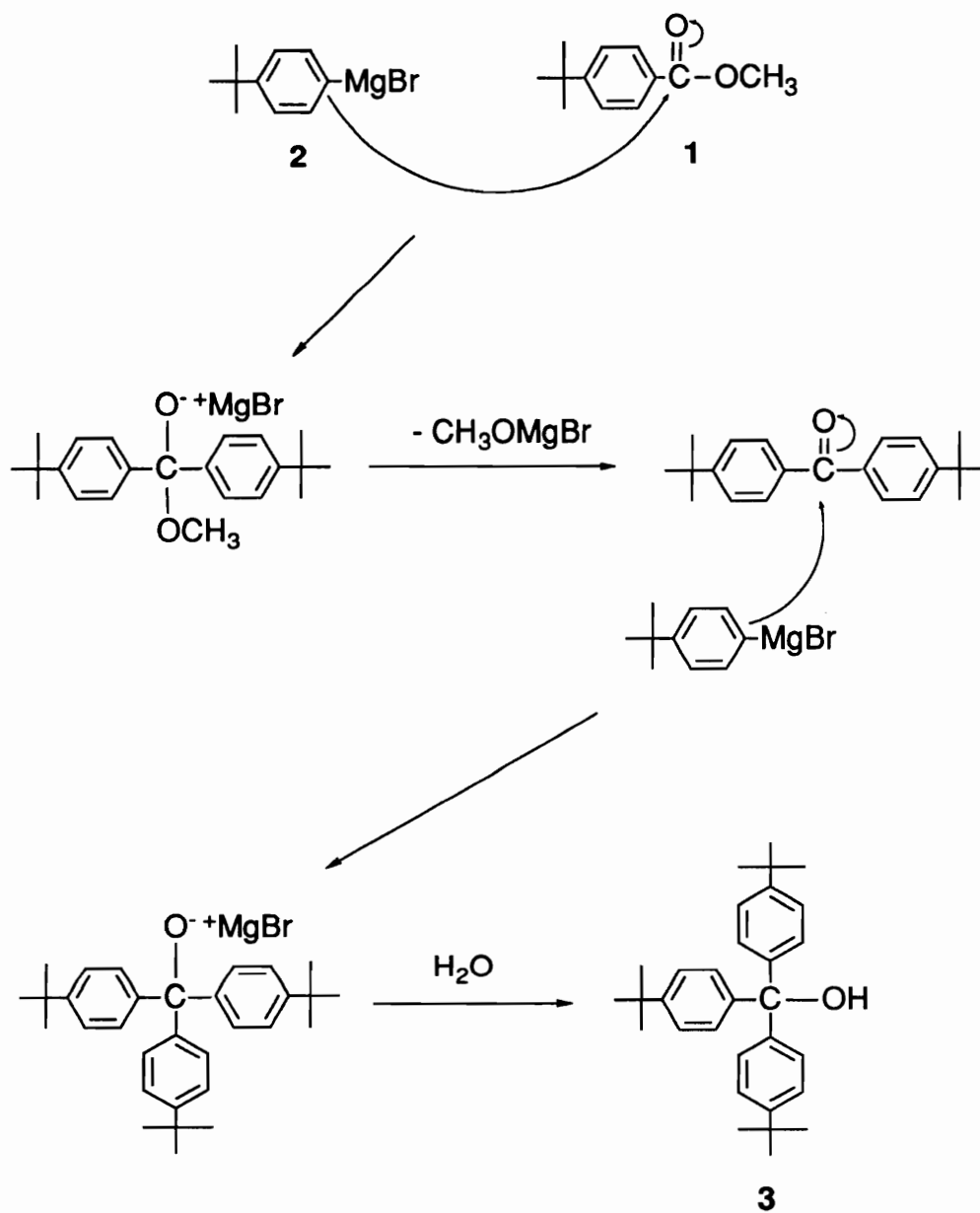
## REFERENCES

1. Gibson, H. W.; Marand, H. *Adv. Mater*, **1993**, *6*, 11; Gibson, H. W.; Bheda, M. C.; Engen, P. T. *Prog. Polym. Sci.* **1994**, *19*, 843.
2. Harrison, I. T. *J. Chem.Soc., Chem. Commun.* **1972**, 231; *J. Chem. Soc., Perkin Trans. 1*, **1974**, 301; *J. Chem. Soc., Chem. Commun.* **1977**, 384.
3. Schill, G.; Beckmann, W.; Schweikert, N.; Fritz H. *Chem. Ber.* **1986**, *199*, 2647.
4. Gibson, H. W.; Lee, S-H.; Engen, P. T.; Lecavalier, P.; Sze, J.; Shen, Y. X.; Bheda, M., *J. Org. Chem.* **1993**, *58*, 3748.
5. Marvel, C. S.; Kaplan, J. F.; Himel, C. M. *J. Am. Chem. Soc.* **1941**, *63*, 1892.
6. Ashton, P.R.; Philp, D.; Spencer, N.; Stoddart, J. F. *J. Chem. Soc. Chem. Commun.* **1992**, 1124.
7. Furniss, B. S.; Hannaford, A, J.; rogers, V.; Smith, P. W. G.; Tachell, A. R. *Vogel's Textbook of Practical Organic Chemistry, 4th Ed.*, Jwang Yuan Publishing Co., New York, **1978**, p367.
8. Bachmann, W. E.; Shankland, R. V. *J. Am. Chem. Soc.* **1929**,*51*, 306; Gomberg, M.; Van Natta, F. J. *J. Am. Chem. Soc.* **1929**, *51*, 2238.
9. Mikroyannidis, J. A. *Eur. Poly. J.* **1985**, *21*, 895.

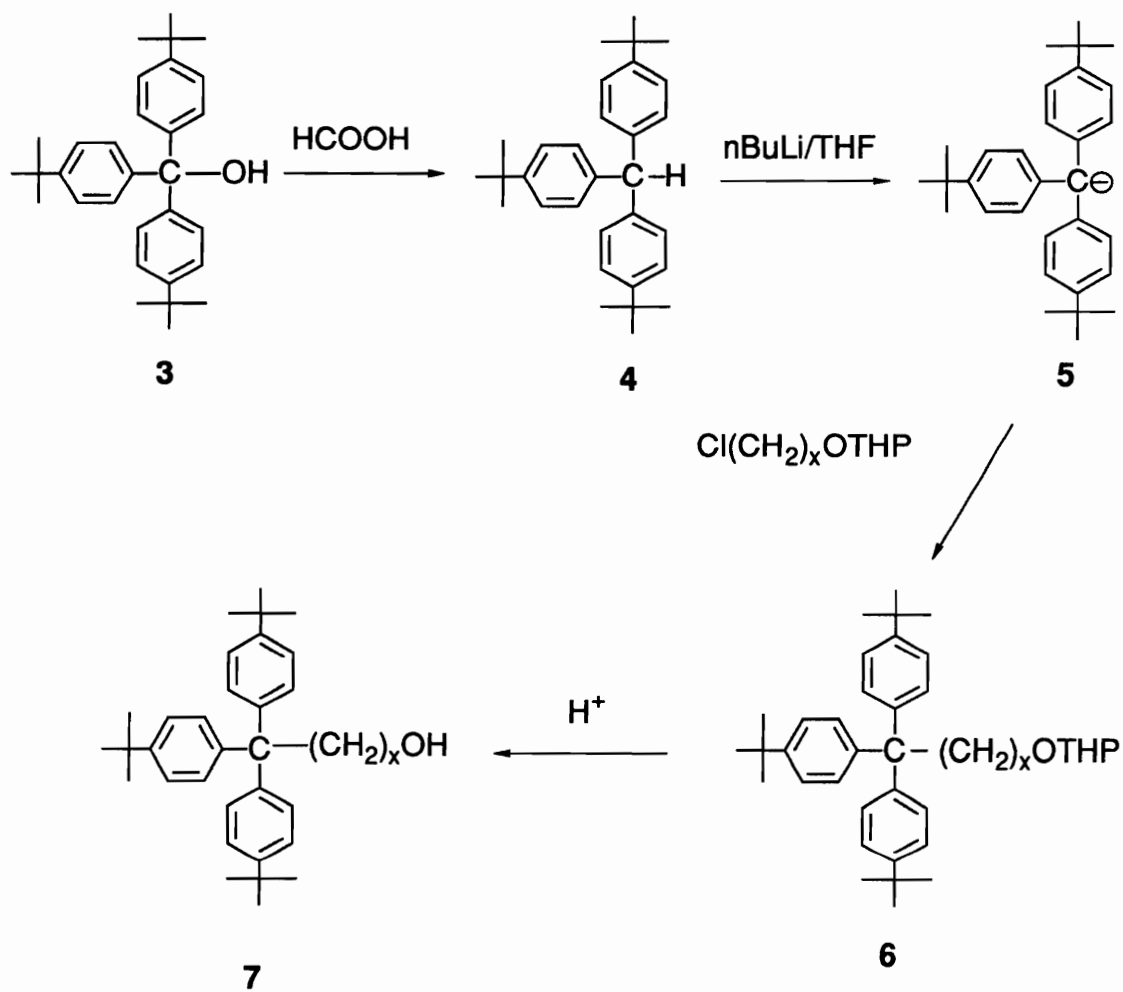


Scheme 1. Syntheses of tris(*p-t*-butylphenyl)methyl compounds

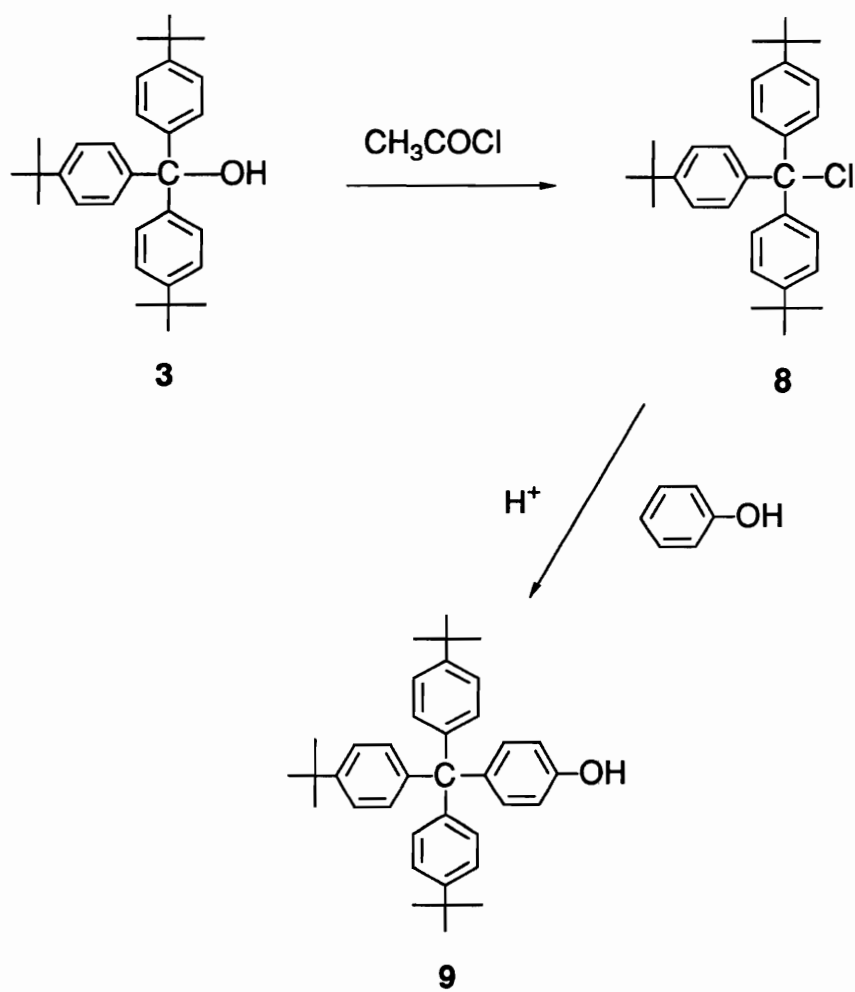




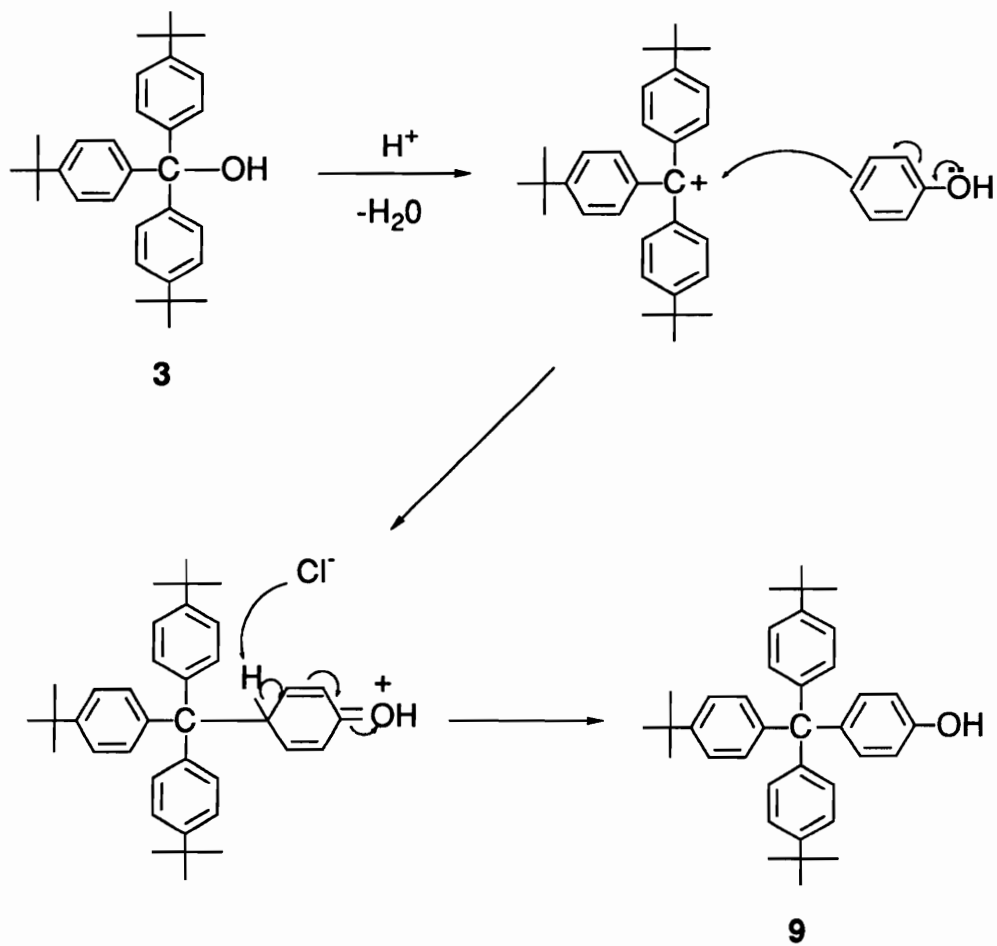
Scheme 2. Mechanism of the Grignard reaction



Scheme 3. Modification of **3** (carbanion chemistry)



Scheme 4. Modification of **3** (carbocationic process)



Scheme 5. Mechanism of the aromatic electrophilic substitution reaction

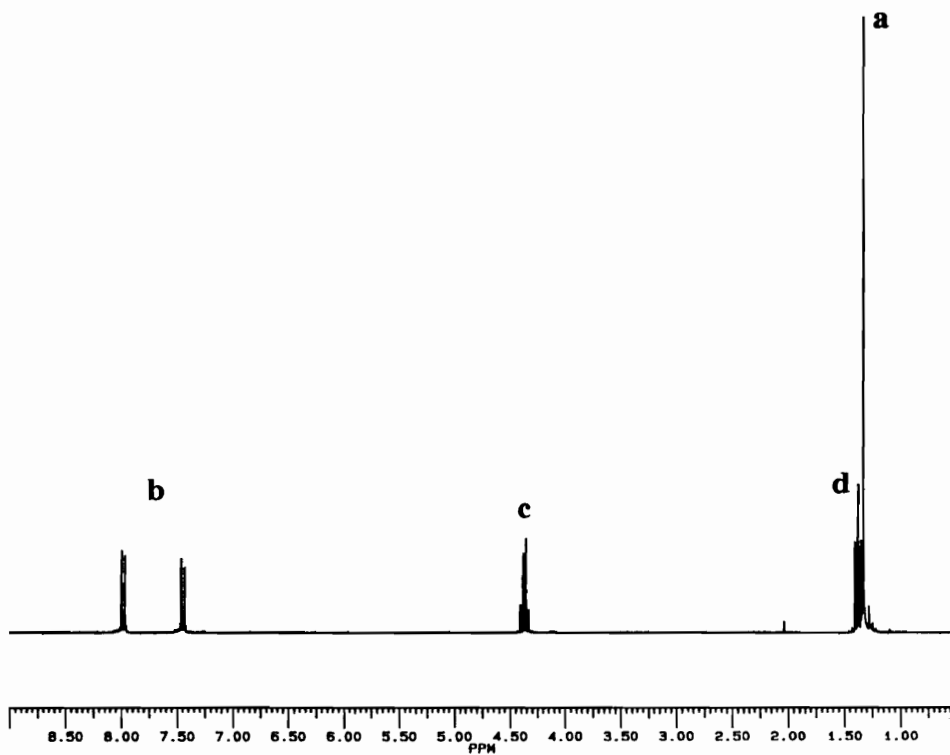
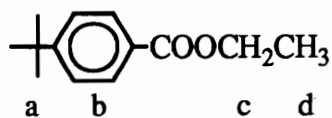


Figure 1. 270 MHz <sup>1</sup>H NMR spectrum of ethyl *p*-*t*-butylbenzoate (1) in CDCl<sub>3</sub>

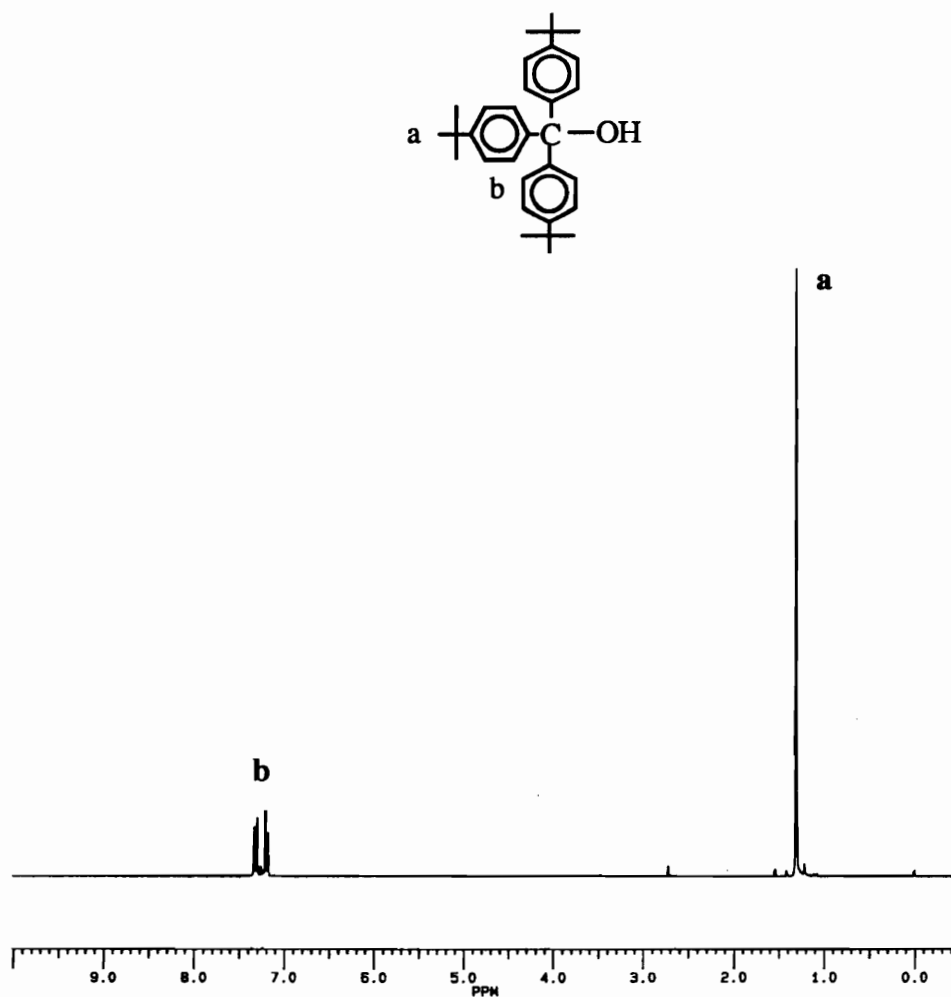


Figure 2. 270 MHz <sup>1</sup>H NMR spectrum of tris(*p*-*t*-butylphenyl)methanol (**3**) in CDCl<sub>3</sub>. The signal at 7.26 ppm is due to CDCl<sub>3</sub>

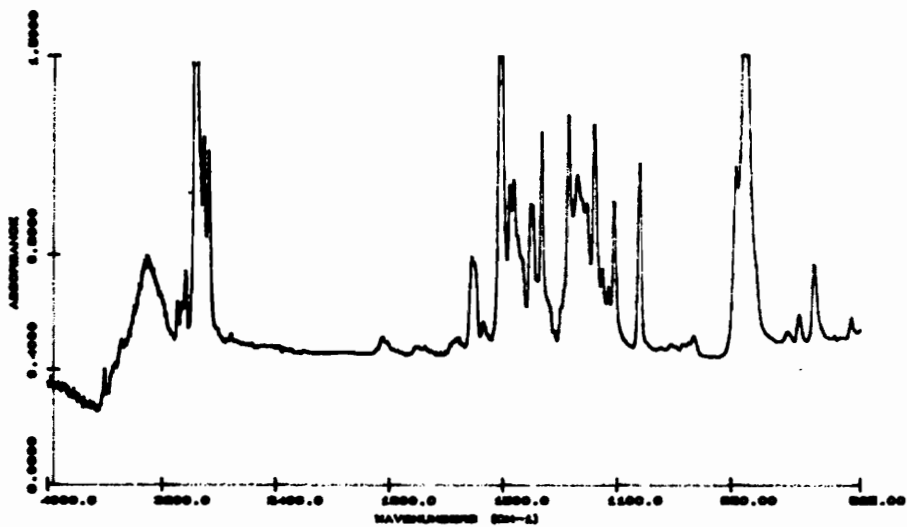


Figure 3. FTIR spectrum of tris(*p*-*t*-butylphenyl)(*p*'-hydroxyphenyl)methane (9) on KBr plate

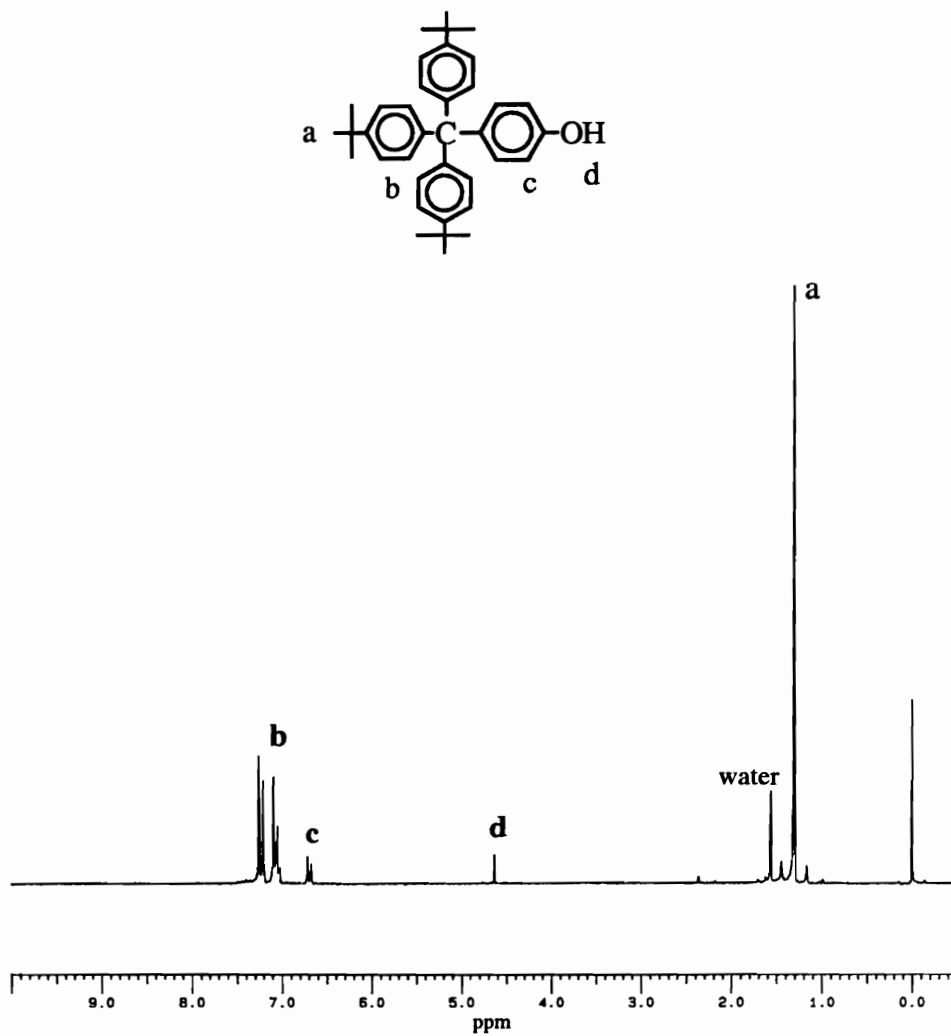


Figure 4. 270 MHz <sup>1</sup>H NMR Spectrum of tris(*p*-*t*-butylphenyl)(*p*'-hydroxyphenyl)methane (9) in CDCl<sub>3</sub>. The signal at 7.26 ppm is due to CDCl<sub>3</sub>



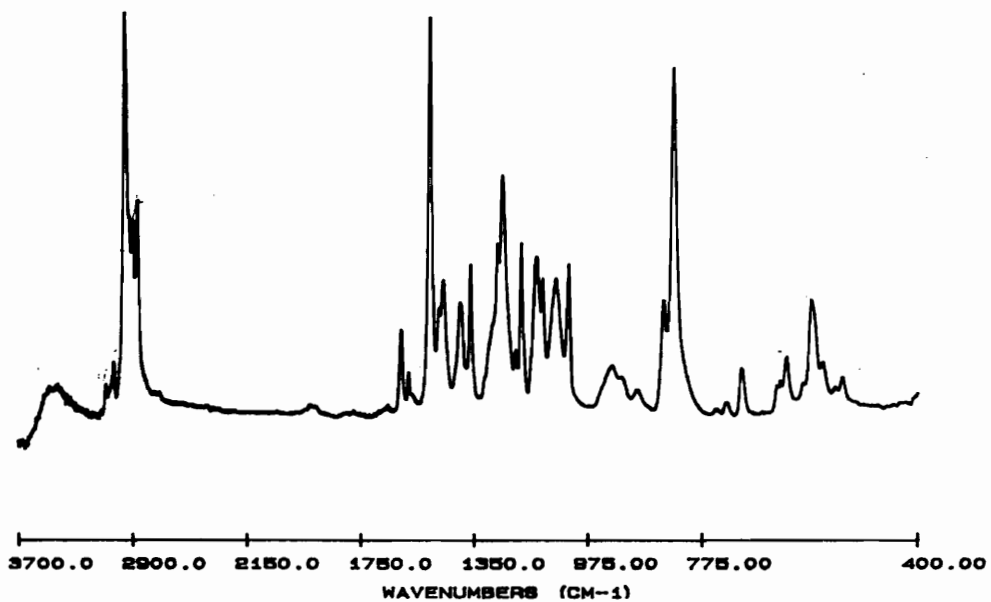


Figure 5. FTIR spectrum of Mono-*p*-[tris(*p'*-*t*-butylphenyl)methyl]phenyl ether of di(ethylene glycol) (**10**) on KBr plate

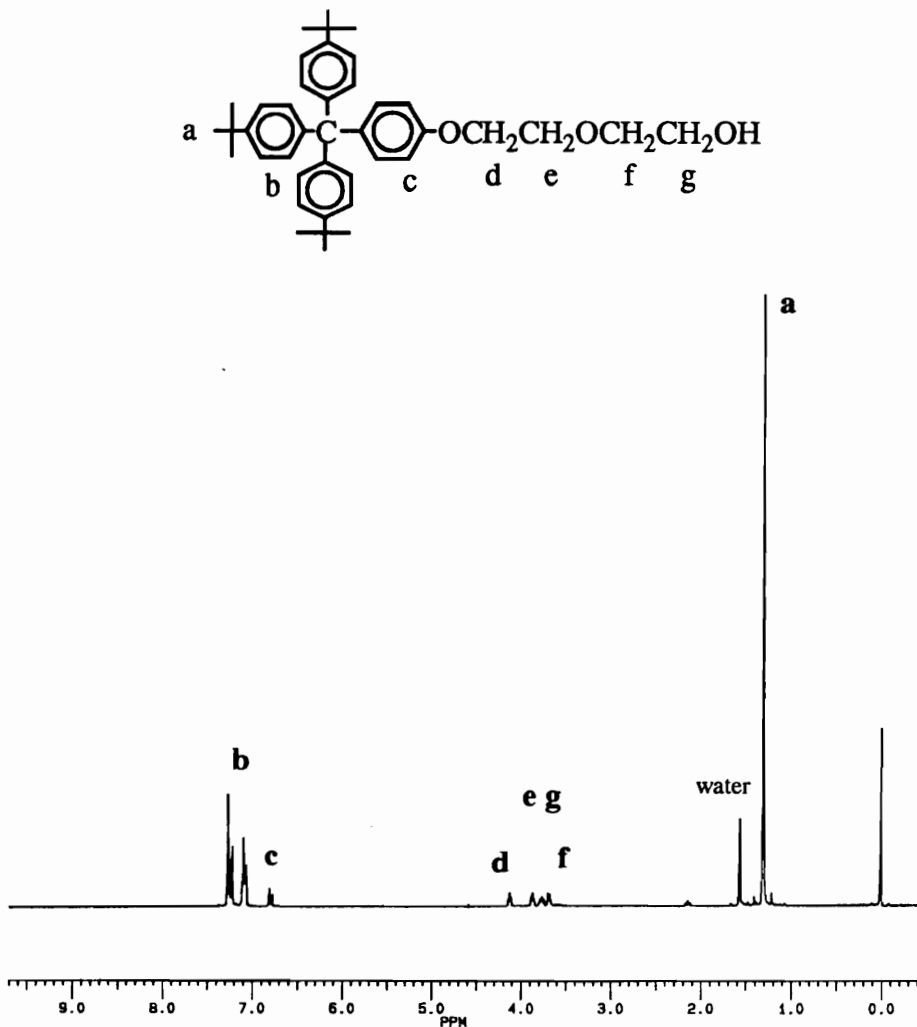


Figure 6. 270 <sup>1</sup>H NMR spectrum of mono-*p*-[tris(*p*'-*t*-butylphenyl)methyl]-phenyl ether of di(ethylene glycol) (**10**) in CDCl<sub>3</sub>. The signal at 7.26 ppm is due to CDCl<sub>3</sub>

**CHAPTER VI**  
**KNOTS FOR MOLECULAR STRINGS OF BEADS:**  
**DIFUNCTIONAL BLOCKING GROUPS**

Polyrotaxanes are supermolecular composites consisting of macrocycles whose cavities are pierced by linear polymer chains [1]. Triarylmethyl derivatives are a family of the monofunctional end blocking groups used in the polyrotaxane syntheses to prevent threaded macrocycles from dethreading [2]. However, the end capping of polymer chains by monofunctional blocking groups is often not complete and molecular weights of polyrotaxanes are reduced by addition of monofunctional blocking groups [3].

However, if the bulky groups can be polymerized into polymer backbones of polyrotaxanes, as depicted by Scheme 1, that is, using blocking groups **3** which have two functional groups to react with other monomers, **1** and **2**, during the polymerization process, we can permanently and completely constrain the macrocycles **4** onto polymer chains and obtain polyrotaxanes **5** with high molecular weights. Furthermore, it has been found that polyrotaxanes show interesting independent crystallization behavior due to the movement, aggregation and crystallization of threaded macrocycles along the polymer backbones [1, 3]. This movement could be limited by the incorporation of bulky spacers along the polymer chains. Such systems are micro-composites in which two immiscible components are held together by physical barriers. The difunctional bulky compounds can also form rotaxanes by their reactions with monofunctional blocking groups in the presence of macrocycles.

In this chapter, the syntheses and characterization of several difunctional blocking groups are reported [4]. All the compounds synthesized possess two or four *p-t*-butylphenyl moieties, which confer solubility while exerting a large steric influence, capable of constraining rings comprised up to 30 to 42 C, N, O, or S atoms.

## RESULTS AND DISCUSSION

### I. DIFUNCTIONAL BLOCKING GROUPS FOR STEP GROWTH POLYMERIZATION

#### A. $\alpha,\alpha,\omega,\omega$ -Tetraaryl- $\alpha,\omega$ -difunctional Blocking Groups

Similarly to the syntheses of monofunctional triarylmethyl derivatives [2], syntheses of difunctional blocking groups started from the reaction of  $\alpha,\omega$ -diesters **6** with the Grignard reagent **7** derived from *p*-bromo-*t*-butylbenzene in tetrahydrofuran (THF) (Scheme 2), using the procedure reported by Marvel et al. [5] and Stoddart et al. [6] and later by ourselves [2].

The starting material **6a** was prepared in 86 % yield by the reaction of ethyl *p*-hydroxybenzoate with 1,10-dibromodecane in absolute ethanol under reflux, using sodium to deprotonate the phenol [7]. The  $^1\text{H}$  NMR spectrum of **6a** is shown in Figure 1. Usually Grignard reactions require a cold bath to absorb the

heat generated during the formation of Grignard reagents. In our case, however, refluxing is needed due to the low reactivity of *p*-bromo-*t*-butylbenzene. Using iodine as an initiator for the formation of the Grignard reagent was avoided because it also catalyzes a Gomberg-Bachman reaction [2, 8]. Compounds **8a** - **8c** were obtained in 40 -72 % yields and were purified by recrystallization. Figures 2-4 are their <sup>1</sup>H NMR spectra.

Harrison investigated the steric influence of various blocking groups. He reacted di(cyclohexyl)acetyl chloride, triphenylmethyl chloride, and tris(*p-t*-butylphenyl)-methanol with 1,10-decanediol in the presence of a cyclic species [9] and found that these three blocking groups could constrain macrocycles comprised of up to 28, 29, and 42 methylene groups, respectively [10]. Therefore, the  $\alpha,\alpha,\omega,\omega$ -tetraaryl- $\alpha,\omega$ -diols **8a** and **8b** can constrain 42-membered rings because of their larger size compared to tris(*p-t*-butylphenyl)methanol. **8c** is also probably capable of blocking the loss of 42-membered rings.

However, diols **8** can not be used directly in the polyrotaxane syntheses because the steric hindrance around the functional group reduces the reactivities and also the resultant ether linkages are hydrolytically unstable. Therefore, it is necessary to have the functional groups remote from the region of steric hindrance. This was achieved by adding a spacer between the triarylmethyl moiety and the functional group. We studied carbocationic processes to incorporate the spacer and functional group.

There are two approaches for this purpose. One approach involves the conversion of the alcohol to the corresponding chloride by the reaction with acetyl chloride [5] followed by the Friedel-Crafts reaction with phenol, as reported by Mikroyannidis in his preparation of bis-(*p*-hydroxyphenyl)diphenylmethane [11]. Alternatively, we reported the direct reactions of tris(*p*-*t*-butylphenyl)methanol with an excess of phenol to produce *p*-substituted trityl phenolic blocking groups [2]. This approach is simpler compared to the first one and, therefore, was adopted in the present work, as shown in Scheme 3. The bisphenol **9** was generated (96 %) via a carbocationic process by refluxing **8a** in phenol, using HCl as a catalyst. This is an aromatic electrophilic substitution reaction involving attack on the para-position of phenol by the carbocation formed by the acid catalyzed ionization of the tetraaryldiol. Two additional phenyl rings in bisphenol **9** increase its crystallinity in comparison to its precursor, diol **8a**. Hence **9** was easily purified by recrystallization.

In the <sup>1</sup>H NMR spectrum of **9** (Figure 5) the central twelve protons of the decamethylene unit and the *t*-butyl protons (labelled **a**) appear at 1.29-1.47 δ. The four protons β to ether oxygens (labelled **b**) appear at 1.76 δ as a pentet. The OCH<sub>2</sub> protons (labelled **c**) occur as a four proton triplet at 3.93 δ. The hydroxyl protons (**g**) appear at 4.66 δ. The eight aromatic protons (labelled **d**) occur at 6.67 and 6.73 δ as two doublets. The remaining 24 aromatic protons (**e**) appear at 7.02 - 7.24 δ.

The attempt to synthesize a bisphenol by the reaction of **8b** with phenol, however, led to a product which showed virtually no solubility in any common

solvents. Consequently, purification and characterization efforts were severely hampered. The elemental analysis suggested the presence of impurities.

The reaction of **8c** with phenol, surprisingly, did not generate the expected bisphenol but instead produced  $\alpha,\alpha,\omega,\omega$ -tetraarylhexane **10** in 80 % yield (Scheme 4). The  $^1\text{H}$  NMR spectrum of **10** is shown in Figure 6. The mechanism of the reaction is not clear at this time, but plausibly could involve electron transfer from phenol to the triarylmethyl carbocation, followed by hydrogen atom abstraction. **10** can be converted via its dianion to other difunctional blocking groups by the addition of linear chains via nucleophilic substitution reactions of the type shown in our synthesis of monofunctional blocking groups [2] and can possibly form polyrotaxanes directly by  $\text{S}_{\text{N}}2$  reactions with dielectrophiles such as dihalides.

The bisphenolic blocking group **9** is itself useful. It has been incorporated into aliphatic polyester rotaxane backbones [see Chapter VII]. In fact, due to the lower reactivity of phenolic compared to alcoholic monomers the blocking groups are expected to occur in long sequences along polymer chains. Therefore, there is still enough freedom for the macrocycles to move along the polymer backbones so that both polymer backbone and macrocycle can aggregate and crystallize independently, the same as in the polyrotaxanes without bulky spacers in their polymer chains. Indeed this phenomenon has been observed by DSC measurement. The polyrotaxane with bulky spacers originating from the bisphenolic blocking group **9** showed two melting temperatures and two

crystallization temperatures, as did the polyrotaxane without blocking groups, while its linear model polymer showed only one.

On the other hand we also wished to have an aliphatic hydroxyl terminated difunctional blocking group. This was done by elaboration of the bisphenol **9**. **9** was allowed to react with an excess of di(ethylene glycol) monochloride in butanol at reflux, using an excess of  $K_2CO_3$  as a base, as shown in Scheme 5. The product **11** was obtained in 83 % yield and was purified by recrystallization in ethanol.

In the  $^1H$  NMR spectrum of **11** (Figure 7) the signal of the phenolic -OH protons of starting material **9** is not present. The terminal hydroxyl protons (labelled **j**) appear at 2.17  $\delta$  as a triplet. The protons of the ethyleneoxy units (labelled **h**, **i**, **g**, and **f**) occur at 3.67, 3.75, 3.85, and 4.11  $\delta$ . The signals of decamethylene protons and aromatic protons are similar to those of starting material **9** in Figure 5.

**11** will be utilized in polyester syntheses as a comonomer and the properties of the resultant polyrotaxanes will be compared with the polyrotaxanes synthesized using bisphenolic blocking group **9**. Unlike **9** which is incorporated in long sequences **11** is expected to be included more randomly along polymer chains due to its nearly equal reactivity with diol monomers. Therefore, the threaded macrocycles are expected to be randomly separated by the bulky spacer and their movement along polymer backbones will be limited. Accordingly,



independent crystallization of linear polymer chains and macrocycles may not occur, depending on the ability of aggregates of critical nucleation size to form.

## B. Diethyl Di(*p-t*-butylbenzyl)malonate

The Grignard approach for syntheses of difunctional blocking groups involves several steps and the final products are huge. A new smaller difunctional blocking group was synthesized via a one step route (Scheme 6). Diethyl malonate (**12**) is an ideal starting material for difunctional blocking group syntheses because it has two pairs of reactive sites: two methylene protons and two ester groups. The two pairs have different reactivity. Therefore, one can be used for the incorporation of bulky *t*-butylphenyl groups while the other can participate in polymerization. *p-t*-Butylbenzyl bromide (**13**) was chosen because of its size and its high reactivity toward nucleophiles without the side reaction of elimination. However, the blocking ability of the product **14** is reduced by the free rotation of the methylene group. It is only able to constrain rings comprised of up to 30 atoms, according to a CPK model study.

Antonioletti et al. found that reaction of dimethyl malonate with benzyl bromide in THF using lithium hydroxide gave mainly monoalkylation product [12]. Oediger and Möller demonstrated that use of 1,8-diazabicyclo[5,4,0]undec-7-en (DBU) in DMF gave 84 % dialkylation products [13]. However, application of the latter reaction conditions in our system did not generate the desired product. Therefore, we choose sodium ethoxide as a base and ethanol as a solvent. This condition prevents the hydrolysis or transesterification of the ester groups of the

malonate. Pure product was obtained by recrystallization in ethanol. The relatively low yield (55 %) was attributed to the fact that ethanol can solvate the enolate anion and thus reduce its reactivity as a nucleophile, leading to the monoalkylation [14]. However, the byproducts generated by the monoalkylation and O-alkylation were easily removed by the recrystallization due to their low symmetry.

Figure 8 is the  $^1\text{H}$  NMR spectrum of **14**. The ethyl protons appear at 1.13  $\delta$  (**a**) and 4.08  $\delta$  (**b**). The eighteen *t*-butyl protons appear at 1.29  $\delta$  (labelled **e**). The benzylic methylene protons occur as a four proton singlet at 3.18  $\delta$  (labelled **c**). The signals of the eight aromatic protons appear at 7.09-7.29  $\delta$  (**d**).

## II. A DIFUNCTIONAL BLOCKING GROUP FOR CHAIN GROWTH POLYMERIZATION

We now have phenolic (**9a**), anilinic (**9b**), alkanic (**10**), alcoholic (**11**), and esteric (**14**) difunctional blocking groups which can be used in step growth (condensation) polymerizations. We also wished to have difunctional blocking groups for chain growth (addition) polymerizations. These compounds should be soluble, possess enough steric influence to constrain large macrocycles, and be polymerizable. Compound **17** (Scheme 7) was designed to meet these requirements. Because it has two *p-t*-butylphenyl moieties, in rigid polymer chains such as polystyrene it can block 42-membered rings. The reaction of ethyl acetate (**15**) with Grignard reagent **7** generated di(*p-t*-butylphenyl)ethanol (**16**) in 67 % yield. The product was purified by recrystallization in a mixture of

toluene and hexane (1:2). Figure 9 is the  $^1\text{H}$  NMR spectrum of **16**. Removal of water from **16** under acidic conditions in refluxing toluene gave desired product **17** in 82 % yield. Water generated in the reaction was removed by a Dean-Stark trap to drive the equilibrium toward the product. **17** was purified by recrystallization in ethanol. The procedure was similar to the classical synthesis of 1,1-diphenylethene [15].

In the  $^1\text{H}$  NMR spectrum of compound **17** (Figure 10) the signal of the eighteen *t*-butyl protons appears at 1.34  $\delta$  (labelled **c**). The two vinyl protons appear as a singlet at 5.40  $\delta$  (**a**). The eight aromatic protons occur at 7.27-7.37  $\delta$  (labelled **b**).

## CONCLUSIONS

A series of three  $\alpha,\alpha,\omega,\omega$ -tetraaryl- $\alpha,\omega$ -dicarbinols (**8**) were synthesized via Grignard reactions. The tetraaryldicarbocations derived from the tetraaryldicarbinols (**8**) were utilized in aromatic electrophilic substitution reactions on phenol, producing tetraarylbisphenol **9**. Tetraarylhexane **10** was produced via the reaction of tetraarylhexanediol **8c** and phenol. Williamson ether synthesis was applied to tetraarylmethylbisphenol **9** to form aliphatic hydroxyl terminated difunctional compound **11**. Diethyl di(*p-t*-butylbenzyl)malonate (**14**) was synthesized in one step via two nucleophilic substitution reactions, starting from diethyl malonate. 1,1-Di(*p-t*-butylphenyl)ethene (**17**) was produced by the elimination of water from 1,1-di(*p-t*-butylphenyl)ethanol (**16**) which was prepared via a Grignard reaction. In summary, several difunctional blocking groups were successfully synthesized. These compounds and their intermediates, **8a**, **8b**, **8c**, **9**, **10**, **11**, **12**, **16**, and **17** are new compounds and all of them gave satisfactory  $^1\text{H}$  NMR,  $^{13}\text{C}$  NMR, IR spectra and elemental analysis or mass spectrometry results. While compounds **9**, **10**, **11**, **14** can be used in step growth polymerizations for polyrotaxanes and for preparation of rotaxanes by the reactions with monofunctional blocking groups, compound **17** is suitable for chain growth polymerizations.

## EXPERIMENTAL

**Measurements.** Melting points were taken in capillary tubes and have been corrected, Proton and carbon NMR spectra, reported in ppm, were obtained on 270 or 400 MHz spectrometers using chloroform-d solutions with tetramethylsilane as an internal standard. The following abbreviations have been used in describing the NMR spectra: s (singlet), d (doublet), t (triplet), q (quartet), p (pentet), sx (sextet), and m (multiplet); coupling constants are in Hz. FTIR or IR spectra, reported in  $\text{cm}^{-1}$ , were obtained using KBr pellets unless otherwise noted. Elemental analyses were performed by Atlantic Microlab of Norcross, GA.

**Starting materials.** THF and xylene were dried over Na/benzophenone and distilled just before use. Diethyl malonate and *p-t*-butylbenzyl bromide were dried over  $\text{CaCl}_2$  before use. The other compounds were used without purification as obtained from commercial sources.

### Clean granulated sodium

Lumps of sodium metal were immersed in dry xylene in an Erlenmeyer flask and heated carefully on an electric hot plate with gentle swirling until the sodium just melted and flowed away from the contaminating surface oxide. The flask was then removed from the hot plate and upon cooling the sodium melt solidified in globules which were then removed with a spatula to be immediately reimmersed under dry xylene in a preweighed reaction flask equipped with a condenser and a

magnetic stirrer. The flask was heated by an electric hot plate until the sodium melted. The stirrer was started and after the sodium was suitably granulated, the electric hot plate was removed. When the contents of the flask had cooled to room temperature, the stirrer was stopped. The flask was weighed. Excess sodium was taken out with a spatula and xylene was decanted.

### **1,10-Bis(*p*-carbethoxyphenoxy)decane (6a)**

To a 1 L 3-necked flask equipped with a condenser, a dropping funnel, a mechanical stirrer, and nitrogen inlet clean granulated sodium (11.5 g, 500 mmol) was added. Absolute ethanol (250 mL) was added dropwise. The mixture was heated to reflux and all sodium was reacted. The mixture was cooled until ethoxide commenced to separate out. Ethyl *p*-hydroxybenzoate (83.1 g, 500 mmol) was added slowly. The mixture was refluxed for 1 h and then cooled until phenoxide commenced to separate out. 1,10-Dibromodecane (75.0 g, 250 mmol) was added slowly and the mixture was refluxed for 4 h. After the mixture had been cooled to room temperature, it was poured into ice water (3 L). The product was filtered and washed with water and ethanol. The product was then recrystallized in ethanol to afford a white solid (87.0 g, 74 %), mp 109.8-110.7 °C (Lit.[7] 108.5-110 °C). <sup>1</sup>H NMR: 1.34-1.40 (m, 14 H, CH<sub>3</sub>CH<sub>2</sub>OOC-, -O(CH<sub>2</sub>)<sub>3</sub>(CH<sub>2</sub>)<sub>2</sub>-), 1.46 (p, J = 7, 4 H, -OCH<sub>2</sub>CH<sub>2</sub>CH<sub>2</sub>-), 1.80 (p, J = 7, -OCH<sub>2</sub>CH<sub>2</sub>-), 4.00 (t, J = 7, -OCH<sub>2</sub>CH<sub>2</sub>-), 4.33 (q, J = 7, CH<sub>3</sub>CH<sub>2</sub>OOC-), 6.89-7.99 (m, 8 H, arom.).

**General Procedure for Grignard Reactions: 1,10-Bis(*p*-[di(*p*'-*t*-butylphenyl)hydroxymethyl]phenoxy)decane (8a)**

In an oven dried 500 mL 3-necked flask equipped with a condenser, a dropping funnel, a mechanical stirrer, and nitrogen system were placed magnesium turnings (8.75 g, 360 mmol) with dry THF (Na/benzophenone) (90 mL). *p*-t-Butylbromobenzene (63.9 g, 300 mmol) in dry THF (60 mL) was added dropwise over 1 h. The flask was heated to initiate the reaction. The charge rate of *p*-t-butylbromobenzene was adjusted so that the mixture kept refluxing. The reaction was allowed to go for 2 h at room temperature. A brown color was observed. **6a** (31.4 g, 66.7 mmol) in dry THF (60 mL) was added dropwise. The mixture was stirred at reflux under nitrogen for 12 h. After the solution had been cooled to room temperature, it was neutralized by 5 % HCl (1.5 L) at 0 °C. The organic layer was separated from the aqueous layer in a separation funnel. After solvents had been removed by rotary evaporation, a sticky green solid was obtained. The solid (60.9 g) was recrystallized in a mixture of hexane and ethyl acetate (8:1) 3 times to afford a white powder (33.6 g, 56 %), mp 130.5-132.0 °C. IR: 3560, 2950, 2850, 1610, 1500, 1470, 1250, 1180, 1020, 830, 580. <sup>1</sup>H NMR: 1.30-1.48 (m, 48 H, *t*-butyl, -(CH<sub>2</sub>)<sub>3</sub>(CH<sub>2</sub>)<sub>2</sub>O-), 1.76 (p, J = 7, 4 H, -CH<sub>2</sub>CH<sub>2</sub>O-), 2.69 (s, 2 H, -OH), 3.93 (t, J = 7, 4 H, -CH<sub>2</sub>O-), 6.80-7.32 (m, 24 H, arom.). <sup>13</sup>C NMR: 26.0, 29.2, 29.3, 29.4, 31.3, 34.3, 67.8, 81.3, 113.5, 124.6, 127.4, 129.0, 139.2, 144.2, 149.7, 158.0 (16 signals as required). Anal. calculated for C<sub>64</sub>H<sub>82</sub>O<sub>4</sub>: C, 83.98; H, 9.03; found: C, 83.71; H, 9.04.

### **1,4-Bis[di(*p*-*t*-butylphenyl)hydroxymethyl]benzene (8b)**

**8b** was prepared from 4-bromo-*tert*-butylbenzene and dimethyl terephthalate (**6b**). The product was crystallized from toluene, 16.7 g (40 % yield), mp 291.5-295.5 °C (Lit. [12] mp. ). IR: 3566, 3027, 2959, 2903, 2869, 1508, 1502, 834, 818. <sup>1</sup>H-NMR: 1.30 (s, 36 H, *t*-butyl), 2.75 (s, 2 H, OH), 7.18 (d, J = 9, 8 H, arom.), 7.21 (s, 4 H, arom.), 7.31 (d, J = 9, 8 H, arom.). <sup>13</sup>C NMR: 31.3, 34.4, 81.5, 124.7, 127.3, 127.5, 143.9, 145.8, 149.9 (9 signals as required).

### **1,1,6,6-Tetra(*p*-*t*-butylphenyl)-1,6-hexanediol (8c)**

**8c** was prepared from 4-bromo-*tert*-butylbenzene and dimethyl adipate (**6c**). The product was crystallized from toluene, 10.5 g (72 %), mp. 259.7-260.6 °C. IR: 3592, 3036, 2959, 1911, 1510, 1468, 1405, 1363, 1271, 1201, 1110, 1018, 976, 864, 835, 828, 709, 653, 582, 547. <sup>1</sup>H NMR: 1.29 (m, 40 H, *t*-butyl and -CH<sub>2</sub>(CH<sub>2</sub>)<sub>2</sub>CH<sub>2</sub>-), 2.01 (s, 2 H, -OH), 2.20 (t, J = 7, 4 H, -CH<sub>2</sub>(CH<sub>2</sub>)<sub>2</sub>CH<sub>2</sub>-), 7.29 (s, 16 H, arom.). <sup>13</sup>C NMR: 22.1, 31.3, 34.4, 42.1, 78.0, 124.9, 125.6, 144.1, 149.4 (9 signals as required). Anal. calculated for C<sub>46</sub>H<sub>62</sub>O<sub>2</sub>: C, 85.53; H, 9.52; found: C, 85.33; H, 9.62.

### **1,1-Di(*p*-*t*-butylphenyl)ethanol (16)**

**16** was prepared from 4-bromo-*t*-butylbenzene and ethyl acetate. The product was crystallized three times in a mixture of hexane and toluene, 20.6 g (67 %),



mp 138.7-139.9 °C. IR: 3560, 2960, 2860, 1400, 1270, 1170, 1090, 1020, 910, 840, 810, 690, 580. <sup>1</sup>H NMR: 1.30 (s, 18 H, t-butyl), 1.94 (s, 3 H, methyl), 2.13 (s, 1 H, -OH), 7.33 (m, 8 H, arom.). <sup>13</sup>C NMR: 30.9, 31.3, 34.4, 75.9, 124.9, 125.4, 145.1, 149.6 (8 signals as required). Anal. calculated for C<sub>22</sub>H<sub>30</sub>O: C, 85.11; H, 9.74; found: C, 85.12; H, 9.78.

**1,10-Bis{*p*-[di(*p*'-*t*-butylphenyl)-(*p*''-hydroxyphenyl)methyl]phenoxy}decane (9)**

**8a** (13.4 g, 14.6 mmol) was dissolved in phenol (48.4 g, 514 mmol) by warming in a 500 mL 1-necked flask equipped with a condenser and nitrogen system. HCl (36 %, 1.0 mL) was added as a catalyst. A deep reddish color was observed immediately. The mixture was heated at reflux for 24 h. After the system had been cooled to room temperature, the product was boiled in water, dissolved in toluene (200 mL), extracted with aqueous NaOH (20 g/L, 5 x 250 mL) and water (3 x 250 mL). A brown solid (14.9 g, 96 %) was obtained after toluene had been removed. The solid was recrystallized in a mixture of ethyl acetate and toluene (4:1) 3 times to afford a white solid, mp 162.5-165.7 °C. IR: 3400, 2940, 2840, 1600, 1490, 1240, 1170, 1010, 830, 590. <sup>1</sup>H NMR: 1.29-1.47 (m, 48 H, t-butyl, -(CH<sub>2</sub>)<sub>3</sub>(CH<sub>2</sub>)<sub>2</sub>O-), 1.76 (p, J = 7, 4 H, -CH<sub>2</sub>CH<sub>2</sub>O-), 3.92 (t, J = 7, 4 H, -CH<sub>2</sub>O-), 4.66 (s, 2 H, -OH), 6.68-7.27 (m, 32 H, arom.). <sup>13</sup>C NMR: 26.0, 29.2, 29.3, 29.4, 31.3, 34.2, 62.7, 67.8, 112.9, 113.9, 124.0, 130.5, 132.0, 132.3, 139.3, 139.8, 144.1, 148.2, 153.2, 156.8 (20 signals as required). Anal. calculated for C<sub>76</sub>H<sub>90</sub>O<sub>4</sub>: C, 85.51; H, 8.50; found: C, 85.26; H, 8.43.

## Attempted Synthesis of 1,4-Bis[di(*p-t*-butylphenyl)-*p'*-hydroxyphenylmethyl] benzene

**8b** (1.46 g, 2.19 mmol) was dissolved in phenol (7.21 g, 76.7 mmol) by refluxing at 150 °C in a 100 mL 1-necked flask equipped with a condenser and nitrogen system. HCl (36 %, 0.2 mL) was added as a catalyst. A deep reddish color was observed immediately. The mixture was refluxed for 24 h. During the reaction, some solids precipitated out of the solution. After the system had been cooled to room temperature, the product was boiled in CH<sub>2</sub>Cl<sub>2</sub> (200 mL). The product was not soluble in CH<sub>2</sub>Cl<sub>2</sub>. The CH<sub>2</sub>Cl<sub>2</sub> solution was extracted with NaOH aqueous solution (20 g/L, 5 x 150 mL) and water (3 x 150 mL). A pale yellow solid (1.69 g, 94 %) was obtained after CH<sub>2</sub>Cl<sub>2</sub> had been removed. The solid showed virtually no solubility in any common solvents and did not melt up to 413 °C. The solid was then washed with solvents at boiling including hexane, ethyl acetate, cyclohexane, toluene, ethanol, CH<sub>2</sub>Cl<sub>2</sub>, and THF and then was vacuum dried. Anal. calculated for C<sub>59</sub>H<sub>66</sub>O<sub>2</sub>: C, 87.97; H, 8.12; found: C, 44.35; H, 6.43.

## 1,1,6,6-Tetra(*p-t*-butylphenyl)hexane (**10**)

**10** was prepared from 1,1,6,6-tetra(*p-t*-butylphenyl)-1,6-hexanediol (**8c**) and phenol. The product was crystallized in a mixture of hexane and ethanol, 1.54 g (80 %), mp 231.7-232.3 °C. IR: 2965, 2865, 1515, 1465, 1370, 1275, 1110, 1020, 820, 810, 590. <sup>1</sup>H NMR: 1.27 (m, 40 H, *t*-butyl, Ar<sub>2</sub>CHCH<sub>2</sub>CH<sub>2</sub>-), 1.95 (sx, J = 8, 4 H, Ar<sub>2</sub>CHCH<sub>2</sub>-), 3.75 (t, J = 8, 2 H, Ar<sub>2</sub>CH-), 7.15-7.27 (m, 16 H, arom.). <sup>13</sup>C NMR: 27.8, 31.3, 34.2, 35.6, 50.3, 125.0, 127.3, 142.3, 148.4 (9

signals as required). Anal. calculated for C<sub>46</sub>H<sub>62</sub>: C, 89.84; H, 10.16; found: C, 89.61; H, 10.22.

**1,10-Bis{*p*-(di[*p*'-*t*-butylphenyl]-[*p*''-2-(2'-hydroxyethoxy)ethoxy]phenyl methyl) phenoxy}decane (11)**

**9** (2.00 g, 1.87 mmol) was dissolved in butanol (50 mL) by heating in a 250 mL one-necked flask equipped with a condenser and a magnetic stirring bar. K<sub>2</sub>CO<sub>3</sub> (5.67 g, 41.0 mmol) in water (15 mL) was added and the mixture was refluxed for 2 h. 2-(2'-Chloroethoxy)ethanol (7.30 g, 58.6 mmol) in butanol (10 mL) was added. The mixture was refluxed for 6 days. After it had been cooled to room temperature, the mixture was dissolved in methylene chloride (50 mL) and washed with water (2 x 50 mL). A transparent oil was obtained after methylene chloride had been removed. The oil was recrystallized in ethanol 3 times to afford a white solid (1.93 g, 83%), mp 146.7-151.2 °C. IR: 3500, 3080, 3000, 2900, 1630, 1520, 1420, 1385, 1270, 1205, 1150, 1080, 840. <sup>1</sup>H NMR: 1.29-1.47 (m, 48 H, *t*-butyl, -(CH<sub>2</sub>)<sub>3</sub>(CH<sub>2</sub>)<sub>2</sub>O-), 1.76 (p, J = 7, 4 H, -(CH<sub>2</sub>)<sub>3</sub>CH<sub>2</sub>CH<sub>2</sub>O-), 2.17 (t, J = 6, 2 H, -OH), 3.67 (t, J = 5, 4 H, HOCH<sub>2</sub>CH<sub>2</sub>-), 3.75 (m, 4 H, -CH<sub>2</sub>OH), 3.85 (t, J = 5, 4 H, HOCH<sub>2</sub>CH<sub>2</sub>OCH<sub>2</sub>-), 3.92 (t, J = 7, 4 H, -CH<sub>2</sub>OAr-), 4.11 (t, J = 5, 4 H, HOCH<sub>2</sub>CH<sub>2</sub>OCH<sub>2</sub>CH<sub>2</sub>-), 6.73-7.23 (m, 32 H, arom.). <sup>13</sup>C NMR: 26.0, 29.3, 29.4, 29.5, 31.3, 34.2, 61.7, 62.7, 67.1, 67.8, 69.7, 72.5, 112.9, 113.0, 124.0, 130.6, 132.0, 132.1, 139.2, 140.0, 144.1, 148.2, 156.3, 156.9 (24 signals as required). Anal. calculated for C<sub>84</sub>H<sub>106</sub>O<sub>8</sub>: C, 81.12; H, 8.59; found: C, 81.01; H, 8.67.

### Diethyl Di(*p*-*t*-butylbenzyl)malonate (14)

To a 100 mL 3-necked flask equipped with a magnetic stirrer, a dropping funnel, and a condenser, clean sodium (2.02 g, 88 mmol) was added. Absolute ethanol (15 mL) was added dropwise. The mixture was heated to reflux and all the sodium was reacted. The mixture was then cooled until ethoxide commenced to separate out. Diethyl malonate (4.70 g, 29.4 mmol) was added dropwise. The mixture was then refluxed for 2 h. The solution was cooled. When the malonate salt commenced to separate out, *p*-*t*-butylbenzylbromide was added dropwise. The mixture was refluxed for 19 h. After it had been cooled to room temperature, the mixture was poured into water (500 mL). The crystals formed were recrystallized in ethanol (7.2 g, 55 %), mp 84.9-86.6 °C. IR: 2850, 2760, 1725, 1510, 1360, 1265, 1190, 1170, 1650, 860, 810, 570. <sup>1</sup>H NMR: 1.13 (t, J = 7, 6 H, CH<sub>3</sub>CH<sub>2</sub>OOC-), 1.29, (s, 18 H, *t*-butyl), 3.18 (s, 4 H, C<sub>6</sub>H<sub>4</sub>-CH<sub>2</sub>-), 4.08 (q, J = 7, 4 H, CH<sub>3</sub>CH<sub>2</sub>-), 7.09-7.29 (m, 8 H, arom.). <sup>13</sup>C NMR: 13.8, 31.3, 34.3, 38.4, 60.2, 61.1, 125.0, 129.8, 133.2, 149.5, 171.1 (11 signals as required). Anal. calculated for C<sub>29</sub>H<sub>40</sub>O<sub>4</sub>: C, 76.95; H, 8.91; found: C, 77.21, H, 8.90.

### 1,1-Di(*p*-*t*-butylphenyl)ethene (17)

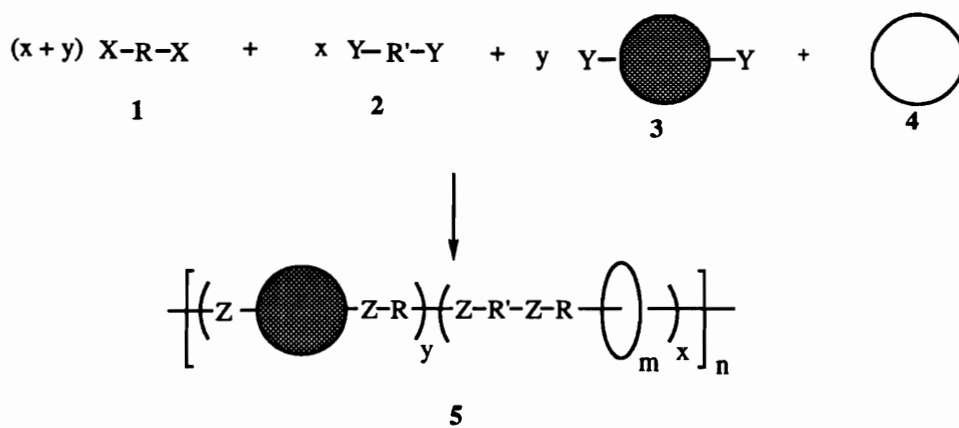
**16** (3.00 g, 9.66 mmol) was dissolved in toluene (50 mL) in a 100 mL 3-necked flask equipped with a Dean-Stark trap, a condenser, and a magnetic stirrer. Phosphoric acid (10.1 g, 87.6 mmol) was added. The mixture was then refluxed over night. After the mixture had been cooled to room temperature, it was filtered and a yellow solid was discarded. A white powder was obtained after toluene

had been removed from the filtrate. The product was recrystallized in ethanol twice to afford a white solid (2.30 g, 82 %), mp 100.8-101.6 °C. IR: 3080, 2960, 2870, 1840, 1685, 1605, 1470, 1370, 1275, 1120, 920, 845, 620, 580. <sup>1</sup>H NMR: 1.34 (s, 18 H, t-butyl), 5.40 (s, 2 H, vinyl), 7.27-7.37(m, 8 H, arom.). <sup>13</sup>C NMR: 31.3, 34.5, 113.1, 124.9, 127.9, 138.6, 149.5, 150.6 (8 signals as required). Anal. calculated for C<sub>22</sub>H<sub>28</sub>: C, 90.35; H, 9.65; found: C, 90.32; H, 9.62.

## REFERENCES

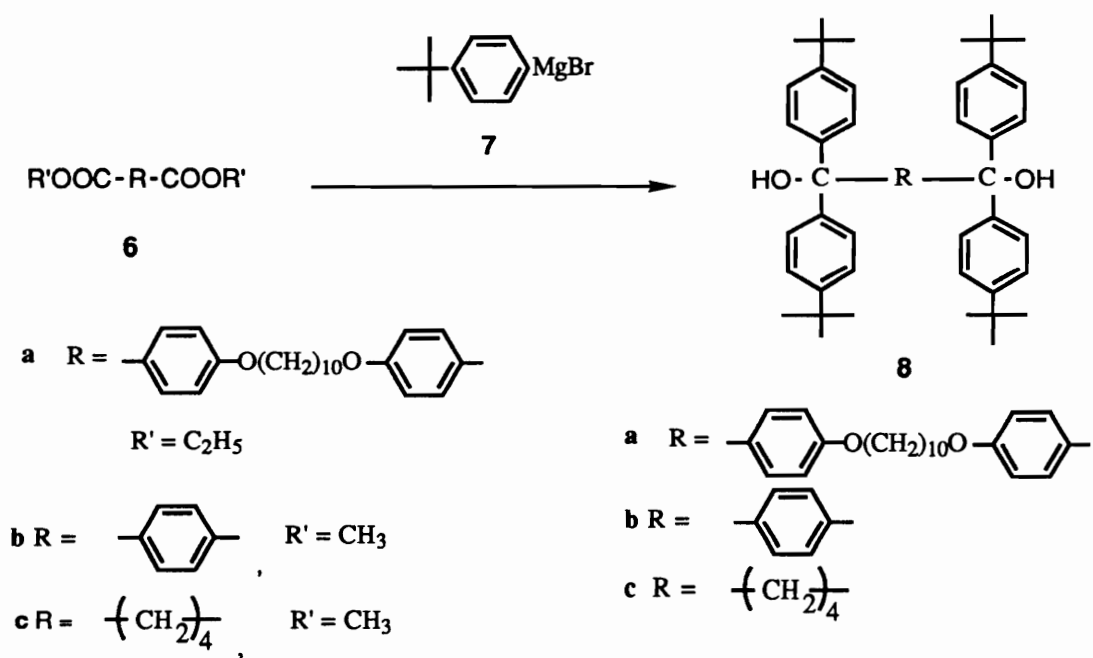
1. Gibson, H. W.; Marand, H. *Adv. Mater.* **1993**, *5*, 11; Gibson, H. W.; Bheda, M. C.; Engen, P. T. *Prog. Polym. Sci.* **1994**, *19*, 843; Shen, Y. X.; Xie, D.; Gibson, H. W. *J. Am. Chem. Soc.* **1994**, *116*, 537.
2. Gibson, H. W.; Lee, S-H.; Engen, P. T.; Lecavalier, P.; Sze, J.; Shen, Y. X.; Bheda, M. C. *J. Org. Chem.* **1993**, *58*, 3748.
3. Gibson, H. W.; Liu, S.; Lecavalier, P.; Wu, C.; Shen, Y. X. *J. Am. Chem. Soc.*, **1995**, *117*, in press.
4. The contents of this chapter have been reported: Liu, S.; Gibson, H. W.; *Tetrahedron Lett.*, **1994**, *35* (46), 8533; Liu, S.; Lee, S-H.; Shen, Y. *J. Org. Chem.*, accepted.
5. Marvel, C.S.; Kaplan, J. F.; Himel, C. M.; *J. Am. Chem. Soc.* **1941**, *63*, 1892.
6. Ashton, P. R.; Philp, D.; Spencer, N.; Stoddart, J. F. *J. Chem. Soc. Chem. Commun.* **1992**, 1124.
7. Bonahoe, H. B.; Benjamin, L. E.; Fennoy, L. V.; Greiff, D. J. *J. Org. Chem.* **1961**, *26*, 474.
8. Bachmann, W. E.; Shankland, R. V. *J. Am. Chem. Soc.* **1929**, *51*, 306; Gomberg, M.; Van Natta, F. J. *J. Am. Chem. Soc.* **1929**, *51*, 2238.
9. Harrison, I. T.; Harrison, S. *J. Am. Chem. Soc.* **1967**, *89*, 5732.
10. Harrison, I. T. *J. Chem. Soc. Chem. Commun.* **1972**, 231; Harrison, I, T. *J. Chem. Soc. Perkin 1* **1974**, 301.
11. Mikroyannidis, J. A. *Eur. Polym. J.* **1985**, *10*, 895.

12. Antonioletti, R.; Bonadies, F.; Orelli, L. R.; Scettri, A. *Gazz. Chim. Ital.* **1992**, *122*, 237.
13. Oediger, H.; Möller, F. *Liebigs Ann. Chem.* **1976**, 348.
14. House, H. O. "*Modern Synthetic Reactions*", 2nd, ed. Benjamin, Menlo Park, CA, **1972**, pp 492-546.
15. Blatt, A. H. "*Organic Synthesis*", Coll. Vol. 1, 2nd. ed., New York, Wiley & Sons, **1972**, p. 226.

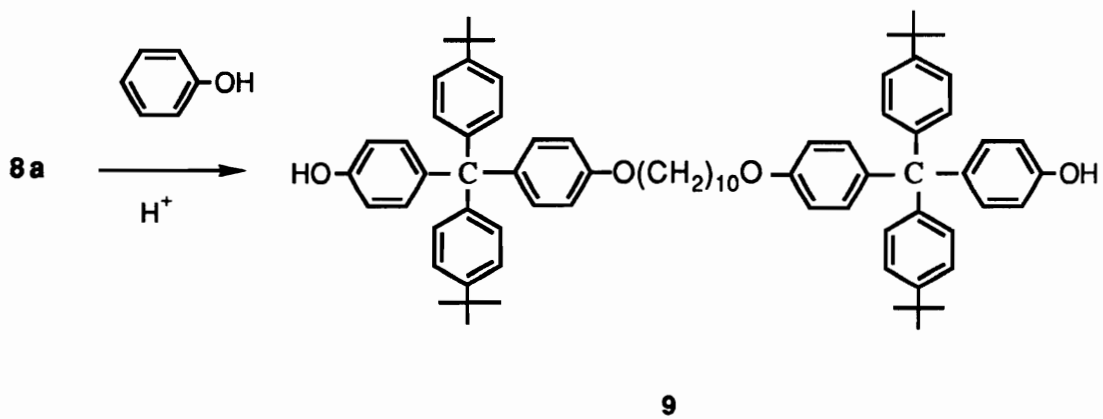


Scheme 1. Syntheses of molecular strings of beads with knots

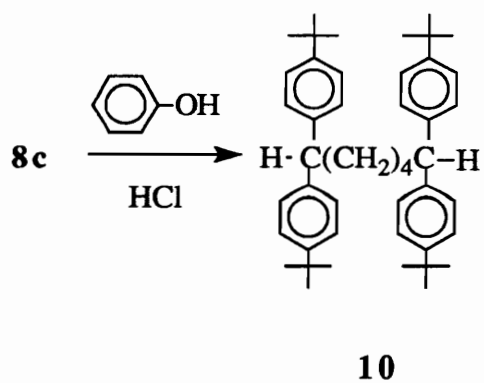




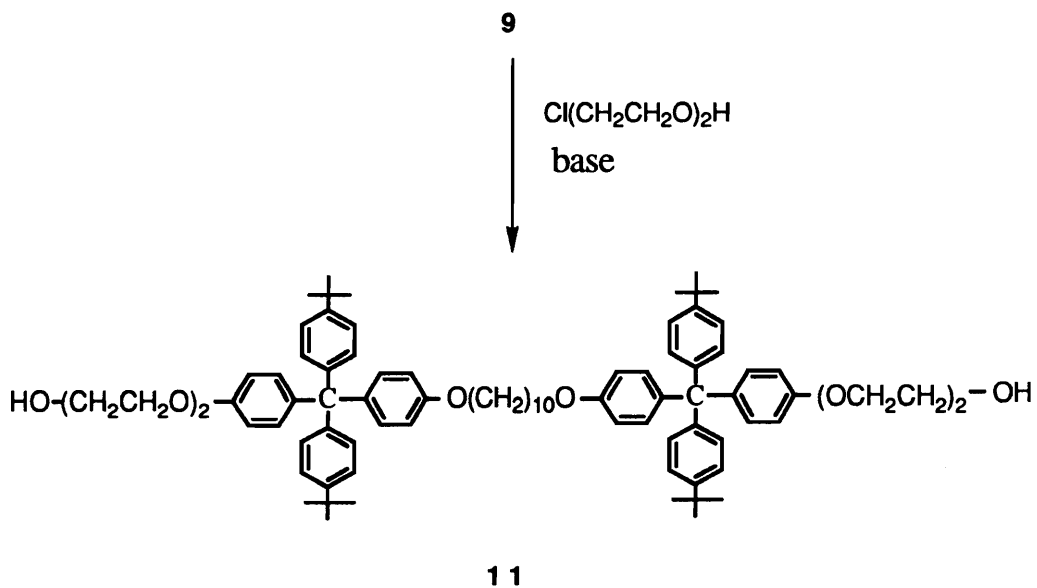
Scheme 2. Syntheses of **8**



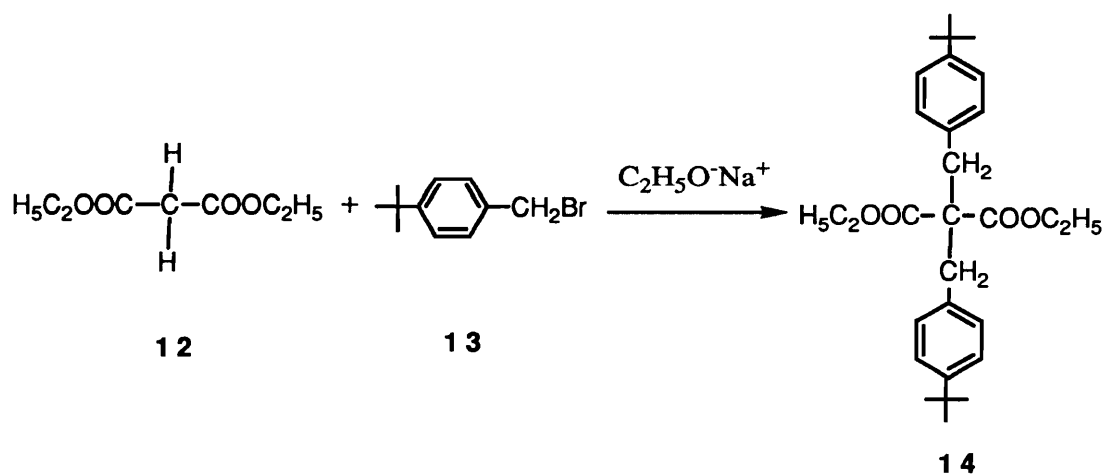
Scheme 3. Synthesis of **9**



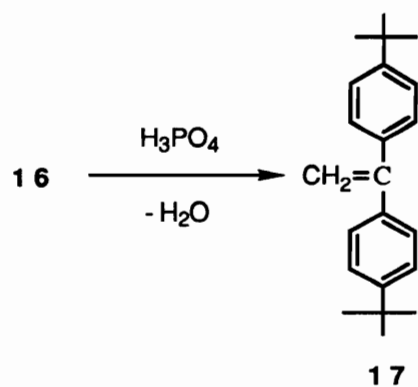
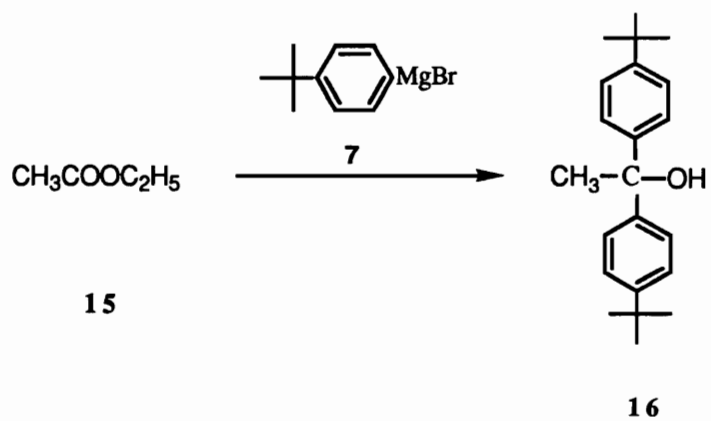
Scheme 4. Synthesis of **10**



Scheme 5. Synthesis of **11**



Scheme 6. Synthesis of **14**



Scheme 7. Synthesis of 17

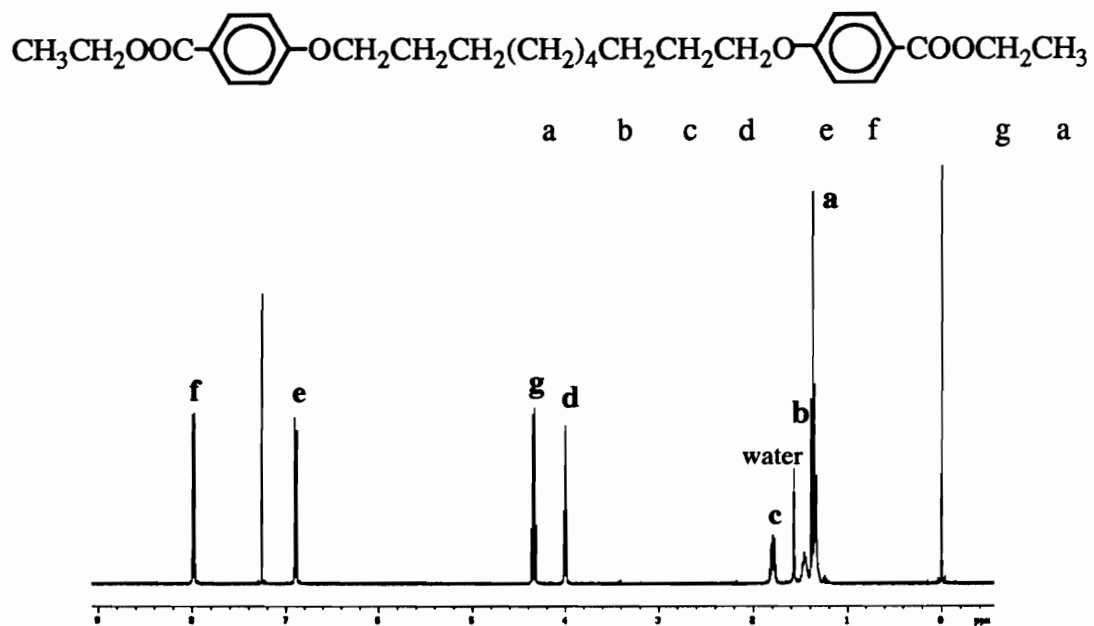


Figure 1. 400 MHz  $^1\text{H}$  NMR spectrum of **6a** in  $\text{CDCl}_3$ . The signal at 7.26 ppm is due to  $\text{CDCl}_3$

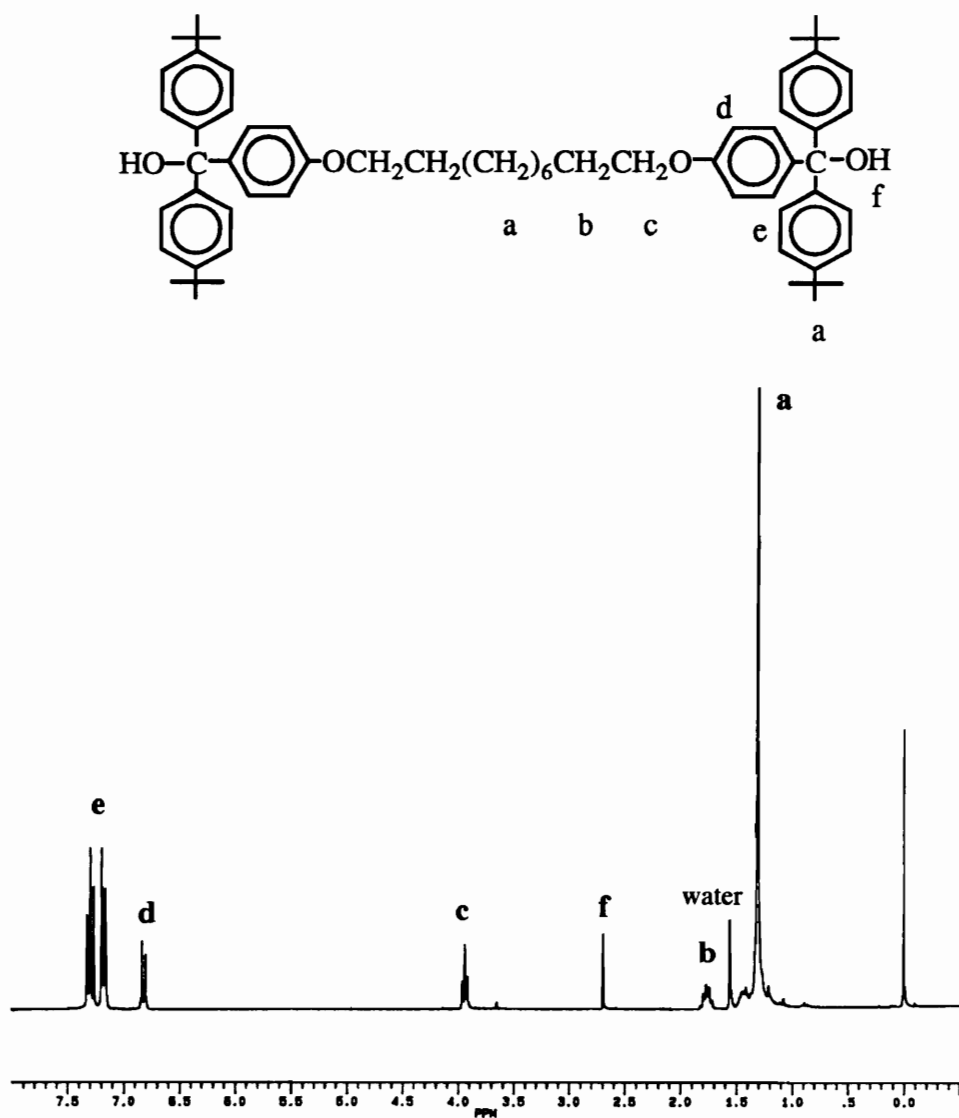


Figure 2. 270 MHz <sup>1</sup>H NMR spectrum of **8a** in CDCl<sub>3</sub>. The signal at 7.26 ppm is due to CDCl<sub>3</sub>

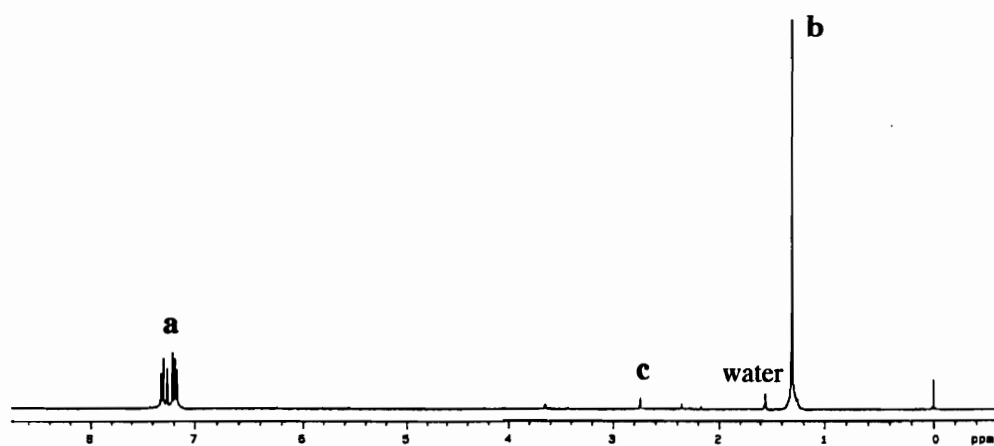
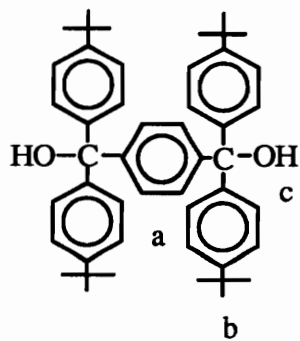


Figure 3. 400 MHz <sup>1</sup>H NMR spectrum of **8b** in CDCl<sub>3</sub>. The signal at 7.26 ppm is due to CDCl<sub>3</sub>

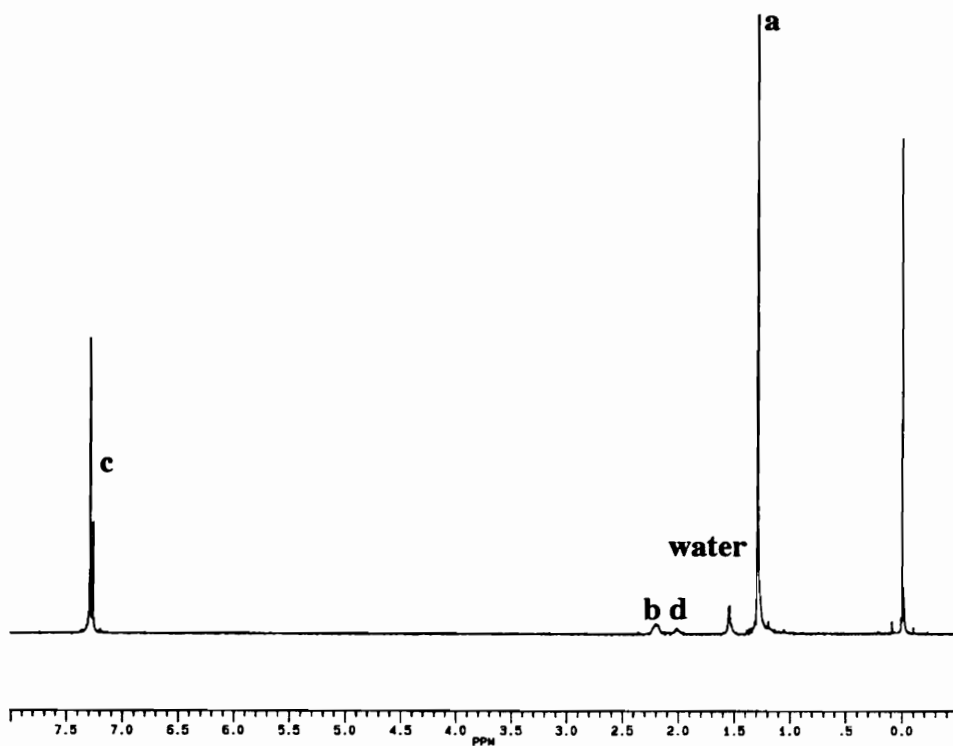
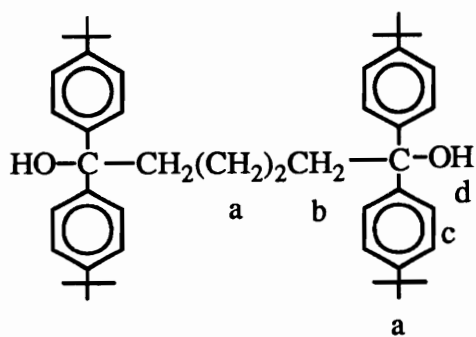


Figure 4. 400 MHz  $^1\text{H}$  NMR spectrum of **8c** in  $\text{CDCl}_3$ . The signal at 7.26 ppm is due to  $\text{CDCl}_3$



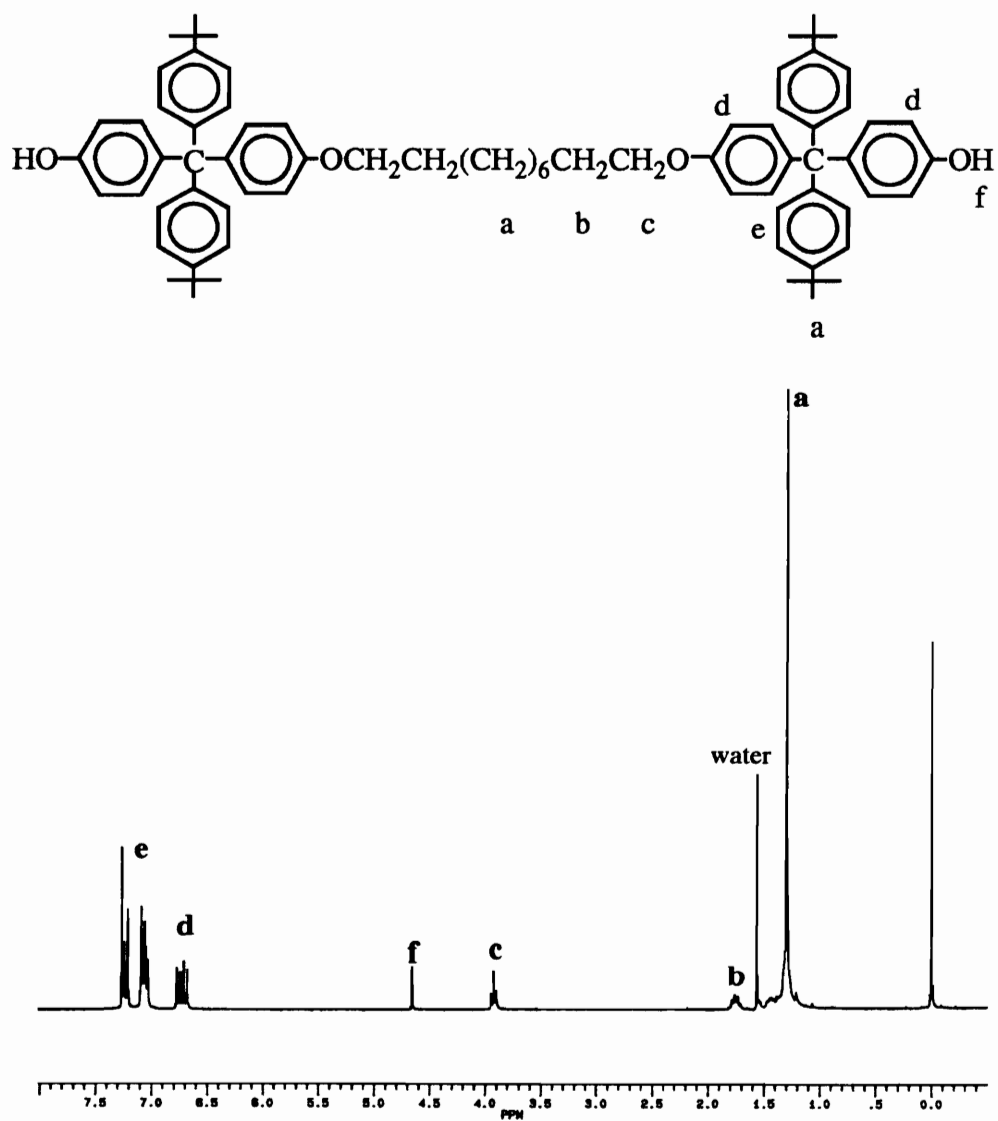


Figure 5. 270 MHz  $^1\text{H}$  NMR spectrum of **9** in  $\text{CDCl}_3$ . The signal at 7.26 ppm is due to  $\text{CDCl}_3$

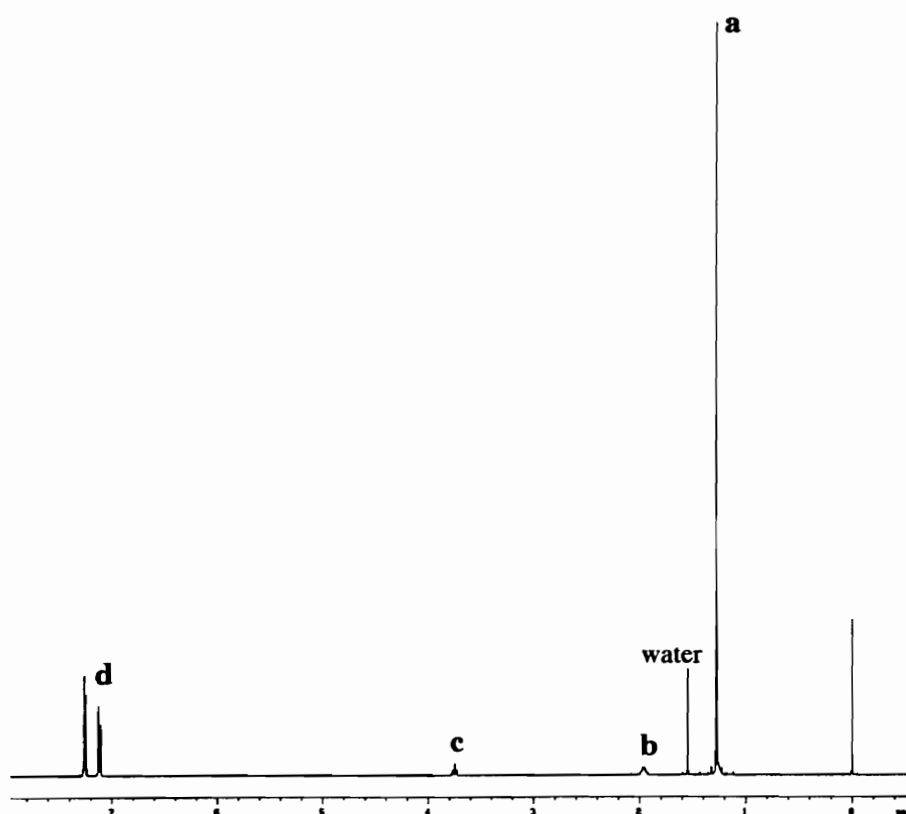
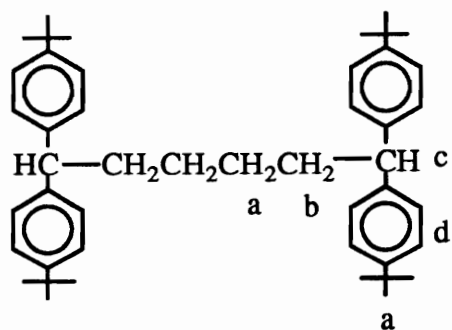


Figure 6. 270 MHz  $^1\text{H}$  NMR spectrum of **10** in  $\text{CDCl}_3$ . The signal at 7.26 ppm is due to  $\text{CDCl}_3$

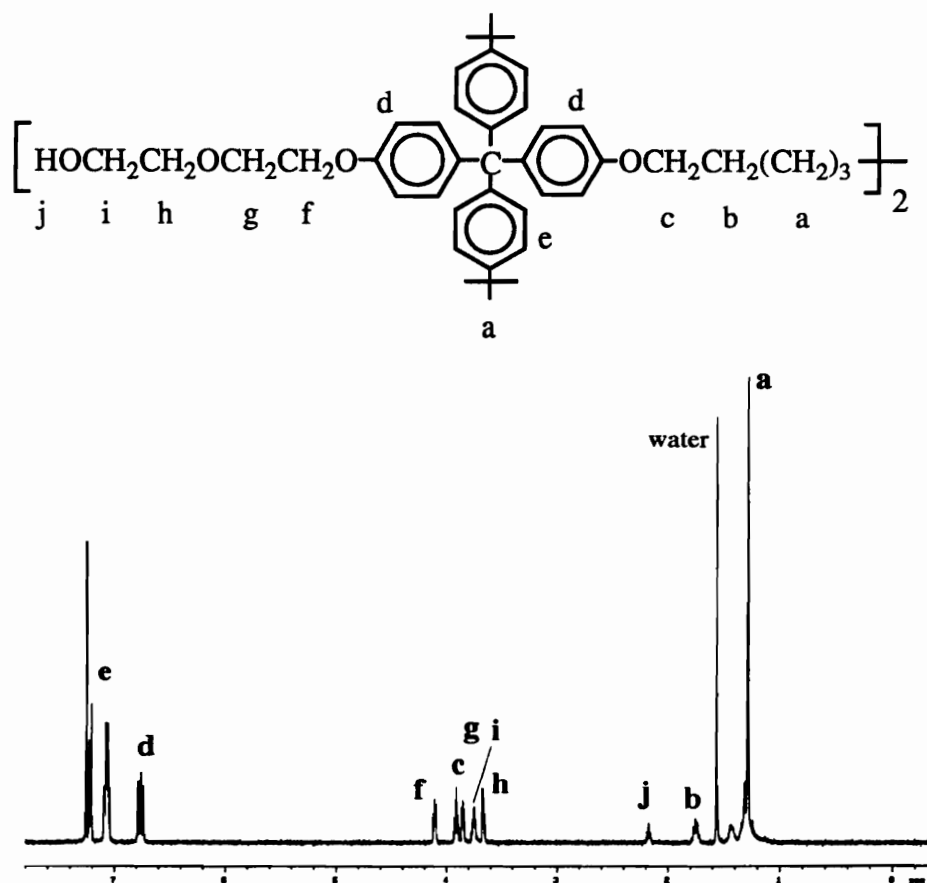


Figure 7. 400 MHz  $^1\text{H}$  NMR spectrum of 11 in  $\text{CDCl}_3$ . The signal at 7.26 ppm is due to  $\text{CDCl}_3$

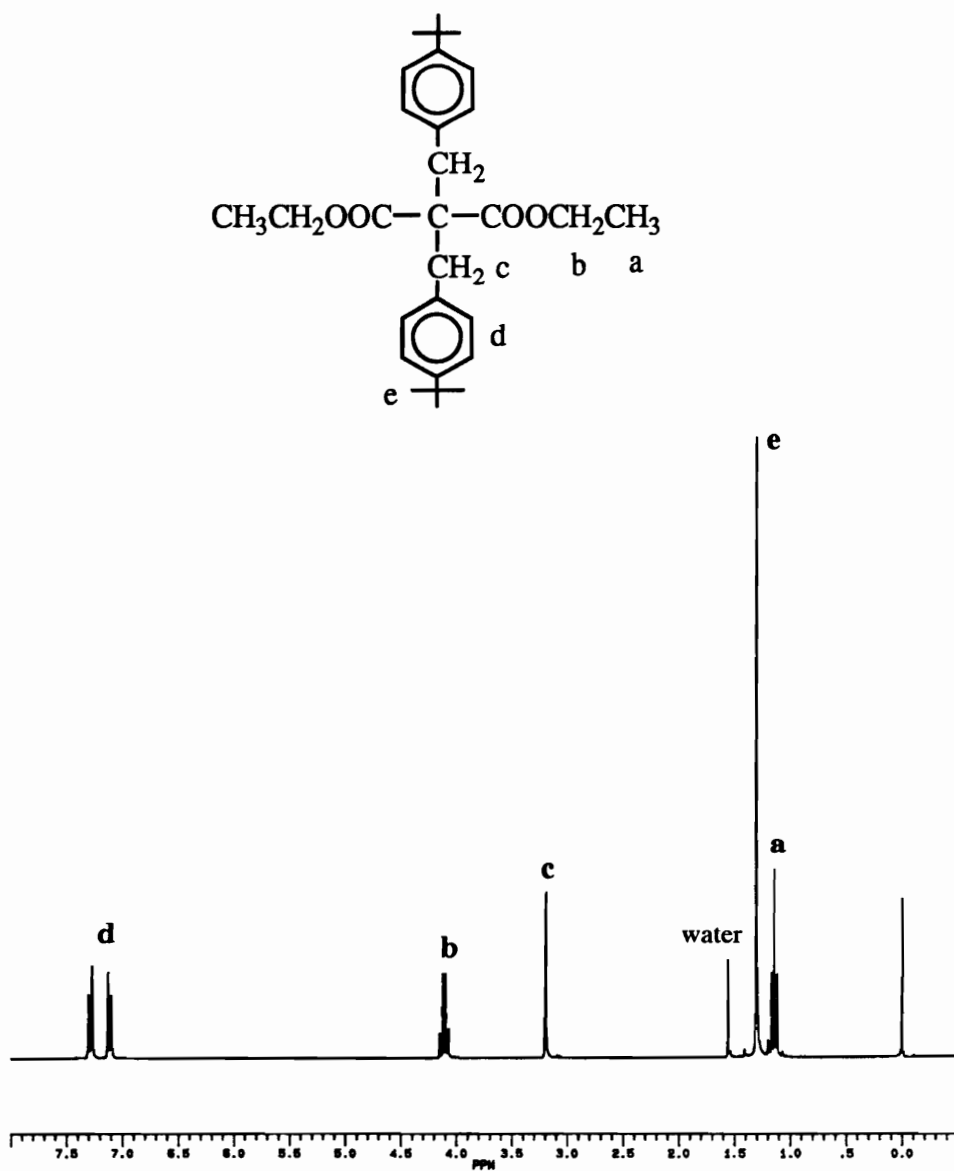


Figure 8. 270 MHz  $^1\text{H}$  NMR spectrum of **14** in  $\text{CDCl}_3$ . The signal at 7.26 ppm is due to  $\text{CDCl}_3$

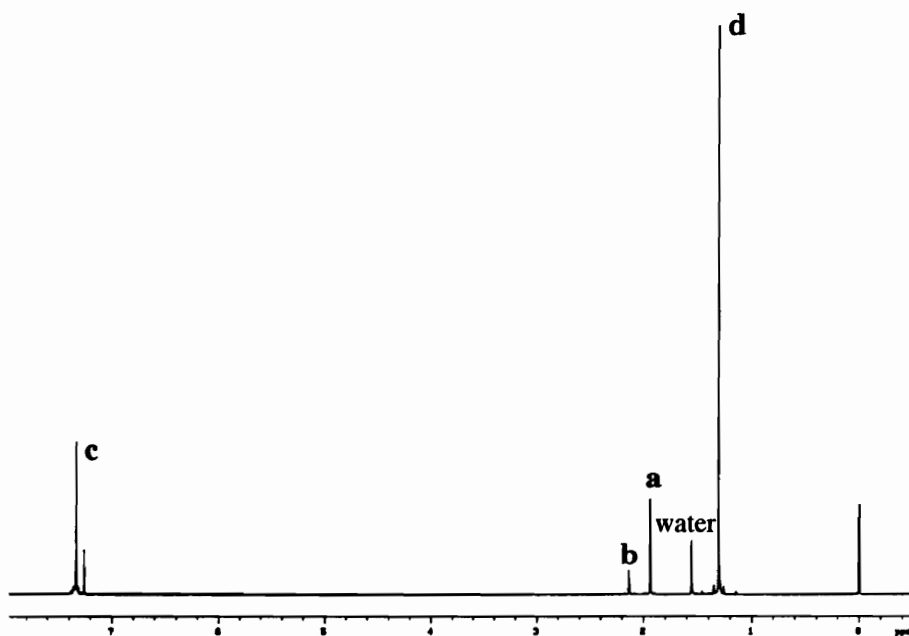
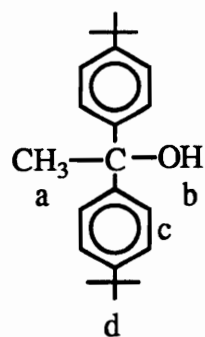


Figure 9. 400 MHz <sup>1</sup>H NMR spectrum of **16** in CDCl<sub>3</sub>. The signal at 7.26 ppm is due to CDCl<sub>3</sub>

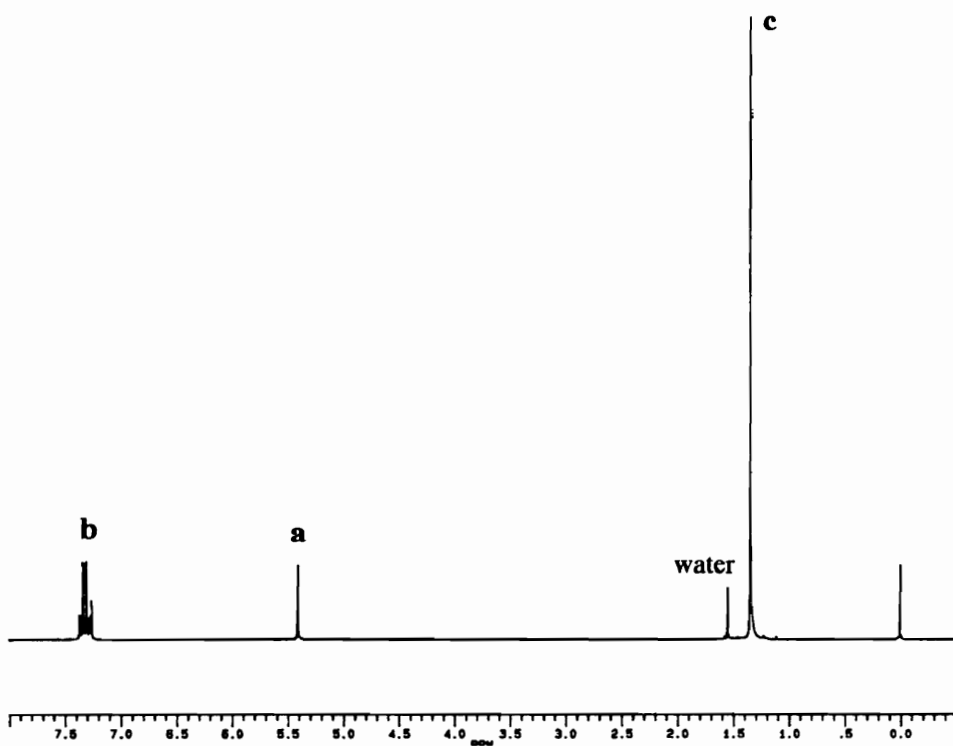
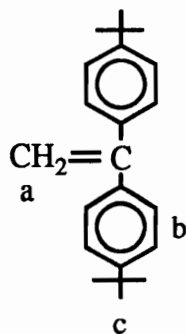


Figure 10. 270 MHz  $^1\text{H}$  NMR spectrum of 17 in  $\text{CDCl}_3$ . The signal at 7.26 ppm is due to  $\text{CDCl}_3$

## CHAPTER VII

### POLYESTER ROTAXANES (TRANSESTERIFICATION METHOD)

There are five main approaches for the syntheses of polyrotaxanes which are schematically illustrated in Scheme 1 [1]. The first approach is comprised of the formation of macrocycles in the presence of preformed linear polymers. The application of this approach is limited by the fact that cyclization reactions must be carried out under high dilution conditions [2], which do not favor the formation of rotaxanes unless the solvent is a linear polymer. However, most polymers are not good solvents for this purpose because of the high viscosity of polymer melts.

The second method of Scheme 1 consists of the preparation of rotaxane monomers. The monorotaxanes are then polymerized to give polymeric rotaxanes. One of the examples of this method is the utilization of complexation to prepare a series of difunctional rotaxane monomers comprised of dibenzo crown ether and difunctional quaternary salts of 4,4-bipyridine [3]. The difunctional rotaxane monomer was formed quantitatively *in situ* and then polymerized to form a series of elastomeric viologen based segmented polyurethanes [3].

The third method of rotaxane syntheses involves the syntheses of prepolyrotaxanes in which the cyclic and linear species are covalently linked. The elective bond cleavage generates polyrotaxane structures. Although Schill and coworkers demonstrated this elegant approach with monomeric species [4, 5], no polymeric rotaxanes have been prepared via this approach. The drawback

of this approach is that preparation of prerotaxanes or prepolyrotaxanes involves complex chemistry.

The fourth method indicated involves the threading of preformed cyclic molecules by preformed linear polymers. Agam et al. demonstrated that the degree of threading of oligomeric ethylene glycol into crown ethers first increased and then decreased with increasing molecular weight of the linear species [6]. The result seems to indicate that this approach, in the absence of template effects between the cyclic and linear species, has limitations in terms of threading percentage of macrocycles because of the kinetic limitations due to the low concentration of chain ends. At high molecular weights in neat systems the threading rate and efficiency will be reduced by the decreased mobility of chain ends due to the high viscosity. On the other hand, work of Harada et al. [7-11] suggests this approach is useful via template threadings.

The fifth approach to polyrotaxanes consists of the formation of linear polymers in the presence of the preformed cyclic component. Within method 5 there are two general approaches. The first is "template threading" involving attractive interactions between the linear species and the macrocycle. Therefore, the enthalpy of the threading in Scheme 2 is negative. A high degree of threading can be achieved and macrocycle content of the polyrotaxanes can be stoichiometrically controlled. The difficulty of formation of the template system is a disadvantage of this approach unless the macrocycles are readily available such as cyclodextrins.



The alternative approach is the "statistical approach", in which the interaction between cyclic and linear species is weakly attractive, negligible or perhaps repulsive. The equilibrium for threading is driven to completion by the use of an excess of macrocycle. This method is attractive because 1) the high concentration conditions of polymerizations favors rotaxane formation, especially if the cyclic species is a major constituent of the solvent; 2) the cyclic and linear components are independently variable and the methodology can be applied to common commercial polymers. The work in our group has established that polyrotaxanes can be prepared by this method via a variety of step and chain growth techniques [12-14].

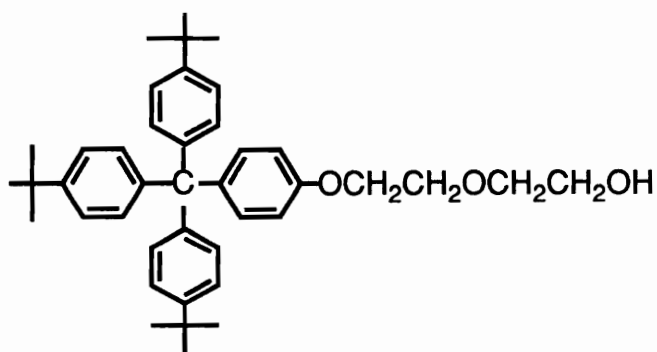
In the present work a series of polysebacate rotaxanes was synthesized using the statistical threading approach of method 5 discussed above. These polyester rotaxanes consist of poly(triethyleneoxy sebacate) or poly(butylene sebacate) backbone and 30-60 membered-crown ethers. In this chapter, the synthesis, purification, characterization, and preliminary physical analyses of these novel polymeric materials will be discussed [15].

## RESULTS AND DISCUSSIONS

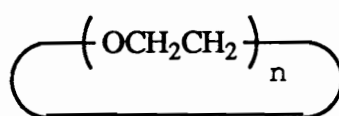
Transesterification, the most important step growth polymerization method for the preparation of polyesters [16], was adopted in the synthesis of polyester rotaxanes because it does not require precise stoichiometry. This is important for our polyrotaxane syntheses because the trace amount of poly(ethylene glycol) that may exist in crown ethers does not influence the polymerization by upsetting the stoichiometry, providing the major diol is relatively more volatile.

The polymerization reactions for the syntheses of the polysebacate rotaxanes were carried out in the presence of a large amount of melted macrocycle as solvents, so that random threading could take place in monomer, oligomer, and polymer stages. The reaction system was under the threading equilibrium condition throughout the polymerization. The threaded macrocycles were trapped on the polymer backbones by the random coiling of linear polymer chains and macrocycles or by introducing a bulky compound, mono[tris(*p*-*t*-butylphenyl)methyl-*p*'-hydroxyphenyl] ether of di(ethylene glycol) (**1**), onto the polymer chain ends. Large aliphatic crown ethers, 30-crown-10 (**2**), 42-crown-14 (**3**), and 60-crown-20 (**4**), were chosen as the macrocyclic components in this work.

Because the blocking group **1** can only constrain crown ethers with ring size up to 42 atoms [17], no blocking group was used for the syntheses of polyrotaxanes with 60-crown-20 as the macrocycle.



1 (BG-OH)



2, n = 10      30-crown-10

3, n = 14      42-crown-14

4, n = 20      60-crown-20

The polyester backbones of polyrotaxanes consist of sebacate units and triethyleneoxy or butylene units. Dimethyl sebacate was chosen as a monomer because of its nonpolar property and the optimum chain length to thread the macrocycle via a statistical approach [15, 18, 19]. The ratio of the macrocycle and the diester was kept low because the supply of crown ethers was initially limited. Since tri(ethylene glycol) has a similar structure to crown ethers and hence was believed to offer high threading percentages, it was used as a diol monomer. On the other hand, 1,4-butanediol was chosen because it will form tetrahydrofuran under the influence of the acidic catalyst during the polymerization. Elimination of the THF drives the esterification equilibrium toward completion [19]. *p*-Toluenesulfonic acid is an effective catalyst for the polyrotaxane syntheses because it does not form complexes with crown ethers,

while the catalytic function of metallic transesterification catalysts such as manganese or cadmium acetate or antimony oxide are hampered or eliminated by the strong complexing capabilities of the crown ethers [15].

In order to choose the reaction temperatures, the thermal stabilities of the crown ethers were examined by thermogravimetric analyses (TGA). The onset of decomposition of crown ethers occurred at around 180 °C and 5 % weight losses of 30-60 membered crown ethers occurred at temperatures ranging from 205-214 °C in air and from 265 to 376 °C in nitrogen [20]. For this reason, initial polymerizations were carried out at 180 °C.

While poly(butylene sebacate) as well as poly(butylene sebacate) rotaxanes with relatively high molecular weights were successfully synthesized under this condition, poly(triethylene sebacate) and its rotaxane counterparts were not obtained under this condition due to the high boiling point of tri(ethylene glycol). It is obvious that the polycondensation reactions for synthesis of poly(triethyleneoxy sebacate) rotaxanes should be carried out at temperatures higher than the onset decomposition temperatures of the crown ethers in air.

The high vacuum condition of the polycondensation reaction offers a hope to break through this dilemma. Because of the absolute absence of the oxygen the crown ethers may be more stable under high vacuum than in air or nitrogen. It is also not clear if the onset of mass loss of crown ethers observed by TGA is due to volatilization or decomposition. A study was performed to examine the thermal stability of the crown ethers under the conditions for the polymerization.

After 42C14 (**3**) was heated at 240 °C in the presence of a trace amount of *p*-toluenesulfonic acid under vacuum, the sample was then analyzed by melting point measurement, <sup>1</sup>H NMR, and <sup>13</sup>C NMR. The sample had the same melting point as standard 42C14. Both <sup>1</sup>H NMR and <sup>13</sup>C NMR showed only pure 42C14 peaks. The analytical results demonstrated that 42C14 does not decompose under the test conditions. Based upon the result of the thermal study, the polycondensation reactions for synthesis of poly(triethyleneoxy sebacate) rotaxanes were carried out at 200-260 °C.

## I. SYNTHESIS AND PURIFICATION

### A. Model Polymers

The model polymers, poly(triethyleneoxy sebacate) (**5**) and poly(butylene sebacate) (**6**), were synthesized from the condensation polymerization of dimethyl sebacate with tri(ethylene glycol) and with 1,4-butanediol, respectively (Scheme 2). In a typical polymerization, 1.0 eq of dimethyl sebacate, 2.2 eq of diol, 0.01 eq of *p*-toluenesulfonic acid (transesterification catalyst), and the blocking group **1** were mixed and heated to 120-150 °C under nitrogen to allow the initial transesterification to occur, as shown in Scheme 2. The system was then heated to 180-200 °C (for **6**) or 200-260 °C (for **5**) gradually under 0.1 mmHg vacuum, and the polycondensation was allowed to proceed for 6-30 hours. Excess diol was removed during this period. Because the excess 1,4-butanediol forms volatile tetrahydrofuran under the influence of the acidic catalyst, the esterification equilibrium is driven toward completion at relatively low

temperatures. In some case the mono[*p*-tris(*p*'-*t*-butylphenyl)methylphenyl] ether of di(ethylene glycol) (**1**) was used as an end blocking group to both control the molecular weights of the polymers and to prevent the dethreading of threaded macrocycles.

Figure 1 is the proton NMR spectrum of poly(triethyleneoxy sebacate) (**5**) which contains signals as follows: 1.3  $\delta$  (labelled **a**), a broad peak for the eight "central" protons of the sebacoyl moiety and the methyl protons of the blocking groups; 1.65  $\delta$  (**b**), a triplet for the four methylene protons  $\beta$  to the carbonyl groups; 2.35  $\delta$  (**c**), a triplet for the four protons  $\alpha$  to the carbonyl group; 3.6-3.7  $\delta$  (**e**), a complex signal for the eight central ethyleneoxy protons, 4.25  $\delta$  (**d**), a triplet for the four protons  $\alpha$  to carbonyl groups; 7.15-7.35  $\delta$  (**f**).

The  $^{13}\text{C}$  NMR spectrum (Figure 2) of **5** contains seven peaks in total. Only three peaks (**a**, **b**, **c**) at 24-35  $\delta$  are observed for the central methylene carbons of the sebacoyl unit, but all three signals of the non-equivalent ethyleneoxy carbons (labelled **e**, **f**, **g**) appear at 63-72  $\delta$ . The carbonyl carbon (**d**) occurs at 174  $\delta$ .

The proton NMR spectrum of poly(butylene sebacate) (**6a**) is shown in Figure 3a. The polyester **6a** displays resonances at 1.3  $\delta$  (labelled **a**) for the central  $(\text{CH}_2)_4$  units (8 H) of the sebacoyl moiety, at 1.6  $\delta$  (**b**) for the  $\text{COCCH}_2$  protons (4 H), at 1.7  $\delta$  (**c**) for the  $\text{OCCH}_2$  protons (4H), at 2.3  $\delta$  (**d**) for the  $\text{COCH}_2$  group (4 H), and at 4.1  $\delta$  (**e**) for the  $\text{OCH}_2$  protons (4H).

The  $^{13}\text{C}$  NMR spectrum of poly(butylene sebacate) (**6a**) is shown in Figure 4. **6a**

displays six of a possible seven signals. Apparently the four central carbon atoms of the sebacoyl unit are indistinguishable as they were in **5** (Figure 2); these are assigned to the upfield signal at 24.8  $\delta$  (labelled **a**). The two equivalent central carbons of the diol moiety are assigned as the 25.3  $\delta$  signal (**f**). Carbons  $\beta$  to the carbonyl are designated as giving rise to the 29.0  $\delta$  signal (**b**) and those  $\alpha$  to the carbonyl the 34.2  $\delta$  signal (**c**). The carbons  $\alpha$  to the ether oxygen are responsible for the 63.6  $\delta$  peak (**e**) and the carbonyl carbon is observed at 173.7  $\delta$  (**d**).

## B. Polyester Rotaxanes

The poly (triethylenoxy sebacate) rotaxanes (**7** and **8**) and poly(butylene sebacate) rotaxanes (**9-11**) were synthesized similarly in the presence of crown ethers as solvents (Scheme 2) [21].

To isolate polyrotaxanes from the unthreaded macrocycles, the polymeric materials obtained were dissolved in good solvents for both the backbone polymers and the macrocycles (methylene chloride or THF), and repeatedly reprecipitated into solvents which are good solvents for macrocycles but non-solvents for the polyesters (methanol or water). After each reprecipitation, the composition of the dried polymer was determined by quantitative  $^1\text{H}$  NMR or  $^{13}\text{C}$  NMR spectroscopy, affording a measure of  $m/n$  values, the molar ratios of macrocycle to repeat units of the polymer backbones. After constant composition was achieved, the polyrotaxanes were believed to contain only threaded macrocycles. The absence of unthreaded macrocycles in the polyrotaxanes was

also demonstrated by gel permeation chromatograms which also provided the molecular weights.

#### a. Poly(triethyleneoxy sebacate) Rotaxanes

The proton NMR spectrum of poly[(triethyleneoxy sebacate)-rotaxa-(60C20)] (**8**) (Figure 5) is the same as that of its model polymer, Figure 1, except for an enhancement of the cluster at at 3.6-3.7  $\delta$  due to the crown ether singlet at 3.67  $\delta$ . The  $^{13}\text{C}$  NMR spectrum of **8** is shown in Figure 6. The signal of crown ether carbons appears at 70.5  $\delta$  which is the only difference between the  $^{13}\text{C}$  NMR spectrum of the polyrotaxane and that of model polyester (Figure 2).

The proton and carbon NMR spectra of poly[(triethyleneoxy sebacate)-rotaxa-(30-crown-10)] (**7**) are qualitatively similar to those of the 60-crown-20 analogs shown in Figures 5 and 6. The only differences are small changes in chemical shifts and the relative intensities of the crown ether signals as well as the additional signals of the blocking group for **7**.

The macrocycle content ( $m/n$ ) in polyrotaxanes **7** and **8** was determined by integration of the proton NMR signals from 3.5-3.8  $\delta$  (**e**) versus 4.1-4.4  $\delta$  (**d**) (Figure 5). The former peaks (**e**) contain the crown ether protons and the central eight protons of the triethyleneoxy moiety, while the **d** signal corresponds to the four protons  $\alpha$  to the carbonyl group. Because 60-crown-20 contains 80 protons per molecule, the precision of the  $m/n$  determination is high. For  $m/n = 1$  the **e/d** ratio would be  $88/4 = 22$ ; for  $m/n = 0.1$ , the ratio would be 2.2. In this case (**8**,



Figure 5) m/n was 0.42.

A systematic study of the macrocycle contents in the poly(triethyleneoxy sebacate) rotaxanes after each reprecipitation is shown in Table 1. The macrocycle contents in all the polyrotaxanes reached constant values after the third reprecipitation, indicating complete removal of free macrocycles from the polyrotaxanes. For example, poly[(triethyleneoxy sebacate)-rotaxa-(30-crown-10)] (**7**) had a ratio of repeating units to 30-crown-10 (n/m) of 3.2 after the the first precipitation. This ratio did not change upon second and third reprecipitation. Therefore, a stable composition had been reached. This corresponds to a macrocycle content of 30 % by weight in the polyrotaxane. Poly[(triethyleneoxy sebacate)-rotaxa-(60-crown-20)] (**8**) was analogously produced, purified and analysed as shown in Table 1. On the other hand, after three reprecipitations, no 30C10 was detected in a physical blend of poly(triethyleneoxy sebacate) and 30-crown-10 [19]. These results indicate that the materials synthesized are not simple physical blends of polyesters and crown ethers, but polyrotaxanes, stable "copolymers" of linear polyesters and crown ethers.

#### b. Poly(butylene sebacate) Rotaxanes

Polyrotaxanes **9-11** comprised of poly[(butylene sebacate) backbones and 30-crown-10 (**2**)] [21], 42-crown-14 (**3**), and 60-crown-20 (**4**), were prepared, purified and analyzed in analogous fashion. The results are summarized in Table 1.

The  $^1\text{H}$  NMR spectrum of **10** (Figure3b) contains only one additional peak at 3.7

$\delta$  (f) due to the crown ether, compared to the  $^1\text{H}$  NMR spectrum of its linear counterpart (6a) in Figure 3a. As observed with polyrotaxanes 7 and 8 there are no changes in chemical shifts in the polyrotaxane relative to the two individual components. With butylene sebacate polymers integration of the 3.7  $\delta$  (f) peak (56 H in the case of 10, Figure 3b) directly versus the integrals of the peaks for all the "internal" protons from 1.2 to 1.9  $\delta$  (a, b, c; 16 H) yields m/n. For 10 then an  $m/n = 1$  would yield an integral ratio  $[e/(a + b + c)]$  of  $56/16 = 3.5$ ; again composition can be determined with good precision because of the large number of protons in the crown ether. In this case (Figure 3b) m/n was 0.22.

60-crown-20 based poly(butylene sebacate) 11 afforded qualitatively identical spectra relative to 10 (Figure 3b). Only the relative intensities of the crown ether signals at 3.7  $\delta$  varied.

The  $^{13}\text{C}$  NMR spectrum of poly[(butylene sebacate)-rotaxa-(42-crown-14)] (10) is shown in Figure 7. It differs from that of the model polymer (6a) (Figure 4) only by the resonance at 70.5  $\delta$  (g), the signal of the carbons of the 42-crown-14 component of the polyrotaxane.

## B. PROOF OF STRUCTURES:

At the early stage of the work, attempts to prepare polyrotaxanes were hampered by the small amount of poly(ethylene glycol)s present as impurities in the crown ethers. These poly(ethylene glycol)s were found to copolymerize into the

polymer backbones of the polyrotaxanes, leading to a triplet at 4.2  $\delta$  and multiplets at 3.5-3.8  $\delta$  in  $^1\text{H}$  NMR spectra. The triplet is assigned to  $\text{OCH}_2\text{CH}_2\text{OOC}$  and the 3.5-3.8 multiplet to the ethyleneoxy protons. Two signals at 63.1 and 69.0  $\delta$  in  $^{13}\text{C}$  NMR spectra are also attributed to the poly(ethylene glycol) impurities,  $\text{C}\text{H}_2\text{OOC}$  and  $\text{C}\text{H}_2\text{COOC}$ , respectively. Fortunately, we developed a technique to remove poly(ethylene glycol)s by treating the crown ethers with poly(methacryloyl chloride) [20]. Utilizing purified crown ethers we generated polyrotaxanes whose purity was demonstrated by the lack of these impurity-derived signals in both  $^1\text{H}$  and  $^{13}\text{C}$  NMR spectra (e.g., see Figures 3b and 7).

Crown ethers could also decompose under high temperature and acidic conditions to form oligo(ethylene glycol)s, which could be incorporated into the polymer through the transesterification reaction. In contrast to the crown ethers **1**, **2** and **3** which display single  $^1\text{H}$  and  $^{13}\text{C}$  NMR resonances, oligo(ethylene glycol)s display multiple resonances. Since polymers **7** and **8** contain triethyleneoxy units, the presence of crown ether derived oligoethyleneoxy units is not obvious from the NMR spectra, as exemplified by Figures 5 and 6, the  $^1\text{H}$  and  $^{13}\text{C}$  NMR spectra for **8**.

On the other hand, butylene sebacate polymers **9-11** afford simpler NMR spectra, so that the presence of oligoethyleneoxy units could be detected by  $^1\text{H}$  and  $^{13}\text{C}$  NMR spectroscopy; in fact no evidence of incorporation of oligo(ethylene glycol)s was observed in **9-11**. For example, polyrotaxanes **10** contains only a single additional peak (for the crown ether component) relative to the model

polyester **6a** in  $^1\text{H}$  and  $^{13}\text{C}$  NMR spectra (Figures 3b and 7, respectively).

The lack of decomposition of crown ethers under this condition was further proved by an experiment in which poly(butylene sebacate) was prepared at 180 °C in the presence of 18-crown-6 whose cavity is too small to be threaded by polyester chains. After two reprecipitations from  $\text{CH}_2\text{Cl}_2$  solution into methanol, the  $^1\text{H}$  NMR and  $^{13}\text{C}$  NMR spectra of the product did not show any evidence of extraneous signals. Two conclusions can be drawn from this result. First, 18C6 molecules do not decompose under polymerization conditions and are not incorporated into the polyester in any way. Second, reprecipitation is an efficient method to remove unthreaded macrocycles. This purification method has been discussed in more detail above in this chapter. Some 18-crown-6 was lost through distillation, however. Thus, some loss of the larger crown ethers by volatilization is possible.

The above experiment showed that the threading was impossible for small macrocycles. On the other hand, is threading possible for a polymer whose chain ends are larger than the size of macrocycle? This possibility was studied by a threading experiment. In the experiment, 1.0 g of completely endcapped polymer **6b** (Sample C) and 4.0 g of 42C14 were stirred in THF (10 mL) at 60 °C under nitrogen for 11 days. After three precipitations, only a trace amount of 42C14 was found in the polymer by  $^1\text{H}$  NMR,  $m/n = 3.0 \times 10^{-4}$ , corresponding to 0.07 mass percent of 42C14. The results demonstrated that the tris(*t*-butylphenyl)methyl type group is big enough to block 42C14. The threading of macrocycles onto the polymer chain occurs only when the diameter of the

polymer chain is smaller in size than the cavity of the macrocycle.

In contrast, in the absence of blocking groups, threading of 42-crown-14 onto preformed poly(butylene sebacate) chains was observed. Scheme 3 summarizes the whole experiment. In the experiment, one gram of poly(butylene sebacate) (**6a**, sample b) was mixed with 4.8 g of 42C14 in a mole ratio of 1:146.8 in the melt at 120 °C for three days. After three precipitations, 0.8 g of polyrotaxane **10** with  $m/n = 2.0 \times 10^{-2}$  (4.6 mass percent of 42-crown-14) was obtained. The recovered crown ether and the polymer were then dissolved in THF (20 mL) and the mixture was stirred at 55 °C for three days. After three precipitations, 0.59 g of poly[(butylene sebacate)-rotaxa-(42C14)] (**10**) with  $m/n = 1.7 \times 10^{-2}$  (4.0 mass percent of 42-crown-14) was obtained. The recovered polymer and 42-crown-14 were again dissolved in mixed solvent (60 mL) of THF (75%) and acetonitrile (25%) at 55 °C for 16 days. After three reprecipitations, polyrotaxane **10** (0.43 g) with  $m/n = 1.3 \times 10^{-2}$  (3.0 mass percent of 42-crown-14) was obtained. Surprisingly, another sample taken from inside wall of the flask after the removal of solvent shows a high macrocycle content:  $m/n = 8.6 \times 10^{-2}$  (17.2 mass percent of 42-crown-14). The reason for the fractionation is not clear at this time, but plausibly could involve the enhanced solubility of the higher cyclic content systems. The results of intrinsic viscosity measurements for the final polyrotaxane containing 3 mass percent of 42-crown-14 and its precursor polymer are surprising : the viscosity of the former is twice of that of the latter (1.654 vs 0.847). Number average molecular weight determined by GPC with polystyrene standards was also doubled (48.7 vs 19.6 kg/mol). These dramatic changes could have been caused by the fractionation of the polymer **6a** during

multiple precipitations. However, the number average molecular weights determined by VPO did not change very much:  $M_n$  of the linear polymer **6a** is 27.6 kg/mol and that of the final polyrotaxane **10** is 29.8 kg/mol. Therefore, polymer fractionation is not the main reason for the changes in the viscosity and the GPC results. These changes reflect the changes in the hydrodynamic volume of polymer chains, that is, the polymer chains were stiffened by the incorporation of macrocycles.

### III. MOLECULAR WEIGHT DETERMINATIONS AND BLOCKING EFFICIENCY

#### A. Gel Permeation Chromatography (GPC) with Polystyrene Standards

Molecular weights of polyesters and polyester rotaxanes were measured by gel permeation chromatography based on polystyrene standards. The results are listed in Table 2.

The molecular weights of poly(butylene sebacate)s (**6**) were generally higher than those of poly(triethyleneoxy sebacate)s (**5**) because of formation of THF as discussed before. Since transesterification polymerization was carried out under high vacuum at high temperature and no solvent was used during the reaction, the viscosity of the systems increased at high conversion under these conditions, and magnetic stirring became ineffective at this critical period of polymerization. It is believed that higher molecular weight polymers can be produced by using a mechanical stirrer in larger scale reactions.

Other experimental results in our laboratory demonstrated a common phenomenon that the molecular weights of step growth polyrotaxanes are often lower than those of the corresponding model polymers [12, 13]. Two factors may be involved: 1) the reaction is retarded by the dilution, solvation, and viscosity effects of the crown ethers, 2) the chain orientations are obstructed or burdened by the threaded macrocycle molecules. Among polyrotaxanes, the poly(butylene sebacate) rotaxanes had much higher molecular weights than the triethyleneoxy analogs. Formation of THF may play a major role in this phenomenon. The high boiling temperature of tri(ethylene glycol) makes it difficult to remove excess glycol and drive the equilibrium to high molecular weight polyester.

Because the molecular weights of poly(triethyleneoxy sebacate) rotaxanes (**7** and **8**) are low, the GPC signals of the polymers will overlap with signals of free crown ethers, if they exist. the GPC measurements can not detect free macrocycles in these polyrotaxanes. On the other hand, GPC is a powerful tool to detect the free macrocycles in poly(butylene sebacate) rotaxanes (**9-11**) because the molecular weights of the polymers (> 5,000 g/mol) are much higher than those of the crown ethers (< 900 g/mol).

Figure 8 contains GPC traces for (a) poly(butylene sebacate) (**6a**) without end-capping groups (**6a**), (b) a physical mixture of poly(butylene sebacate) (**6a**) and 42-crown-14 (**3**), (c) 42-crown-14 (**3**) alone and (d) poly(butylene sebacate)-rotaxa-(42-crown-14)] (**10**), all in chloroform. For the physical blend the presence of the free crown ether is clearly detected by the shoulder at larger elution volume as shown in the trace (b). On the other hand, the trace (d) for the

polyrotaxane is quite symmetric and shows no evidence of the presence of unthreaded macrocycle. In fact the polydispersity of the polyrotaxane is less than that of the polyester model system (1.86 vs. 2.19). Polyrotaxane **10** contained 35 mass percent of 42-crown-14, as determined by  $^1\text{H}$  NMR spectroscopy.

Figure 9 displays similar results for poly(butylene sebacate) (**6a**), a blend of **6a** and 60-crown-20 (**4**), 60-crown-20 (**4**) and poly[(butylene sebacate)-rotaxa-(60-crown-20)] (**11**). Although the resolution of the peak for the free macrocycle is somewhat less than with 42-crown-14 due to the higher molecular weight of 60-crown-20, it can still be clearly seen that polyrotaxane **11** does not contain free crown ether based on the fact that the peak in curve d is quite symmetric while the peak of the blend (curve b) shows two overlapped signals; the one at large elution volume is due to 60-crown-20. Again, the polydispersity of the polyrotaxane (2.01) is less than that of model polyester **6a** (2.19). Polyrotaxane **11** contained 51 mass percent of 60-crown-20, as determined by  $^1\text{H}$  NMR spectroscopy.

## B. NMR Spectroscopy

The blocking group **1** is a huge compound. After it has been incorporated as an end group into polymer chains, it could be quantitatively detected by  $^1\text{H}$  NMR or  $^{13}\text{C}$  NMR spectroscopy, providing that the molecular weight of the polymer is not very high. The presence of 27 methyl protons in each endblocking moiety (**1**) enables proton NMR estimation of  $M_n$  from integration of the 1.35  $\delta$  signal relative to polyester backbone signals, under the assumption of 100 %



endblocking, and knowing the molar ratio of macrocycle to repeat unit.  $^{13}\text{C}$  NMR can also be utilized to estimate  $M_n$  by comparing the integrals for the *t*-butyl methyl signal (31.4  $\delta$ ) to that of the four central sebacoyl carbons (29.1  $\delta$ ) or for the quaternary aromatic carbon (148.2  $\delta$ ) to the carbonyl carbon (173.8  $\delta$ ). In the quantitative  $^{13}\text{C}$  NMR measurement, chromium acetyl acetonate was used to reduce the relaxation time ( $T_1$ ).

### C. Ultraviolet Spectroscopy

Because the blocking group **1** contains four phenyl groups, a strong chromophore responsible for the electronic absorption in near UV region due to aromatic  $\pi \longrightarrow \pi^*$  transition. Taking advantage of the UV absorption of **1**, one can calculate  $M_n$  under the assumption of 100 % endcapping. The measurements were calibrated by four standard solutions of **1** and the calibration curve is shown in Figure 10. The curve was correlated perfectly to a linear equation:

$$A = 0.03779 + k C \quad (1)$$

where:  $A$  = absorbance (%)

$$k = b \epsilon$$

$b$  = path length through the sample ( 1.000 cm)

$\epsilon$  = molar absorptivity (L /cm mol)

$C$  = concentration (mol/L)

Therefore, Equation (1) obeys Beer's law with a baseline correction of 0.03779 absorbance units. The number average molecular weights of the polymer were calculated by equation (2):

$$M_n = 2 M (\epsilon)/10 (A - 0.037) \quad (\text{g/mol}) \quad (2)$$

where M is the mass of polymer in mg dissolved in 10.00 ml of chloroform.

#### D. Vapor Pressure Osmometry (VPO)

The number average molecular weights of the model polyesters and their rotaxane counterparts were also determined by vapor pressure osmometry. The voltage changes ( $\Delta V$ ) recorded is proportional to the temperature change ( $\Delta T$ ) which is related to the decrease of vapor pressure of toluene solvent in the polymer solution. The  $\Delta V$  values are proportional to the concentration of polymer (C):

$$\Delta V = (k/M_n) \cdot C \quad (3)$$

where K is a constant [22].

Polystyrene standards with narrow molecular weight distribution (1.3 , 8.0, and 17.5 kg/mol) were used to construct the calibration curve. Figure 11 shows the plots of  $\Delta V$  vs the concentration of the standards. All the plots are quite linear.

It can be seen from Equation (3) that the slopes of the linear plots in Figure 11 are proportional to the reciprocal of molecular weight. Therefore, a calibration curve was constructed by plotting the reciprocal of  $M_n$  against the slopes, as shown in figure 12.

The polyesters and polyester rotaxanes were measured similarly. The plots of voltage change vs. concentration of polymers are shown in Figure 13. The molecular weights of the polymers were determined by the interpolation of the slopes of these plots to the calibration curve.

#### E. Gel Permeation Chromatography with Viscosity Detection and Universal Calibration ("Absolute GPC")

The validity of using universal calibration to analyze highly branched polymers has not been clearly documented. This assertion was evaluated by Siochi et al. for PMMA-g-PMMA system [23]. They found that these graft polymers containing up to 40 mass % of long-chain branching obeyed the universal calibration. Since our polyrotaxanes contain up to 51 mass percent macrocycles, one questions if polyrotaxanes also obey the universal calibration. This problem was studied by the comparison of molecular weights determined by VPO with those by GPC using universal calibration. The results of VPO measurements and absolute GPC (universal calibration using viscosity detector) are in good agreement. For example, the molecular weight of polyrotaxane **7** determined by VPO is 2.2 kg/mol and that determined by GPC with viscosity detector is 2.4 kg/mol. The relative error between the two is 8.3 %. Another sample of **7** (not listed in Table

2) also showed good agreement between the two techniques (error = 9.8 %) [24]. The molecular weight of **11** determined by VPO is 8.6 kg/mol while that determined by absolute GPC is 10.1 kg/mol. The relative error between the two is 14.9 %. Therefore, the universal calibration is valid for polyrotaxanes. This conclusion is important in two aspects. First, the absolute molecular weight can be conveniently determined by GPC with a viscosity detector instead of tedious VPO measurements. Second, polyrotaxane backbones are still flexible although they are stiffened to some extent by the incorporated crown ethers, as will be discussed below. It is worth noting that the molecular weights of polyrotaxanes determined by VPO are always lower compared to those determined by GPC with universal calibration. It is probably due to the chain stiffening by the macrocycles.

However, the molecular determination by VPO is subject to greater error for high molecular weight polymers due to the fact that polymer solutions for VPO measurements deviate from ideal conditions at high molecular weights. A large difference between the molecular weights determined by GPC and VPO was found for poly(butylene sebacate) (**6a**) with high molecular weight. The molecular weight determined by VPO is 27.6 kg/mol while that determined by absolute GPC is 18.8 kg/mol.

#### F. End Blocking Efficiency

The number average molecular weights of polymers determined by VPO and absolute GPC are compared with those determined by other methods in Table 2.

The end capping efficiency using blocking group 1 is calculated by comparison of the number average molecular weight measured by VPO or absolute GPC with that determined by the techniques of end group analysis such as UV,  $^1\text{H}$  NMR, and  $^{13}\text{C}$  NMR spectroscopy assuming two end groups per macromolecule .

For the end capped poly[(triethyleneoxy sebacate)-rotaxa-(30ClO)] (**7**),  $M_n$  values from end groups analyses were much higher than the VPO value (Table 2). For example, the UV value was 3.4 times as high as the VPO value, indicating that the end capping is only 29% percent complete, i.e., on average there were only 58 blocking groups per 100 molecules.

All the results for poly(butylene sebacate) (**6b**, Sample C) from different end group techniques are in good agreement with the VPO value (Table 2), indicating the complete end capping in the case of low molecular weight. For the higher molecular weight poly(butylene sebacate) (**6b**, Sample D), moreover, end capping also appears to be complete given the larger error inherent in the end group analyses at higher molar masses.

#### G. Effect of Rotaxane Structure on Hydrodynamic Volume

For poly(butylene sebacate) (**6a**) there was good agreement between absolute GPC and GPC with polystyrene standards, while VPO yielded a higher value (Table 2). However, end blocked poly(butylene sebacate) (**6b**) gave good correlation between VPO and GPC with polystyrene standards. For poly(triethyleneoxy sebacate) (**5**) absolute GPC and GPC with polystyrene

standards also agreed well (Table 2). That is, the hydrodynamic volumes of model polymers **6a**, **6b** and **5** are similar to those of polystyrene at the same molecular weight.

However, for the polyrotaxanes, GPC values with polystyrene standards were always higher than the absolute GPC values and VPO values because of the larger hydrodynamic values of polyrotaxanes relative to polystyrene. For example poly[(triethyleneoxy sebacate)rotaxa-(30-crown-10)] (**7**) with polystyrene standards yielded an  $M_n$  value that was twice that of the absolute methods (VPO and absolute GPC) (Table 2) and poly[(butylene sebacate)-rotaxa-(60-crown-20)] (**11**) also yielded a polystyrene equivalent value nearly twice those obtained by absolute methods (Table 2). These results again support the idea that rotaxane formation leads to chain stiffening, thereby increasing hydrodynamic volume. The only log "K" and "a" values available for comparison (**6a** vs. **11**, Table 2) were indicative of more negative log "K" and more positive "a" values. More detailed rationalization of the solution behavior of polyrotaxanes requires more extensive data on the effects of solvents, temperature, etc (See Chapter VIII for some preliminary results).

#### IV. THREADING EFFICIENCIES OF MACROCYCLES: EFFECTS OF RING SIZE AND BACKBONE STRUCTURE

It has been found that the threading efficiency of the macrocycles is affected by their sizes and their concentrations relative to the monomers.

A higher macrocycle incorporation rate was found in poly[(triethyleneoxy sebacate)-rotaxa-(60-crown-20)] (**8**) than in poly [(triethyleneoxy sebacate)-rotaxa-(30-crown-10)] (**7**), and the same phenomenon, i.e., higher cyclic incorporation for larger crowns, was observed for poly(butylene sebacate) rotaxanes **9**, **10** and **11**, with 30-crown-10 (**2**), 42-crown-14 (**3**), and 60-crown-20 (**4**), respectively.

Agam reported that at 1:1 molar ratios of neat components using trideca(ethylene glycol) as the linear component dibenzo-57-crown-19, a 57-membered ring, leads to 63% threading, while dibenzo-45-crown-15, a 45-membered ring, produces 41 % threading. [6] The area of the cavity of the ring is a key variable; it is proportional to the square of the circumference. Thus the cavity area of a fully open 57 membered ring will be 1.60 ( $57^2/45^2$ ) times as great as that of a 45 membered ring. In this case, the ratio of threading efficiencies ( $63/41 = 1.54$ ) is very close to this value.

The cavity of a 60-crown-20 molecule (**4**) is two times as large in area as that of a 42-crown-14 molecule (**3**) and 4 times as large as that of a 30-crown-10 molecule (**2**) when the macrocycles are fully open. Although studies on cyclic(dimethylsiloxane)s using both calculations and experiments demonstrated that the rings are not fully open and the percentage of threadable conformations is higher for large rings than for small rings [25], the possibility for a given linear chain to thread should be about twofold greater for 60-crown-20 than with 42-crown-14 and fourfold greater than with 30-crown-10.

For the triethyleneoxy case even though only half as much 60-crown-20 was used as 30-crown-10 on a molar basis (Table 1, **8** vs **7**) 1.3 times more threading was observed for the larger macrocycle, an overall factor of 2.6 enhancement in threading efficiency. Similarly for the poly(butylene sebacate) rotaxanes a factor of 4.8 more threading was observed for 60-crown-20 (Table 1, **11**) and 2.4 times more efficient threading for 42-crown-14 (**10**) compared to 30-crown-10 (**9**).

When the total mass of crown ether in the neat reaction was kept constant, in the syntheses of **9**, **10**, and **11** (Table 1) as shown in Figure 14 the m/n values were proportional to ring size and the mass percentage of macrocycles in the purified polyrotaxanes also increased linearly with increasing ring size. This phenomenon was also observed in polyurethane rotaxane syntheses [12]. Detailed quantitative analysis of these results is rendered questionable by several factors including: 1) differences in molar concentrations of the crown ethers and 2) the possibility of loss of macrocycles from the non-encapped polyrotaxanes by dethreading during purification, particularly in the first precipitation [26].

The importance of interactions of the macrocycle with the backbone was probed by comparison of the threading efficiencies of the triethyleneoxy and butylene systems with 60-crown-20 (Table 1, **8** vs **11**). For the same feed ratio the triethyleneoxy polymer **8** contained 1 macrocycle per 2.4 repeat units as compared to one per 3.3 in the butylene system **11**. On a backbone atom basis (20 per repeat unit in **11** vs. 16 in **8**) the triethyleneoxy polymer had an average one 60-crown-20 per 48 atoms, while the butylene polymer had one per 53



atoms; in other words the triethyleneoxy threading efficiency was ca 10 % higher on this basis. Probably the greater compatibility of the triethyleneoxy moiety with the crown ether plays a role in the threading.

## V. SOLUBILITY PROPERTIES OF POLYROTAXANES

As shown in Table 3 all of the polyrotaxanes displayed solubility behavior that differed from the simple linear polyesters themselves. The former display higher solubility in polar solvents than the latter. This was also observed with polyurethane rotaxanes [12] and most strikingly poly[(acrylonitrile)-rotaxa-(60-crown-20)] which is completely soluble in methanol while polyacrylonitrile is completely insoluble [14].

Poly(triethyleneoxy sebacate) rotaxanes **7** and **8** are substantially more soluble in polar solvents than the parent polyester **5**. For example, **7**,  $n/m = 3.2$  in spite of its hydrophobic blocking groups is somewhat soluble in methanol and acetone while poly(triethyleneoxy sebacate) (**5**) is completely insoluble in methanol and acetone.

Likewise the rotaxanes based on poly(butylene sebacate) reflect the enhanced polar contribution of the macrocycles. For example, while the parent polyester **6a** is virtually insoluble in methanol and acetone and is isolated in 96 % yield after two precipitations from methanol, polyrotaxane **11**,  $n/m = 3.3$  is slightly soluble in methanol and completely soluble in acetone, affording only a 32% yield after two precipitations from methanol. Even with the use of water as a precipitation

medium only 30% of the polymer was recovered after three reprecipitations!

Just as in covalently bonded copolymers the solubility properties of polyrotaxanes should reflect the properties of the two components. Thus the solubility parameter of a polyrotaxane should be a function of its composition, as well as the size and flexibility of the macrocycles. Enhancement of solubilities of polyrotaxanes in polar solvents increases with increasing crown ether content; for example, polyrotaxane **10** is only partially soluble in acetone because of its lower crown ether content compared to polyrotaxane **11**, which is completely soluble in acetone. However, because of the mobility of the cyclic species along the linear backbone some unusual behavior may be anticipated. For example, good solvents for the backbone which are poor solvents for the macrocycle may lead to aggregation and crystallization of the cyclic component. Conversely, good solvents for the macrocycle that are poor solvents for the backbone may force backbone segments that are not in the vicinity of the cyclic species to remain in a highly coiled state. These possibilities should significantly affect solution properties such as radius of gyration, hydrodynamic volume and dethreading, micelle formation [27] as well as crystallization of the cyclics.

Crown ethers are polar organic compounds. Because they are soluble in very polar solvents such as water and methanol but not soluble in acetone, the solubility parameters of crown ethers are higher than that of acetone. On the other hand, poly(butylene sebacate) is not soluble in acetone. The solubility parameter of poly(butylene sebacate) is lower than that of acetone due to its hydrocarbon nature. It is interesting to note that polyrotaxane **11** is totally soluble

and **10** is partially soluble in acetone. Physical interlocking of polar crown ethers with non-polar poly(butylene sebacate) makes the resultant polyrotaxanes dissolve in acetone whose polarity is between those of the two components of the polyrotaxanes.

## VI. THERMAL TRANSITIONS, SOLUTION PROPERTIES OF POLYROTAXANES

All of the polyrotaxanes exhibited phase transition behavior that differed from that of the simple corresponding model polyester. Both glass transitions and melting points were altered and in some cases the macrocycles were able to crystallize without dethreading, as shown in Table 4.

### A. Poly(triethyleneoxy sebacate) Systems

The model system poly(triethyleneoxy sebacate) (**5**) displayed complex phase transition behavior as shown in Figure 15. Upon heating (Figure 15a) a glass transition occurred at  $-56\text{ }^{\circ}\text{C}$  immediately followed by a crystallization exotherm at  $-47\text{ }^{\circ}\text{C}$ , then a melting endotherm at  $-26\text{ }^{\circ}\text{C}$ , another crystallization exotherm at  $-23\text{ }^{\circ}\text{C}$ , a broad double-peaked melting transition at  $19\text{ }^{\circ}\text{C}$ , a small endothermic transition at  $30\text{ }^{\circ}\text{C}$  and finally a melting transition at  $36\text{ }^{\circ}\text{C}$ . The second run after slow cooling (Figure 15b) essentially reproduced the first heating, except that the two uppermost endothermic transitions were absent. These two transitions reappear only after several days of "annealing" at room temperature. The nature

of the complex set of transitions was not further investigated, since our intent was to use the parent system as a point of reference for the corresponding polyrotaxane derivatives. In the only report we found on this system  $T_m$  was reported to be 28 °C. [28]

The DSC trace for the heating of the endblocked triethyleneoxy sebacate polyrotaxane **7** based on 30-crown-10 is shown in Figure 16. The glass transition is clearly obvious at -56 °C. Similarly to the model polyester **5** (Figure 15) a crystallization exotherm was observed at -8 °C, followed by a double-peaked maximum at 10 °C. Upon cooling at 5 °C/min to -40 °C, no transitions were observed. Subsequent heating curves reproduced the first heating curve. Thus in this case rotaxane formation did not significantly alter the phase behavior of the polyester.

However, in the 60-crown-20 based system **8**, whose DSC curves are shown in Figure 17, a new phenomenon was observed. Upon heating (Figure 17a) In addition to the glass transition temperature at -57 °C a small melting endotherm occurred at 12 °C and then a large melting transition at 43 °C. Upon cooling at 10 °C/min (Figure 17b) a single large crystallization exotherm was seen at 13 °C. After rapid cooling to -100 °C, heating produced a crystallization exotherm at -45 °C and the subsequent melting transition at 43 °C. Figure 18 illustrates the phase transition behavior of 60-crown-20 (**4**), which underwent melting at 56 °C (Figure 18a) and upon slow cooling crystallized at 36 °C (Figure 18b); after rapid cooling the glass transition was observed at -67 °C. In view of the fact that poly(triethyleneoxy sebacate) (**5**) itself displayed no endothermic transitions

above 36 °C and did not readily reform this crystalline phase upon cooling (Figure 15), the crystalline phase in polyrotaxane **8** is attributed to the crown ether. The transition temperatures observed in polyrotaxane **8** were somewhat depressed relative to the pure macrocycle **4** as would be expected. The perfection of the crystal of the macrocyclic component of the polyrotaxane should be lower than that of the macrocycle itself due to the constraints of the linear backbone penetrating the crown ether; the aggregation of the cyclic species required for recrystallization will likewise be retarded by the physical linkage. Such crystallization of the cyclic component of polyrotaxanes was observed with amorphous polyurethane backbones as well [12].

#### B. Poly(butylene sebacate) Systems

Poly(butylene sebacate) (**6a**) is a highly crystalline polymer,  $T_m = 64-67$  °C, and  $T_g$  was not observed by DSC (Table 4); the heating and cooling curves (DSC) are shown in Figure 19.  $T_m$  of **6a** has been reported as 63-65 °C and  $T_g$  as -57 to -75 °C [29-31]. Endcapped poly(butylene sebacate) **6b** shows a somewhat lower  $T_m$ , dependent of course on molecular weight; compare **6a** and **6b** in Table 4.

However, poly[(butylene sebacate)-rotaxa-(42-crown-14)] (**10**), as shown in Table 4 and Figure 20a displayed a  $T_g$  at -58 °C and two melting transitions, one at 53 °C and the other at 59 °C. Upon cooling, crystallization exotherms occurred at 48 and 16 °C (Figure 20b). The melting point of pure 42-crown-14 is 56 °C as shown in Figure 21a. Upon cooling from the melt it crystallized at 32 °C

(Figure 21b). Its  $T_g$  is  $-68\text{ }^\circ\text{C}$  [20].

Thus, it appears that for polyrotaxane **10**  $T_g$  corresponds to that of the crown ether and that the two melting and crystallization transitions are associated with crown ether and backbone rich domains. That is, the sharper transitions at higher temperature on heating and cooling (Figure 20) are due to backbone transitions and the smaller lower temperature events are due to the crown ether. The polyester melting and crystallization transitions are sharper and closer to those of the pure component than those of the crown ether, indicating that the backbone crystallization process is less influenced by rotaxane formation than the crystallization of the crown ether. Hence the lamellar perfection of the polyester is greater than the ordering of the crown regions of the polyrotaxane. Taking into account the fact that the sample was 35 mass percent macrocycle comparison of the heats of crystallization of Figures 20b, 19b and 21b indicates that ~133% of the backbone and ~33% of the macrocycle species of **10** crystallized with respect to the pure components **4** and **6a**. The higher crystallinity of linear component of **10** compared to **6a** may be the result of low molecular weight of **10** backbone.

Moreover, polyrotaxane **11** showed a  $T_g$  at  $-60.5\text{ }^\circ\text{C}$  (Table 4), in the vicinity of glass transition temperature of 60-crown-20 itself ( $-67\text{ }^\circ\text{C}$ ). Two melting points were observed for polyrotaxane **11** (Figure 22a) at  $33\text{ }^\circ\text{C}$  and  $37\text{ }^\circ\text{C}$ , which were somewhat below the melting points of 60-crown-20 (**4**) ( $57\text{ }^\circ\text{C}$ , Figure 18a) and polymer **6a**, ( $66\text{ }^\circ\text{C}$ , Figure 19) respectively. Two crystallization temperatures were also observed upon cooling for polyrotaxane **11** (Figure 22b). This

behavior is similar to block copolymers which are often heterogeneous on a microscopic scale. Phase separation might possibly take place via dethreading. However, our tests show that no dethreading occurs at room temperature in solution and this conclusion was corroborated for the melt state by the reproducibility of the DSC results and by the results described below.

The fact that polyrotaxanes **10** and **11** possessed two melting points and two crystallization temperatures is quite interesting, especially coupled to the similar results for polyrotaxane **8**. Two deductions can be made. 1) Since there are two kinds of crystalline phases in these systems, there must be enough freedom for the macrocycles to move along the polymer backbone during the crystallization process, so that both the macrocycle and the polymer backbone can aggregate and crystallize independently. 2) The significant depression in both the melting points and the crystallization temperatures and the lower degree of crystallization as indicated by a lower heats of fusion for the polyrotaxanes relative to the pure linear and cyclic components indicate that the crystallization process, however, is hindered by the "permanent" physical linkages between macrocycles and linear polymer chains in the polyester rotaxanes.

## VII. THERMO-OXIDATIVE STABILITY OF POLYROTAXANES

Because crown ethers are not thermally stable in air, polyrotaxanes tend to decompose at lower temperatures compared to their linear analogs, as shown by the TGA results in Table 4.

## CONCLUSIONS

It has been demonstrated here that polymeric rotaxanes containing polysebacate backbones [tri(ethyleneoxy) and 1,4-butylene] and ethylene oxide-based crown ethers [30-crown-10, 42-crown-14, and 60-crown-20] can be synthesized by polyesterification using macrocycles as solvents in transesterification methods. The polyrotaxanes were purified by multiple reprecipitations into good solvents for the crown ethers. The compositions and the physical properties of the polyrotaxanes were measured by a variety of characterization techniques including NMR, GPC, VPO, UV, DSC, TGA, as well as intrinsic viscosity measurements. Significant amounts, up to 51 mass %, of the macrocyclic component can be incorporated, depending on the size of the macrocycle and the feed ratios employed.

The threading of macrocycles onto the backbone leads to changes in physical properties. In all cases the solubilities of the polyrotaxanes were strongly influenced by the cyclic component; enhanced solubilities in polar solvents were observed relative to the simple parent polysebacates. Thermal behavior was also affected. In the tri(ethyleneoxy) system  $T_g$  is lowered in the rotaxanes. In the butylene system, a glass transition was observed in rotaxanes, but not in the model system; the transition was attributed to the crown ether component. Due to the ability of the macrocycles to move along the backbone and aggregate, the macrocycles are able to crystallize without dethreading.



## EXPERIMENTAL

**Measurements.** All melting points were determined on a Haake-Buchler melting point apparatus and are corrected.  $^1\text{H}$  nuclear magnetic resonance (NMR) spectra were recorded with chloroform solutions (unless otherwise noted) with tetramethylsilane as an internal standard on a Bruker 270 MHz instrument and a Hewlett Packard 7550A graphics plotter or on a Varian Unity 400 MHz instrument. The following abbreviations have been used in describing the NMR spectra: s (singlet), d (doublet), t (triplet), q (quartet), p (pentet), and m (multiplet); coupling constants are represented by J in Hz.  $^{13}\text{C}$  NMR spectra were recorded on chloroform solutions (unless otherwise noted) using Varian Unity 400 MHz instruments; chemical shifts are relative to the center line of the  $\text{CDCl}_3$  triplet at 77.0 ppm. Fourier transform infra-red (FTIR) (KBr pellets unless otherwise noted) spectra, reported in  $\text{cm}^{-1}$ , were recorded on a Nicolet MX-1. Thermogravimetric analyses (TGA) were carried out on a DuPont 951 TGA coupled to a DuPont instruments Thermal Analyst 2100. Transition temperatures ( $T_g$ ,  $T_m$ ) were determined by a dual cell DuPont Instruments 912 differential scanning calorimeter (DSC) coupled to the same data station as in TGA or a Perkin Elmer DSC 2 at a heating rate of  $10^\circ\text{C}/\text{min}$  or less. Absolute molecular weights were determined from gel permeation chromatographic (GPC) analyses run on a Waters 150C equipped with a refractive index detector and Viscotek model no. 100 differential viscosity detector using the universal calibration approach which relates elution volume to the product  $[\eta]M$ . GPC measurements were also done using a Waters 590 instrument fitted with refractive index and UV

detectors which was calibrated with polystyrene standards. Permagel 10<sup>2</sup> - 10<sup>6</sup> Å polystyrene-divinylbenzene columns were employed in both instruments. VPO data were recorded on a Wescan-232A Molecular Weight Apparatus at 63 °C using toluene as solvent, and the molecular weights were calculated using a calibration curve obtained from polystyrene (MW's 1250, 2150, 2950, 5050, 9200, and 22000). Ultraviolet spectra were obtained on a Perkin Elmer Model 330 instrument. Intrinsic viscosities were measured on polymer solutions by the successive dilution technique beginning with a 1% by weight solution of the polymer in a Cannon-Fenske type viscometer; care was taken to have the measured "t" (flow time, solution) values between 1.7 and 1.1 t<sub>0</sub> (flow time, solvent).

**Starting materials.** Dimethyl sebacate was purified by sublimation. Tri(ethylene glycol) and 1,4-butanediol were distilled before use. Crown ethers were prepared using procedures described in Chapter 3. The mono-*p*-[tris(*p*'-*t*-butylphenyl)methyl]phenyl ether of di(ethylene glycol) (**1**) was synthesized using the method described in Chapter 4. The other chemicals were used without purification as obtained from commercial sources.

### **Poly(triethyleneoxy sebacate) (**5**) (General Procedure)**

Stage 1: To a 15 mL flask were added dimethyl sebacate (1.83 g, 7.96 mmol), tri(ethylene glycol) (2.65 g, 17.7 mmol), and *p*-toluenesulfonic acid (30 mg, 0.16 mmol). The mixture was heated to 120 °C under nitrogen and stirred with a magnetic stirrer for 12 h. Stage 2: The system was then cooled to room

temperature and connected to a vacuum distillation apparatus. After the vacuum reached 0.1 mm Hg, the system was slowly heated to 200 °C in 2 h and then maintained at this temperature and pressure for 24 h. During this period, about 0.95 mL of colorless distillate was collected; in theory 1.46 g or 1.3 mL of triethylene glycol should be collected. The magnetic stirring stopped towards the end of the polymerization due to the high viscosity of the system. The reaction product solidified quickly upon cooling and became a pale yellow solid at room temperature. **Purification:** This material was dissolved in 30 mL of CH<sub>2</sub>Cl<sub>2</sub> and precipitated into 300 mL of methanol. After the precipitate was filtered and dried, a pale yellow solid material was obtained (2.36 g, 94%). <sup>1</sup>H NMR: 4.24 (t, J = 4.5, 4 H), 3.70 (t, J = 4.5, 4 H), 3.67 (s, 4 H), 2.34 (t, J = 6.5, 4 H), 1.62 (m, 4 H), 1.32 (br 5, 8 H). <sup>13</sup>C NMR: 173.4, 70.5, 69.2, 63.2, 34.0, 28.9, 24.7. IR (neat): 1128 (s), 1177 (s), 1249 (m), 1736 (vs), 2857 (s), 2929 (s).

### **Poly(butylene sebacate) (6a)**

**Stage 1:** Dimethyl sebacate (2.57 g, 11.2 mmol), 1,4-butanediol (2.25 g, 25.0 mmol), and *p*-toluenesulfonic acid (35 mg, 0.18 mmol), 120 °C under nitrogen, 10 h, 0.6 mL distillate. **Stage 2:** 0.1 mmHg, to 200 °C in 2 h, then 24 h. The magnetic stirring stopped towards the end of the polymerization due to the high viscosity of the system. **Purification:** white solid in methylene chloride (30 mL) precipitated into methanol (300 mL). White powdery solid (2.60 g, 88 %) was obtained after the precipitate was filtered and dried, T<sub>m</sub> = 67 °C, no T<sub>g</sub> (from DSC). <sup>1</sup>H NMR : 7.10 (m, 0.44 H), 6.78 (d, 0.04 H), 4.09 (t, J = 5.5, 4H), 2.29 (t, J = 7.0, 4H), 1.70 (m, 4H), 1.61 (m, 4H), 1.30 (br 5, 11.6 H); <sup>13</sup>C NMR: 173.7,

130.6, 123.9, 110, 63.6, 34.2, 31.3, 29.0, 25.3, 24.8. IR (CHCl<sub>3</sub>): 3021 (s), 2933 (m), 1727 (vs), 1223 (vs), 1177 (m).

### **Endblocked poly(butylene sebacate) (6b)**

Stage 1: Dimethyl sebacate (1.38 g, 6.0 mmol), 1,4-butanediol (1.19 g, 13.2 mmol), *p*-toluenesulfonic acid (18.3 mg, 0.096 mmol) and mono[*p*-tri(*p*'-*t*-butylphenyl)methylphenyl ether of di(ethylene glycol)] (0.4286 g, 0.723 mmol) (**1**), 120 °C under nitrogen, 10 h, 0.6 mL distillate. Stage 2: 0.1 mmHg, to 200 °C in 2 h, then 24 h. The magnetic stirring stopped towards the end of the polymerization due to the high viscosity of the system. Purification: white solid in methylene chloride (30 mL) precipitated into methanol (300 mL). White powdery solid (1.72 g, 100%) was obtained after the precipitate was filtered and dried,  $T_m = 65$  °C, no  $T_g$  (from DSC). <sup>1</sup>H NMR : 7.10 (m, 0.44 H), 6.78 (d, 0.04 H), 4.09 (t, *J* = 5.5, 4H), 2.29 (t, *J* = 7.0, 4H), 1.70 (m, 4H), 1.61 (m, 4H), 1.30 (br s, 11.6 H); <sup>13</sup>C NMR: 173.7, 130.6, 123.9, 110, 63.6, 34.2, 31.3, 29.0, 25.3, 24.8. IR (CHCl<sub>3</sub>): 3021 (s), 2933 (m), 1727 (vs), 1223 (vs), 1177 (m). UV:  $A = 0.217$  (1 cm cell, 1.78 mg in 10 mL THF); calcd.  $M_n = 5.7$  kg/mol assuming 100% end capping.

### **Poly(butylene sebacate) (6a) in the presence of 18-Crown-6**

Stage 1: Dimethyl sebacate (1.38 g, 6.0 mmol), 1,4-butanediol (1.19 g, 13.2 mmol), *p*-toluenesulfonic acid (18.3 mg, 0.096 mmol) and 18C6 (1.10 g, 4.2 mmol), 120 °C under nitrogen, 10 h. Stage 2: 0.1 mm Hg, 200 °C in 2h, then 15

h. Purification: product in methylene chloride (30 mL) precipitated into methanol (300 mL) 2 times: white powdery solid (1.55 g, 90%).  $^1\text{H}$  NMR same as above except there were no signals for end blocking groups; no signals of 18-crown-6 or oligomeric glycols were found.

### **Endblocked Poly[(triethyleneoxy sebacate)-rotaxa-(30-crown-10)] (7)**

Stage 1: Dimethyl sebacate (1.80 g, 7.83 mmol), tri(ethylene glycol) (2.85 g, 19.0 mmol), *p*-toluenesulfonic acid (90.0 mg, 0.47 mmol), and mono[*p*-tri(*p*'-*t*-butylphenyl)methylphenyl ether of di(ethylene glycol)] (1), (0.186 g, 0.314 mmol), 120 °C under nitrogen, 21 h. Stage 2: 30C10 (3.80 g, 8.64 mmol) was added after the system had been cooled to room temperature. After the vacuum had reached 0.1 mm Hg, the system was heated to 260 °C in 2 h, then 5 h. Purification: yellow viscous material reprecipitated 3 times from methylene chloride (15 mL) into methanol (300 mL). Third precipitation: 1.40 g (44 %).  $^1\text{H}$  NMR: 7.25 (m, 0.96 H), 4.24 (t,  $J = 4.5$ , 4 H), 3.70 (t,  $J = 4.5$ , 4 H), 3.67 (s, variable), 2.34 (t,  $J = 6.5$ , 4 H), 1.62 (m, 4 H), 1.32 (br s, 8 H); the resonance of 30-crown-10 occurs at 3.67  $\delta$ .  $^{13}\text{C}$  NMR: 173.4, 70.5, 69.2, 63.2, 34.0, 28.9, 24.7; the 70.5  $\delta$  peak corresponds to the carbon of 30-crown-10. IR (neat): 1127 (s), 1177 (m), 1736 (vs), 2859 (s), 2930 (s).

### **Poly[(triethyleneoxy sebacate)-rotaxa-(60-crown-20)] (8)**

Stage 1: Dimethyl sebacate (1.29 g, 5.60 mmol), tri(ethylene glycol) (1.40 g, 9.32 mmol), and *p*-toluenesulfonic acid (10.0 mg, 0.05 mmol), 120 °C under nitrogen,

12 h. Stage 2: cooled to room temperature, 60C20 (2.71 g, 3.08 mmol), 0.1 mm Hg, 260 °C in 2 h then 12 h. Purification: yellow viscous material reprecipitated 3 times from 10 mL of THF into 300 mL of H<sub>2</sub>O. <sup>1</sup>H NMR: 7.25 (m, 0.96 H), 4.24 (t, J = 4.5, 4 H), 3.70 (t, J = 4.5, 4 H), 3.67 (s, variable), 2.34 (t, J = 6.5, 4 H), 1.62 (m, 4 H), 1.32 (br s, 8 H); the resonance of 60-crown-20 occurs at 3.64 δ. <sup>13</sup>C NMR: 173.4, 70.5, 69.2, 63.2, 34.0, 28.9, 24.7; the 70.5 δ peak corresponds to the carbon of 30-crown-10. IR (neat): 1127 (s), 1177 (m), 1736 (vs), 2859 (s), 2930 (s).

### **Poly[(butylene sebacate)-rotaxa-(42-crown-14)] (10)**

Stage 1: Dimethyl sebacate (0.3040 g, 1.321 mmol), 1,4-butanediol (0.2715 g, 3.013 mmol), *p*-toluenesulfonic acid (4.6 mg, 0.0242 mmol), and 42C14 (0.6404 g, 1.038 mmol), 120 °C under nitrogen, 10 h. Stage 2: 0.1 mmHg, 180 °C in 2 h then 20 h. Purification: product in CH<sub>2</sub>Cl<sub>2</sub> (10 mL) precipitated into methanol (250 mL) three times. <sup>1</sup>H NMR: 1.31 (br s, 8 H), 1.61 (m, 4H), 1.71 (m, 4H), 2.29 (t, J = 7.0), 3.65 (s, variable, 42C14), 4.09 (t, J = 5.5). <sup>13</sup>C NMR: 24.89, 25.30, 29.05, 34.23, 63.69, 70.53 (42C14), 173.77.

### **Poly[(butylene sebacate)-rotaxa-(60-crown-20)] (11)**

Stage 1: Dimethyl sebacate (1.29 g, 5.60 mmol), 1,4-butanediol (1.40 g, 9.32 mmol), and *p*-toluenesulfonic acid (10 mg, 0.05 mmol), 120 °C under nitrogen, 24 h. Stage 2: cooled to room temperature, 60C20 (2.71 g, 3.08 mmol), 0.1 mm Hg, 180 °C in 2 h, then 24 h. Purification: viscous pale yellow material in 10 mL

of THF precipitated into 300 mL of H<sub>2</sub>O. <sup>1</sup>H NMR: 1.31 (br s, 8 H), 1.61 (m, 4H), 1.71 (m, 4H), 2.29 (t, J = 7.0), 3.65 (s, variable, 60C20), 4.09 (t, J = 5.5). <sup>13</sup>C NMR: 24.89, 25.30, 29.05, 34.23, 63.69, 70.53 (60C20), 173.77.

### Threading Experiment I

Endcapped poly(butylene sebacate) (**6b**, sample c)(1.0 g, 0.19 mmol) and 42-crown-14 (4.0 g, 6.5 mmol) were dissolved in THF (10 mL) and the mixture was stirred at 55 °C under nitrogen for 11 days. After three precipitations from CH<sub>2</sub>Cl<sub>2</sub> into methanol, polymer (0.65 g) was obtained. Only a trace amount of 42-crown-14 was observed by <sup>1</sup>H NMR: m/n = 3.0 × 10<sup>-4</sup>, 42C14 wt% = 0.07 %.

### Threading Experiment II

Poly(butylene sebacate) (**6a**, sample b, M<sub>n</sub> = 19.6 kg/mol by GPC with polystyrene standards and M<sub>n</sub> = 27.6 kg/mol determined by VPO) (1.0 g, 0.053 mmol) was mixed with 42C14 (4.8 g, 7.7 mmol) in THF (20 mL) at 60 °C under nitrogen. After all starting materials had dissolved, the temperature was raised to 120 °C to remove THF. The mixture was stirred at this condition for three days. After it had been cooled to room temperature, the mixture was dissolved in CH<sub>2</sub>Cl<sub>2</sub> and precipitated in methanol three times. Polyrotaxane **10** (0.8 g) with m/n = 2.0 × 10<sup>-2</sup> (4.6 mass percent of 42-crown-14) was obtained and 95.8 % 42C14 was recovered from methanol. The recovered crown ether and the polymer were then dissolved in THF (20 mL) and the mixture was stirred at 55 °C under nitrogen for three days. After three precipitations from CH<sub>2</sub>Cl<sub>2</sub> into

methanol, poly(butylene sebacate)-rotaxa-(42C14) (**10**) (0.59 g) with  $m/n = 1.7 \times 10^{-2}$  (4.0 mass percent of 42-crown-14) was obtained. 42C14 (3.65 g, 79 %) was recovered. The recovered polymer and 42-crown-14 were then stirred in mixed solvent (60 mL) of THF (75%) and acetonitrile (25%) at 55 °C for 16 days. After three reprecipitations, polyrotaxane **10** (0.43 g) with  $m/n = 1.3 \times 10^{-2}$  (3.0 mass percent of 42-crown-14) was obtained.  $M_n = 48.7$  kg/mol determined by GPC with polystyrene standards and  $M_n = 29.8$  kg/mol determined by VPO.



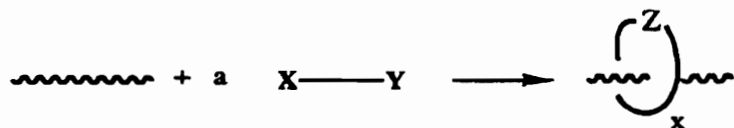
## REFERENCES

1. Gibson, H. W.; Bheda, M. C.; Engen, P. *Prog. in Polym. Sci.* **1994**, *19*, 843.
2. Knops, P.; Sendhoff, N.; Mekelburger, H-B.; Vögtle, F. *Top. Curr. Chem.* **1991**, *161*, 1.
3. van Gulick, N. *New J. Chem.* **1993**, *17*, 618.
4. Schill, G.; Zöllenkopf, H. *Nachr. Chem.*, **1967**, *79*, 149; Schill, G.; Zöllenkopf, H. *Ann. Chem.* **1969**, *721*, 53.
5. Schill, G.; Beckmann, W.; Vetter, W. *Chem. Ber.* **1980**, *113*, 941.
6. Agam, G.; Gravier, D.; Zikha, A. *J. Am. Chem. Soc.* **1976**, *98*, 5206.
7. Harada, A.; Kamachi, M. *Macromolecules*, **1990**, *23*, 2821; Harada, H.; Li, J.; Kamachi, M. *Macromolecules*, **1993**, *26*, 5698.
8. Harada, A.; Li, J.; Kamachi, M. *Nature*, **1992**, *356*, 325.
9. Harada, A.; Li, J.; Kamachi, M. *Nature*, **1993**, *364*, 516.
10. Harada, A.; Kamachi, M. *J. Chem. Soc., Chem. Commun.*, **1990**, 1322.
11. Harada, A.; Li, J.; Suzuki, S.; Kamachi, M. *Macromolecules*, **1993**, *26*, 5267.
12. Shen, Y. X.; Gibson, H. W. *Macromolecules* **1992**, *25*, 2058; Shen, Y. X.; Xie, D.; Gibson, H. W. *J. Am. Chem. Soc.* **1994**, *116*, 537.
13. Gibson, H. W.; Marand, H. *Adv. Mater.*, **1993**, *5*, 11; Gibson, H. W.; Engen, P. T.; Shen, Y. X.; Sze, J.; Lim, C.; Bheda, M. C.; Wu, C. *Makromol. Chem., Macromol. Symp.* **1992**, *54/55*, 519.
14. Gibson, H. W.; Engen, P. T. *New J. Chem.* **1993**, *17*, 723.

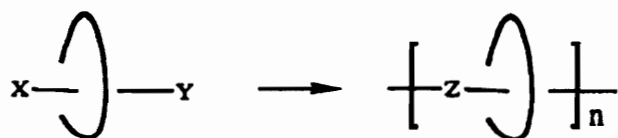
15. The contents of this chapter have been reported: Gibson, H. W.; Liu, S.; Lecavalier, P.; Wu, C.; Shen, Y. X.; *J. Am. Chem. Soc.*, **1995**, *117*, in press.
16. Lenz, R. W., *Organic Chemistry of Synthetic High Polymers*, Inter. Publi., N.Y., **1967**, 83.
17. Gibson, H. W.; Lee, S. H.; Engen, P. T.; Lecavalier, P.; Sze, J.; Shen, Y. X.; Bheda, M. *J. Org. Chem.*, **1993**, *58*, 3748.
18. Lecavalier, P. R.; Engen, P. T.; Shen, Y. X.; Joardar, S.; Ward, T. C.; Gibson, H. W. *Polym. Prepr.*, **1989**, *30* (1), 189.
19. Wu, C.; Bheda, M. C.; Lim, C.; Shen, Y. X.; Sze, J.; and Gibson, H. W., *Polym. Comm.*, **1991**, *32* (7), 204.
20. Gibson, H. W.; Bheda, M. C.; Engen, P.; Shen, Y. X.; Liu, S.; Zhang, H.; Gibson, M. D.; Delaviz, Y.; Lee, S. H.; Wang, L.; Rancourt, J.; Taylor, L. T. *J. Org. Chem.*, **1994**, *59*, 2186.
21. Poly[(butylene sebacate)-rotaxa-(30-crown-10)] (**9**) was prepared by Dr. Charles Wu.
22. *Instruction Manual for Vapor Pressure Osmometry*, WESCAN Instrument Inc. **1987**, pp 3-6. Kroschwitz, J. I. *Polymers: Polymer Characterization and Analysis*, John Wiley & sons, New York, **1990**, pp 486-488.
23. Siochi, E. J.; DeSimone, J. M.; Hellstern, A. M.; McGrath, J. E.; Ward, T. C. *Macromolecules* **1990**, *23*, 4696.
24. This sample was prepared by Dr. Charles Wu.  $M_n$  determined by VPO was 11.0 kg/mol and that determined by GPC with viscosity detector was 12.2 kg/mol.
25. Garrido, L.; Mark, J. E.; Clarson, S. J.; Semlyen, J. A. *Polym. Commun.*

- Polym. Commun.* **1985**, *26*, 55; Clarson, S. J.; Mark, J. E.; Semlyen, J. A. *Polymer Commun.* **1987**, *27*, 244; Fyvie, T. J.; Frisch, H. L.; Semlyen, J. A.; Clarson, S. J.; Mark, J. E. *J. Poly. Sci., Part A, Poly. Chem.* **1987**, *25*, 2503; Hubbard, R. E.; Semlyen, J. A. *Eur. Polym. J.* **1993**, *29*, 305.
26. See Chapter VII.
27. Indeed rotaxanes based on crown ethers and polyurethanes are soluble in water at room temperature and display lower critical solution temperatures at 80 °C. Micelles have been detected by light scattering [unpublished results of R. Davis, Y. X. Shen and H. W. Gibson]. Poly[(styrene)-rotaxa-(crown ether)]s form emulsions in water and alcohols [unpublished results of S.-H. Lee and H. W. Gibson].
28. Korshak, V. V.; Vinogradova, S. V.; Vlasova, E. S. *Doklady Akad. Nauk S.S.S.R.* **1954**, *94*, 61.
29. Woo, E. M.; Barlow, J. W.; Paul, D. R. *Polymer*, **1985**, *26*, 763.
30. Fernandes, A. C.; Barlow, J. W.; Paul, D. R. *Polymer*, **1986**, *27*, 1799.
31. Marvel, C. S.; Johnson, J. H. *J. Am. Chem. Soc.*, **1950**, *72*, 1674.

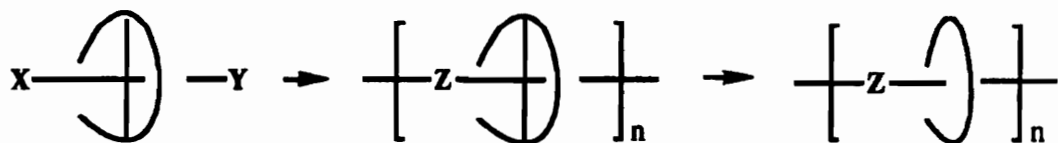
1. Cyclization in presence of linear macromolecules



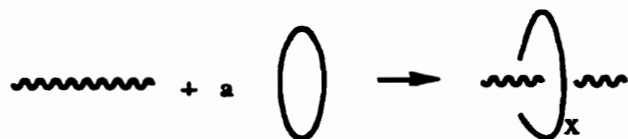
2. Polymerization of monomeric rotaxanes



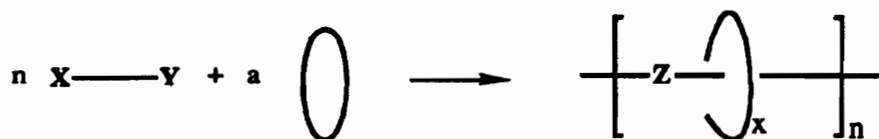
3. Chemical Conversion



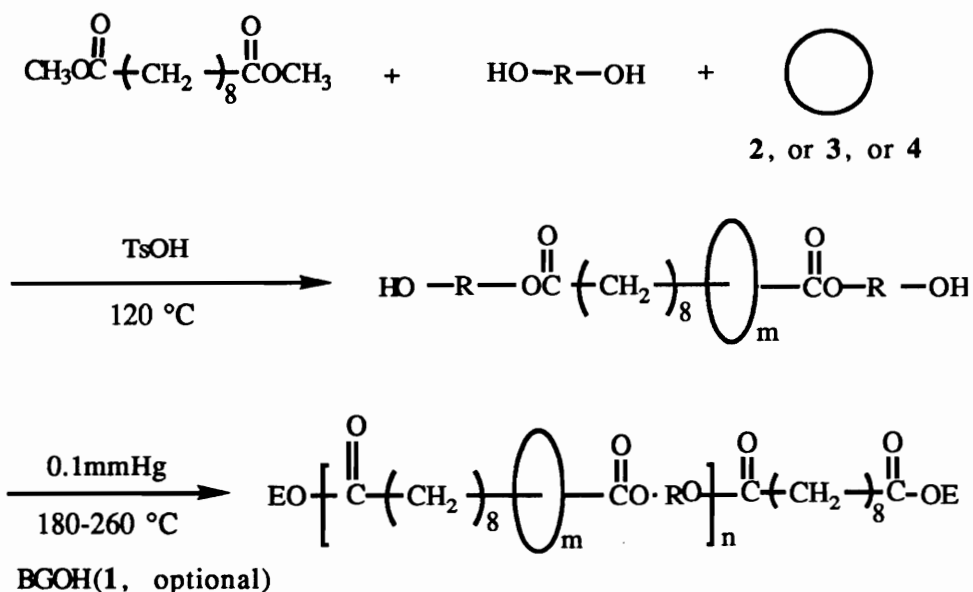
4. Threading of preformed linear macromolecules through preformed macrocycles



5. Production of linear macromolecule in the presence of preformed macrocycle

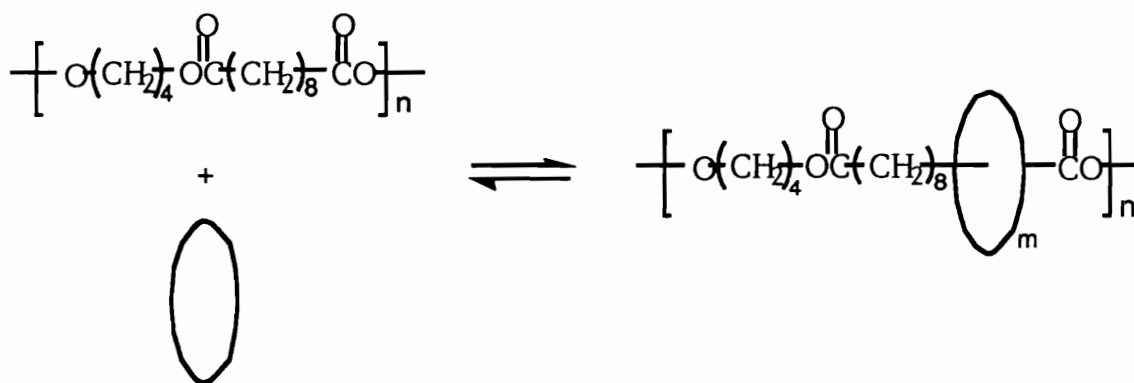


Scheme 1. Potential routes to polyrotaxanes in which functional groups X and Y react to form Z (from ref. 1)



- 5:** R =  $-(\text{CH}_2\text{CH}_2\text{O})_2\text{CH}_2\text{CH}_2-$ , m = 0, E = H  
**6a:** R =  $-(\text{CH}_2)_4-$ , m = 0, E = H  
**6b:** R =  $-(\text{CH}_2)_4-$ , m = 0, E = BG  
**7:** R =  $-(\text{CH}_2\text{CH}_2\text{O})_2\text{CH}_2\text{CH}_2-$ ,  $\text{O} = 2$ , E = BG  
**8:** R =  $-(\text{CH}_2\text{CH}_2\text{O})_2\text{CH}_2\text{CH}_2-$ ,  $\text{O} = 4$ , E = H  
**9:** R =  $-(\text{CH}_2)_4-$ , m = 0,  $\text{O} = 2$ , E = H  
**10:** R =  $-(\text{CH}_2)_4-$ , m = 0,  $\text{O} = 3$ , E = H  
**11:** R =  $-(\text{CH}_2)_4-$ , m = 0,  $\text{O} = 4$ , E = H

Scheme 2: Syntheses of polysebacates and corresponding polyotaxanes



Polymer (g)	42C14 (g)	Solvent	Time (day)	Temp. (°C)	wt % of 42C14		
					1st ppt	2nd ppt	3rd ppt
1.0 <sup>a</sup>	4.80		3	120	23	4.9	4.6
0.8 <sup>b</sup>	4.60	THF (10 mL)	3	55	10	4.4	4.0
0.59 <sup>b</sup>	3.65	THF(45 mL) Acetonitrile (15 mL)	16	62	5.8	4.4	17 <sup>c</sup> 3.0 <sup>c</sup>

- Poly(butylene sebacate).  $M_n = 18.8$  K (determined by GPC with differential viscosity detector).
- Resultant polymers from previous experiments.
- Fractionated.

Scheme 3. Preparation of polyrotaxane **10** from preformed polymer **6a**

Table 1

## Reprecipitation results for polysebacate rotaxanes

Sample ID.	Polymer	Cyclic	S/M Ratio <sup>a</sup>	BGOH Used	Rxn. Cond. <sup>b</sup>	n/m Ratio in Polymer			Final Backbone Atoms per Cyclic	Final wt % Macrocycle
						1st ppt	2nd ppt	3rd ppt		
E	7	30C10	0.91	Yes	I	3.2 <sup>d</sup>	3.2	3.2	64	30 <sup>i</sup>
F	8	60C20	1.81	No	I	1.9 <sup>e</sup>	2.4	2.4	48	54 <sup>i</sup>
G	9 <sup>c</sup>	30C10	0.91	Yes	II	6.5 <sup>f</sup>	7.5	7.8	125	18 <sup>j</sup>
H	10	42C14	1.27	No	IV	4.3 <sup>g</sup>	4.4	4.5	73	35 <sup>j</sup>
I	11	60C20	1.86	Yes	V	2.6 <sup>h</sup>	3.5	3.3	53	51 <sup>j</sup>

**a** S/M was the molar ratio of dimethyl sebacate to macrocycle in the monomer feed.

**b.** I: 120 °N<sub>2</sub>, 21 h; 260 °/0.3 Torr, 5 h; II: 120 °N<sub>2</sub>, 12 h; 260 °/0.2 Torr, 12 h; III: 140 °N<sub>2</sub>, 24 h; 180 °/0.2 Torr, 30 h; IV: 120 °N<sub>2</sub>, 10 h; 180 °/0.1 Torr, 20 h; V: 120 °N<sub>2</sub>, 24 h; 180 °/0.1 Torr, 24 h.

**c.** See ref. 21.

**d.** Determined by the formula  $n/m = [10A/(B-2A)]$  where A is the integral for signals in the range 4.1-4.4  $\delta$  (-COOCH<sub>2</sub>- of polyester, 4H) and B is the integral for signals in the range 3.5-3.9  $\delta$  [all other -OCH<sub>2</sub>'s of polyester (8H) and crown ether (40H)]. Estimated error:  $\leq \pm 0.1$ .

**e.** Calculated from  $n/m = [20A/(B-2A)]$  where A and B are defined as in footnote d; crown has 80H. Estimated error:  $\leq \pm 0.1$ .

**f.** Calculated from  $n/m = 5A/2B$  where A is the integration of signals in the range 1.20-1.80  $\delta$  (internal CH<sub>2</sub>'s of backbone, 16 H) and B is that for the 3.67  $\delta$  signal for the 40 H of 30C10. Estimated error:  $\pm 0.2$ .

**g.** Calculated from  $n/m = 7A/2B$  where A is the integration of signals in the range 1.20-1.80  $\delta$  (internal CH<sub>2</sub>'s of backbone, 16 H) and B is that for the 3.67  $\delta$  signal for the 56 H of 42C14. Estimated error:  $\leq \pm 0.1$ .

**h.** Calculated from  $n/m = 5A/B$  where A is the integration of signals in the range 1.20-1.80  $\delta$  (internal CH<sub>2</sub>'s of backbone, 16 H) and B is that for the 3.67  $\delta$  signal for the 80 H of 60C20. Estimated error:  $\pm 0.2$ .

**i.** End groups ignored in this calculation: wt. % =  $M_{\text{crown}}/[M_{\text{crown}} + (n/m)]$  (316)].

**j.** End groups ignored in this calculation: wt. % =  $M_{\text{crown}}/[M_{\text{crown}} + (n/m)]$  (256)].

Table 2

Molecular weights of polysebacates and corresponding polyrotaxanes a

Sample ID	Polymer	$[\eta]^b$ (dL/g)	Target $M_n^c$	$M_n$ $^1H$ NMR	$M_n$ $^{13}C$ NMR	$M_n$ UV	$M_n$ VPO	$M_n$ GPC (abs)	$M_w$ GPC (abs)	$-\log K$	$\alpha$	$M_n$ GPC (PS)	$M_w$ GPC (PS)	Cyclic per Macrol.
A	5	0.12	$\infty$	-	-	-	-	1.9	2.5	-	-	2.3	3.9	0
B	6a	0.85	$\infty$	-	-	-	27.6	18.8	35.7	2.66	0.51	19.6	41.7	0
C	6b	0.46	11.4	18.0 d	-	18.9	19.3	-	-	-	-	19.9	33.3	0
D	6b	0.27	5.4	5.2 d; 5.0 e	5.9 f; 5.4 g	5.7	5.3	-	-	-	-	5.0	9.4	0
E	7	0.28	15.7	9.0 h	-	7.5	2.2	2.4	3.6	4.83	1.03	4.4	10.0	2.3 i
F	8	-	$\infty$	-	-	-	-	-	-	-	-	3.6	11.6	2.4 j
H	10	0.46	$\infty$	-	-	-	-	-	-	-	-	17.0	28.9	15 k
I	11	0.51	$\infty$	-	-	-	8.6	10.1	18.2	3.02	0.54	15.0	24.8	5.9 l

a. Molecular weights are in kg/mol.

b. In  $CHCl_3$  at 30 °C.c. The  $M_n$  values of polymer backbones determined by the amount of the blocking group (1) used.d. Calculated from  $M_n = \{256(27)/4[(A/B) - 1]\} + 2(592) - 88$  Where A is the integration of the 1.3  $\delta$  signal [ $CH_3$  (54 H) +  $COCC(CH_2)_4CCCO$  (8H)] and B is that for the 1.5 - 1.9  $\delta$  signal [ $COCC(CH_2)_4CH_2CCO$  (4 H) +  $OCCH_2CH_2CO$  (4 H)]. Estimated error:  $\pm 10\%$ .




- e. Calculated from  $M_n = \{256(27)/2[(A/B) - 2]\} + 2(592) - 88$  Where A is the integration of the 1.3  $\delta$  signal [CH<sub>3</sub> (54 H) + COCC(CH<sub>2</sub>)<sub>4</sub>CCCO (8H)] and B is that for the 2.3  $\delta$  signal [COCH<sub>2</sub>C<sub>6</sub>H<sub>4</sub>CH<sub>2</sub>CO (4 H) + OCCH<sub>2</sub>CH<sub>2</sub>CO (4 H)]. Estimated error:  $\pm 5\%$ .
- f. Calculated from  $M_n = [256 (9) /2(A/B)] + 2(592) - 88$  where A is the integration for the 31.17  $\delta$  signal [CH<sub>3</sub> (18C)] and B is that for the 29.05  $\delta$  signal (COCCC<sub>4</sub>CCCO). Estimated error:  $\pm 5\%$ .
- g. Calculated from  $M_n = [256 (3)/(A/B)] + 2 (592) - 88$  where A is the integration for the 148.2  $\delta$  signal [  (6C)] and B is the integration for the 173.7  $\delta$  signal [C=O (2C)]. Estimated error:  $\pm 7\%$ .
- h. Calculated from  $M_n = \{316 + 0.31 (440) (9B)/[(A/B) - 2]\} + 2(591) - 132 - 0.31(440)$  where A is the integration of the 1.3  $\delta$  signal [CH<sub>3</sub> (36 H) + COCC(CH<sub>2</sub>)<sub>4</sub>CCO (8 H)] and B is that for the 1.6  $\delta$  signal [COCCCH<sub>2</sub>C<sub>4</sub>H<sub>2</sub>CCO (4 H)]. Estimated error:  $+ 5\%$ .
- i. Based on  $M_n = 2.3$  kg/mol.
- j. Based on  $M_n = 3.6$  kg/mol.
- k. Based on  $M_n = 17.0$  kg/mol.
- l. Based on  $M_n = 9.4$  kg/mol (average of VPO and abs. GPC results).

Table 3  
Solubility of polysebacates and corresponding polyrotaxanes

Sample ID	Polymer	Water	Methanol	Acetone (hot)	CH <sub>2</sub> Cl <sub>2</sub>	THF
A	5	no	no	no	yes	yes
B	6 a	no	no	no	yes	yes
E	7	slightly	slightly	yes	yes	yes
F	8	slightly	slightly	yes	yes	yes
H	10	slightly	slightly	partially	yes	yes
I	11	slightly	slightly	yes	yes	yes

Table 4  
Thermal properties of model polymers and polyrotaxanes

Sample ID	Polymer	TGA <sup>a</sup> (°C, 5% loss)	T <sub>g</sub> <sup>b</sup> (°C)	T <sub>m</sub> <sup>b</sup> (°C)	ΔH <sub>f</sub> (cal/g)	T <sub>c</sub> <sup>c</sup> (heating, °C)	T <sub>c</sub> <sup>d</sup> (cooling, °C)
A	5	273	-55.5	-26, 19 <sup>e</sup>	7.4, 15.3	-47, -23	-0.6
B	6a	340	-	67 <sup>f</sup>	18.5 <sup>f</sup>	-	48
C	6b	320	-	65	20.1	-	-
D	6b	312	-	62	14.7	-	40.7
E	7	222	-55.7	9, 13	1.06 tot <sup>e</sup>	-8	-
F	8	277	-56.9	43	11.6	-44	15
H	10	258	-58	53, 59	5.1, 16.0	-	48, 16
I	11	298	-60.5	33, 37	15.5 tot <sup>e</sup>	-49	19, 9

- a. Measured in air at 10 °C/min.  
b. At 10 °C/min after heating to melt and cooling to -100 °C; corrected.  
c. At 10 °C/min after rapid cooling from the melt; corrected.  
d. At 2.5 °C/min; corrected.  
e. Broad peak; two maxima.  
f. Reported T<sub>m</sub> 62.6,<sup>34</sup> 64.8,<sup>35</sup> 64.5 °C; <sup>40</sup> ΔH<sub>m</sub> = 37.0 cal/g for sample of M<sub>v</sub> = 2.5 kg/mol.<sup>35</sup>

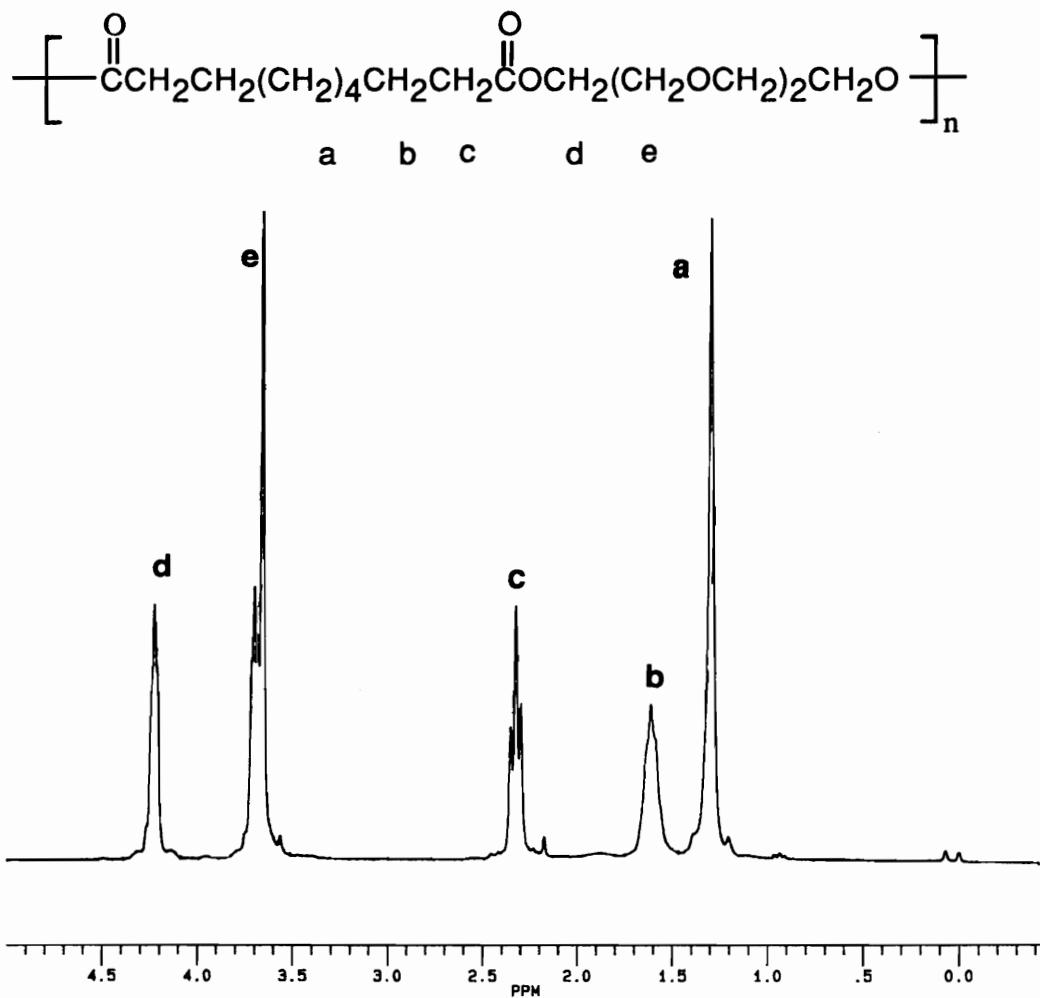


Figure 1. 270 MHz <sup>1</sup>H NMR spectrum of poly(triethyleneoxy sebacate) (5) in CDCl<sub>3</sub>

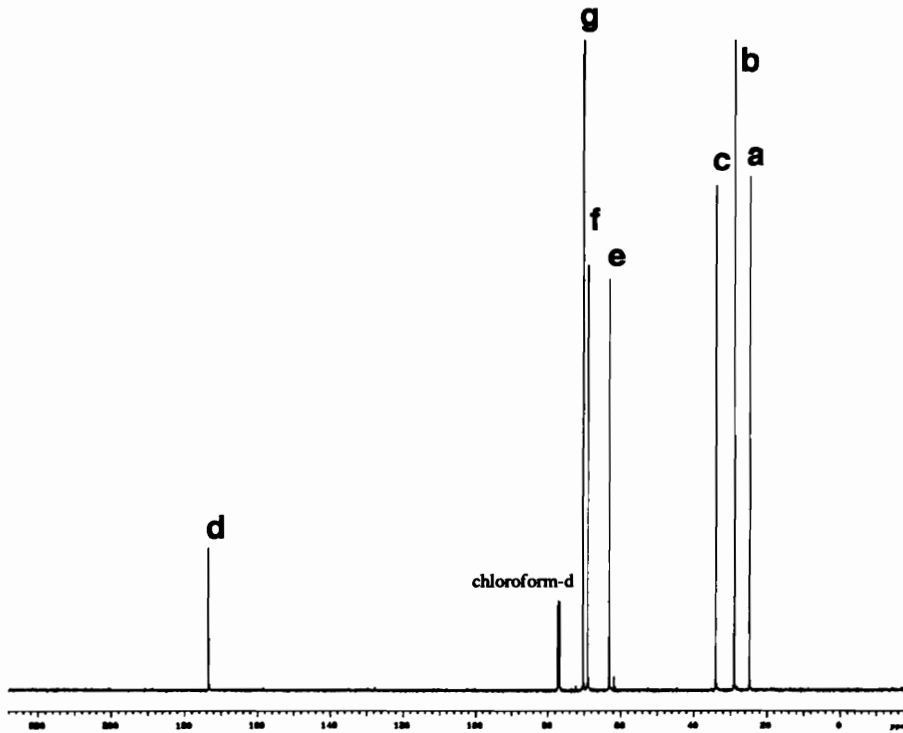
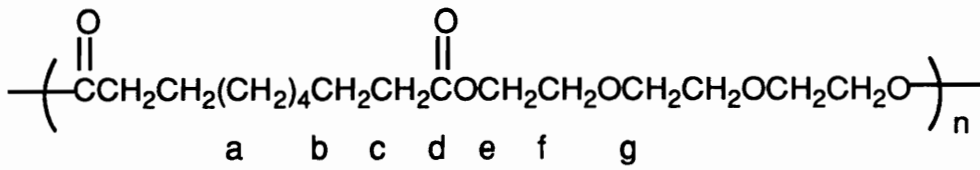


Figure 2. 100 MHz  $^{13}\text{C}$  NMR spectrum of poly(triethyleneoxy sebacate) (5) in  $\text{CDCl}_3$

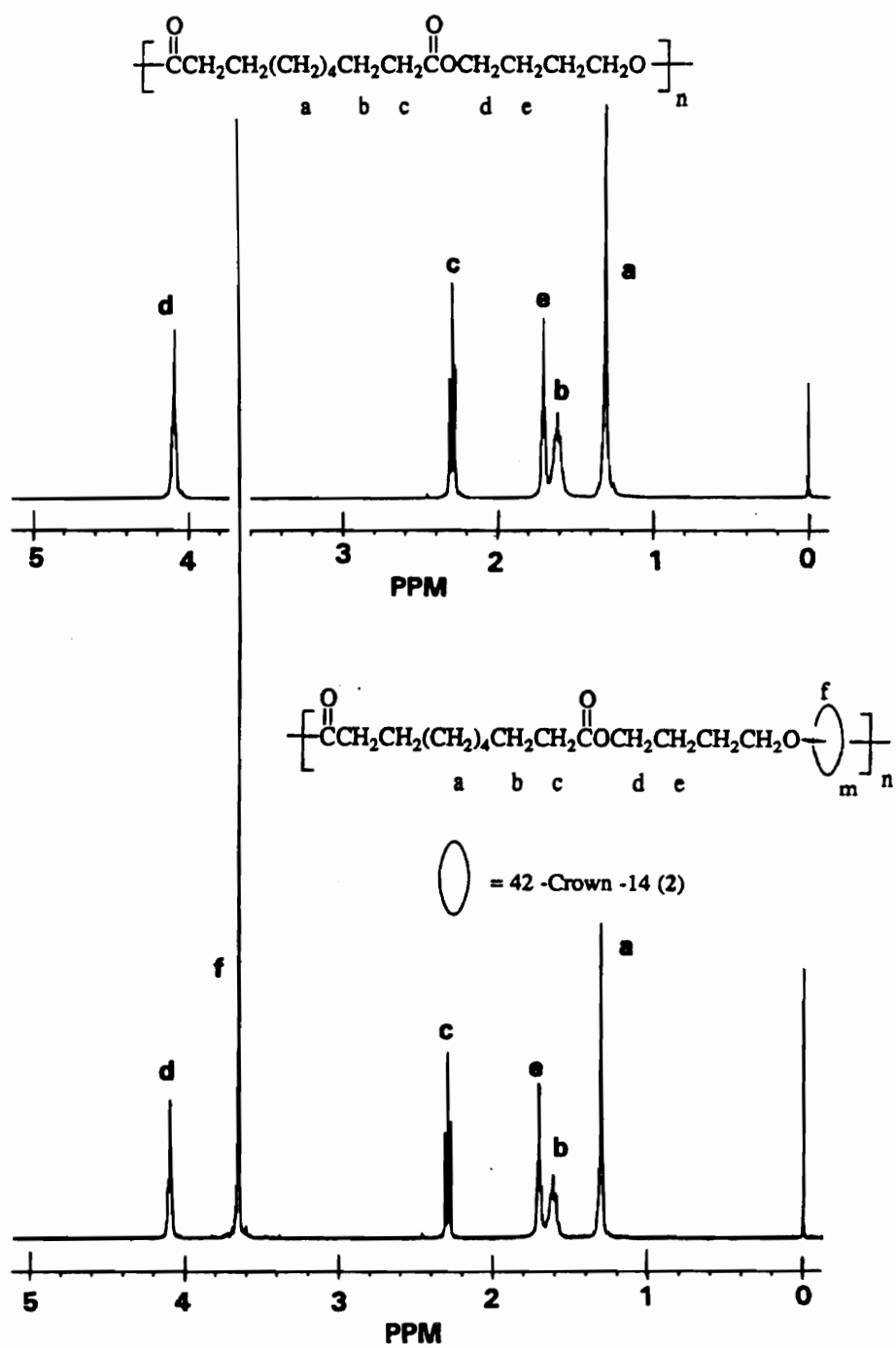


Figure 3. 400 MHz  $^1\text{H}$  NMR spectrum of a) poly(butylene sebacate) (6a) (top) and b) poly[(butylene sebacate)-rotaxa-(42-crown-14)] (10) (bottom) in  $\text{CDCl}_3$ .

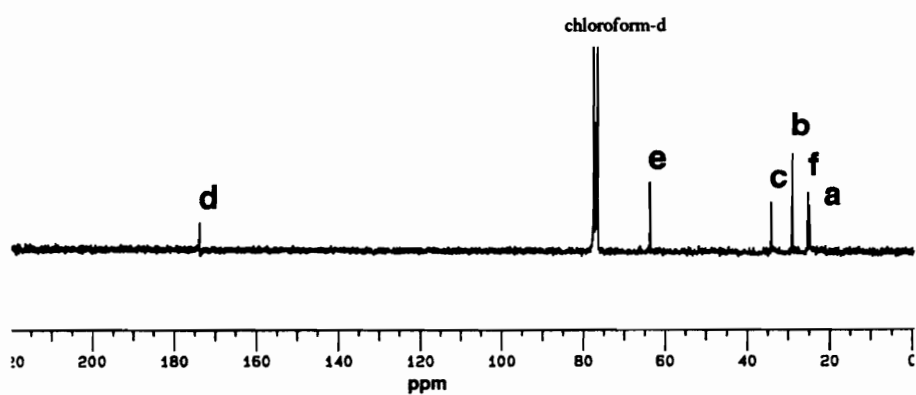
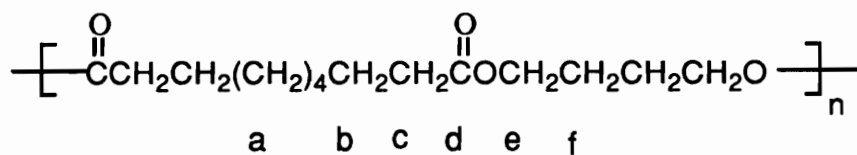


Figure 4. 100 MHz <sup>13</sup>C NMR spectrum of poly(butylene sebacate) (**6a**) in CDCl<sub>3</sub>

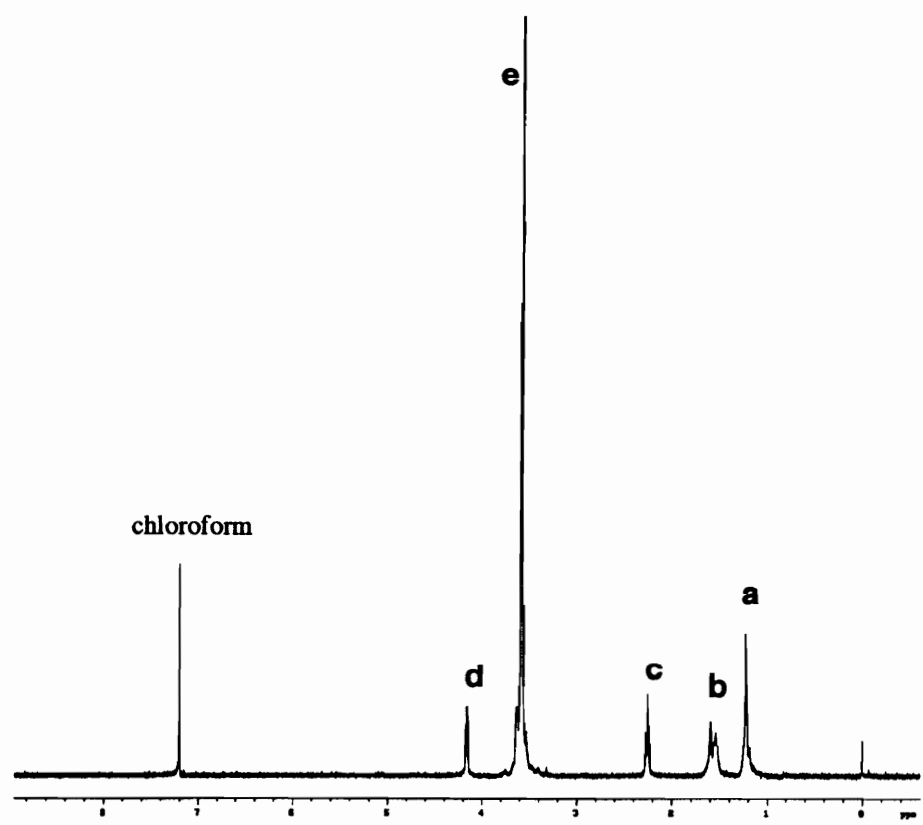
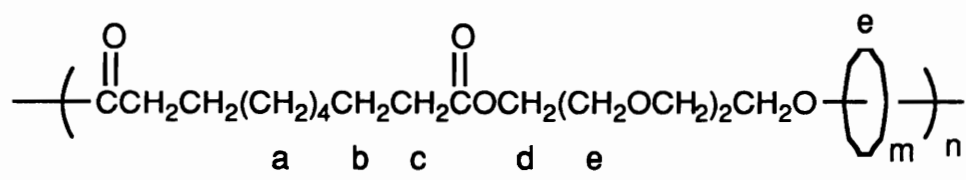


Figure 5. 400 MHz <sup>1</sup>H NMR spectrum of poly[(triethyleneoxy sebacate)-rotaxa-(60-crown-20)] (**8**) in CDCl<sub>3</sub>



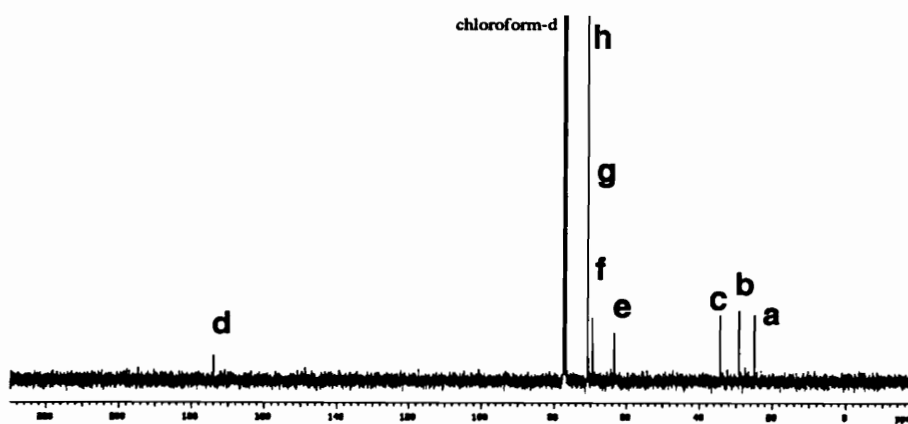
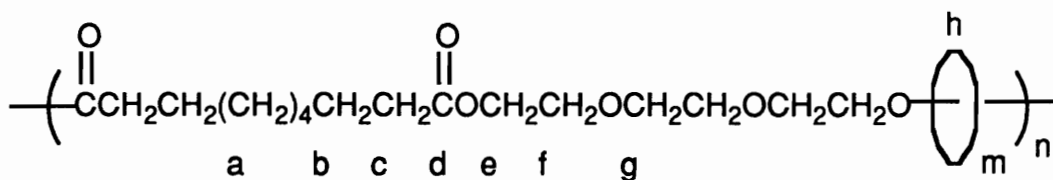


Figure 6. 100 MHz  $^{13}\text{C}$  NMR spectrum of poly[(triethyleneoxy sebacate)-rotaxa-(60-crown-20)] (**8**) in  $\text{CDCl}_3$

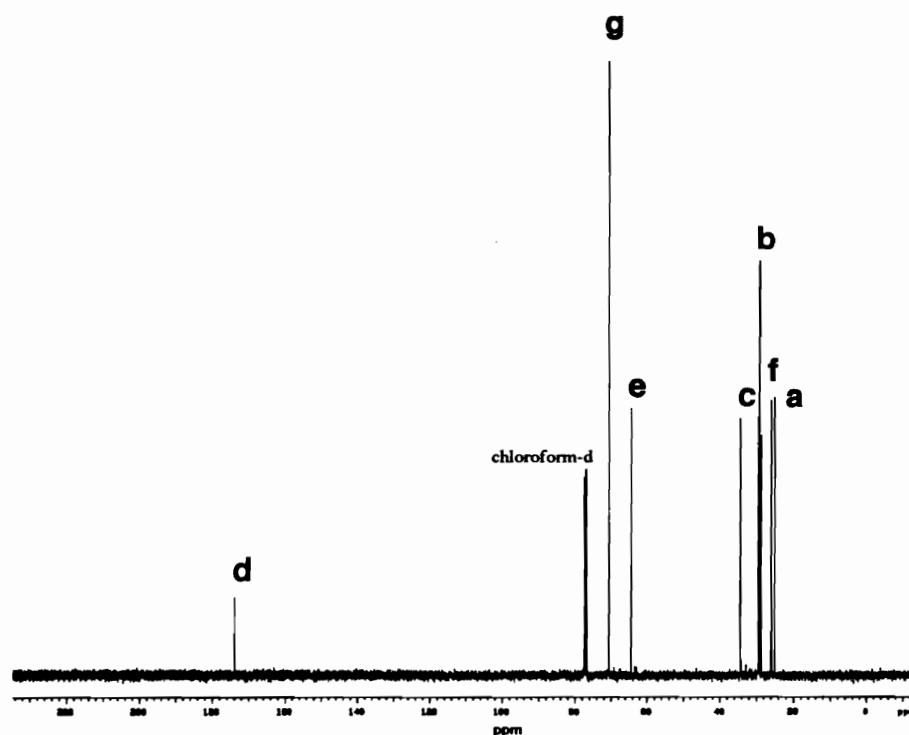
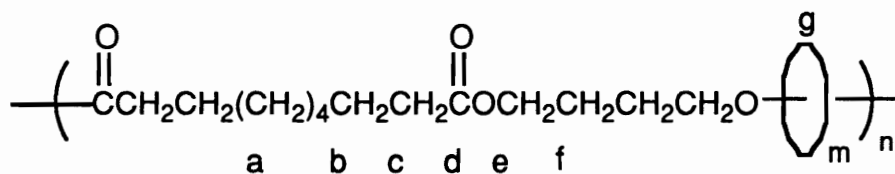


Figure 7. 100 MHz  $^{13}\text{C}$  NMR spectrum of poly[(butylene sebacate)-rotaxa-(42-crown-14)] (**10**) in  $\text{CDCl}_3$

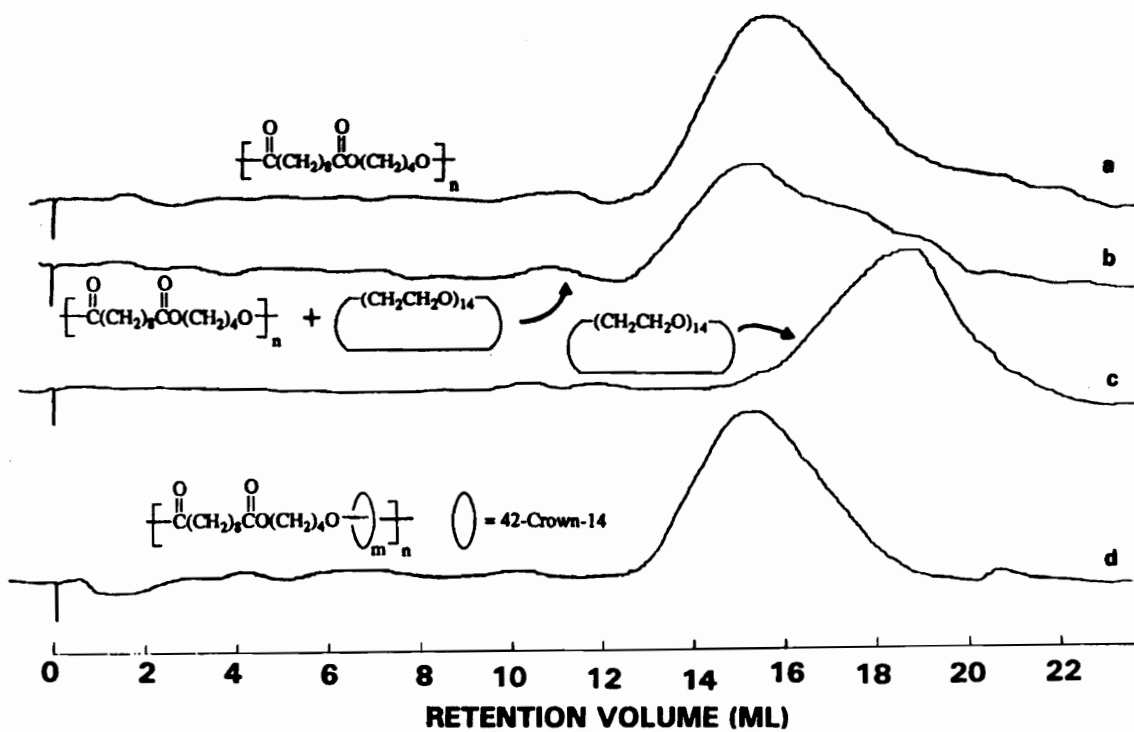


Figure 8. GPC traces for a) poly(butylene sebacate) (**6a**); b) a physical mixture of **6a** and 42-crown-14 (**3**) 70:30 by mass; c) 42-crown-14 (**3**) and d) poly[(butylene sebacate)-rotaxa-(42-crown-14)] (**10**) in CHCl<sub>3</sub> at 30 °C; refractive index detector.

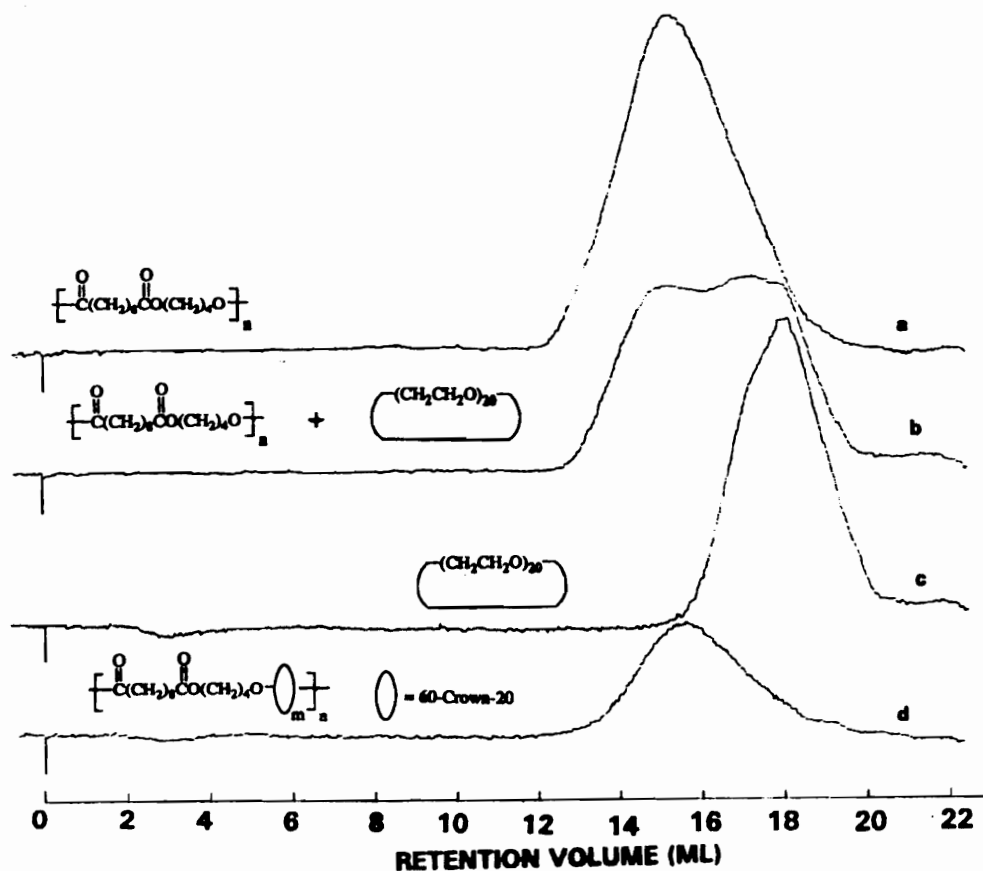


Figure 9. GPC traces for a) poly(butylene sebacate) (**6a**); b) a physical mixture of **6a** and 60-crown-20 (**4**) 55:45 by mass; c) 60-crown-20 (**4**) and d) poly[(butylene sebacate)-rotaxa-(60-crown-20)] (**11**) in  $\text{CHCl}_3$  at  $30^\circ\text{C}$ ; refractive index detector.

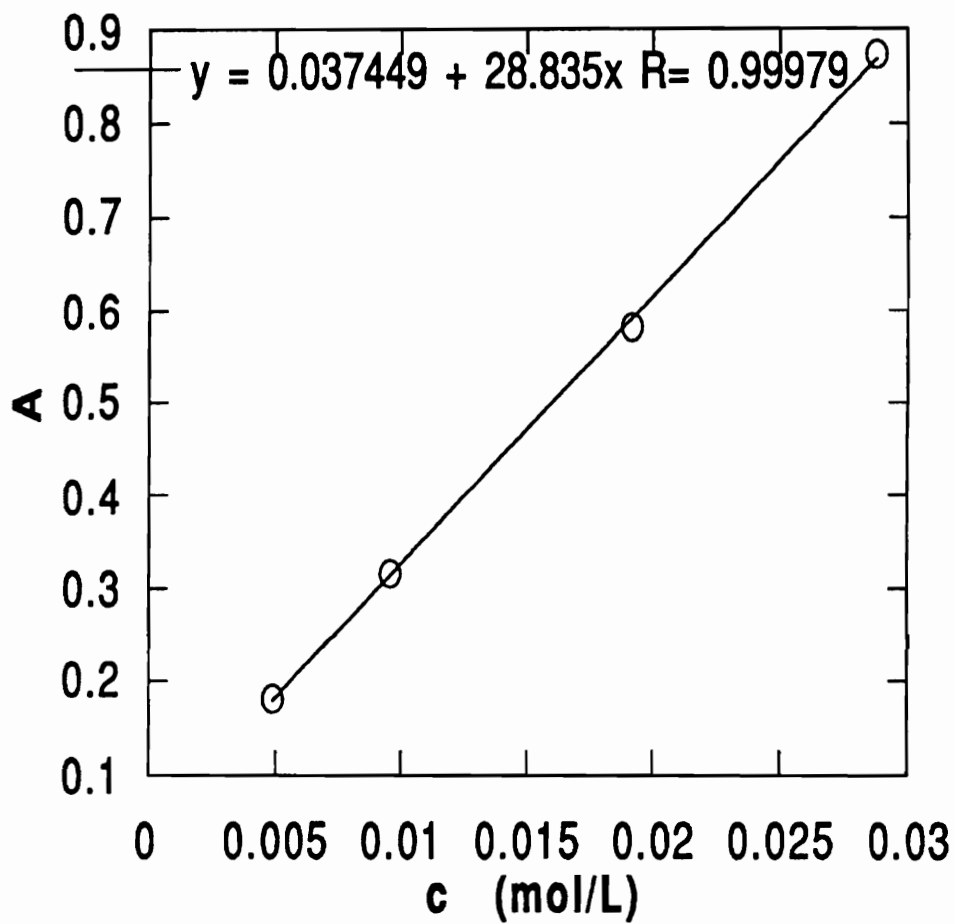


Figure 10. Calibration curve for UV measurement of 1. 25 °C in THF.

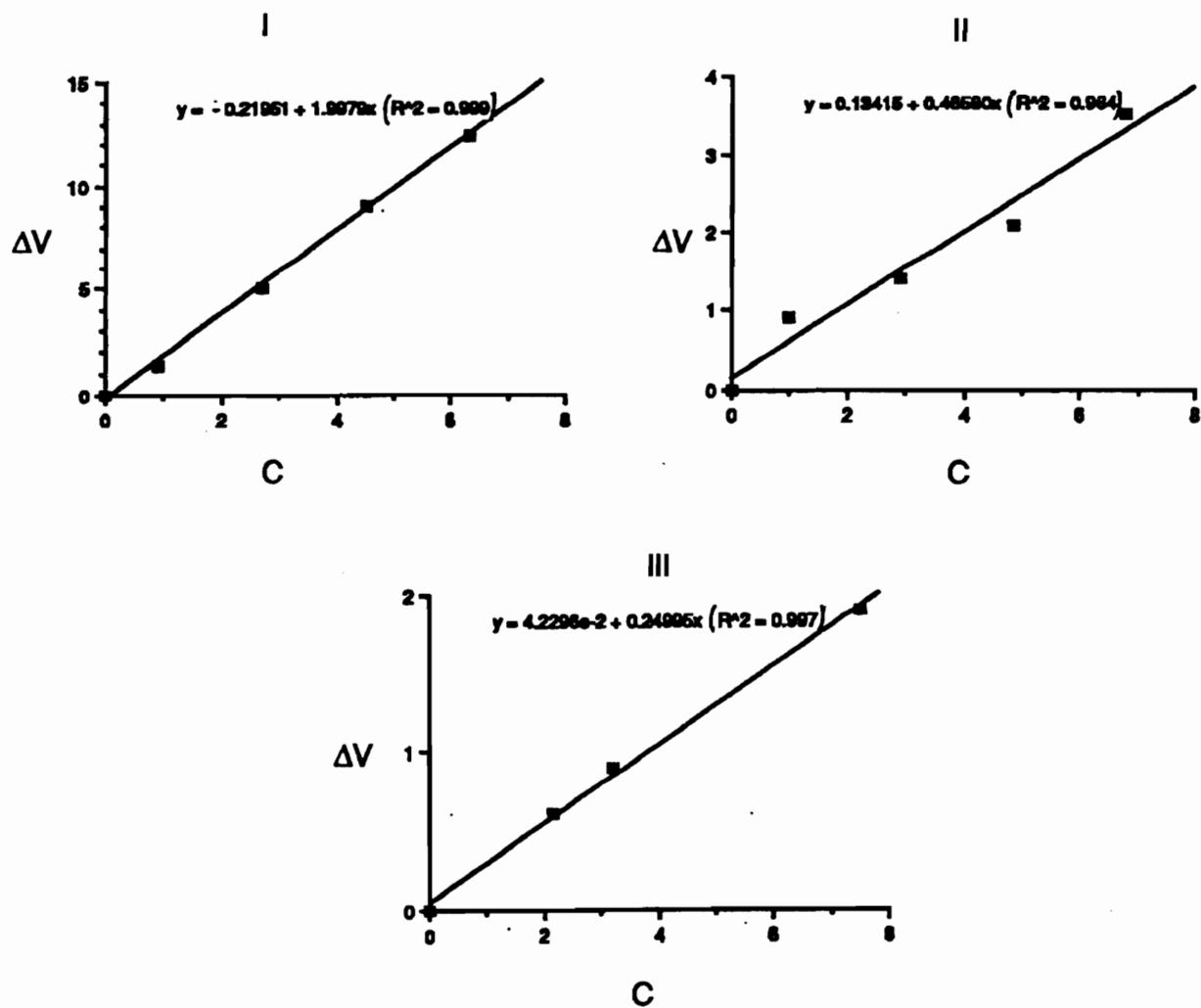


Figure 11. Plots of  $\Delta V$  vs. concentration  $c$  (g/L) for polystyrene standards: I)  $M_n = 1,320$ ; II)  $M_n = 8,000$ ; and III)  $M_n = 17,500$ . 50 °C in toluene.

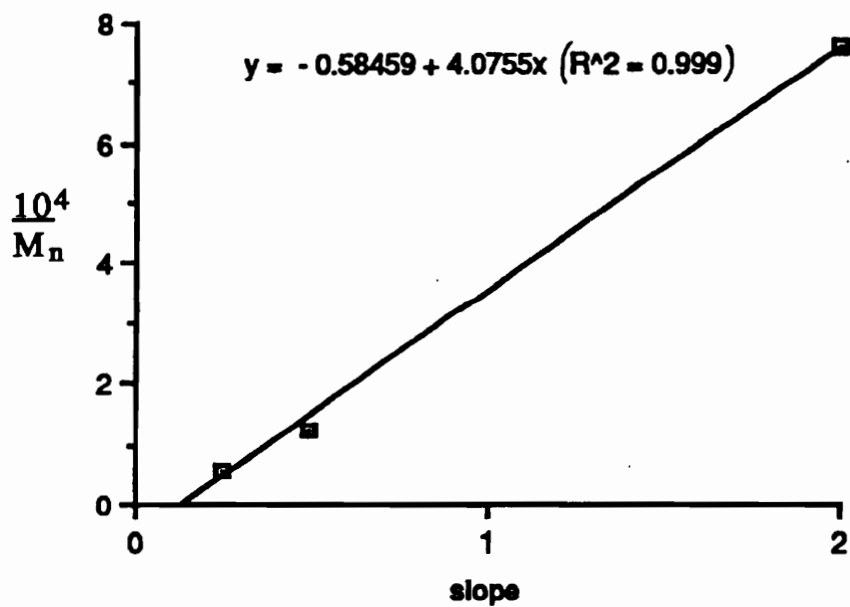


Figure 12. Calibration curve for VPO measurements

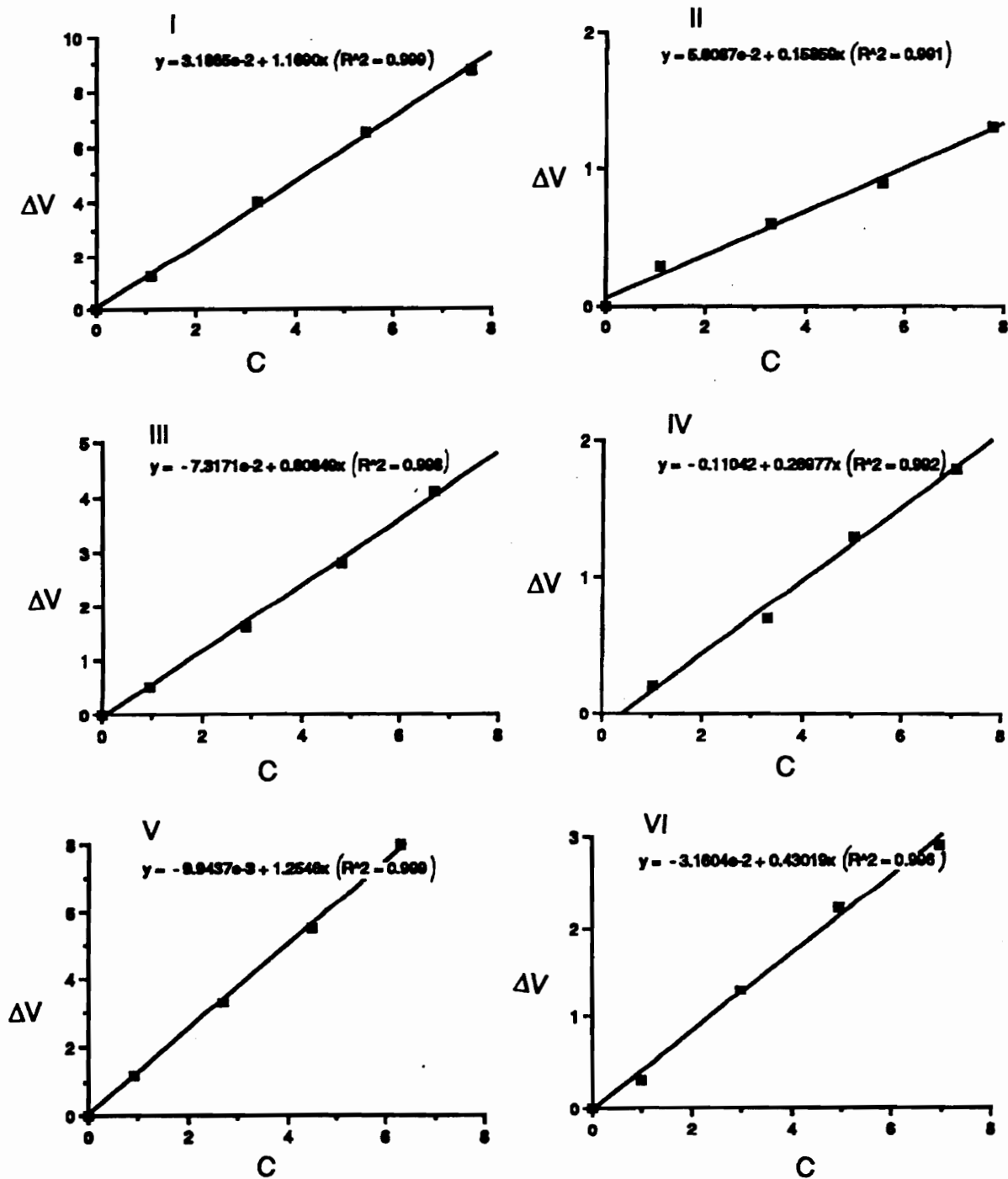


Figure 13. Plots of  $\Delta V$  vs. concentration  $c$  (g/L) for I) polymer 5; II) polymer 6a; III) polymer 6b (sample C); IV) polymer 6b (sample D); V) polymer 7; and VI) polymer 11. 50 °C in toluene.



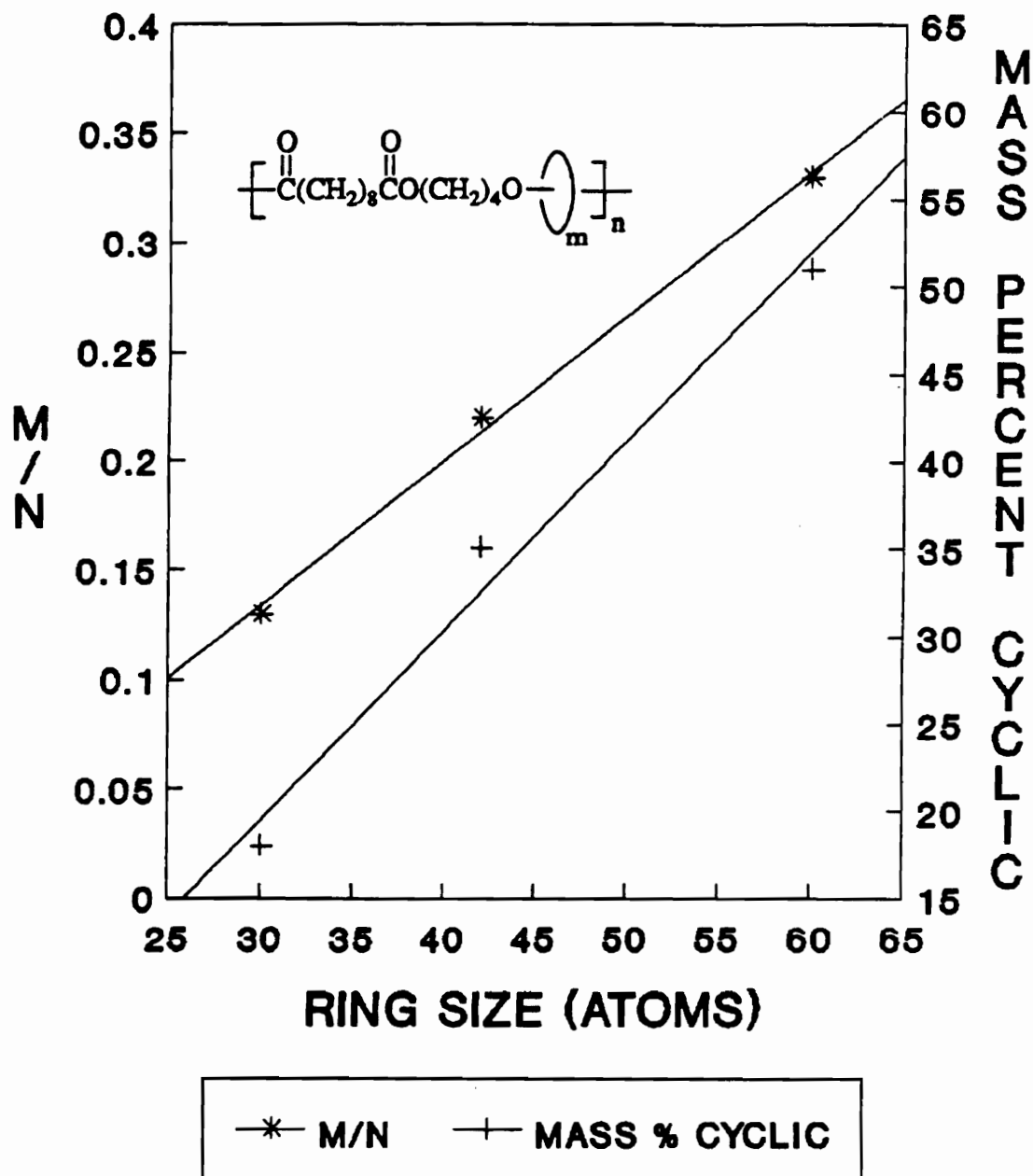


Figure 14. Cyclic ratio (m/n) and mass percent cyclic in polyrotaxanes 9, 10 and 11 as a function of crown ether ring size for neat polymerizations (120 °C, 10h; 180 °C, 0.1 Torr, 20 h) using the same mass (2.01 g) of each macrocycle per gram of dimethyl sebacate.

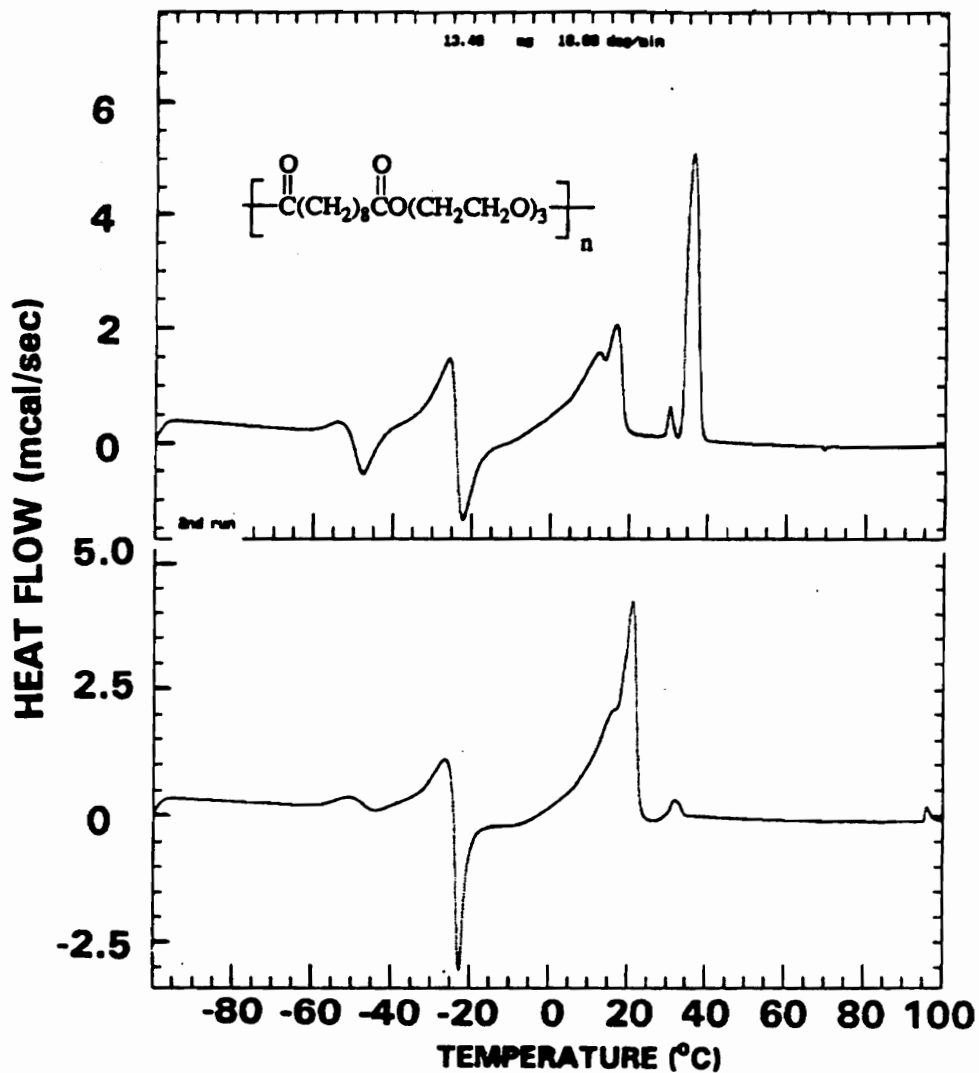


Figure 15. DSC traces for poly(triethyleneoxy sebacate) (5): a) first heating scan (top), b) second heating scan after slow cooling (bottom); 10 °C/min. Temperature scale is uncorrected.

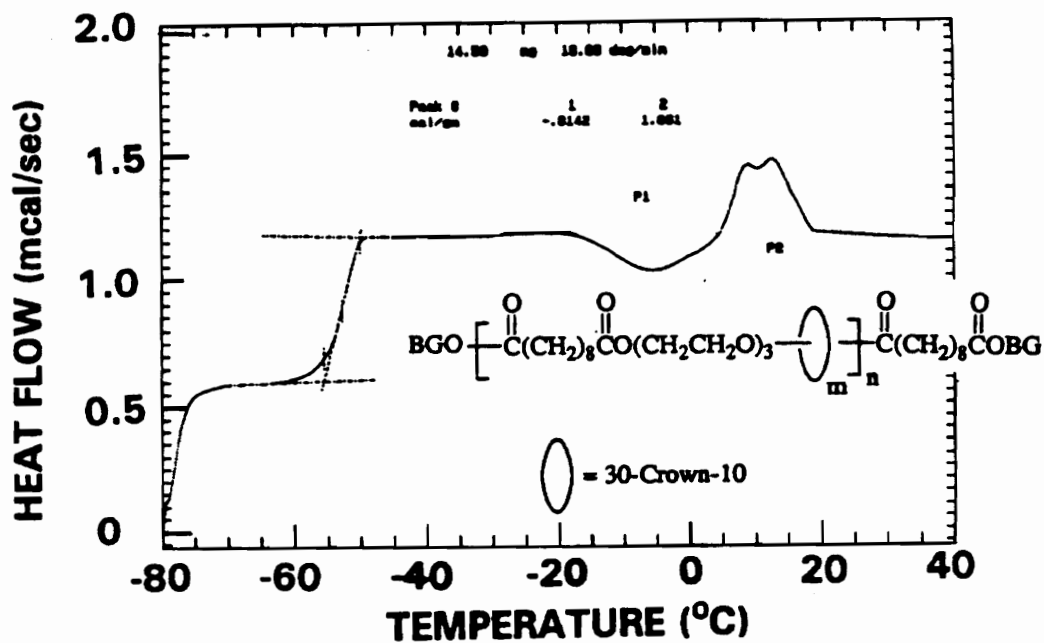


Figure 16. DSC trace for poly[(triethyleneoxy sebacate)-rotaxa-(30-crown-10)] (7), 10 °C/min. Temperature scale is uncorrected.

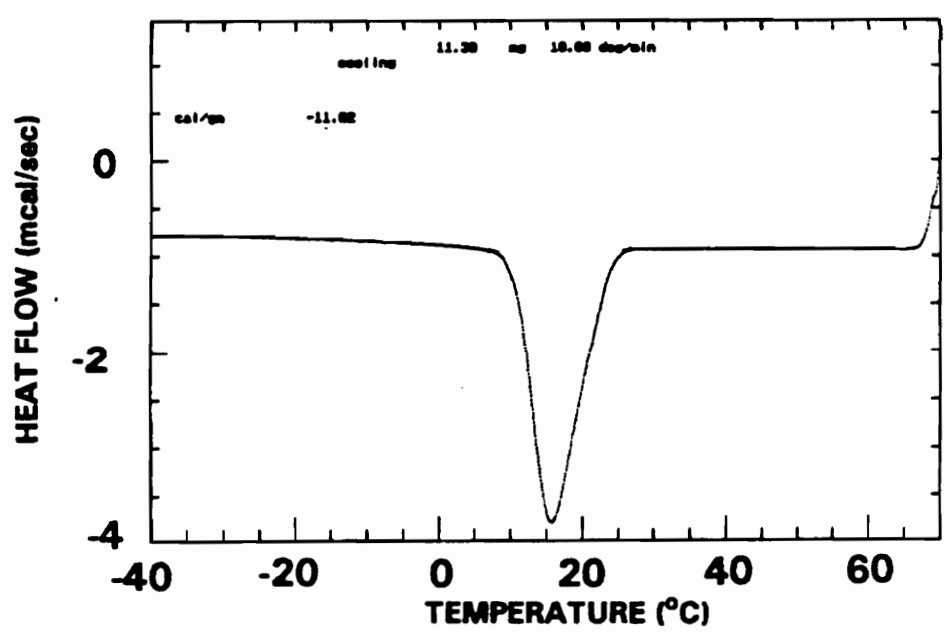
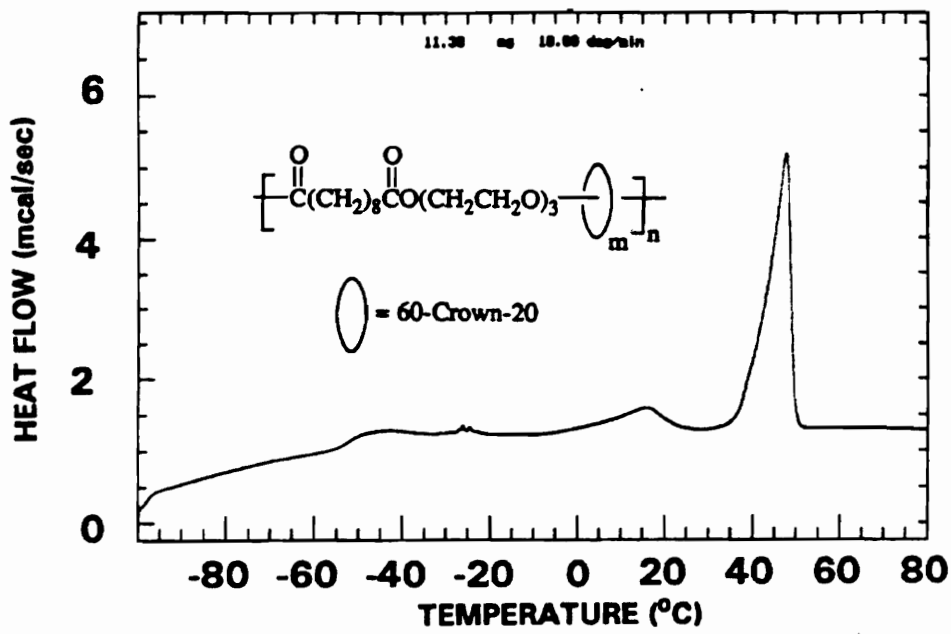


Figure 17. DSC traces for poly[(tri(ethyleneoxy sebacate)-rotaxa-(60-crown-20))<sub>n</sub>](8): a) heating (top); b) cooling (bottom), 10 °C/min. Temperature scale is uncorrected.

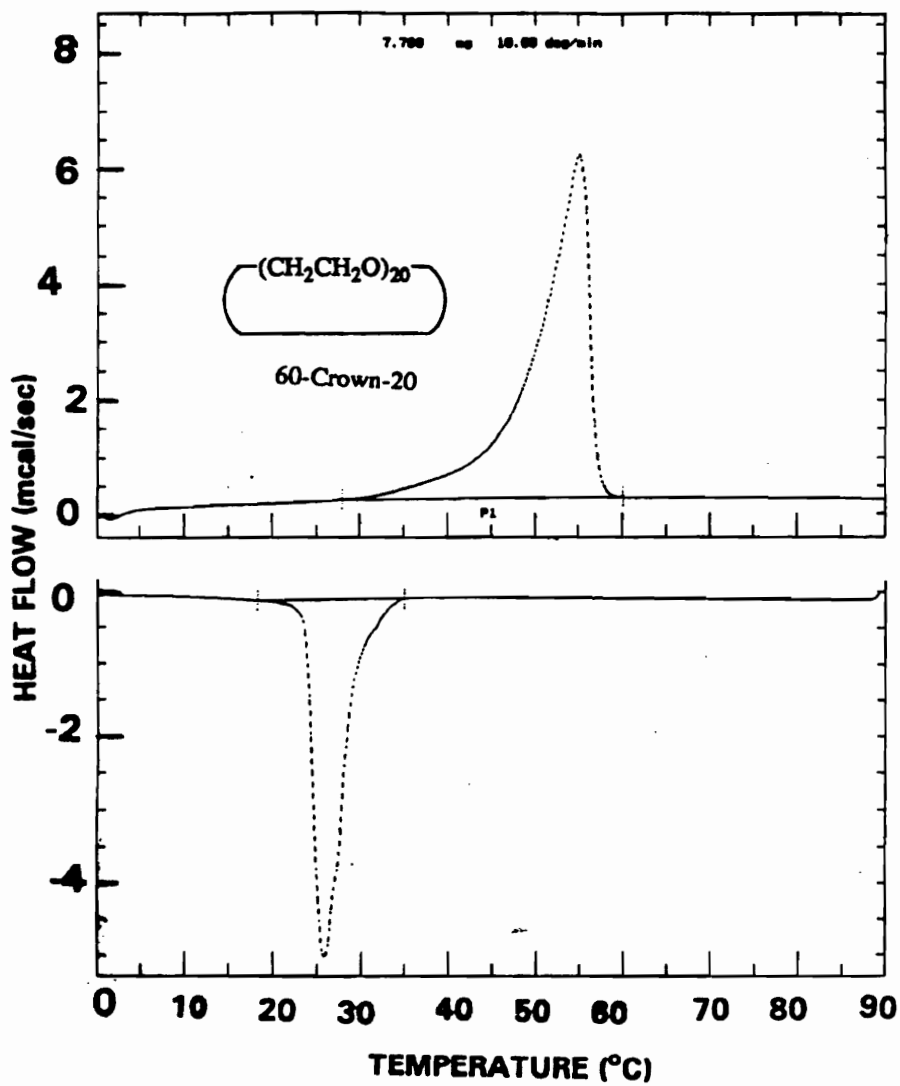


Figure 18. DSC traces for 60-crown-20 (4): a) heating (top), 10 °C/min. cooling (bottom), 5 °C/min. Temperature scale is uncorrected.

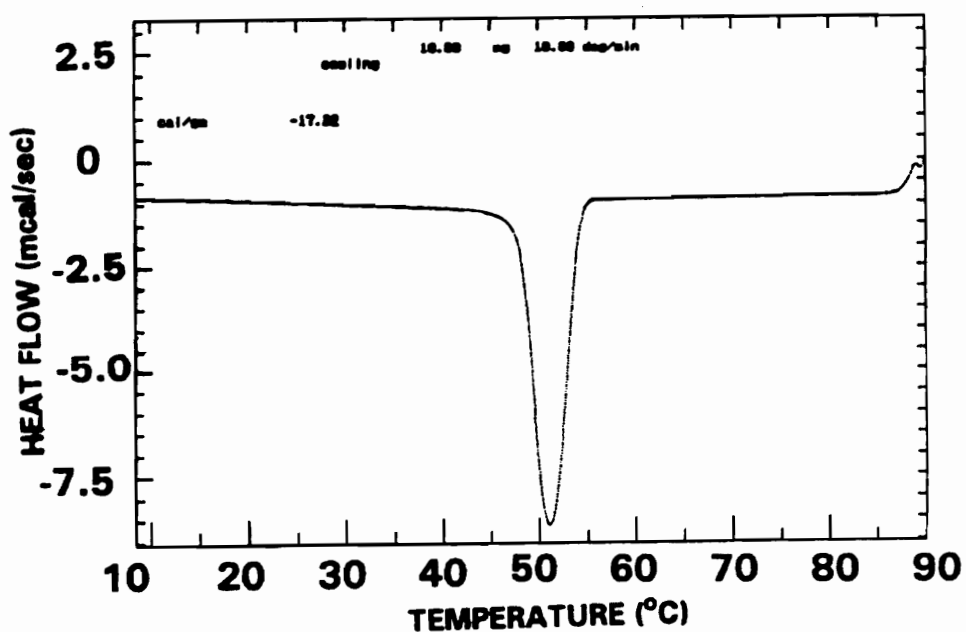
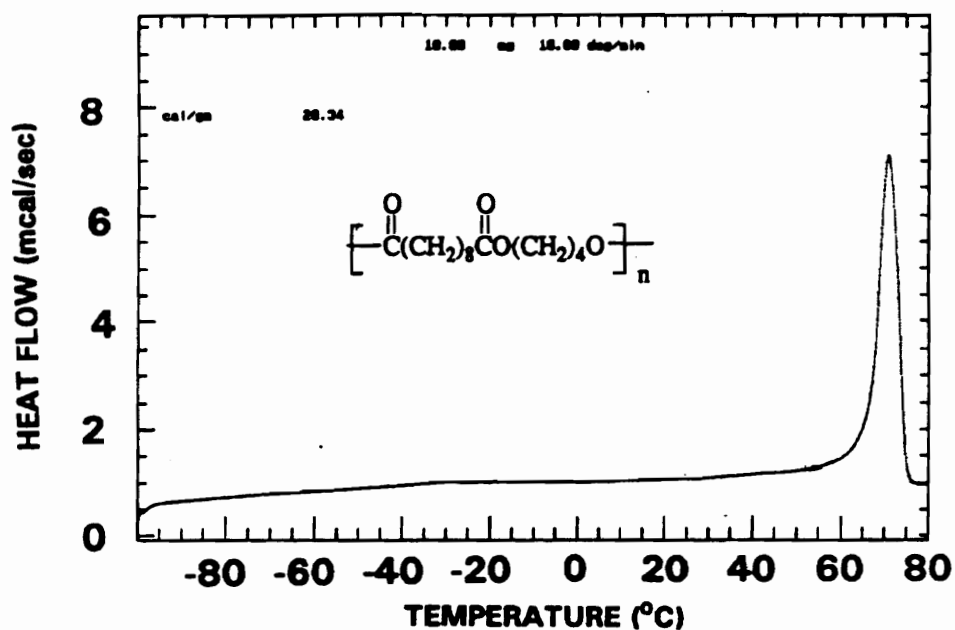


Figure 19. DSC traces for poly(butylene sebacate) (6a): a) heating (top), b) cooling (bottom), 10 °C/min. Temperature scale is uncorrected.

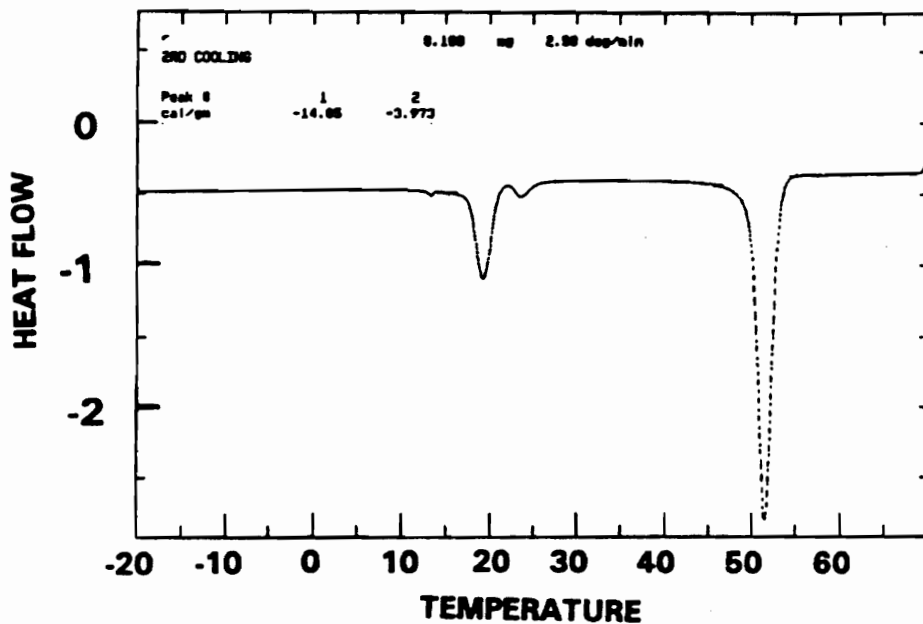
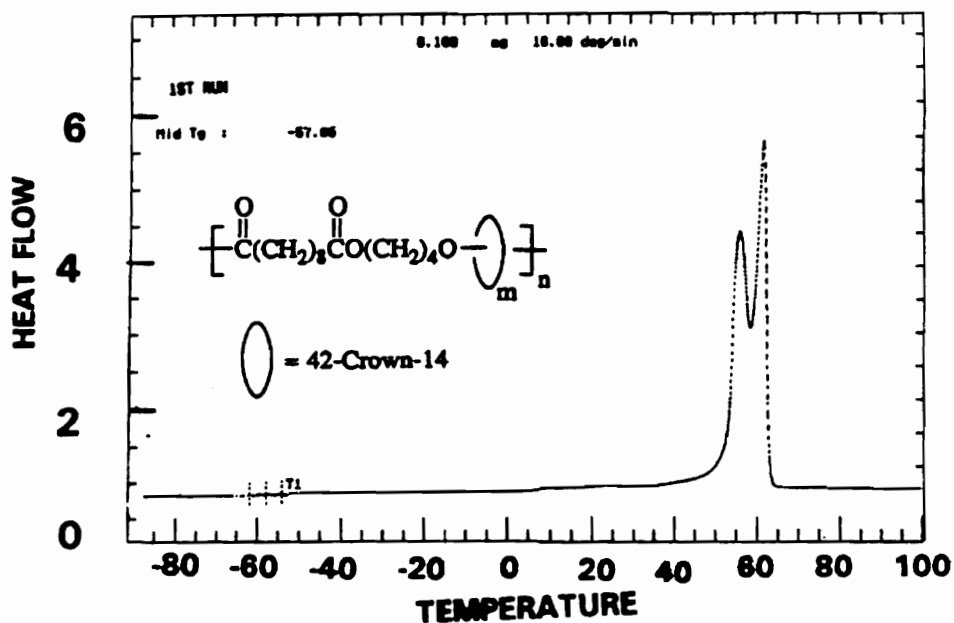


Figure 20. DSC traces for poly[(butylene sebacate)-rotaxa-(42-crown-14)] (10): a) heating (10 °C/min) (top); b) cooling (bottom), 2.5 °C/min. Temperature scale is uncorrected.

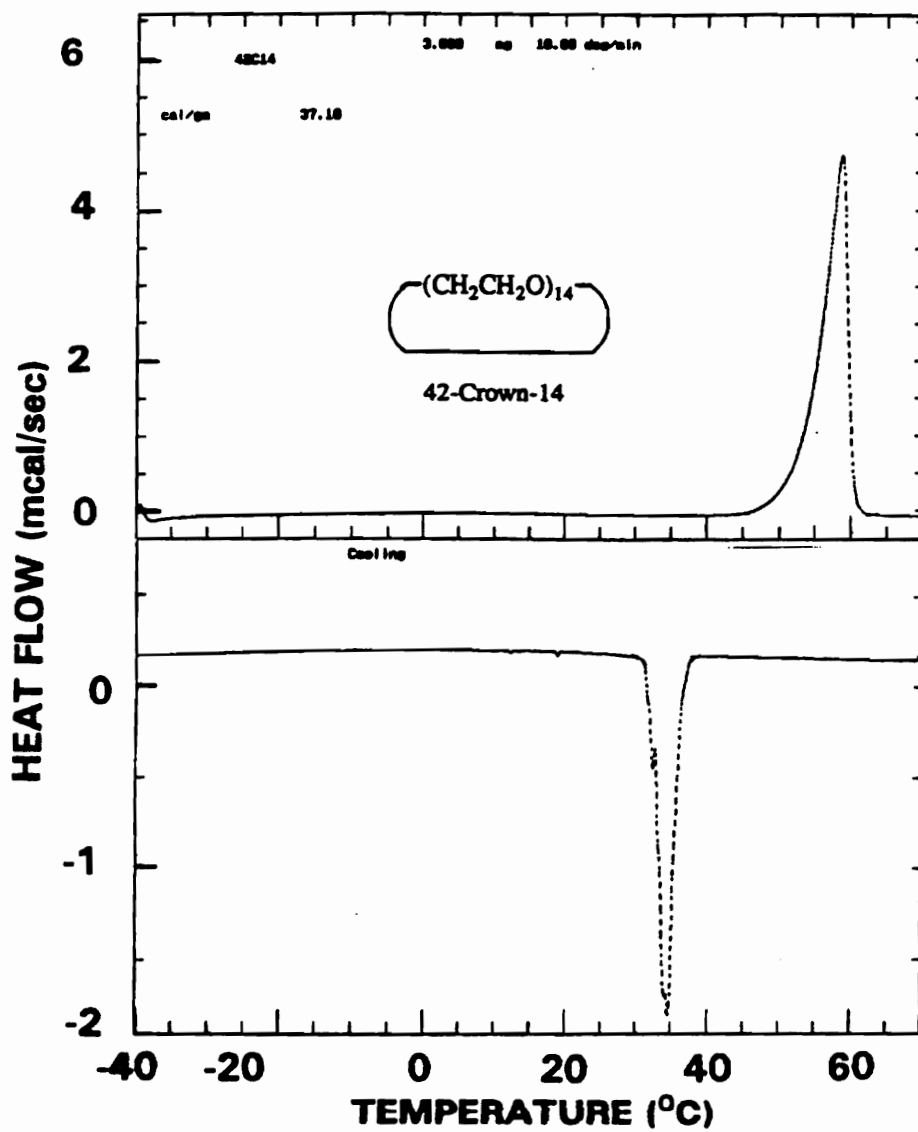


Figure 21. DSC traces for 42-crown-14 (2): a) heating (top), b) cooling (bottom), 10 °C/min. Temperature scale is uncorrected.



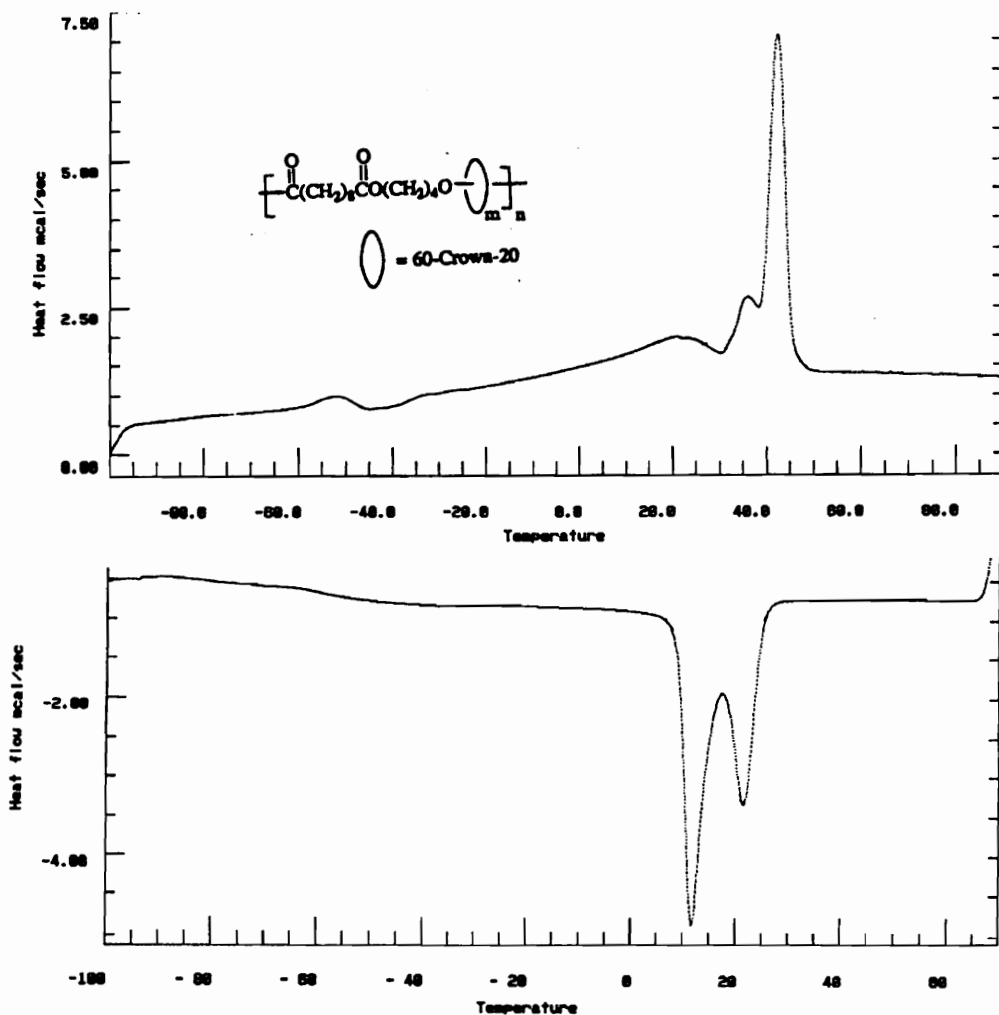


Figure 22. DSC traces for poly[(butylene sebacate)-rotaxa-(60-crown-20)] (11): a) heating (top), 10 °C/min; b) cooling (bottom), 10 °C/min. Temperature scale is uncorrected.

## **CHAPTER VIII**

### **POLYESTER ROTAXANES (ACID CHLORIDE METHOD)**

Since the special properties of polyrotaxanes arise from the physical linkage of linear and cyclic molecules, a high degree of threading of macrocycles onto linear species has been diligently pursued. The key step in the construction of a rotaxane is to create conditions which allow the threading of the linear chain through the cyclic component to take place. Therefore, it is necessary to understand the nature of the threading process. Parameters of interest are the size of the macrocycles, the length and nature of linear monomers, the molar ratio of cyclic to linear species, temperature, and time. The stoichiometry of the two monomers in the acid chloride method, a well known polymerization technique for the syntheses of polyesters, allows us to systematically study the effects of these parameters in the threading process.

## **RESULTS AND DISCUSSION**

### **I. SOLUTION POLYMERIZATION**

#### **A. Optimization of Reaction Conditions in Model Studies**

Poly(decamethylene sebacate), a model compound for the corresponding polyrotaxanes, was prepared by the acid chloride approach. In model reactions

(Scheme 1) sebacoyl chloride reacted with equimolar 1,10-decanediol in diglyme. Diglyme was chosen as a model for the crown ethers.

The polymerization of diacid chlorides with diols is a typical step growth polymerization of an A-A monomer with a B-B monomer [1]. High molecular weight polymers can be produced by using pure starting monomers, by choosing appropriate reaction conditions to reduce side reactions, and by controlling the precise stoichiometry of monomers [1].

Therefore, all the monomers and the solvent were carefully purified before use. Sebacoyl chloride was vacuum distilled twice. Alkylene diols were recrystallized in dry dichloroethane twice. Diglyme was stored over NaOH, refluxed with sodium and then vacuum distilled.

During the reactions, a nitrogen flow passed through the reaction system to remove the hydrogen chloride generated in the reactions. An attempt to use pyridine as an acid capturer was not successful because the polymer is not soluble in the mixture of pyridine and diglyme.

Two important reaction parameters, temperature and time, were optimized by a series of reactions under different reaction conditions. The results are listed as experiments 1-4 in Table 1. The conditions of experiment 2, 80 °C and 48 hours, gave the highest molecular weight.

Precise stoichiometry of the two monomers is another important factor in achieving high molecular weight polymers. Polyrotaxanes are usually synthesized on a small scale because the supply of crown ethers is limited. Unfortunately, the exact equivalent ratio of monomers is very difficult to attain on a small scale because of relatively large measurement errors. Precisely weighing the liquid monomer, sebacoyl chloride, in a small quantity is especially difficult. Therefore, even when temperature and reaction time had been optimized, the molecular weight was still low. The situation is more complicated in syntheses of polyrotaxanes in which the diol monomer and crown ether are mixed in the melt prior to the addition of liquid sebacoyl chloride. The acid chloride needed to be weighed in a separate flask instead of in the reaction flask directly. The problem was circumvented by using a two chamber reaction flask where the two monomers were weighed directly into separate chambers. Liquid sebacoyl chloride was weighed first so that the quantity of diol monomer could be adjusted to maintain the exact 1:1 molar ratio of the two monomers. After the diol monomer was melted in chamber 1, the two monomers were mixed directly inside the flask at the reaction temperature under nitrogen. Using this method, the molecular weight was greatly increased, as shown in Table 1, the results of experiment 5.

In the  $^1\text{H}$  NMR spectrum of poly(decamethylene sebacate) (**9**) (Figure 1) the central eight protons of the sebacoyl unit and the central twelve protons of the diol moiety appear at 1.3  $\delta$  (labeled **a**). The signal at 1.6  $\delta$  (**b**) includes the eight protons  $\beta$  to both the carbonyl and ether oxygen atoms. The four protons  $\alpha$  to

the carbonyl group appear at 2.3  $\delta$  (c). The OCH<sub>2</sub> protons appear as a four proton triplet at 4.05  $\delta$  (d).

The <sup>13</sup>C NMR spectrum of **9** is shown in Figure 2. **9** displays nine of a possible ten signals. Apparently the four central carbon atoms of the sebacoyl unit are indistinguishable and are assigned to the upfield signal at 24.9 $\delta$  (labelled a). The two most central carbons of the diol moiety are assigned as the 25.8 $\delta$  signal (i) and the next two carbons are designated as giving rise to the 28.6 $\delta$  signal (h). The carbons  $\beta$  to carbonyl are assigned to 29.0 $\delta$  signal (b). The two carbons of the diol unit  $\gamma$  to the ether oxygen are responsible for the 29.2 $\delta$  peak (g), and those  $\beta$  to the ether oxygen are assigned as the 29.4 $\delta$  signal (f). The carbons  $\alpha$  to the carbonyl are observed at 34.3 $\delta$  (c) and those  $\alpha$  to the ether oxygen are assigned as the 64.3 $\delta$  signal (e). The carbonyl carbons are observed at 173.9 $\delta$  (d).

## B. Studies of Threading Processes in Polyrotaxane Syntheses

Our studies were performed in polysebacate-crown ether rotaxane systems by the statistical threading method. As depicted in Scheme 1, the polyrotaxanes were prepared by the condensation of alkylene diols and sebacoyl chloride using melted crown ethers as solvents. The diol and the crown ether were stirred in the melt to allow threading of the linear species through the macrocycle prior to the addition of sebacoyl chloride. This threading process is termed "prethreading".

The purification protocol for polyrotaxanes prepared by transesterification polymerization was also employed here: the polyrotaxanes were purified by multiple reprecipitations from CH<sub>2</sub>Cl<sub>2</sub> solution into methanol which is a good solvent for the crown ether but not for the polyrotaxane. After each precipitation the polymer composition was determined by quantitative <sup>1</sup>H NMR, affording a measure of m/n values, the molar ratio of macrocycle to repeat units of polymer backbones. All the polyrotaxanes synthesized reached a constant m/n value after three precipitations, indicating the complete removal of free macrocycles.

The single peak in the GPC diagrams of the polyrotaxanes also demonstrated the absence of free macrocycles, as shown in Figure 3 (d). The number average molecular weight of polyrotaxane **14** determined by GPC with polystyrene standards is 8.3 kg/mole, higher than the previous results, due to the use of optimized reaction conditions [2]. Also shown in Figure 3 are GPC traces for (a) poly(decamethylene sebacate) (**9**); (b) a physical mixture of poly(decamethylene sebacate) (**9**) and 42-crown-14 (**6**), and (c) 42-crown-14 alone, all in chloroform. Note that in the trace (b) for the physical blend the presence of the free crown ether is readily detected by the shoulder at larger elution volume. Polyrotaxane **14** was shown by NMR spectroscopy to contain 35 mass percent of 42-crown-14.

Although there were no blocking groups at the ends of the polymer chains, no free macrocycles were found in polyrotaxanes, as demonstrated by both constant m/n values after the second and third reprecipitations and by GPC measurements. This phenomenon was also observed in the syntheses of

polyester rotaxanes prepared by transesterification polymerization [2] and polyurethane rotaxanes [3], probably due to the random coiling of the chains and the macrocycles, the interaction between cyclic and linear species, and the "wobble effect" of the chain ends which enhances the mobility of macrocycles towards the middle of the chain, analogous to a button-on-a-string toy.

The process of threading linear chains through macrocycles may be very complicated. In order to simplify the situation, the studies began in neat systems so that solvent effects were not considered. Furthermore, it was assumed that the threading of linear species through macrocycles only occurs during the prethreading process, and that the threading of oligomers and polymers through macrocycles during the polymerization process is not significant.

#### a. Determination of Measurement Error of $m/n$ Values

The  $m/n$  values, the molar ratios of the macrocycle to the repeat unit of the polymer backbone, were determined by quantitative  $^1\text{H}$  NMR measurements. Indeterminate error of the analysis, arising from sampling and measuring, were statistically treated. Each treatment dealt with 20 data sets to obtain the populational results.

## 1) Sampling

Twenty samples were taken from a poly(decamethylene sebacate)-rotaxa-(42C14) (14) sample which had been thoroughly stirred before the samplings. These samples were then measured by  $^1\text{H}$  NMR and m/n values were calculated by 4 methods based on different protons of the polysebacate backbone (Figure 4).

Method 1 is based on protons d compared to protons e:

$$m/n = A_{3.6} / [14 A_{4.1}] \quad (1)$$

Where A represents the integration of signals whose chemical shifts in ppm are indicated by subscripts.

Method 2 uses protons c and d compared to protons e:

$$m/n = A_{3.6} / [7(A_{4.1} + A_{2.3})] \quad (2)$$

Method 3 depends on the comparison of protons a, c, and d compared to protons e:

$$m/n = A_{3.6} / [2(A_{4.1} + A_{2.3} + A_{1.3})] \quad (3)$$

and protons c are compared to protons e in method 4:



$$m/n = A_{3.6} / [14 A_{2.3}] \quad (4)$$

Protons b were not taken into account because the peaks are overlapped by that of water. Results are summarized in Table 2. The population standard deviation,  $\sigma$ , is calculated by equation (5):

$$\sigma = \sqrt{\frac{\sum \left( \frac{m}{n} - \mu \right)^2}{20}} \quad (5)$$

where  $\mu$  is the population mean. Among the four methods method 4 is the best with respect to both the spread and the standard deviation.

## 2). Measuring

One NMR sample of **14** was measured 20 times and  $m/n$  values were calculated using methods 1 and 4. Results are listed in Table 3. Method 4 again appears to be the better one, having a smaller standard deviation ( $3.46 \times 10^{-3}$ ).

Therefore, method 4 was used in calculations and the resultant overall error is  $6.90 \times 10^{-3}$ . It is concluded that the error in  $m/n$  is  $\leq 0.01$ .

## b. Ring Size

Crown ethers with different ring sizes were involved in the study. The following conditions were adopted in the syntheses of poly(decamethylene sebacate) rotaxanes with different crown ethers: the prethreading time was 0.5 hour, the reaction temperature was 80 °C and the molar ratio of crown ether to diol was one. The results are shown in Table 4. In Figure 5 the m/n values of polyrotaxanes are plotted against the ring sizes of crown ethers. The results demonstrate that m/n values increase non-linearly with ring size.

Harrison studied the influence of macrocycle size on rotaxane yields [4]. His procedure consisted of combining a mixture of cyclic alkanes with ring sizes of 14 to 42 atoms and 1,13-bis[tri-(*p-tert*-butylphenyl)methoxy]tridecane, with an acid catalyst. He found a monotonic increase in the yield of rotaxane as the size of the macrocycle increased from 24-33 atoms. Schill and his colleagues carried out similar studies to address the issue of ring size [5]. The yield of rotaxane was found to increase with macrocycle size (Figure 6). Zilkha synthesized oligomeric rotaxanes by statistical threading of crown ether macrocycles onto poly(ethylene glycol)s [6]. The proportion of threading was found to increase with increasing ring size of crown ethers. Similar observations were also obtained in polyurethane-crown ether rotaxanes synthesized by Shen [3]. Clarson, Mark, and Semlyen threaded narrow molecular weight distribution cyclic poly(dimethylsiloxane)s with linear  $\alpha,\omega$ -dihydroxy poly(dimethylsiloxane)s (PDMS) of  $M_n$  18 kg/mol to form homosiloxane polyrotaxanes [7]. They immobilized the threaded rings by cross-

linking the linear PDMS. The unthreaded rings were then extracted from the matrix. They found that the mass percentage of cyclics in the cured polyrotaxane increased with ring size. Gibson et al. calculated equilibrium constants from Clarson's data on a molar basis taking into account the total molar masses of the components [3]. The results are shown in Figure 7 in the form  $\log K$  vs ring size.

As defined in Chapter II, homorotaxanes are comprised of cyclic and linear species which are chemically equivalent. Heterorotaxanes, on the other hand, involve cyclic and linear species having different chemical structures. In the literature cited above, the results are all from homorotaxane systems, except for polyurethane rotaxanes which are a semi-homorotaxane system because of the chemical equivalence of crown ethers and tetra(ethyleneoxy) units in the polymeric backbones [3].

The ring size effects of macrocycles in the homorotaxane systems can be divided into three regions. In the small ring size region, the repulsive interaction between the cyclic and linear species is the most important factor that affects threading because of the short distance between the two components of rotaxanes. Therefore, the degree of threading is an exponential function of ring size, following the formula of the Lennard-Jones potential [8], as shown in the region of ring size  $\leq 24$  atom of Figure 5. Other interactions are not considered here because their changes relative to the ring size may not be as large as that of the repulsive interaction. For the middle and large ring regions, repulsive interaction is less important compared to that the small ring size region because

of the larger distance between the two components. Above the small ring region, the plot of threading constant vs. ring size shows a logarithmic pattern, as demonstrated in Figure 7. The curve can be roughly treated as two straight lines, one in the middle ring size region and one in the large ring size region. The two regions may reflect the fact that below a certain ring size, the ability to be threaded is strongly governed by conformational possibilities, that is, up to a certain size, there is a large fraction of unthreadable conformations, but once that size is exceeded, the fraction of unthreadable conformations diminishes. Therefore, the increase of threading yield with increasing ring size in the large ring size region is slower than that in the small ring size region. The break point would depend on the flexibility of the cyclic component and the nature of the linear species. Indeed, recent molecular modeling studies by Semlyen and coworkers indicated that such is the case [9]. The polyurethane rotaxane system showed a linear line [3]. This system seems to be in the middle ring size region.

Although the poly(decamethylene sebacate)-crown ether rotaxanes are heterorotaxanes and the threading process is more complicated than those in homorotaxane systems, the principles discussed above are still suitable in this system. Therefore, the curve in Figure 5 can be divided into two straight lines with the break point at about 38 atoms. 36-crown-12 differs greatly from 30-crown-10 in term of degree of threading, probably due to the great differences in repulsive interaction and threadable conformations.

In a separate experiment, 1 mole of 1,10-decanediol was stirred with 0.5 mole of 30-crown-10 and 0.5 moles of 42-crown-14 before the addition of sebacyl chloride. 30-Crown-10 can be differentiated from 42-crown-14 because it shows a singlet at 3.671  $\delta$  and 42-crown-14 displays a singlet at 3.647  $\delta$  in  $^1\text{H}$  NMR spectra in  $\text{CDCl}_3$ . After three precipitation into methanol no 30-crown-10 molecules were found in the polyrotaxane. This experiment again demonstrated the important effect of ring size on degree of threading.

The  $^1\text{H}$  and  $^{13}\text{C}$  NMR spectra of poly[(decamethylene sebacate)-rotaxa-(42-crown-14)] (**14**) are shown in Figures 4 and 8. These spectra are same as those of their linear counterpart **9** shown in Figures 1 and 2, except for the signals of the crown ethers. The  $^1\text{H}$  NMR spectrum of **14** contains only one additional peak at 3.7  $\delta$  (**e**) due to the crown ether. Likewise, the  $^{13}\text{C}$  NMR spectrum of **14** differs from that of the model polymer **9** only by the resonance at 70.5  $\delta$  (**g**), easily assigned to the carbons of the 42-crown-14 component of the polyrotaxane.

### c. Feed Ratio

The next parameter studied was the feed ratio of crown ether to diol monomer. The polyrotaxanes were prepared by the polymerization of sebacyl chloride with 1,10-decanediol at 80  $^\circ\text{C}$ . The 42-crown-14 (**6**) was stirred with 1,10-decanediol (1:1 molar ratio) in the melt for half an hour before the addition of sebacyl chloride. As shown in Figure 9, the macrocycle content increases with

increasing feed ratio until the feed ratio reaches two. After that the macrocycle content becomes constant. These results are listed in Table 5.

Zilkha et al. found that the threaded proportions of the cyclic species can be maximized by using an excess of macrocycles [6]. The same phenomenon was observed in polyurethane-crown ether rotaxanes [3] and polyacrylonitrile-crown ether rotaxanes [10]. All these results demonstrate that the formation of polyrotaxanes follows le Chatelier's principle [11].

The fact that the equivalence point is two indicates that one diol molecule was "saturated" by two crown ether molecules during the prethreading process. The ratio equals the number of hydroxyl groups of the linear molecules and may imply that one diol monomer hydrogen bonds with two crown ether molecules during the prethreading process.

#### d. The Length of the Diol

If the hydrogen bonding between the diol monomers and crown ethers plays an important role on the threading, the degree of the threading,  $m/n$ , should not be significantly affected by the length of the diol monomers. This is exactly what was observed. The study of the effect of the length of diols on threading yield was performed by the preparation of polyrotaxanes by the condensation of sebacoyl chloride with 1,4-butanediol (**1**), 1,6-hexanediol (**2**), and 1,10-decanediol (**3**), respectively, in the presence of 42-crown-14 (**6**). Again, the prethreading time was 0.5 hours, the temperature was 80 °C and the molar feed

ratio of cyclic to linear monomer in the prethreading process was 1. The results (Table 6 and Figure 10) revealed that the  $m/n$  values did not change with increasing length of alkynene diol molecules. Because the increase of the length of the diols does not increase the degree of threading but does increase the molecular weight of the repeat units of the polymer backbones, the mass percentage of macrocycles in the polyrotaxanes decreases with increasing diol length.

The above result is different from the results obtained for *homorotaxane* formation in which threading increases with increased length of the linear species. For example, Schill and coworkers studied the effect of the length of linear alkane chains of 10-38 carbons blocked by trityl groups on their threading into a 29-carbon cycloalkane [5]. The yield of rotaxane increased from 4.5 % to 11.3 % when the chain length increased from 10 carbons to 38 carbons. In this system the linear species can not hydrogen bond with the cyclic alkanes. Hence the threading equilibrium is determined by the length of the linear species.

Zilkha and coworkers found from their synthesis of poly(ethylene glycol)-crown ether rotaxanes that the percent of threading vs. linear species length increased and then decreased, the maximum apparently being a function of ring size [6]. Although in this case the hydroxyl groups of the linear oligo(ethylene glycol)s can hydrogen bond with the crown ethers, the effect of the hydrogen bonding on the threading is greatly reduced by the hydrogen bonding between the terminal hydroxyl groups of the glycols and the oxygen atoms of the glycol molecules.

The  $^1\text{H}$  and  $^{13}\text{C}$  NMR spectra of poly[(butylene sebacate)-rotaxa-(42-crown-14)] have been shown in Figure 3b and 4b of Chapter VI.  $^1\text{H}$  and  $^{13}\text{C}$  NMR spectra of poly[(hexamethylene sebacate)-rotaxa-(42-crown-14)] (**11**) are shown in Figures 11 and 12. In the proton NMR spectrum (Figure 11) the polyester **11** displays resonances at 1.30 $\delta$  (labelled **c**) for the central  $(\text{CH}_2)_4$  unit (8H) of the sebacoyl moiety, at 1.38 $\delta$  for  $(\text{CH}_2)_2$  unit (4H) of the diol moiety (**e**), at 1.62 $\delta$  for protons  $\beta$  to the ether oxygen and those  $\beta$  to the carbonyl (**b**), at 2.28 $\delta$  for the protons  $\alpha$  to the carbonyl (**a**) and at 4.05 $\delta$  for the protons  $\alpha$  to the ether oxygen (**d**).

Figure 13 is the GPC traces for polyrotaxanes **10-16**. Note that all the polyrotaxanes display single symmetric signals in their GPC traces and no free crown signals were observed.

#### e. Prethreading Time

Zilkha and his colleagues observed that the equilibrium for threading of linear poly(ethylene glycol) into dibenzo crown ethers was established within 30 minutes [6]. Similarly, I found that the threading yield of 1,10-decanediol by 42-crown-14 did not increase with increased prethreading time even though the time was extended from <1 minute to 48 hours, as shown in Table 6. All the reactions were at 80 °C with a 1:1 feed molar ratio of 42-crown-14 to 1,10-decanediol. This result is attributed to the fast formation of hydrogen bonds between the cyclic and linear species during the prethreading process.



#### f. Double Prethreading

The importance of prethreading invites consideration of double prethreading, that is, prethreading both monomers through macrocycles simultaneously. An experiment was performed in which sebacoyl chloride and 1,10-decanediol had been mixed with an equivalent of 42C14 independently and separately prior to the polymerization, at 80 °C for half an hour. The final m/n value was 0.35, higher than that of diol monoprethreading with  $M_O/L_O = 1$  ( $m/n = 0.29$ ) but lower than that with  $M_O/L_O = 2$  ( $m/n = 0.41$ ) (Table 8). Apparently the threading yield of the diol is higher than that of the diacid chloride due to hydrogen bonding between the hydroxyl end groups of the diol with oxygen atoms in crown ether molecules.

Based upon the above results, it is believed that one diol molecule hydrogen bonds with two crown ether molecules during the prethreading process. The polymerization takes place after the threading equilibrium has been established. This concept is depicted in Scheme 2.

#### g. Temperature

Because hydrogen bonding is a favorable interaction between the cyclic and linear species, the term for the enthalpy change ( $\Delta H^\circ$ ) in the free energy equation:

$$\Delta G^\circ = \Delta H^\circ - T\Delta S^\circ \quad (6)$$

was expected to be negative. Since:

$$\Delta G^\circ = -RT \ln K = \Delta H^\circ - T\Delta S^\circ \quad (7)$$

the natural log of the equilibrium constant for threading is a function of the reciprocal of temperature:

$$\ln K = -(\Delta H^\circ)/(RT) + \Delta S^\circ/R \quad (8)$$

Therefore, temperature dependence of the degree of the threading was expected. In order to determine the significance of enthalpic interactions in the threading process, prethreading of 1,10-decanediol with 42-crown-14 (1:1 molar ratio, 0.5 hour) was performed at different temperatures followed by polymerization at those temperatures. However, the similarity of all m/n values in the temperature range of 80°C to 160 °C, as shown in Table 9, suggested that threading is independent of temperature. The temperature independence of the threading was also observed by Zilkha et al. [6]. They suggested that due to the chemical similarity between the macrocycle and linear polymer, the chain ends show no preferred interaction with any element in the system.

Several factors need to be taken into account in our heterorotaxane systems:

- 1) Not all crown ethers hydrogen bonding with diol will be threaded onto the polymer backbones. Whether they can be threaded onto polymer chains depends on their conformations. Conformational changes of the linear species

also affect the degree of threading, although they may not be as significant as conformational changes of the macrocycles. Unfortunately, the influence of temperature on threadable conformations is not well understood at this time.

2) Contrary to the hydrogen bonding, a favorable interaction between the cyclic and linear molecules, the non-compatibility of the non-polar linear chain and the polar cyclic species is an unfavorable interaction between the two species which contributes to a positive enthalpy for threading.

3) The constant macrocycle contents of all polyrotaxane synthesized after the second precipitation demonstrated that threaded macrocycles can be constrained onto the polymer chains even though there are no blocking groups at the chain ends. However, the threaded macrocycles in the proximity of chain ends are susceptible to diffusion from polymer chains, especially during the first precipitation. This hypothesis was supported as the most plausible explanation of the lack of temperature dependence by the synthesis of a polyrotaxane with bulky spacers on its backbone, which will be discussed below.

4) Molecular weights of polyrotaxanes may also influence the dethreading of macrocycles from polymer chains due to the differences in numbers of chain ends. However, as shown in Table 9,  $m/n$  values do not vary with molecular weights.

#### h. Intrinsic Viscosities as Functions of Solvents

The solution behavior of polyrotaxanes depends on the differential solvation of the cyclic and linear species of the polymers. The differential solvation effect could in the extreme case cause either the macrocycle or the linear backbone to be fully expanded or to collapse into a  $\theta$  state. A good solvent for both the cyclic and linear species leads to expansion of both components. A good solvent for the linear macromolecule but a poor solvent for the cyclic species leads to an expanded backbone but collapsed macrocycle. A poor solvent for the linear backbone but a good solvent for the macrocycle provides a collapsed state of the linear component and an expanded state for the rings. A poor solvent for both the linear and cyclic components affords collapsed conformations of both. In order to address the issue how hydrodynamic volumes of polyrotaxanes change with solvents, the intrinsic viscosities of poly(decamethylene sebacate) (**9**) and poly[(decamethylene sebacate)-rotaxa-(42-crown-14)] (**14**) were measured in pure THF and in mixture of THF and methanol with different ratios (Table 10). THF is a good solvent for both linear and cyclic species of the polyrotaxane, while methanol is a good solvent for the crown ether but a poor solvent for poly(decamethylene sebacate). Furthermore, methanol can form complexes with crown ethers [12]. Thus, a change in the intrinsic viscosity of the polyrotaxane with the ratio of THF:methanol is expected. Indeed, the viscosity of **14** was reduced from 0.331 to 0.248 as the solvents changed from pure THF to the mixture of THF and methanol (100:10, v:v). On the other hand, the  $[\eta]$  value of polymer **9** does not change as the ratio of THF:methanol

changes from 100:0 to 100:20. The results can not be rationalized based on the limited data until more measurements have been done.

### C. Molecular Strings of Beads with Knots

Purification of polyrotaxanes is source of the experimental errors. While the macrocycles in the middle of the polymer chains can be constrained by the random coiling of polymer chains and the “wobble effects” of the chain ends, as demonstrated by the constant  $m/n$  values of all the polyrotaxanes after the second and third reprecipitations, the macrocycles near the chain ends are susceptible to diffusion from the polymer chains during the first precipitation. In order to prevent macrocycles from dethreading, blocking groups are needed. Since the end-capping of polymer chains by monofunctional blocking groups is often not efficient in the cases of high molecular weight polymers [2], difunctional bulky monomers are employed to completely constrain all the threaded macrocycles.

Therefore, a bisphenolic blocking group, 1,10-bis(*p*-[di(*p*'-*t*-butylphenyl)(-*p*''-hydroxyphenylmethyl)]phenoxy)decane (**17**), was used in a polyrotaxane synthesis, as depicted by Scheme 3. In the reaction, the molar ratio of **17** to 1,10-decanediol (**3**) was 1:4 and the molar ratio of 42-crown-14 to sebacoyl chloride was 1. After three precipitations, the  $m/x$  value, the molar ratio of macrocycle to the decamethylene sebacate unit of the polymer backbone, was 0.74, as determined by the proton NMR spectroscopy (Figure 14). The macrocycle content in **18** was 2.4-fold higher than that of **14** under comparable

conditions. This result revealed the fact that for polyrotaxanes without any blocking groups significant loss of threaded macrocycles does occur during the first precipitation in the purification process.

Because the blocking group **17** is difunctional, the molecular weight of the polyrotaxane is high. GPC measurement with polystyrene standards showed a single peak with  $M_n = 18,700$  and polydispersity = 1.57.

#### D. Dethreading Experiments

The lack of dethreading is supported by the results from long term experiments in which poly[(decamethylene sebacate)-rotaxa-(42-crown-14)] (**14**) was heated in tetrahydrofuran solutions (Scheme 4). Table 11 summarizes the results of dethreading experiments obtained so far.

In experiment 1, **14** ( $m/n = 0.33$ , wt % 42C14 = 34) was dissolved in THF and the solution was stirred at 50 °C for seven days. After the purification, the  $m/n$  value was reduced to 0.27, corresponding to 30 mass percent of 42-crown-14. The dethreading rate  $V_d$ , as calculated by equation (9), was  $8.6 \times 10^{-3}$  (day<sup>-1</sup>).

$$V_d = [(m/n) - (m/n)_0]/t \quad (9)$$

where  $m/n$  and  $(m/n)_0$  are final and initial  $m/n$  values, respectively;  $t$  is the dethreading time in days.

In experiment 2, **14** with lower mass percent of 42-crown-14 ( $m/n = 0.18$ ) was treated in refluxing THF for 11 days. Sampling the solution showed a lack of dethreading, as the  $m/n$  value only decreased by 0.01, about the limit of error of the measurement (see above). The rest of the solution was then stirred for another 24 days under the same conditions but only a small change of  $m/n$  value was observed (experiment 3).

The above results demonstrate that the dethreading rate is significantly affected by the initial macrocycle contents of polyrotaxanes as expected from kinetic and thermodynamic considerations. The initial  $m/n$  value in experiment 1 was 1.8 times higher than that of the polyrotaxane in experiment 2. Although the conditions in experiment 1 are more unfavorable for the dethreading of macrocycles than experiment 2, with lower temperature, shorter dethreading time, and higher concentration, the dethreading rate of the former is almost 10-fold higher than the latter. By comparing the results of experiments 2 and 3 it is clear that dethreading rate decreases with increasing dethreading time. Figure 15 is the plot of  $m/n$  value against time, the results of experiments 2 and 3. The dethreading rate derived from the slope was  $8.5 \times 10^{-4}$  per day. The results support the hypothesis that once threaded macrocycles in the proximity of chain ends are lost in the first precipitation, further loss of threaded macrocycles is hindered by the random coiling of both linear and cyclic species and the “wobble effect” of the chain ends which enhances the movement of macrocycles toward the middle of chains.

## E. Thermal Properties of Polyrotaxanes

Polyrotaxanes show different phase transition behavior compared to linear polyesters. Melting temperatures were changed and in some cases the macrocycles were able to crystallize without dethreading. The incorporation of macrocycles also altered transition behavior of polyester backbones (Table 12).

### a. Poly[(decamethylene sebacate) System

The model system poly(decamethylene sebacate) (**9**) is a highly crystalline polymer. It shows a melting transition at 77 °C upon heating (Figure 16 a) and a crystallization exotherm at 62 °C during cooling (Figure 16 b).  $T_g$  was not observed by DSC.  $T_m$  of **9** has been reported as 70-78 °C [13-16], heat of fusion as 33.7-39.9 cal/g [14, 16], and  $T_g$  as -58 to -75 °C [15, 16]. Poly[(decamethylene sebacate)-rotaxa-(30-crown-10)] (**12**), a polyrotaxane containing only 1.5 mass percent macrocycles, demonstrates nearly the same thermal properties:  $T_m = 80$  °C,  $T_c = 63$  °C and no  $T_g$  was observed (Figure 17). A crown ether crystalline phase was not observed due the low quantity of macrocycles present.

However, for poly(decamethylene sebacate) rotaxanes containing larger macrocycles and larger macrocycle contents, glass transitions were observed and three melting temperatures appeared. Poly[(decamethylene sebacate)-rotaxa-(36-crown-12)] (**13**), as shown in Figure 18a, displayed a glass transition signal at -54 °C, at the vicinity of the glass transition of pure 36-crown-12 (-73



°C), a melting endotherm at 42°C, which was somewhat below the melting point of 36-crown-12 (57 °C, Figure 19a), and other two partially overlapped endotherms at 69 and 71 °C, which were somewhat below the melting point of polymer **9** (77 °C, Figure 16a). Upon cooling, a crystallization exotherm appeared first at 56 °C and another exotherm was shown at 21 °C (Figure 18 b). Figure 19 illustrates the phase transition behavior of 36-crown-12 (**5**), which underwent melting at 57 °C (Figure 18a) and upon slow cooling crystallized at 30 °C (Figure 18b); after rapid cooling the glass transition was observed at -73 °C. It is apparent that the glass transition of polyrotaxane **13** corresponds to 36-crown-12 (**5**). In view of the fact that the melting transition of 36-crown-12 (**5**) is lower than that of poly(decamethylene sebacate) (**9**) and the mass percent of macrocycle in polyrotaxane **13** is lower than that of polymer backbone, the lowest melting transition with the lowest heat of fusion is due to the macrocyclic component of polyrotaxanes. Likewise, the lowest crystallization exotherm with the lowest enthalpy of crystallization comes from the crown ether in the polyrotaxane. The two partially overlapped melting endotherms and exotherms at high temperatures are attributed to the polymer backbone.

The reason for two crystalline phases of the polymer backbone is not clear at this time. It has been suspected that macrocycles in the vicinity of the chain ends are lost during purification process. Therefore, the polymer chain ends would lack macrocycles. Perhaps the lamellar thickness of polymer chain ends is thicker than that of chain segments between two macrocyclic lamellae, resulting in two crystalline phases. If this hypothesis is true, the transition

behavior of the polyrotaxane should have a historical effect. Indeed, a sample showed just two melting transitions upon heating after it had been heated above its melting temperature (100 °C) for 65 minutes followed by a rapid cooling.

Taking into account the fact that the sample was 25 mass percent macrocycle, comparison of the heats of fusion of Figures 16a, 18a, and 19a indicates that ~57% of the macrocycle and ~73% of the linear component of **13** crystallized with respect to the pure components **5** and **9**.

Polyrotaxane **14** showed similar phase transition behavior to **13**, as demonstrated in Table 12 and Figure 20. Comparison of the heats of fusion of the polyrotaxane **14** (Figure 20a) with those of pure components **6** (Figure 21a in Chapter VII) and **9** (Figure 16a) indicates that ~32% of the macrocycle and ~100% of the backbone species of **14** crystallized with respect to the pure components **6** and **9**.

Moreover, polyrotaxane **15** showed a  $T_g$  at -58 °C, a melting endotherm at 43°C, and other two partially overlapped endotherms at 71 and 75 °C (Table 12, Figure 21a). Upon cooling, two overlapped crystallization exotherms appeared first at 62 and 60 °C and another exotherm was shown at 25 °C (Figure 18 b). Figure 22 illustrates the phase transition behavior of 48-crown-16 (**7**), which underwent melting at 55 °C (Figure 22a) and upon slow cooling crystallized at 25 °C (Figure 22b); after rapid cooling the glass transition was observed at -73 °C. About 45% of the macrocyclic species of **15** crystallized with respect to the

pure component **7**. Comparison of the heats of fusion of **9** and **15** indicates that the crystallinity of the linear chain of **15** is 28% higher than that of model polymer **9**. This may be due to the fact that the molecular weight of the backbone of **15** is lower than **9**. Indeed, the heat of fusion of **15** backbone is the same as the reported value for the low molecular weight polymer **9** ( $M_v = 5.2 \text{ kg/mol}$ ) [16].

The same phenomenon was observed in poly[(decamethylene sebacate)-rotaxa-(60-crown-20)] (Figure 23). While ~39% of the macrocyclic species of **16** crystallized compared to pure 60-crown-20 (**8**), the crystallinity of the backbone of **16** was 16% higher than model polymer **9** but 10% lower than that of the low molecular weight polymer reported in reference 16.

#### b. Poly(butylene sebacate) and Poly(hexamethylene sebacate) Systems

The phase transition behavior of poly(butylene sebacate) has been described in Chapter VII:  $T_m = 67 \text{ }^\circ\text{C}$ ,  $T_c = 48 \text{ }^\circ\text{C}$ , and  $T_g$  was not observed by DSC.  $T_m$  of the polymer has been reported as 63-65  $^\circ\text{C}$  [15-17], heat of fusion as 37.0 cal/g [16], and  $T_g$  as -57 to -75  $^\circ\text{C}$  [15-17]. Poly[(butylene sebacate)-rotaxa-(42-crown-14)] (**10**) displayed a melting endotherm at 46  $^\circ\text{C}$ , and two overlapped endotherms at 58 and 63  $^\circ\text{C}$  upon first heating, similar to the results shown in Figure 18, 20, 21, and 23 for the decamethylene systems. Upon the second heating after rapid cooling the glass transition was observed at -55  $^\circ\text{C}$ . Although three endotherms were observed upon second heating, the lower melting peak of the two overlapped endotherms was greatly reduced. This transition disappeared upon the third heating (Figure 24a). **10** shows two

crystallization exotherms at 46 and 23 °C upon second cooling. The crystallinity of the cyclic component of **10** is 57% lower than that of pure 42-crown-14 (**6**), but the crystallinity of polyrotaxane **10** backbone is 14% higher with respect to the model polymer. The heat of fusion of linear component of **10** (21.1 cal/g) is lower than the reported value (37.0 cal/g) for low molecular weight model poly(butylene sebacate) ( $M_v = 2.5$  kg/mol) [16].

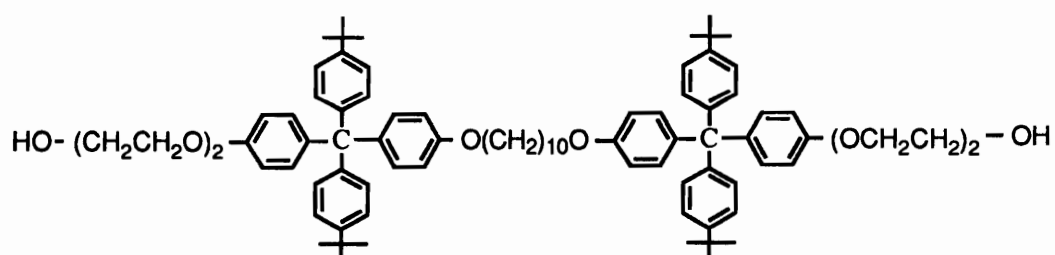
Similarly poly[(hexamethylene sebacate)-rotaxa-(42-crown-14)] (**11**) shows three endotherms upon first heating. In the second heating after rapid cooling the lower endotherm for the backbone nearly disappeared (Figure 25a). Two crystallization exotherms were observed upon the second cooling (Figure 25b). About 39% macrocycle species of **11** was crystallized with respect to the pure **6**. The model polymer, poly(hexamethylene sebacate) was not synthesized, but its  $T_m$  has been reported as 65-71 °C [14-16], heat of fusions as 33.7-37.0 cal/g [14, 16], and  $T_g$  as -60 to -70 °C [15, 16]. Note that the heat of fusion of the polyrotaxane **11** backbone (25.9 cal/g) is lower than the reported values.

### c. Polyrotaxane **18** with bulky spacers

Due to the lower reactivity of the bisphenolic blocking group **17** toward the sebacoyl chloride compared to the alkyene diol monomer, the blocking groups in **18** are expected to be separated by long sequences of alkyene sebacate units. Therefore, macrocycles are still able to move along the polymer backbones, resulting in two crystalline phases: macrocycle and polymer backbone. The DSC measurements showed that indeed this is the case. **18**

shows two broad melting endotherms at 45 and 67 °C upon heating (Figure 26a) and two crystallization exotherms at 47 and 8 °C upon cooling (Figure 26b). Because the bulky group **17** disturbs the packing of the polymer chain and the chain length between two bulky groups is not identical, the crystallinity of the polymer chain is greatly reduced, as shown by the low heat of fusion and broad melting endotherm and crystallization exotherm. The broad melting endotherm and crystallization exotherm of macrocyclic species of **18** are due to the difference in the numbers of macrocycles between two bulky groups.

The bisphenolic blocking group **17** has been converted to a corresponding diolic blocking group **19**, as discussed in Chapter VI. Because of its equal reactivity with diol monomers **19** is expected to be included into polymer chains randomly, resulting in a random separation of the threaded macrocycles. In this situation the crystallization of macrocycles may not occur, depending on the ability of aggregates of critical nucleation size to form.



**19**

## F. Metal Complexation of Crown Ether Components of Polyrotaxanes

It is a well known fact that crown ethers can form complexes with metal ions [12]. If the crown ether components of polyrotaxanes are capable of forming complexes with metal ions, changes in thermal and mechanical properties of the complexed polymer compared to the native polyrotaxanes should be observed. The presence of the metal ion should stiffen the chains, increasing glass transition temperature and modulus. The complexed polyrotaxanes may find some applications in electronic conduction, separation, and so on.

A series of experiments was done to determine qualitatively the metal complexation capability of threaded crown ethers in polyrotaxanes. Poly(decamethylene sebacate) rotaxanes **12, 13, 14, 15, 16** which contain crown ethers **4-10**, respectively, were examined. The metal ions investigated were sodium, potassium, calcium, and cesium. In the experiments the polyrotaxane was dissolved in methylene chloride, which is not miscible with water. Metal picrates (the salts of picric acid, 2,4,6-trinitrophenol) were prepared by dissolving picric acid and the metal hydroxide in water. The picrate anion is intensely yellow. The two solutions were then shaken together in a test tube. A blank methylene chloride solution, methylene chloride solutions of crown ethers and a methylene chloride solution of poly(decamethylene sebacate) were also tested as references. While the blank solution and poly(decamethylene sebacate) solution did not show any color changes after being shaken with the aqueous solutions containing metal picrates, all the crown ether solutions and polyrotaxane solutions displayed a visible yellow

color after being shaken, indicating that metal complexation of crown ethers had taken place (Table 13). Note that poly((decamethylene sebacate)-rotaxa-(30-crown-10)) can also form complexes with metal ions even though 30-crown-10 has a small cavity size, and the crown ether content in the polyrotaxane is low. The internal diameter of a fully opened 30-crown-10 molecule is about 7 Å [18]. It does not have enough room to accommodate a polymer chain (4.5 Å) [19] and a cesium cation (3.6 Å) [20]. However, its flexibility allows it to form a non-circular conformation to contain both the polymer chain and the cesium cation. 30-Crown-10 molecules in the polyrotaxanes, after they form complexes with cesium ions, may not be able to move along the polymer backbone because of steric hindrance. On the other hand, large crown ethers in polyrotaxanes, after they form complexes with a small metal ions, may have enough room in their cavity to allow them to move along the polymer backbone. This movement can probably be hindered by the complexation of the metal ions in the crown ether and carbonyl groups in polymer backbones. Therefore, the movement of threaded macrocycles can be controlled by the adjusting the size of macrocycles, the size and the nature of metal ions as well as the nature of polymer chains. Since the macrocycles can be locked by complexation with metal ions, blocking groups may become unnecessary.

## II. INTERFACIAL POLYMERIZATION

Polyester rotaxanes have been synthesized by the acid chloride method [2] and by the transesterification polymerization approach [2]. However, both synthetic methods are difficult for polyrotaxane syntheses. The acid chloride method

requires high purity of starting materials and precise stoichiometry. The impurities in crown ethers easily react with diacid chlorides and upset the stoichiometry. Precise stoichiometry is difficult to achieve in small scale reactions. On the other hand, the transesterification approach requires high temperature, high vacuum and long reaction times. Impurities in crown ethers can also become involved in the polymerization.

Interfacial polymerization, a polymerization method with mild conditions, has none of these weak points. Crown ethers are stable at the reaction conditions of room temperature and atmospheric pressure. Linear impurities in crown ethers, e.g., poly(ethylene glycol)s, are not likely to be involved in the reaction because of their higher  $pK_a$  values and therefore lower tendency to form glycolate ions in comparison with bisphenols. Furthermore, this method has other advantages such as low requirements for the purity of starting materials and precision of stoichiometry, as well as short reaction times and ease of performance [21]. However, this method has some disadvantages compared to other approaches. First, it is only suitable for the preparation of polyesters from bisphenols. Second, its performance in water and water-immiscible organic solvent systems reduces the concentration of crown ethers and therefore reduces the threading yield. Using a large amount of crown ethers is also restricted because of the loss of a clear phase boundary. However, this weak point is probably compensated by the fact that crown ethers act as phase transfer reagents by forming complexes with metal ions. Both cations and anions pass from the aqueous into the organic phase by the action of a crown ether [22] and free crown ethers recycle between the two phases (Scheme 5).



The use of crown ethers such as 15-crown-5, dibenzo-18-crown-6, and 18-crown-6 in interfacial reactions for syntheses of polysulfonates, polyphosphonates, polyethers and polysulfides has been reported [23-25].

Eareckson systematically investigated the preparation of polyphenyl esters by interfacial polymerization [26]. Polymers prepared with the highest molecular weights were those from bisphenols and aromatic acid chlorides, although both saturated and unsaturated aliphatic acid chlorides have been used with limited success.

Poly(bisphenol-A sebacate)-rotaxa-(42C14) (**19**) was prepared by interfacial polymerization (Scheme 6). In the reaction, an aqueous solution (20 mL) containing bisphenol-A (2.5 mmol), KOH (5.0 mmol) and 42-crown-14 (5.0 mmol) was stirred with a chloroform solution (10 ml) containing sebacoyl chloride (2.5 mmol) for 10 minutes. The mixture was precipitated into methanol and then reprecipitated two times, during which the macrocycle content of the produced polyester became constant at an m/n value of  $6.71 \times 10^{-2}$ , corresponding to 9.5 mass percent of the macrocycle.

Although the molecular weight was relatively low [ $M_n = 2.8$  kg/mol determined by GPC with polystyrene standards] due to the hydrolytic instability of the aliphatic acid chloride, this experiment demonstrates the potential of this methodology. It is particularly encouraging in view of the low macrocycle concentration (0.125 M overall) that was employed. The templating effect of the

potassium counterion of the phenolate must play a strong role in the threading process.

In the  $^1\text{H}$  NMR spectrum (Figure 27), poly[(biphenol A sebacate)-rotaxa-(42-crown-14)] (**19**) displays resonances at 1.38 $\delta$  (labelled **d**) for the four central protons of the sebacoyl moiety and the methyl protons of the bisphenol A moiety, at 1.58 $\delta$  (**c**) for the four methylene protons  $\gamma$  to the carbonyl groups; at 1.75 $\delta$  (**b**) for the four protons  $\beta$  to the carbonyl, at 2.53 $\delta$  (**a**) for the four protons  $\alpha$  to the carbonyl. Aromatic protons are observed at 6.95 $\delta$  (**f**) and 7.20 $\delta$  (**e**).

Although the 42-crown-14 used in the experiment had not been treated with poly(methacryloyl chloride) to remove linear poly(ethylene glycol)s, the by-products generated in the synthesis of crown ethers [27], no poly(ethyleneoxy) segments were found in the resultant polyrotaxane backbones by proton NMR spectroscopy (Figure 20). This is due to the low tendency of the glycol to form the glycolate under basic conditions compared to the bisphenol monomer, and bisphenoxide is more reactive toward diacid chlorides than poly(ethylene glycol)s, as discussed above. In a separate experiment, the crown ether was added into organic solvent with sebacoyl chloride prior to polymerization. An unexpected triplet at 4.22  $\delta$  appeared in the  $^1\text{H}$  NMR spectrum of the resultant polyrotaxane. This triplet is believed to be the signal of the protons of the aliphatic alcoholic unit  $\alpha$  to carbonyl groups in polyester backbones [2]. It is obvious that some poly(ethylene glycol) in the crown ether reacted with sebacoyl chloride.

The polyrotaxane **20**, upon first heating, displays a broad endotherm at 57 °C which may be the overlapped melting transitions of both macrocycle and linear chain (Figure 28a). The crystallized macrocycles delocalize upon melting so that the whole system became totally amorphous. Therefore, the polymer shows a  $T_g$  at -8 °C and a tiny endotherm at 53 °C in the second heating (Figure 28b). No crystallization transitions were observed during the second cooling (Figure 28c).

## CONCLUSIONS

The threading processes of macrocycles onto polymer chains were studied in polysebacate-crown ether rotaxane systems using the acid chloride polymerization method. For polyrotaxanes without blocking groups, the macrocycle content is independent of time, temperature, and length of diol monomers. The macrocycle content is significantly affected by the feed ratio of macrocycle to linear monomers, indicating that the formation of polyrotaxanes follows le Chatelier's principle. The macrocycle content of polyrotaxanes increases non-linearly with the size of the macrocycles, presumably due to changes in the fraction of threadable conformations of the macrocycles. Although they have been threaded by polymer chains, the crown ethers of polyrotaxanes are still able to form complexes with some metal ions.

In order to completely constrain macrocycles onto polymer chains, a difunctional bulky compound was copolymerized into polyester backbones. The

predominant incorporation of the blocking groups near the ends of polymer chains allows independent crystallization of both the cyclic and linear components of the polyrotaxane. The high macrocycle content of the blocked polyrotaxane compared to those of unblocked polyrotaxanes revealed the loss of macrocycles near chain ends during purifications. However, dethreading of macrocycles in the middle of chains is not significant, as demonstrated by long term dethreading experiments.

A poly[(bisphenol-A sebacate)-rotaxa-(42-crown-14)] was prepared by interfacial polymerization. The threading of macrocycles was favored by the complexation of the crown ether with the metal counterion of the phenolate.

## EXPERIMENTAL

**Measurements.**  $^1\text{H}$  nuclear magnetic resonance (NMR) spectra were recorded with chloroform-d solutions (unless otherwise noted) with tetramethylsilane as an internal standard on a Bruker 270 MHz instrument and a Hewlett Packard 7550A graphics plotter or on a Varian Unity 400 MHz instrument. The following abbreviations have been used in describing the NMR spectra: s (singlet), d (doublet), t (triplet), q (quartet), p (pentet), and m (multiplet); coupling constants are represented by J in Hz.  $^{13}\text{C}$  NMR spectra were recorded on chloroform-d solutions (unless otherwise noted) using Varian Unity 400 MHz instruments; chemical shifts are relative to the center line of the  $\text{CDCl}_3$  triplet at 77.0 ppm. Transition temperatures ( $T_g$ ,  $T_m$ ) were determined by a dual cell Perkin Elmer DSC 2 at a heating rate of  $10^\circ\text{C}/\text{min}$  or less. Gel permeation chromatography (GPC) measurements were done using a Waters 590 instrument fitted with refractive index and UV detectors which was calibrated with polystyrene standards. Permagel  $10^2 - 10^6$  Å polystyrene-divinylbenzene columns were employed.

**Starting materials.** Sebacoyl chloride was purified by vacuum distillation. 1,4-Butanediol (1) was distilled before use. 1,6-Hexanediol (2) and 1,10-decanediol (3) were recrystallized twice from water and dichloroethane, respectively, and were vacuum dried at  $45^\circ\text{C}$ . Diglyme was dried by first refluxing it with sodium and then distilled. Crown ethers 4-8 were prepared using procedures described in Chapter 3, and were vacuum dried in the melt. 1,10-Bis{*p*-[di(*p*'-*t*-butylphenyl)hydroxymethyl]phenoxy}decane (17) was

synthesized using the method described in chapter 5 and was vacuum dried at 100 °C before use. Bisphenol-A was purified by recrystallization in 1,2-dichloroethane. The other chemicals were used without purification as obtained from commercial sources.

### **Poly(decamethylene sebacate) (9)**

To chamber one of a two bulb 1-necked flask equipped with magnetic stirring and nitrogen inlet distilled sebacoyl chloride (1.1212 g, 4.6885 mmol) was added via a pipet. Recrystallized 1,10-decanediol (0.8168 g, 4.687 mmol) (with a spatula) and dried diglyme (Na) (6 mL) (with a pipet) were added into chamber 2 of the flask and stirred at 80 °C under nitrogen until the diol was dissolved. The contents of the two bulbs were then mixed in chamber two and the polymerization was allowed to proceed for two days at 80 °C. During the reaction, the flask was continuously flushed with a nitrogen stream to remove HCl. After it had been cooled to room temperature, the product was dissolved in CH<sub>2</sub>Cl<sub>2</sub> (15 mL) and precipitated into methanol (400 mL). The solid was filtered, dried under vacuum and 1.4588g (91 %) of polymer were obtained.  $M_n = 13.9$  kg/mol and  $M_w = 23.5$  kg/mol determined by GPC with polystyrene standards in toluene. <sup>1</sup>H NMR: 1.32 (m, 20 H, -(CH<sub>2</sub>)<sub>6</sub>-(CH<sub>2</sub>)<sub>2</sub>-OOCCH<sub>2</sub>CH<sub>2</sub>(CH<sub>2</sub>)<sub>4</sub>-), 1.64 (t, J = 7 Hz, 8 H, -OCH<sub>2</sub>CH<sub>2</sub>-, -OOCCH<sub>2</sub>CH<sub>2</sub>-), 2.30 (t, J = 8 Hz, 4 H, -OOCCH<sub>2</sub>-), 4.05 (t, J = 8 Hz, 4 H, -OCH<sub>2</sub>-). <sup>13</sup>C NMR: 24.9, 25.8, 28.6, 29.0, 29.1, 29.4, 34.3, 64.35, 173.8 (9 signals, theory: 10).

**General procedure for the syntheses of polysecacate rotaxanes using the acid chloride method: Poly[(decamethylene sebacate)-rotaxa-(42-crown-14)] (14)**

To chamber one of a two bulb 1-necked flask equipped with magnetic stirring and nitrogen inlet distilled sebacoyl chloride (1.2165 g, 5.0869 mmol) was added via a pipet. Recrystallized 1,10-decanediol (0.8866 g, 5.087 mmol) and 42C14 (4.5499 g, 7.3773 mmol) were added with spatulas into chamber 2 of the flask and the mixture was stirred at 80 °C under nitrogen for 0.5 h. The contents of the two bulbs were then mixed in chamber two and the polymerization was allowed to proceed at 80°C for two days. During the reaction, the flask was continuously flushed with a nitrogen stream to remove HCl. After it had been cooled to room temperature, the product was dissolved in CH<sub>2</sub>Cl<sub>2</sub> (15 mL) and precipitated into methanol (600 mL). The precipitation was performed three times. After each precipitation, the polymer was checked by <sup>1</sup>H NMR to determine the macrocycle content. After three precipitations, the polymer was dried under vacuum and 0.9479 g (35.7 %) of polymer was obtained.  $M_n = 8.3$  kg/mol and  $M_w = 14.0$  kg/mol determined by GPC with polystyrene standards in toluene. <sup>1</sup>H NMR: 1.32 (m, 20 H, -(CH<sub>2</sub>)<sub>6</sub>-(CH<sub>2</sub>)<sub>2</sub>-OOCCH<sub>2</sub>CH<sub>2</sub>(CH<sub>2</sub>)<sub>4</sub>-), 1.64 (t, J = 7 Hz, 8 H, -OCH<sub>2</sub>CH<sub>2</sub>-, -OOCCH<sub>2</sub>CH<sub>2</sub>-), 2.30 (t, J = 8 Hz, 4 H, -OOCCH<sub>2</sub>-), 3.65 (s, 42C14), 4.05 (t, J = 8 Hz, 4 H, -OCH<sub>2</sub>-). <sup>13</sup>C NMR: 24.9, 25.8, 28.6, 29.0, 29.1, 29.4, 34.3, 64.3, 70.5 (42C14), 173.8 (10 signals, theory: 11).

### **A. Ring size**

Poly[(decamethylene sebacate)-rotaxa-(30-crown-10)] (**12**), poly[(decamethylene sebacate)-rotaxa-(36-crown-12)] (**13**), poly[(decamethylene sebacate)-rotaxa-(48-crown-16)] (**15**), and poly[(decamethylene sebacate)-rotaxa-(60-crown-20)] (**16**) were prepared from sebacyl chloride (0.2391 g, 1.000 mmol), 1,10-decanediol (0.1743 g, 1.000 mmol), and crown ethers (1.000 mmol).  $M_n$  and  $M_w$  values (kg/mol) determined by GPC with polystyrene standards in THF: **12**: 32.8, 58.9; **13**: 14.3, 22.5; **15**: 11.4, 19.5; and **16**: 10.7, 20.7.

### **B. Feed ratio**

Poly[(decamethylene sebacate)-rotaxa-(42-crown-14)]s (**14**) were prepared from sebacyl chloride (0.2391 g, 1.000 mmol), 1,10-decanediol (0.1743 g, 1.000 mmol), and 42-crown-14 (0.6167 n g, n mmol). The molecular weights of the resultant polyrotaxanes were not measured.

### **C. Prethreading time**

Poly[(decamethylene sebacate)-rotaxa-(42-crown-14)]s (**14**) were prepared from sebacyl chloride (0.2391 g, 1.000 mmol), 1,10-decanediol (0.1743 g, 1.000 mmol), and 42-crown-14 (0.6167 g, 1.000 mmol). Before the polymerization, 1,10-decanediol and 42-crown-14 were stirred in chamber 2 at



80 °C under nitrogen for 0, 0.5, 1, 2, and 13 h., respectively. The molecular weights of the resultant polyrotaxanes were not measured.

#### **D. Double prethreading**

To chamber one of a two bulb 1-necked flask equipped with magnetic stirring and nitrogen inlet distilled sebacoyl chloride (0.5816 g, 2.432 mmol) and 42C14 (1.5000 g, 2.4321 mmol) were added. Recrystallized 1,10-decanediol (0.4238 g, 2.432 mmol) and 42C14 (1.5000 g, 0.4321 mmol) were added into chamber 2 of the flask. The two mixtures were stirred separately at 80 °C under nitrogen for 0.5 hour prior to the polymerization of the diacid chloride and the diol by mixing the contents of the two chambers. The molecular weight of the resultant polyrotaxane was not measured.

#### **E. Temperature**

Poly[(decamethylene sebacate)-rotaxa-(42-crown-14)]s (**14**) were prepared from sebacoyl chloride (0.2391 g, 1.000 mmol), 1,10-decanediol (0.1743 g, 1.000 mmol), and 42-crown-14 (0.6167 g, 1.000 mmol) by equilibration and reaction at 110, 115, 140, and 160 °C, respectively. The  $M_n$  and  $M_w$  values (kg/mol) determined by GPC with polystyrene standards in THF are: 110 °C: 12.8, 22.3; 115 °C: 10.9, 17.8; 140 °C: 6.3, 11.0; 160 °C: 11.6, 19.7.

### **Poly(hexamethylene sebacate)-rotaxa-(42C14) (11)**

**11** was prepared from sebacoyl chloride (0.2391 g, 1.000 mmol), 1,6-hexanediol (0.1182 g, 1.000 mmol), and 42C14 (0.6167 g, 1.000 mmol). Before the polymerization, 1,6-hexanediol and 42-crown-14 were stirred at 80 °C under nitrogen for 0.5 h.  $M_n = 8.3$  kg/mol and  $M_w = 16.1$  kg/mol determined by GPC with polystyrene standards in THF.  $^1\text{H}$  NMR: 1.30 (s, 8 H,  $-(\text{CH}_2)_4(\text{CH}_2)_2\text{COO}-$ ), 1.38 (t,  $J = 7$  Hz, 4 H,  $-\text{OCH}_2(\text{CH}_2)_2-$ ), 1.62 (m, 8 H,  $-\text{CH}_2\text{CH}_2\text{COOCH}_2\text{CH}_2-$ ), 2.29 (t,  $J = 8$  Hz, 4 H,  $-\text{CH}_2\text{COO}-$ ), 3.65 (s, 42C14), 4.06 (t,  $J = 7$  Hz, 4 H,  $-\text{OCH}_2-$ ).  $^{13}\text{C}$  NMR: 24.8, 25.5, 28.5, 29.0, 64.1, 70.5 (42C14), 173.8 (7 signals, theory: 9).

### **Poly(butylene sebacate)-rotaxa-(42C14) (10)**

**10** was prepared from sebacoyl chloride (0.2391 g, 1.000 mmol), 1,4-butanediol (0.0901 g, 1.000 mmol), and 42C14 (0.6167 g, 1.000 mmol). Before the polymerization, 1,4-butanediol and 42-crown-14 were stirred at 80 °C under nitrogen for 0.5 h.  $M_n = 29.5$  kg/mol and  $M_w = 42.5$  kg/mol determined by GPC with polystyrene standards in THF.  $^1\text{H}$  NMR: 1.31 (br s, 8 H,  $-(\text{CH}_2)_4(\text{CH}_2)_2\text{COO}-$ ), 1.61 (m, 4 H,  $-\text{CH}_2\text{CH}_2\text{COO}-$ ), 1.71 (m, 4 H,  $-(\text{CH}_2)_2\text{CH}_2\text{O}-$ ), 2.29 (t,  $J = 7.0$  Hz, 4 H,  $-\text{CH}_2\text{COO}-$ ), 3.65 (s, 42C14), 4.09 (t,  $J = 5.5$  Hz, 4 H,  $-\text{CH}_2\text{O}-$ ).  $^{13}\text{C}$  NMR: 24.8, 25.3, 29.0, 34.2, 63.6, 70.5 (42C14), 173.7 (7 signals, theory: 8).

**Poly{decamethylene sebacate-co-1,10-bis{*p*-[di(*p*'-*t*-butylphenyl)-4-hydroxyphenylmethyl]phenoxy}decamethylene sebacate}-rotaxa-(42-crown-14) (18)**

To chamber one of a two bulb 1-necked flask equipped with magnetic stirring and nitrogen inlet distilled sebacyl chloride (0.2396 g, 1.002 mmol) was added via a pipet. Recrystallized 1,10-decanediol (0.1393 g, 0.7993 mmol), 1,10-bis{*p*-[di(*p*-*t*-butylphenyl)-4-hydroxyphenylmethyl]phenoxy}decane (**17**) (0.2135 g, 0.200 mmol), and 42-crown-14 (0.6165 g, 0.9996 mmol) were added with spatulas to chamber 2 of the flask and the mixture was stirred under nitrogen for 0.5 h. at 130 °C. The contents of the two bulbs were then mixed in chamber two and the polymerization was allowed to proceed for two days at 130 °C. During the reaction, the flask was continuously flushed with a nitrogen stream to remove HCl. After it had been cooled to room temperature, the product was dissolved in CH<sub>2</sub>Cl<sub>2</sub> (10 mL) and precipitated into methanol (250 mL). The precipitation was performed three times. After each precipitation, the polymer was checked by <sup>1</sup>H NMR to determine the macrocycle content.  $M_n = 18.7$  kg/mol and  $M_w = 29.3$  kg/mol determined by GPC with polystyrene in chloroform. <sup>1</sup>H NMR: 1.29 (m, 28 H, protons **a**), 1.61 (m, 10 H, protons **c**), 2.29 (t,  $J = 7.6$  Hz, 5 H, protons **d**), 3.64 (s, 42C14), 3.91 (t,  $J = 6.8$  Hz, 1 H, protons **b**), 4.05 (t,  $J = 6.8$  Hz, 4 H, protons **e**), 6.68-7.23 (m, 8 H, arom.).

## Poly(bisphenol A sebacate)-rotaxa-(42C14) (20)

Potassium hydroxide (3.1034 g, 5.032 mmol) was dissolved in water (20.0 mL), and bisphenol-A (0.5707 g, 2.500 mmol) was added. After bisphenol-A had dissolved, 42C14 (3.1034 g, 5.032 mmol) was added. The mixture was slowly stirred with a mechanical stirrer. An organic solution was prepared by dissolving sebacoyl chloride (0.5979 g, 2.500 mmol) in chloroform (10.0 mL). The organic solution was then added to the aqueous solution which was stirred at maximum speed. The reaction was allowed to proceed for 10 min. The mixture was then precipitated into methanol (200 mL). The precipitation was performed three times. After each precipitation, the polymer was checked by  $^1\text{H}$  NMR to determine the macrocycle content. A white solid polymer (0.0613 g, yield: 6.2 %) was obtained after the third precipitation.  $M_n = 2.8$  kg/mol and  $M_w = 4.1$  kg/mol determined by GPC with polystyrene standards in toluene. The polymer shows a broad endotherm at 57 °C upon first heating in DSC measurement. It shows a  $T_g$  at -8 °C at second heating.  $^1\text{H}$  NMR: 1.38 (m, 10 H,  $-(\text{CH}_3)_2\text{CC}_6\text{H}_4\text{OOC}(\text{CH}_2)_3(\text{CH}_2)_2-$ ), 1.58 (m, 4 H,  $-\text{OOC}(\text{CH}_2)_2\text{CH}_2-$ ), 1.75 (p,  $J = 8$  Hz, 4 H,  $-\text{OOCCH}_2\text{CH}_2-$ ), 2.53 (t,  $J = 8$  Hz, 4 H,  $-\text{OOCCH}_2-$ ), 3.67 (s, 42-crown -14), 6.95 (d,  $J = 9$  Hz, 4 H, arom.), 7.20 (d,  $J = 9$  Hz, 4 H, arom.).

## REFERENCES

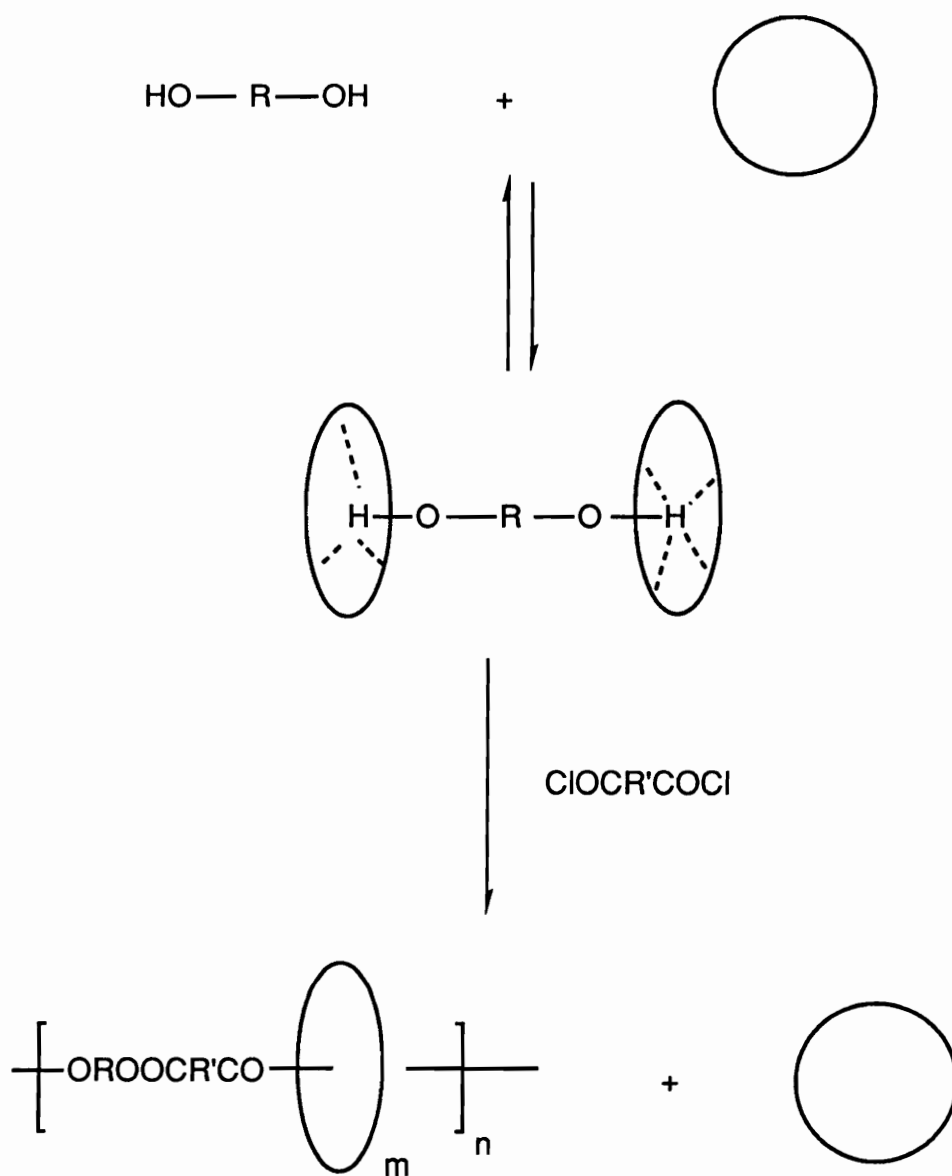
1. Ordian, G. *Principles of Polymerization, 2nd Ed.*, John Wiley & Sons, New York, 1970, pp. 423-445.
2. Gibson, H. W.; Liu, S.; Lecavalier, P.; Wu, C.; Shen, Y. X. *J. Am. Chem. Soc.* 1995, 117, 852.
3. Gibson, H. W.; Xie, D.; Gibson, H. W. *J. Am. Chem. Soc.* 1994, 116, 537.
4. Harrison, I. T. *J. Chem. Soc. Perk. Trans.* 1974, 1, 301.
5. Schill, G.; Beckmann, W., Schweickert, N.; Fritz, H. *Chem. Ber.*, 1986, 119, 2647.
6. Agam, G.; Gravier, D.; Zilkha, A. *J. Am. Chem. Soc.* 1976, 98, 5206.
7. Clarson, S. J.; Mark, J. E.; Semlyen, J. A. *Polym. Commun.* 1987, 27, 244.
8. Atkins, P. W. *Physical Chemistry, 3rd Ed.* W. H. Freeman and Co., New York, 1986, p. 587.
9. Joyce, S. J.; Hubbard, R. E.; Semlyen, J. A. *Eur. Polym. J.* 1993, 29, 305.
10. Gibson, H. W.; Engen, P. T. *New J. Chem.* 1993, 17, 723.
11. Atkins, P. W. *Physical Chemistry, 3rd Ed.* W. H. Freeman and Co., New York, 1986, p. 219.
12. a). Franke, J.; Vögtle, F. *Top. Curr. Chem.* 1986, 132, 135. b). Diederich, F. *Angew. Chem., Int. Ed. Engl.* 1988, 27, 363. c). Inoue, Y.; Gokel, G. W. *Cation Binding by Macrocycles, Complexation of Cationic Species by Crown Ethers*, Marcel Dekker, New York, 1990. d). Izatt, R. M.; Pawlak, K.; Bradshaw, J. S. *Chem. Rev.* 1991, 91, 1721. e). Izatt, R. M.;

- Bradshaw, J. S.; Pawlak, K.; Bruening, R. L.; Taret, B. J. *Chem. Rev.* **1992**, *92*, 1261.
13. Korshak, V. V.; Vingradova, S. V.; Vlasova, E. S. *Doklady Akad. Nauk S.S.S.R.* **1954**, *94*, 61.
  14. Howard, G. J.; Knutton, S. *Polymer*, **1968**, *9* (10), 527.
  15. Woo, E. M.; Barlow, J. W.; Paul, D. R. *Polymer*, **1985**, *26* (5), 763.
  16. Fernandes, A. C.; Barlow, J. W.; Paul, D. R. *polymer*, **1986**, *27*, 1799.
  17. Marvel, C. S.; Johnson, J. H. *J. Am. Chem. Soc.* **1950**, *72*, 1674.
  18. The internal diameter of a fully opened 30-crown-10 is calculated by the equation:  $D = (10/\pi)[(1.52)\sin(108.95/2) + (2)(1.42)\sin(107.00/2)] - 4.5$ , where 1.52 Å is the length of the carbon-carbon bond, 1.42 Å the length of the carbon-oxygen bond, 108.95° is the C-C-C bond angle and 107.00° is the C-O-C bond angle. Above data are from ref 9. 4.5 is the diameter of a poly(ethylene oxide) chain in Å.
  19. Gibson, H. W.; Marand H. *Adv. Mater.* **1993**, *5*, 11.
  20. Douglas, B.; McDaniel, D.; Alexander, J. J. *Concepts and Models of Inorganic Chemistry*, John Wiley & Sons, New York, **1983**, p. 219.
  21. Wittbecker, E. L.; Morgan, P. W. *J. Polym. Sci.* **1959**, *40*, 289.
  22. Korshak, V. V.; Vasnev, V. A. in *Comprehensive Polym. Sci.*, Ed. Geobbery, A. F., Pergamon press, New York, **1989**, Vol. 5, pp. 167-169.
  23. Imai, Y. *J. Macromol. Sci. Chem.* **1981**, *A15*, 833.
  24. Imai, Y.; Ueda, M.; Li, M. *J. Polym. Sci., Polym. Lett. Ed.* **1979**, *17*, 85.
  25. Imai, Y.; Kato, A.; Ueda, M. *J. Polym. Sci., Polym. Lett. Ed.* **1979**, *17*, 579.
  26. Eareckson, W. M. *J. Polym. Sci.* **1959**, *40*, 399.

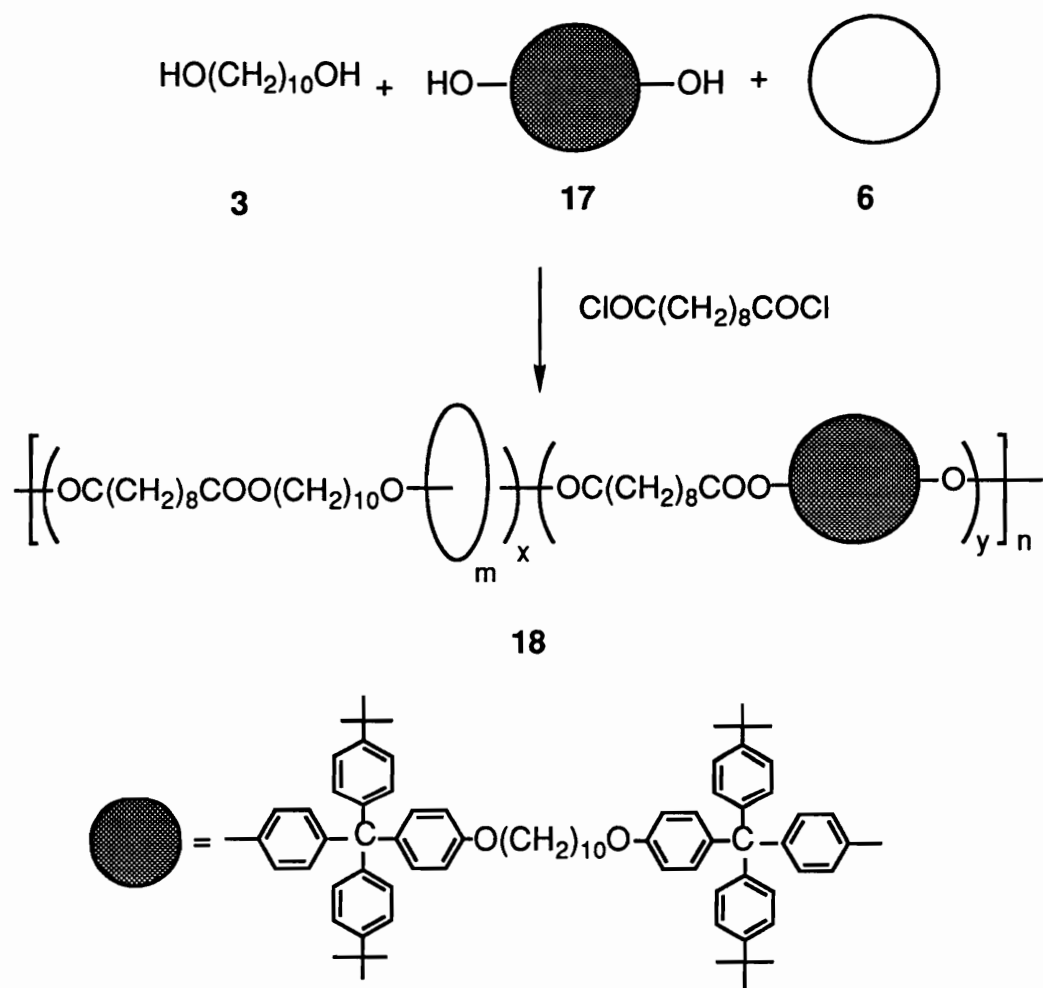
27. Gibson, H. W.; Bheda, M. C.; Engen, P.; Shen, Y. X.; Sze, J.; Zhang, H.; Gibson, M. D.; Delaviz, Y.; Lee, S.-H.; Liu, S.; Wang, L., Rancourt, J.; Taylor, L. T. *J. Org. Chem.* **1994**, *59*, 2186.



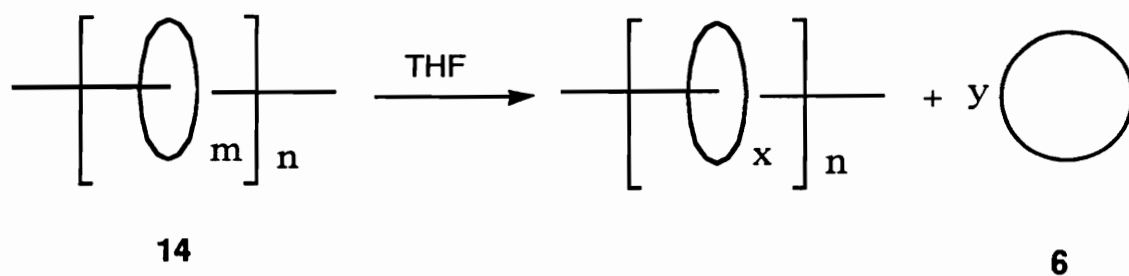




Scheme 2. Hydrogen bonding between diol and crown ether in prethreading process

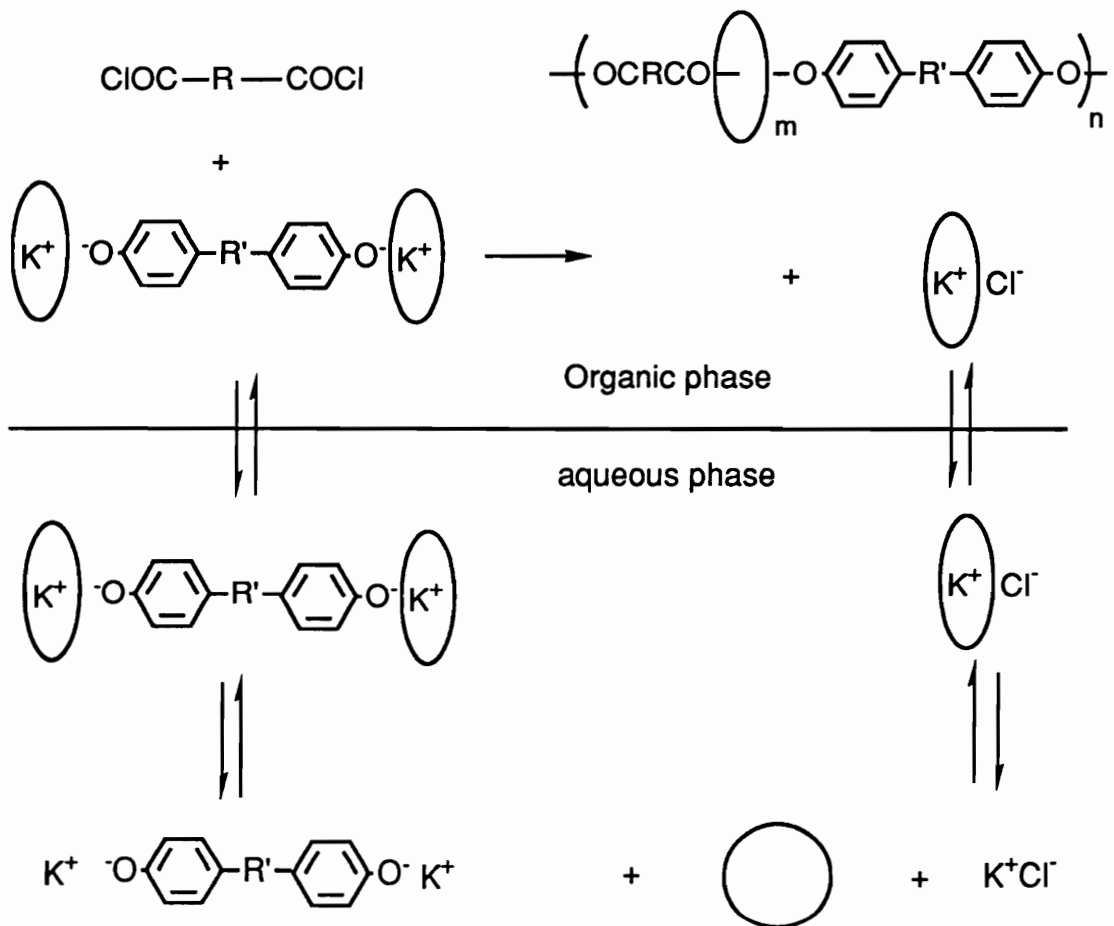


Scheme 3. Synthesis of polyrotaxane (**18**)

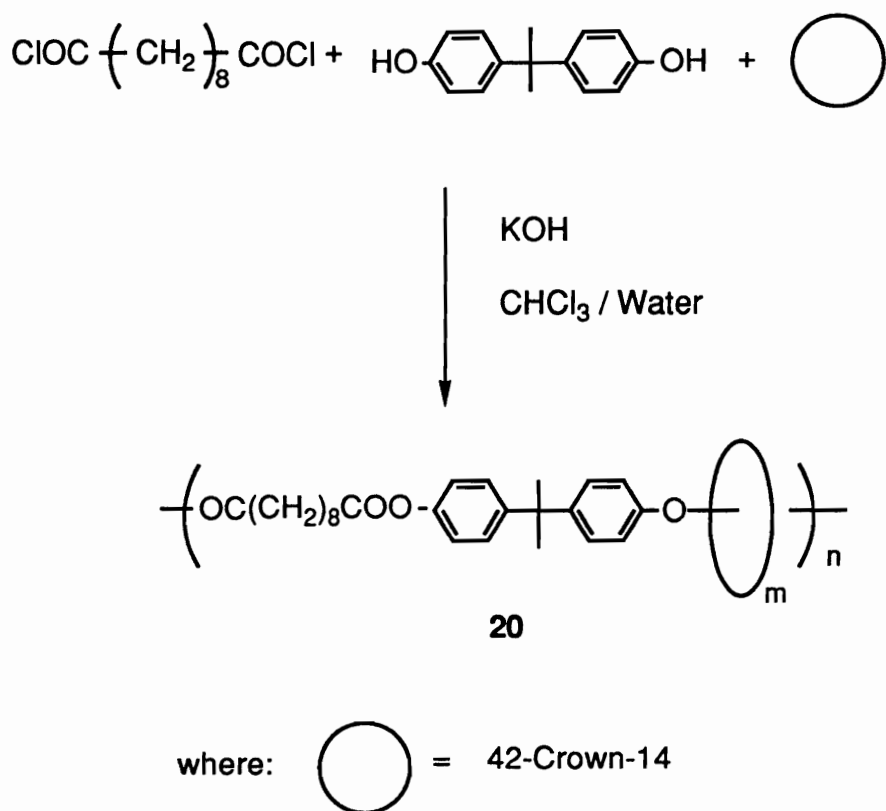


$$Y = n (m - x)$$

Scheme 4. Dethreading experiments of 42-crown-14 (**6**) from poly[(decamethylene sebacate)-rotaxa-(42-crown-14)] (**14**)



Scheme 5. Interfacial polymerization for polyrotaxanes



Scheme 6. Synthesis of poly[(bisphenol A sebacate)-rotaxa-(42-crown-14)]  
**(20)** by interfacial polymerization

Table 1. Optimization for the synthesis of poly(decamethylene sebacate) (9)

Experiment #	Temperature (°C)	Time (h)	M <sub>n</sub> (kg/mol)	M <sub>w</sub> (kg/mol)	M <sub>w</sub> /M <sub>n</sub>
1a	80	24	7.9 <sup>c</sup>	16.1 <sup>c</sup>	2.02
2a	80	48	8.9 <sup>c</sup>	15.2 <sup>c</sup>	1.55
3a	110	48	7.7 <sup>c</sup>	12.9 <sup>c</sup>	1.66
4a	140	48	5.2 <sup>c</sup>	7.1 <sup>c</sup>	1.38
5b	80	48	13.9 <sup>d</sup>	23.5 <sup>d</sup>	1.69

- a. Reactions were done in a single chamber flask.
- b. The reaction was done in a double chamber flask.
- c. Measured by GPC in chloroform at 25 °C with polystyrene standards.
- d. Measured by GPC in toluene at 25 °C with polystyrene standards.

Table 2. Errors of determination of m/n value form sampling of poly[(decamethylene sebacate)-rotaxa-(42-crown-14)] (14): 20 data sets.

method <sup>a</sup>	mean	spread	standard deviation
1	0.356	0.029	0.00719
2	0.340	0.018	0.00443
3	0.325	0.036	0.00754
4	0.326	0.013	0.00344

a. See text (p. 235).

Table 3. Errors of determination of m/n value from measuring of poly[(decamethylene sebacate)-rotaxa-(42-crown-14)] (14): 20 data sets

method	mean	spread	standard deviation
1	0.369	0.017	0.00395
4	0.329	0.013	0.00346

Table 4. The effect of macrocycle size on the threading of crown ethers (**4-8**) by 1,10-decanediol (**3**): neat process, temperature: 80 °C; molar feed ratio of cyclic to linear: 1.0; prethreading time: 30 min.

Ring Size	30C10	36C12	42C14	48C16	60C20
m/n <sup>a</sup>	0.012	0.22	0.29	0.34	0.36
wt% ring	1.5	25	34	41	48

a. Final molar ratio of macrocycle to repeat unit of the polymer backbone in the polyrotaxane, measured by <sup>1</sup>H NMR.

Table 5. The effect of feed ratio on the threading of 42C14 (**6**) by 1,10-decanediol (**3**) (0.5 h, 80 °C)

M <sub>0</sub> /D <sub>0</sub> <sup>a</sup>	m/n <sup>b</sup>	wt % 42C14
1.00	0.29	34
1.45	0.33	37
2.00	0.41	43
4.00	0.42	43

- a. Molar feed ratio of 42-crown-14 to 1,10-decanediol.  
 b. Final molar ratio of macrocycle to repeat unit of the polymer backbone in the polyrotaxane, measured by <sup>1</sup>H NMR.



Table 6. The effect of the diol length on the threading of 42C14 (6) by HO(CH<sub>2</sub>)<sub>x</sub>OH (1-3) (0.5 h, 80 °C)

Length (x)	m/n <sup>a</sup>	wt % 42C14
4	0.32	43
6	0.30	39
10	0.29	34

- a. Final molar ratio of macrocycle to repeat unit of the polymer backbone in the polyrotaxane, measured by <sup>1</sup>H NMR.

Table 7. The effect of prethreading time on the threading of 42-crown-14 (6) by 1,10-decanediol (3): neat process, molar feed ratio of cyclic to linear: 1.0; temperature: 80 °C.

Time (h)	<0.02	0.5	1	2	24	48
m/n <sup>a</sup>	0.32	0.29	0.30	0.31	0.31	0.31

- a. Final molar ratio of macrocycle to repeat unit of the polymer backbone in the polyrotaxane, measured by <sup>1</sup>H NMR.

Table 8. Prethreading of 42-crown-14 (**6**) by sebacoyl chloride (molar ratio of cyclic and linear: 1.0; temperature: 80 °C; 0.5 h) and by 1,10-decanediol (**3**) (molar ratio of cyclic and linear: 1.0; temperature: 80 °C; 0.5 h)

	Double Prethreading	Monoprethreading of 1,10-decanediol	
$M_O / L_O$ <sup>a</sup>	1.00	1.00	2.00
$M_O / S_O$ <sup>b</sup>	1.00	0.00	0.00
$m / n$ <sup>c</sup>	0.35	0.29	0.41

- Molar ratio of 42-crown-14 to 1,10-decanediol in the monomer feed.
- Molar ratio of 42-crown-14 to sebacoyl chloride in the monomer feed.
- Final molar ratio of macrocycle to repeat unit of the polymer backbone in the polyrotaxane, measured by <sup>1</sup>H NMR.

Table 9. The effect of temperature on the threading of 42C14 (**6**) by 1,10-decanediol (**3**): neat process, molar feed ratio of cyclic to linear: 1.0; prethreading time: 30 min.

Temp. (°C)	80	110	115	140	160
$m/n^a$	0.29	0.30	0.29	0.33	0.32
$M_n$ (kg/mol)	8.3 <sup>b</sup>	12.8 <sup>c</sup>	10.9 <sup>c</sup>	6.3 <sup>c</sup>	11.6 <sup>c</sup>
$M_n/M_w$	1.68 <sup>b</sup>	1.74 <sup>c</sup>	1.62 <sup>c</sup>	1.75 <sup>c</sup>	1.69 <sup>c</sup>

- Final molar ratio of macrocycle to repeat unit of the polymer backbone in the polyrotaxane, measured by <sup>1</sup>H NMR.
- Determined by GPC with polystyrene standards in THF.
- Determined by GPC with polystyrene standards in chloroform.

Table 10. Intrinsic viscosities of the model polymer **9** and the polyrotaxane **14** as functions of solvents

Polymer	$M_n$ (kg/mol)	$M_w$ (kg/mol)	$[\eta]^c$ (dL/g)		
			(THF : methanol; v:v)		
			(100:0)	(100:10)	(100:20)
<b>9</b>	5.2 <sup>a</sup>	7.1 <sup>a</sup>	0.141	0.147	0.146
<b>14</b>	8.3 <sup>b</sup>	14 <sup>b</sup>	0.331	0.248	-

- a. Determined by GPC with polystyrene standards in chloroform.
- b. Determined by GPC with polystyrene standards in toluene.
- c. Measured in a Cannon-Fenske type viscometer at 25 °C.

Table 11. Dethreading experiments of 42C14 (6) from poly[(decamethylene sebacate)-rotaxa-(42-crown-14)] (14)

Experiment	1	2	3
Temperature (°C)	50	65	65
Concentra. (g/L)	42	4.8	4.8
Time (days)	7	11	35
Initial m/n	0.33	0.18	0.18
Initial wt % cyclic	34	25	25
Initial $M_n$ (kg/mol)	8.3 <sup>a</sup>	11.3 <sup>b</sup>	11.3 <sup>b</sup>
Initial $M_w$ (kg/mol)	14 <sup>a</sup>	20.5 <sup>b</sup>	20.5 <sup>b</sup>
Final m/n	0.27	0.17	0.15
Final wt % cyclic	30	24	21
Final $M_n$ (kg/mol)	-	9.1 <sup>b</sup>	12.7 <sup>b</sup>
Final $M_w$ (kg/mol)	-	17.9 <sup>b</sup>	22.3 <sup>b</sup>

a. Determined by GPC with polystyrene standards in toluene.

b. Determined by GPC with polystyrene standards in THF.

Table 12. Thermal properties of model polymer and polyrotaxanes measured by DSC at 10 °C/min.

polymer	T <sub>g</sub> <sup>a</sup> (°C)	T <sub>m</sub> <sup>b</sup> (°C)	ΔH <sub>f</sub> <sup>b</sup> (cal/g)	T <sub>c</sub> <sup>c</sup> (°C)
<b>9</b>	-	77	30.8	62.1
<b>10</b>	-55	44, 62	5.7, 12.0	23, 46
<b>11</b>	-55	39, 67	5.6, 15.8	22, 49
<b>12</b>	-	80	25.8	63
<b>13</b>	-54	42, 69, 71	5.0, 16.8 <sup>d</sup>	21, 56
<b>14</b>	-56	42, 70, 74	4.1, 20.9 <sup>d</sup>	25, 59
<b>15</b>	-58	43, 71, 75	5.7, 23.3 <sup>d</sup>	25, 60, 62
<b>16</b>	-58	44, 63, 70	5.4, 18.6 <sup>d</sup>	26, 55, 57
<b>18</b>	-56	45, 67	5.0, 5.0	8, 47

- a. Data from second heating.
- b. Data from second heating except the data of **10** which was from third heating.
- c. Crystallization exotherm data from second cooling.
- d. Heat of fusion of two partially overlapped endotherms.

Table 13. Metal complexation tests of crown ethers (**4-8**), poly(decamethylene sebacate) (**9**), and poly(decamethylene sebacate) rotaxanes (**12-16**) in which the toluene solutions containing organic compounds were shaken with aqueous solution of metal picrates. Complexations were determined by the color changes in the organic phases.

compound	Na	K	Ca	Cs
Blank	no	no	no	no
<b>4</b>	yes	yes	yes	yes
<b>5</b>	yes	yes	yes	yes
<b>6</b>	yes	yes	yes	yes
<b>7</b>	yes	yes	yes	yes
<b>8</b>	yes	yes	yes	yes
<b>9</b>	no	no	no	no
<b>12</b>	yes	yes	yes	yes
<b>13</b>	yes	yes	yes	yes
<b>14</b>	yes	yes	yes	yes
<b>15</b>	yes	yes	yes	yes
<b>16</b>	yes	yes	yes	yes

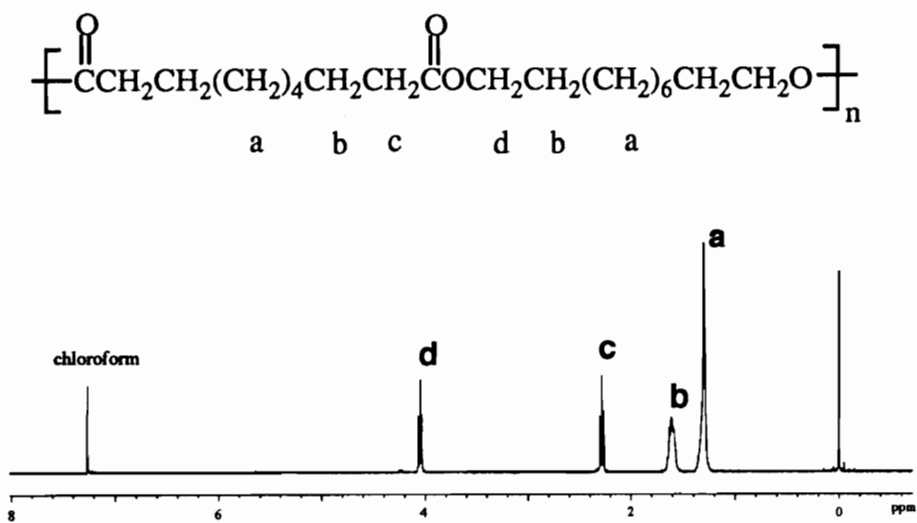


Figure 1. 400 MHz  $^1\text{H}$  NMR spectrum of poly(decamethylene sebacate) (**9**) in  $\text{CDCl}_3$

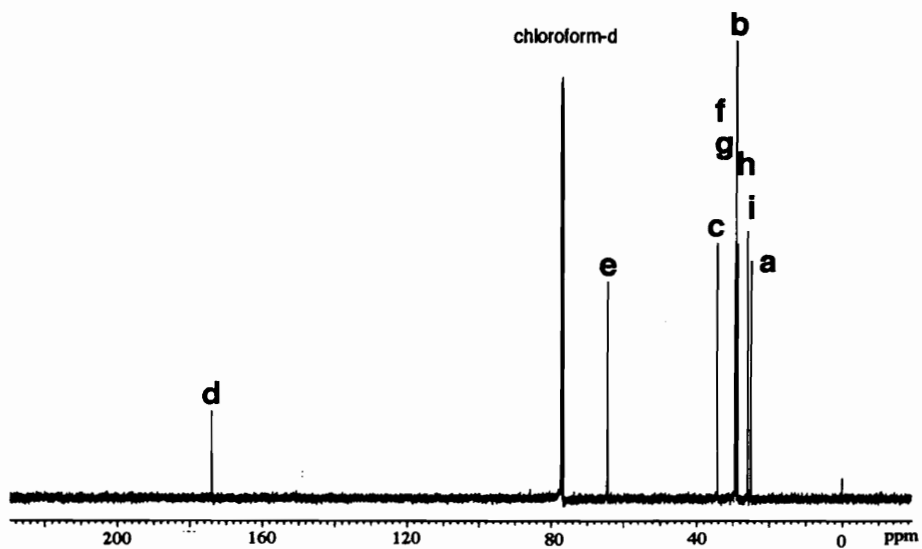
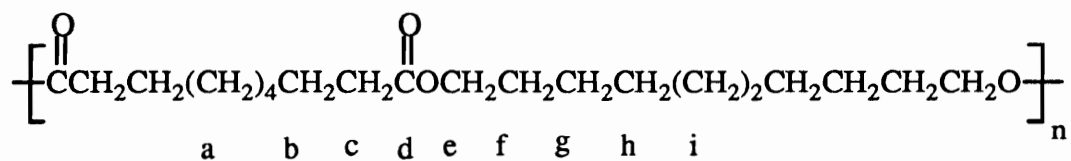


Figure 2. 100 MHz  $^{13}\text{C}$  NMR spectrum of poly(decamethylene sebacate) (9) in  $\text{CDCl}_3$



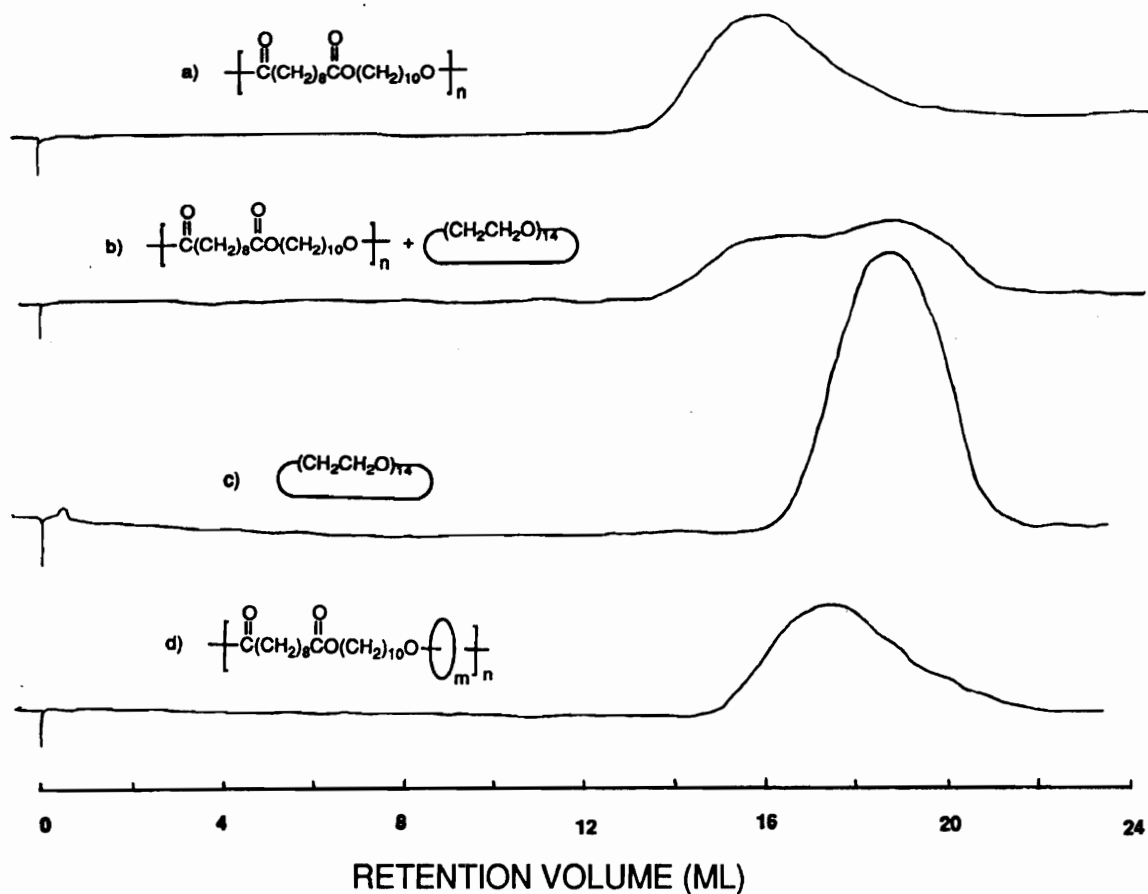


Figure 3. Gel permeation chromatography traces for a) poly(decamethylene sebacate) (**9**); b) a physical mixture of **9** and 42-crown-14 (**6**) 65:35 by mass; c) 42-crown-14 (**6**) and d) poly[(decamethylene sebacate)-rotaxa-(42-crown-14)] (**14**) in  $\text{CHCl}_3$  at 30 °C; refractive index detector.



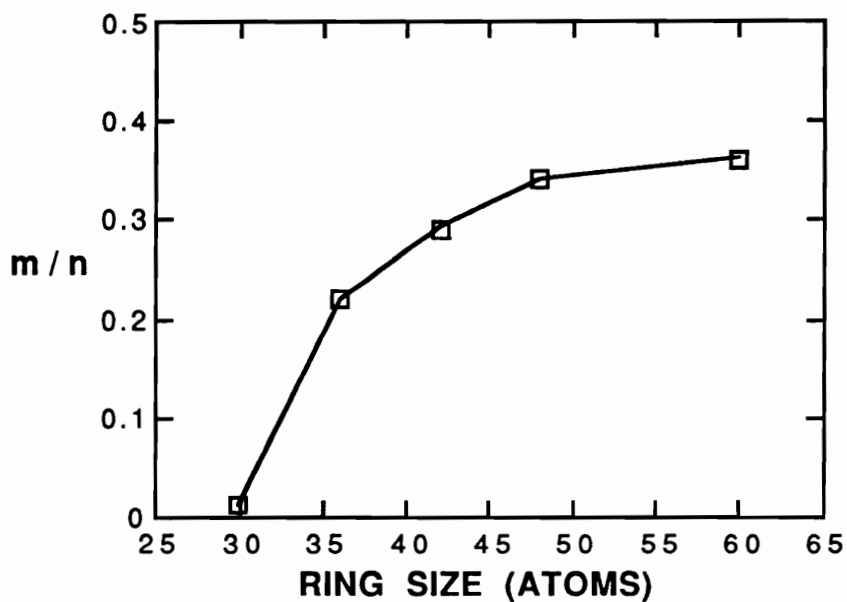


Figure 5.  $m/n$  value of polyrotaxanes (**12**, **13**, **14**, **15**, and **16**) versus ring size of the crown ether: neat process, molar feed ratio of cyclic to linear: 1.0; prethreading time: 30 min; temperature: 80 °C.

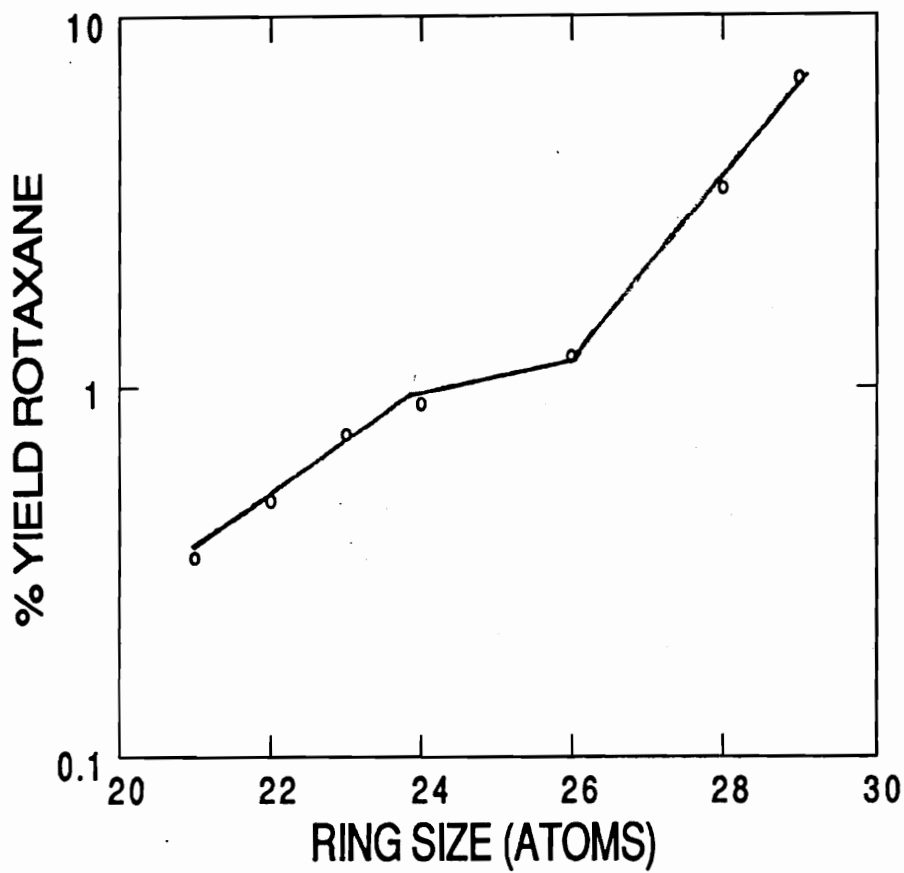


Figure 6. Log of the rotaxane yield as a function of ring size of the macrocycle.

Data from ref. 5.

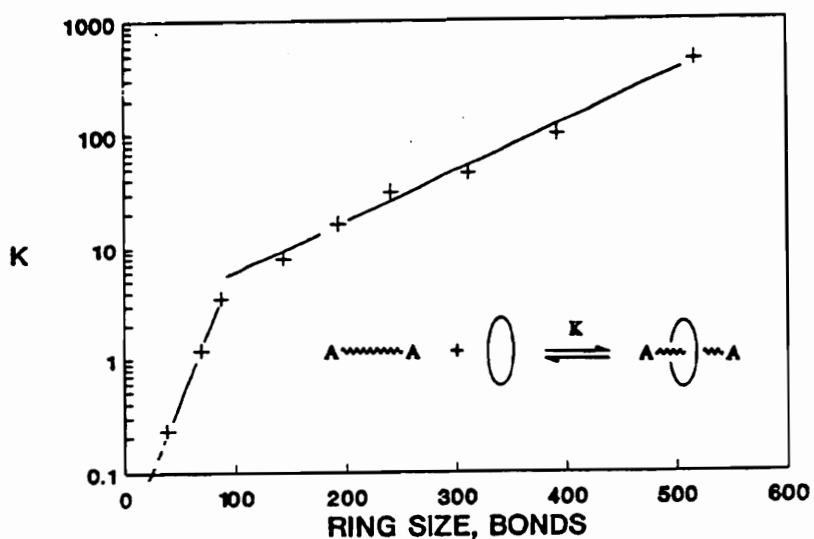


Figure 7. Log of the equilibrium constant,  $K$ , for threading of cyclic poly(dimethylsiloxane)s by linear poly(dimethylsiloxane) of  $M_n$  18 kg/mol versus ring size of the cyclic species: neat process, molar feed ratio of cyclic to linear: variable; temperature: 25 °C; from ref. 3.

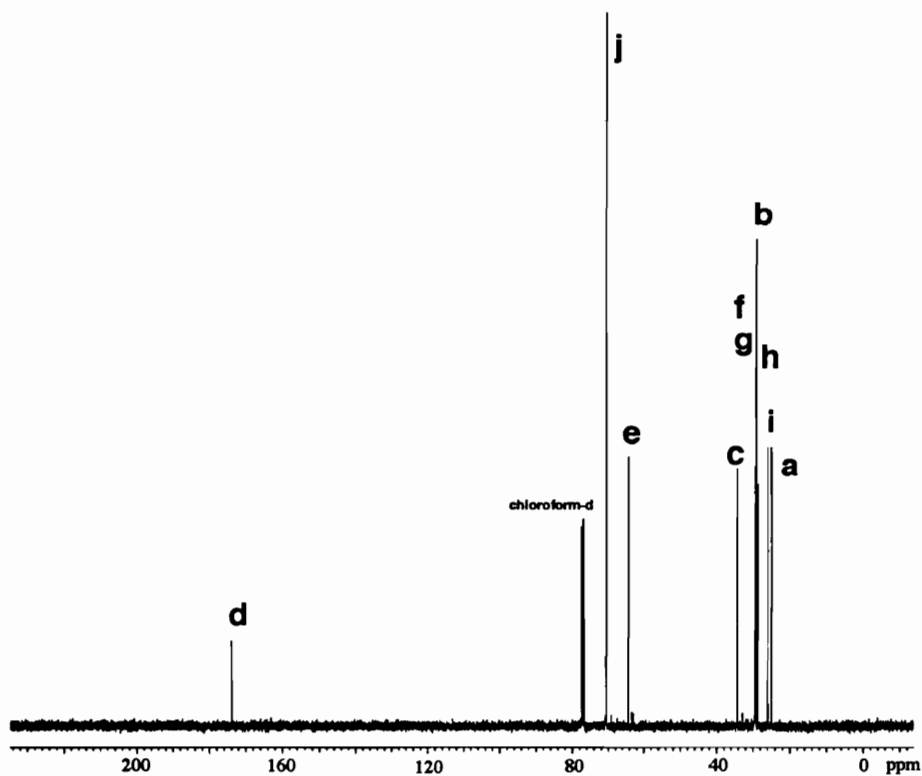
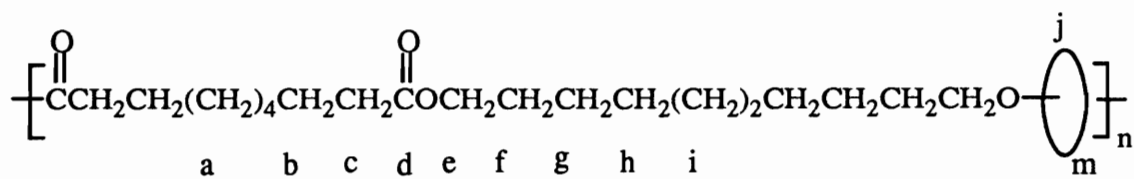


Figure 8. 100 MHz  $^{13}\text{C}$  NMR spectrum of poly[(decamethylene sebacate)-rotaxa-(42-crown-14)] (14) in  $\text{CDCl}_3$

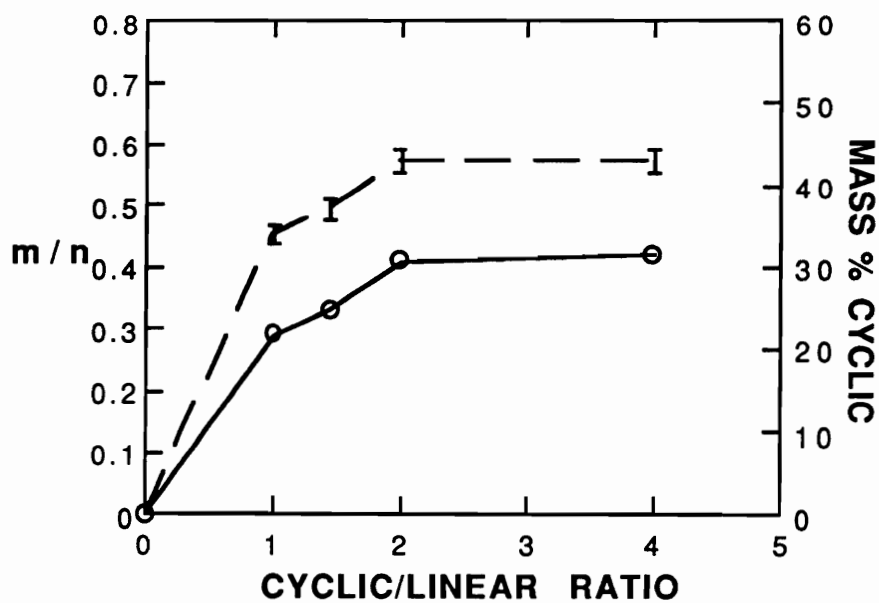


Figure 9.  $m/n$  value (solid line) and mass percent cyclic (broken line) in poly[(decamethylene sebacate)-rotaxa-(42C14)] (**14**) as a function of the mole ratio of 42-crown-14 (**6**) to 1,10-decanediol (**3**): neat process, temperature: 80 °C; prethreading time: 30 min.

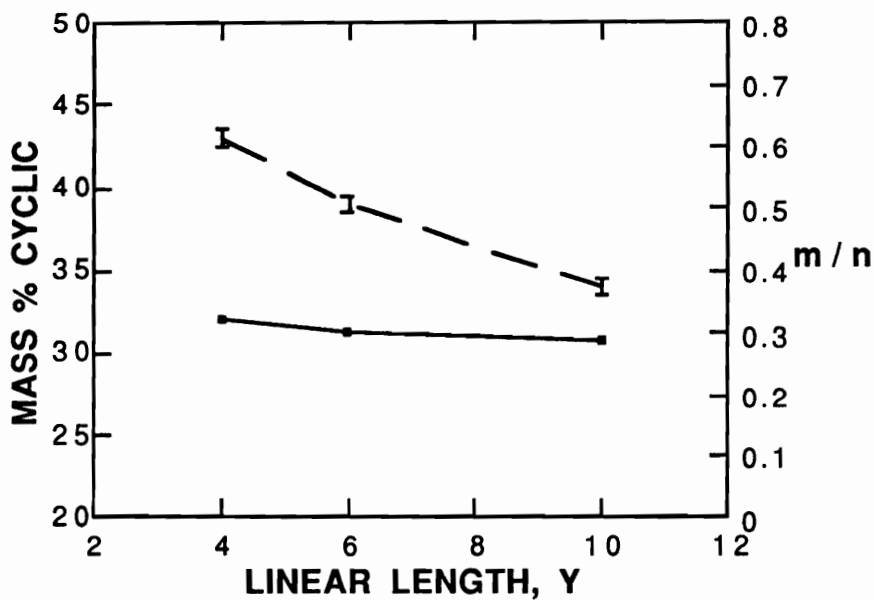


Figure 10.  $m/n$  value of polyrotaxanes (**10**, **11**, and **14**) (solid line) and mass percent 42-crown-14 (**6**) in polysebacate rotaxanes (broken line) as a function of length,  $y$ , of alkylene diols (**1**, **2**, and **3**): neat process, molar feed ratio of cyclic to linear: 1.0; temperature: 80 °C; prethreading time: 30 min.



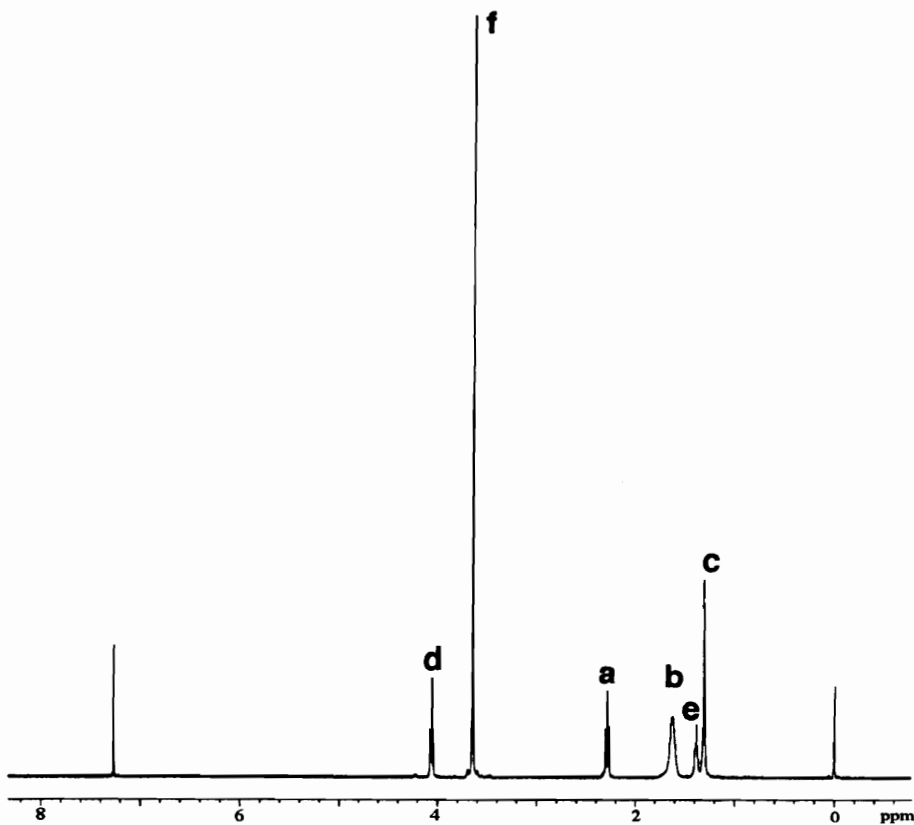
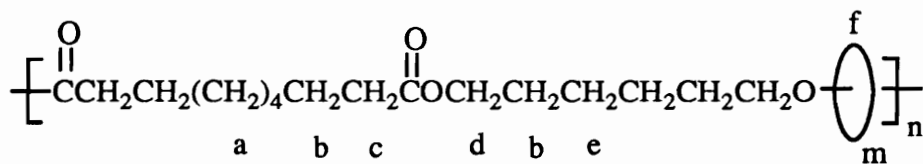


Figure 11. 400 MHz  $^1\text{H}$  NMR spectrum of poly[(hexamethylene sebacate)-rotaxa-(42-crown-14)] (11) in  $\text{CDCl}_3$ . The peak at 7.26  $\delta$  is due to chloroform.

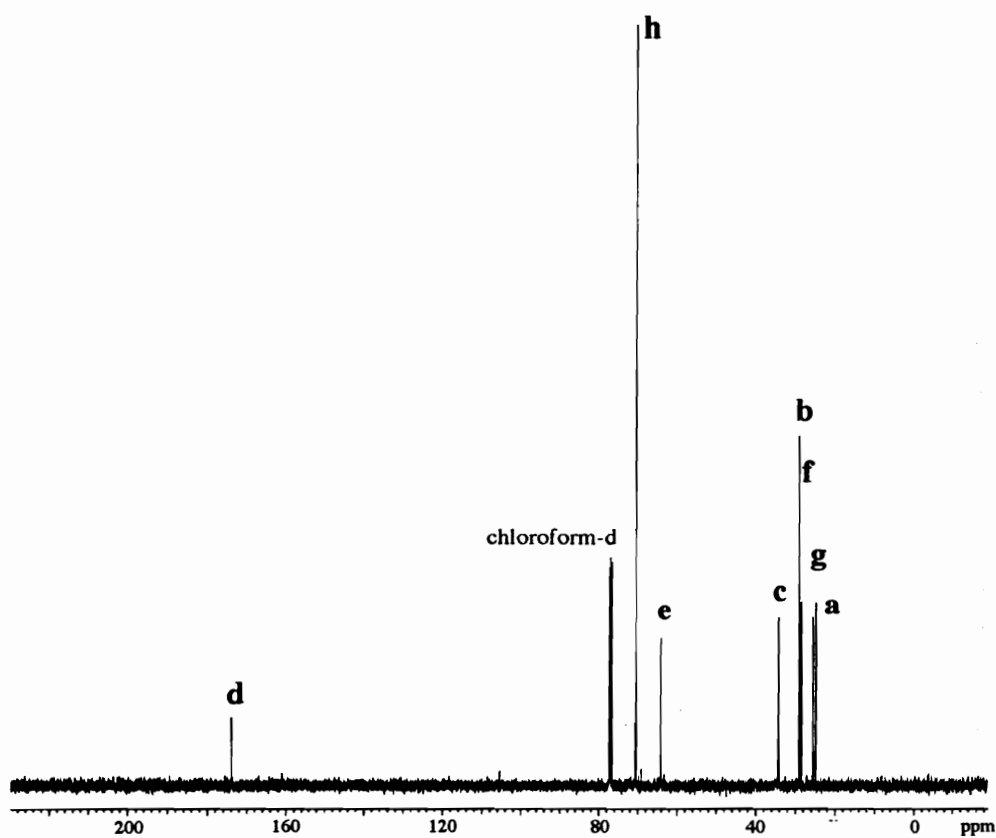
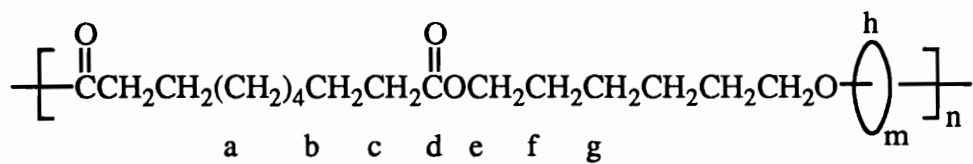


Figure 12. 100 MHz  $^{13}\text{C}$  NMR spectrum of poly[(hexamethylene sebacate)-rotaxa-(42-crown-14)] (11) in  $\text{CDCl}_3$

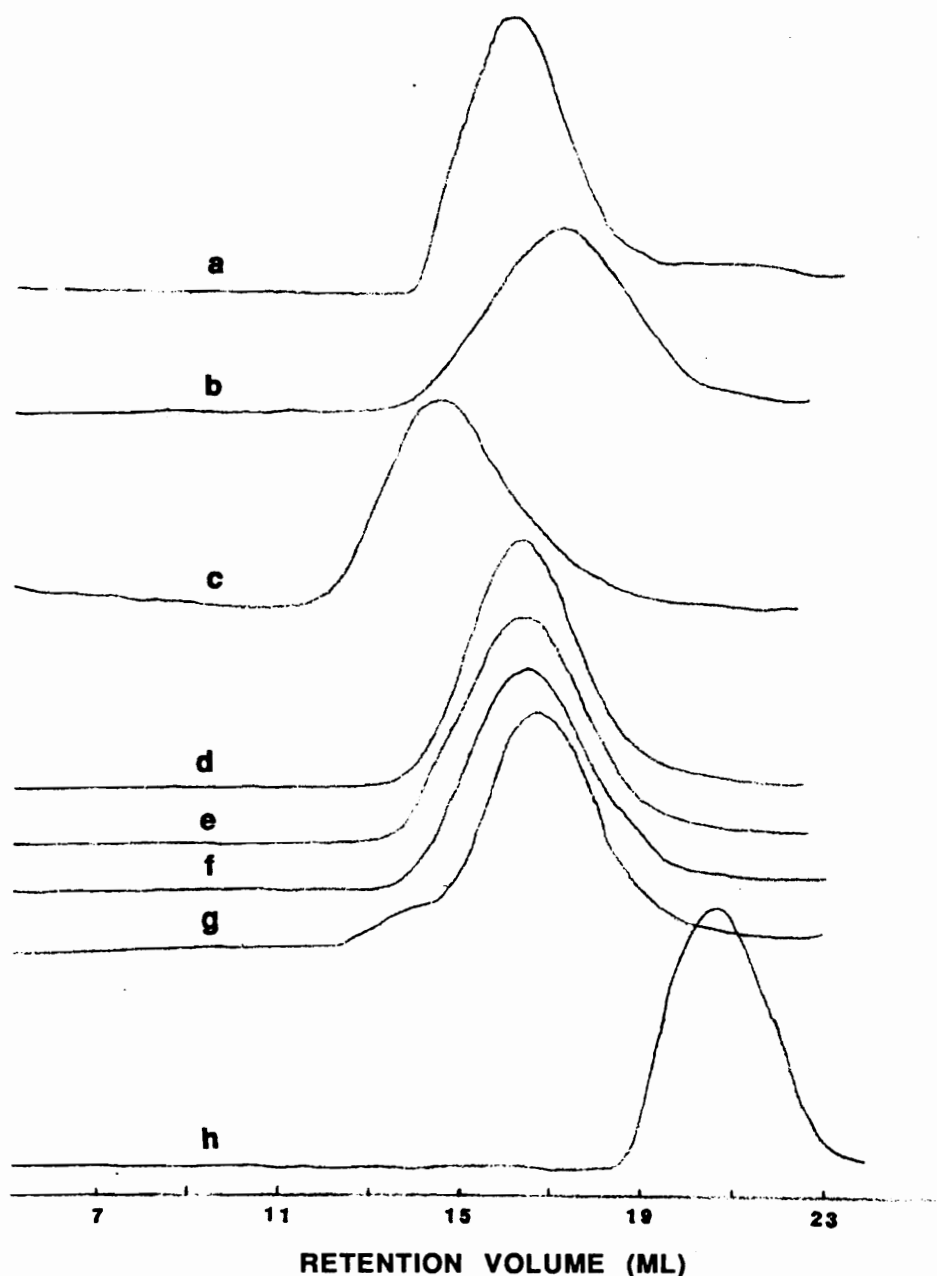


Figure 13. GPC traces for a) poly[(butylene sebacate)-rotaxa-(42-crown-14)] (10); b) poly[(hexamethylene sebacate)-rotaxa-(42-crown-14)] (11); c) poly[(decamethylene sebacate)-rotaxa-(30-crown-10)] (12); d) poly[(decamethylene sebacate)-rotaxa-(36-crown-12)] (13); e) poly[(decamethylene sebacate)-rotaxa-(42-crown-14)] (14); f) poly[(decamethylene sebacate)-rotaxa-(48-crown-16)] (15); g) poly[(decamethylene sebacate)-rotaxa-(60-crown-20)] (16) and h) 42-crown-14 (6) in THF at 30 °C; refractive index detector.



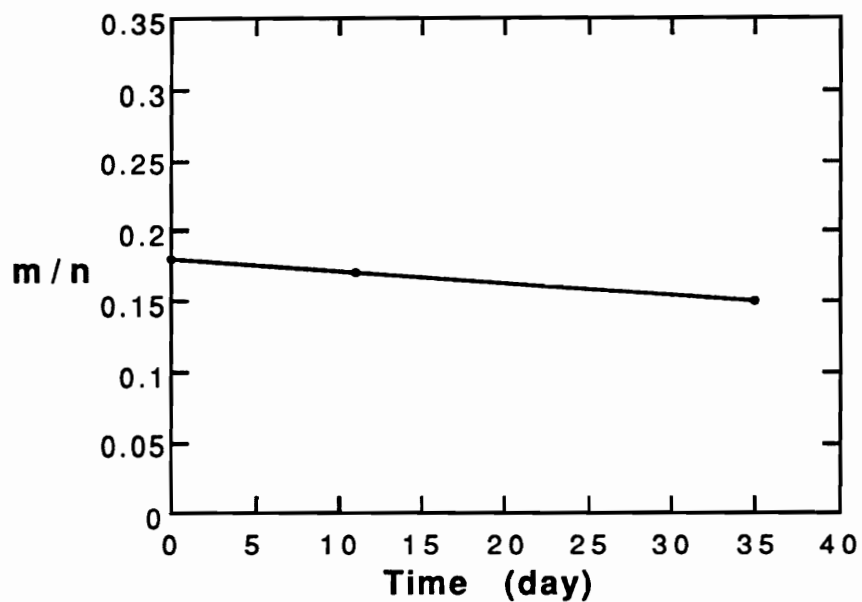


Figure 15.  $m/n$  value of poly[(decamethylene sebacate)-rotaxa-(42-crown-14)] (**14**) as a function of dethreading time: in THF, concentration of **14**: 4.8 gram/L; temperature: 65 C.

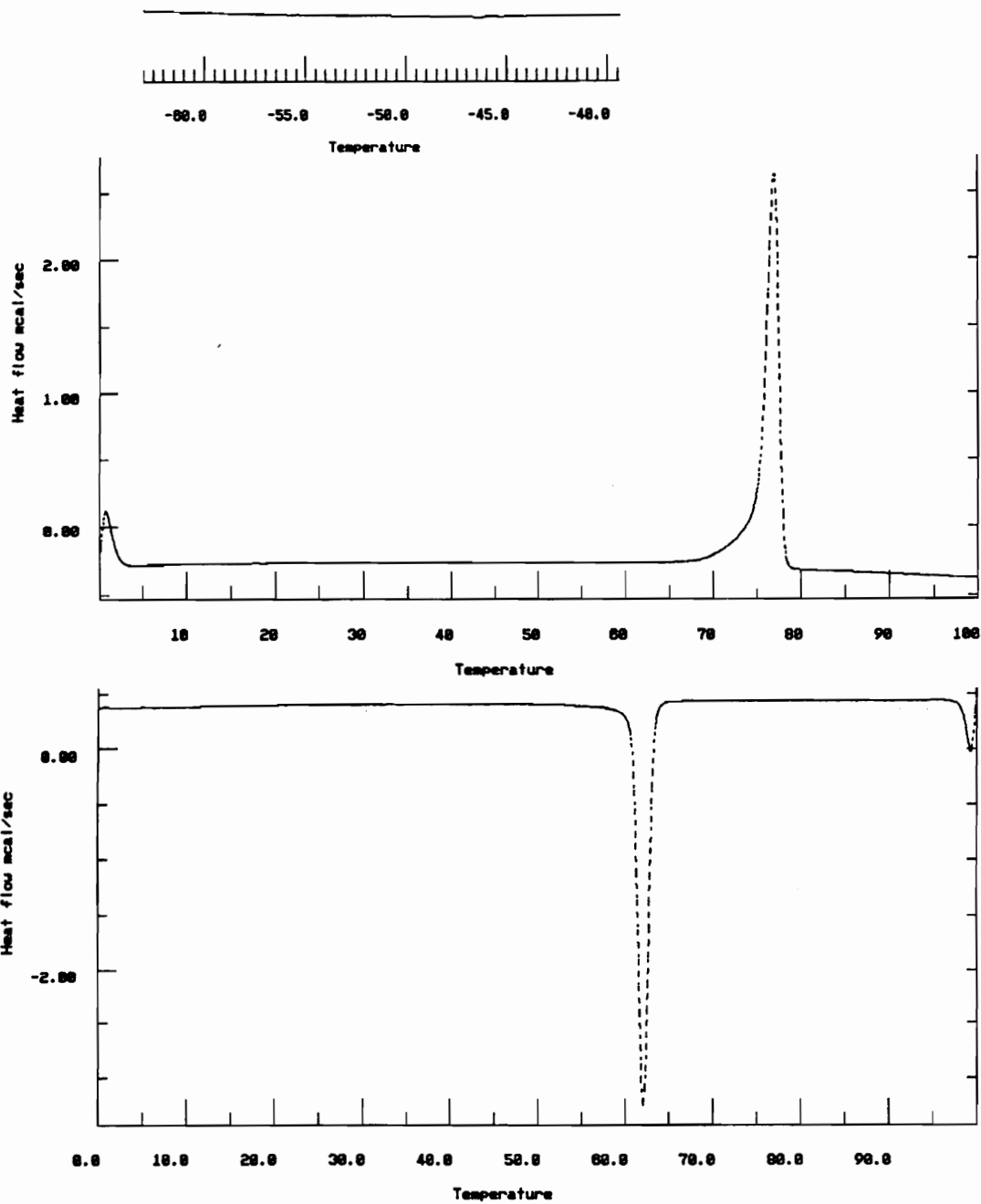


Figure 16. DSC traces for poly(decamethylene sebacate) (9): a) heating scan (top), b) cooling scan (bottom); 10 °C/min.

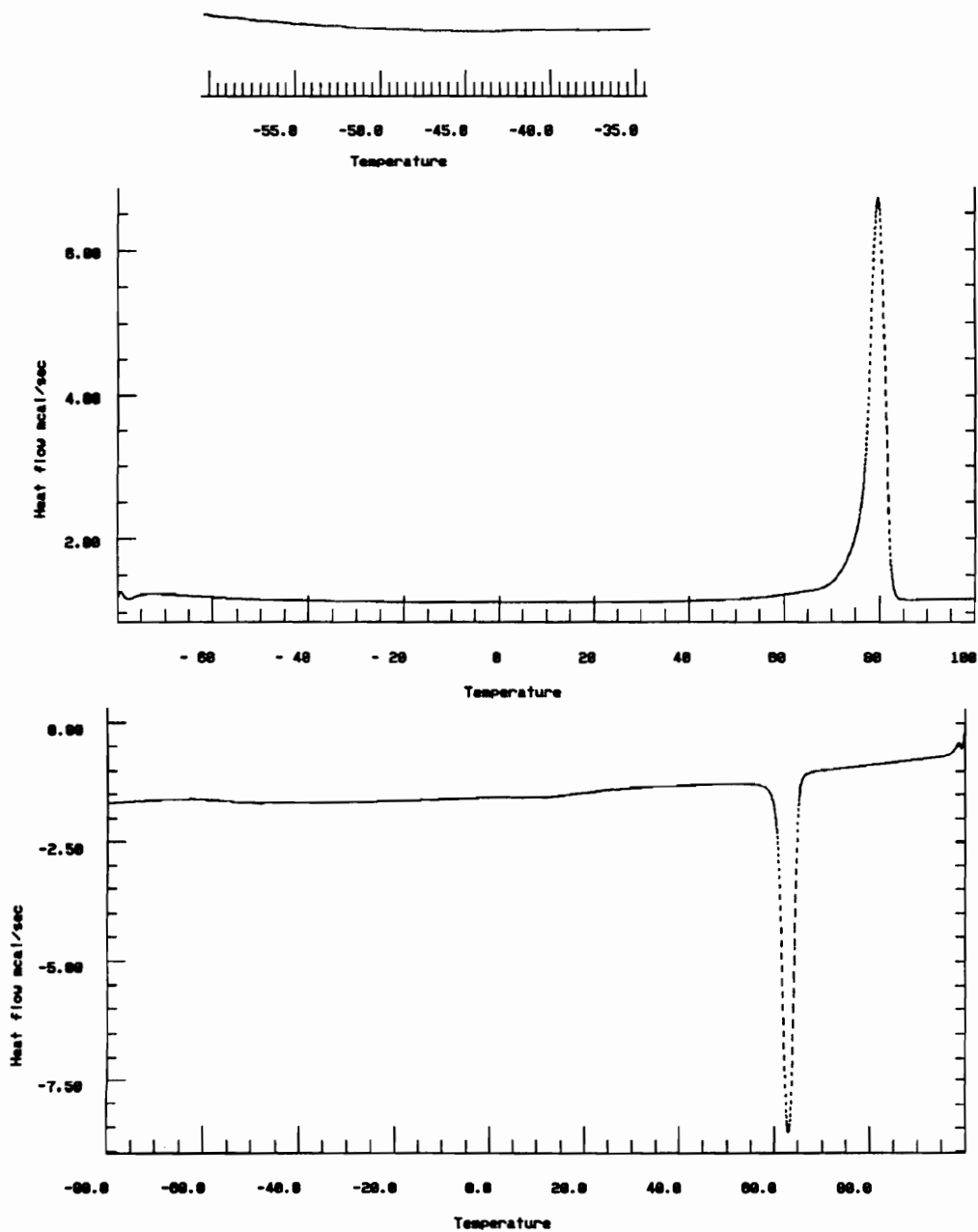


Figure 17. DSC traces for poly[(decamethylene sebacate)-rotaxa-(30-crown-10)] (12): a) second heating scan (top); b) second cooling scan (bottom), 10 °C/min.

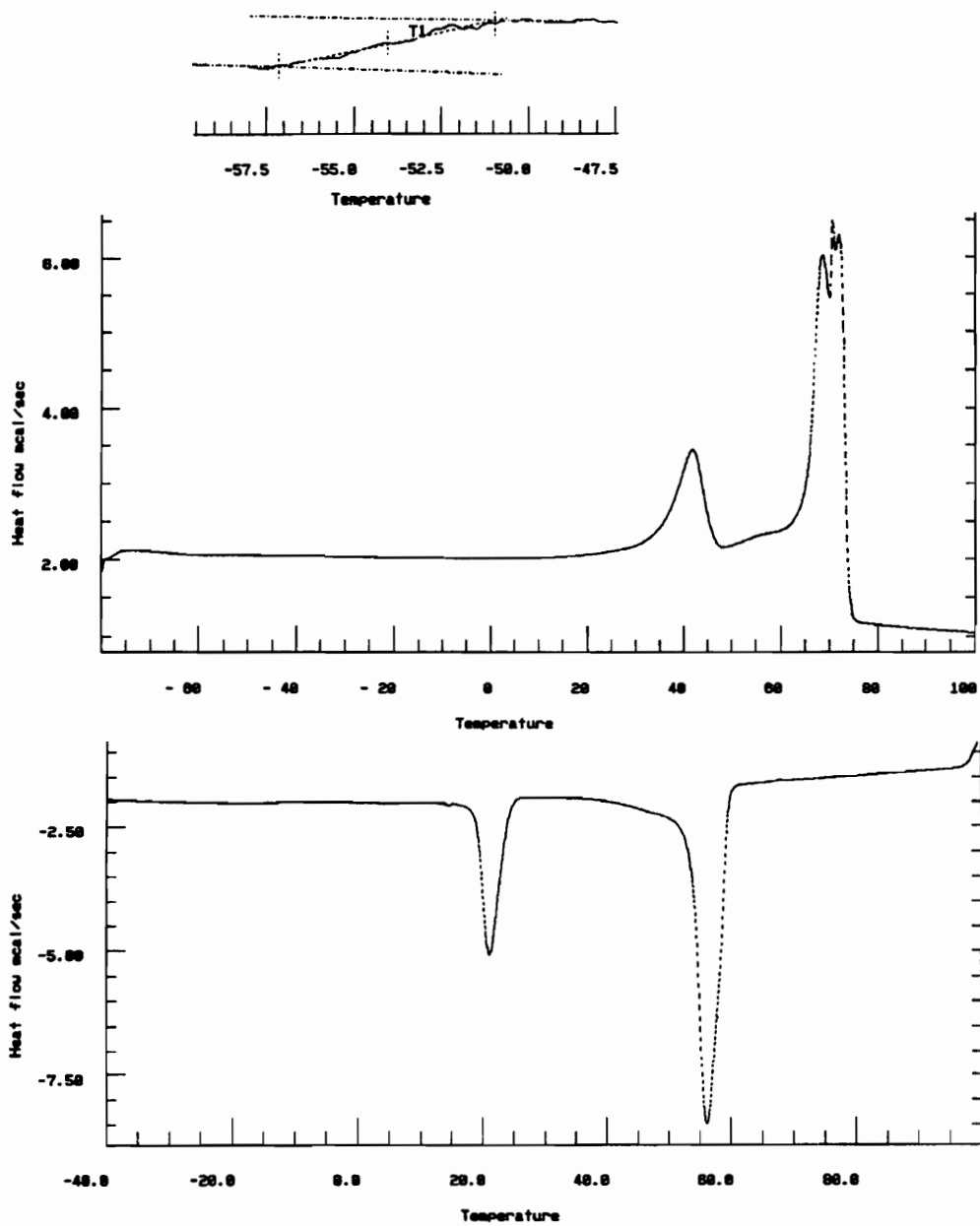


Figure 18. DSC traces for poly[(decamethylene sebacate)-rotaxa-(36-crown-12)] (**13**): a) second heating scan (top); b) second cooling scan (bottom), 10 °C/min.



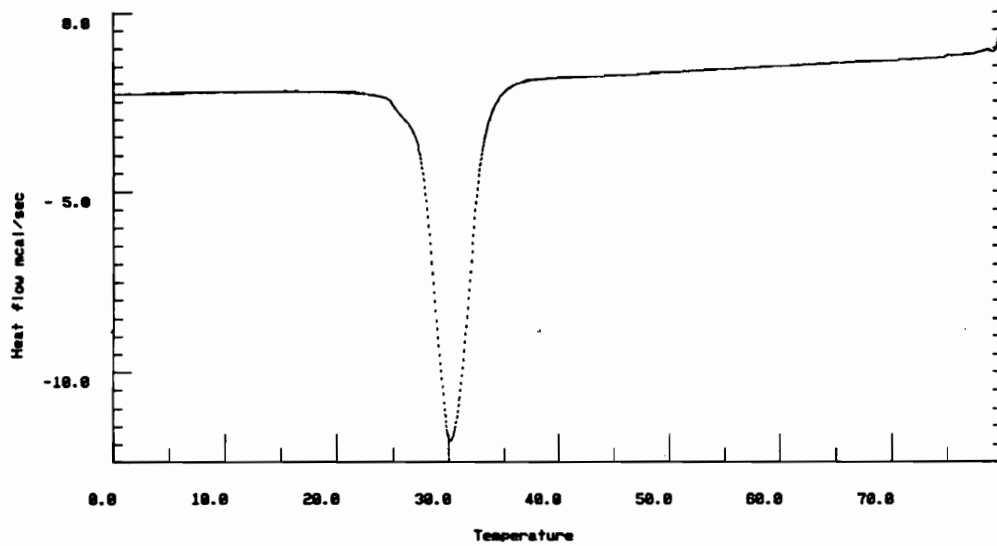
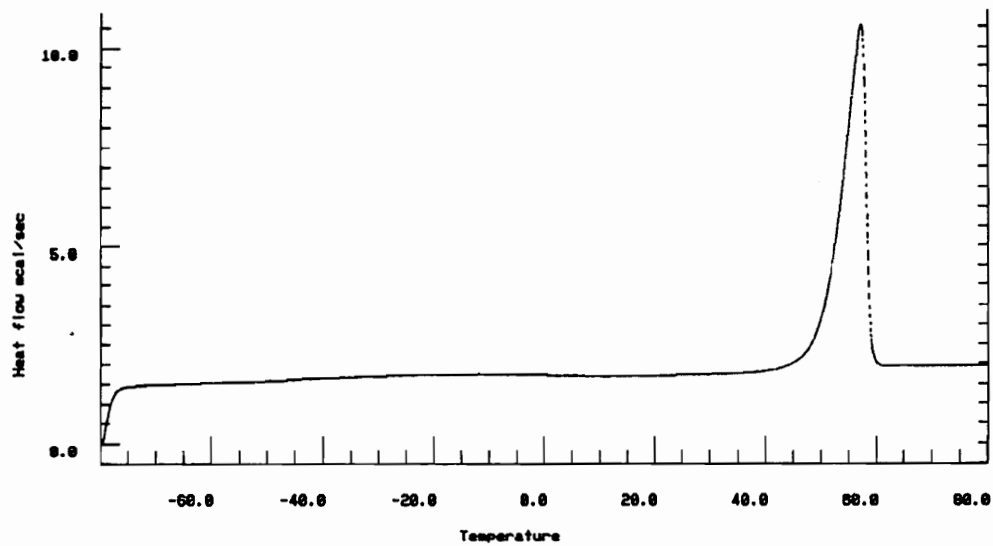


Figure 19. DSC traces for 36-crown-12 (5): a) second heating scan (top); b) second cooling scan (bottom); 10 °C/min.

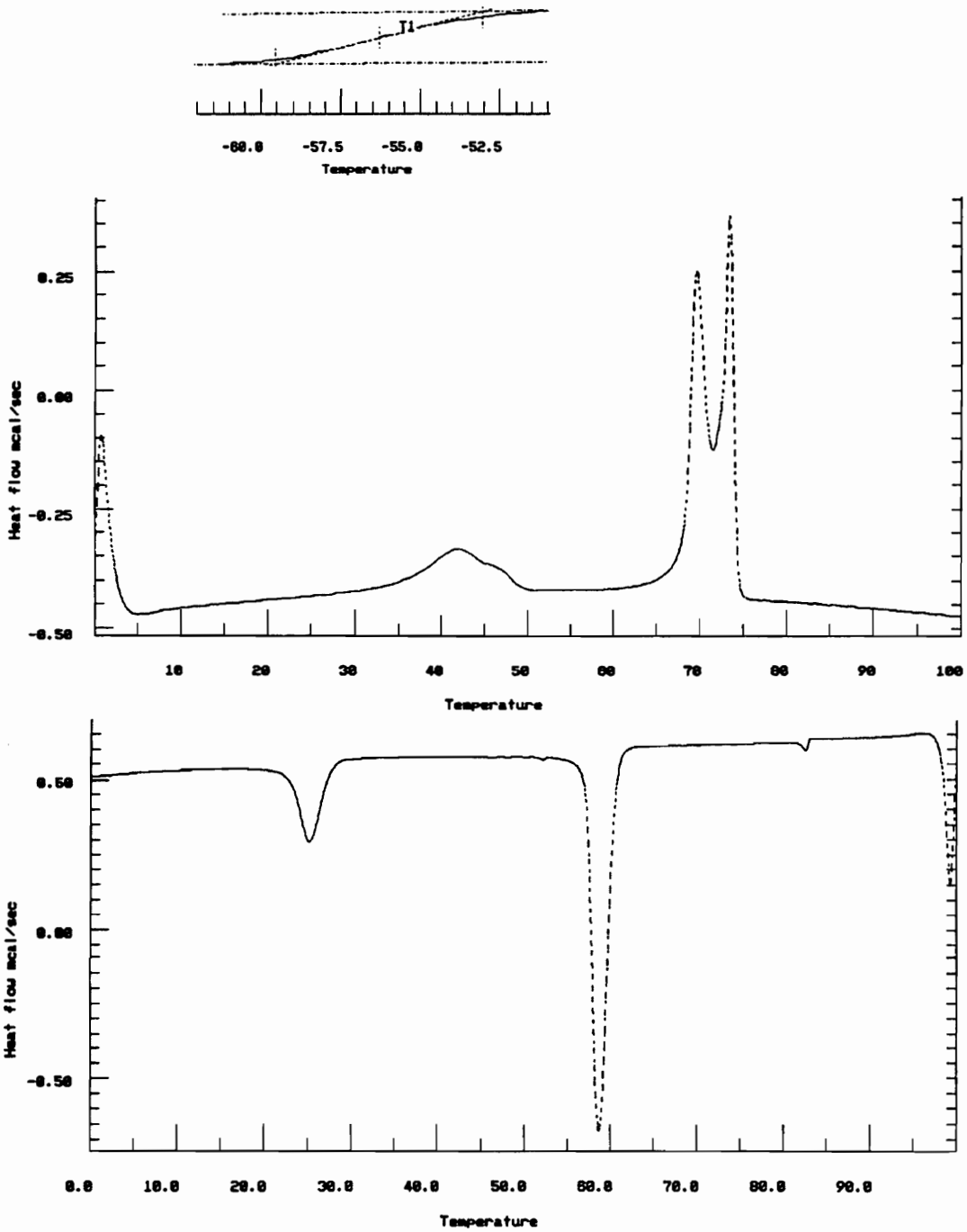


Figure 20. DSC traces for poly[(decamethylene sebacate)-rotaxa-(42-crown-14)] (14): a) second heating scan (top); b) second cooling scan (bottom), 10 °C/min.

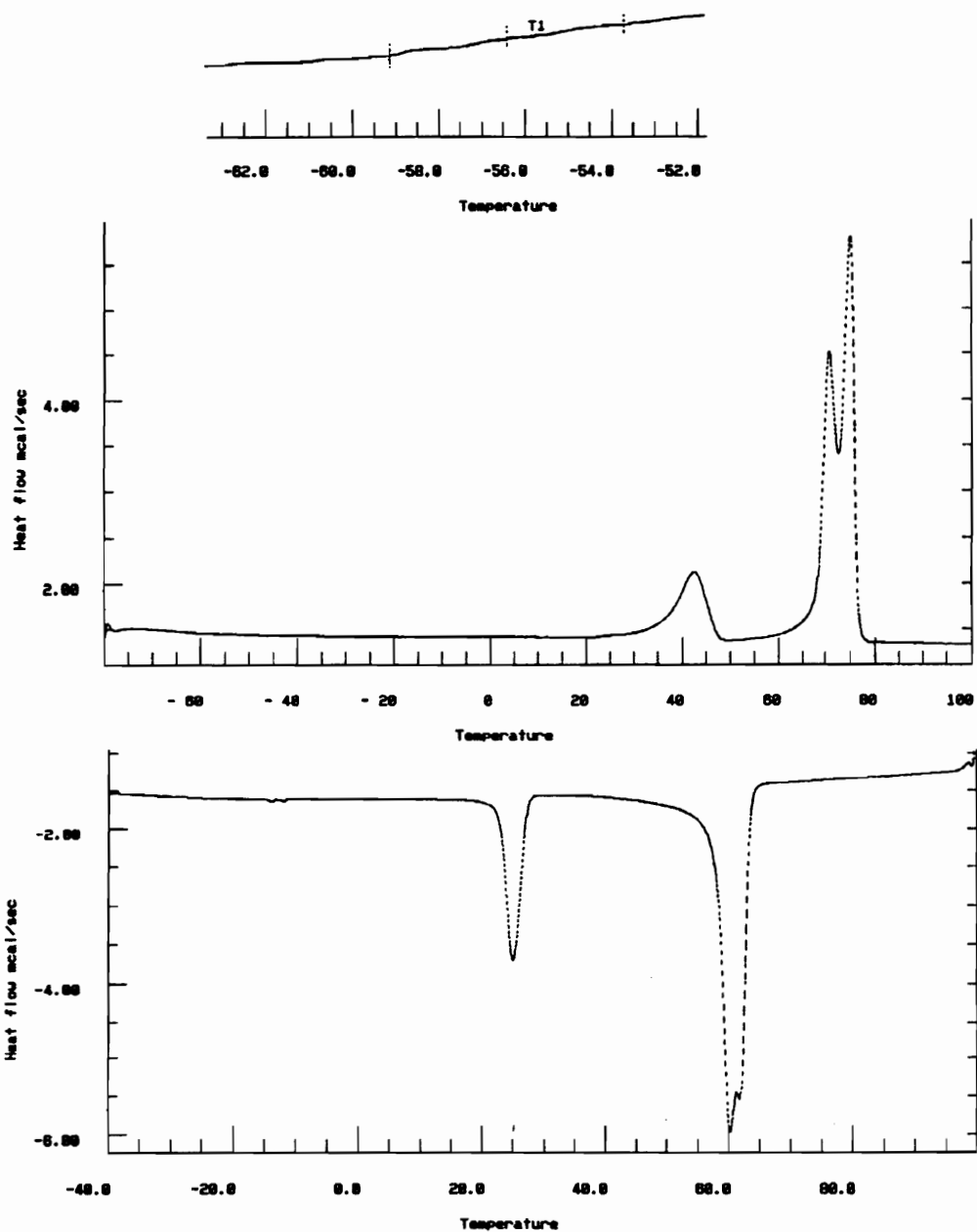


Figure 21. DSC traces for poly[(decamethylene sebacate)-rotaxa-(48-crown-16)] (15): a) second heating scan (top); b) second cooling scan (bottom), 10 °C/min.

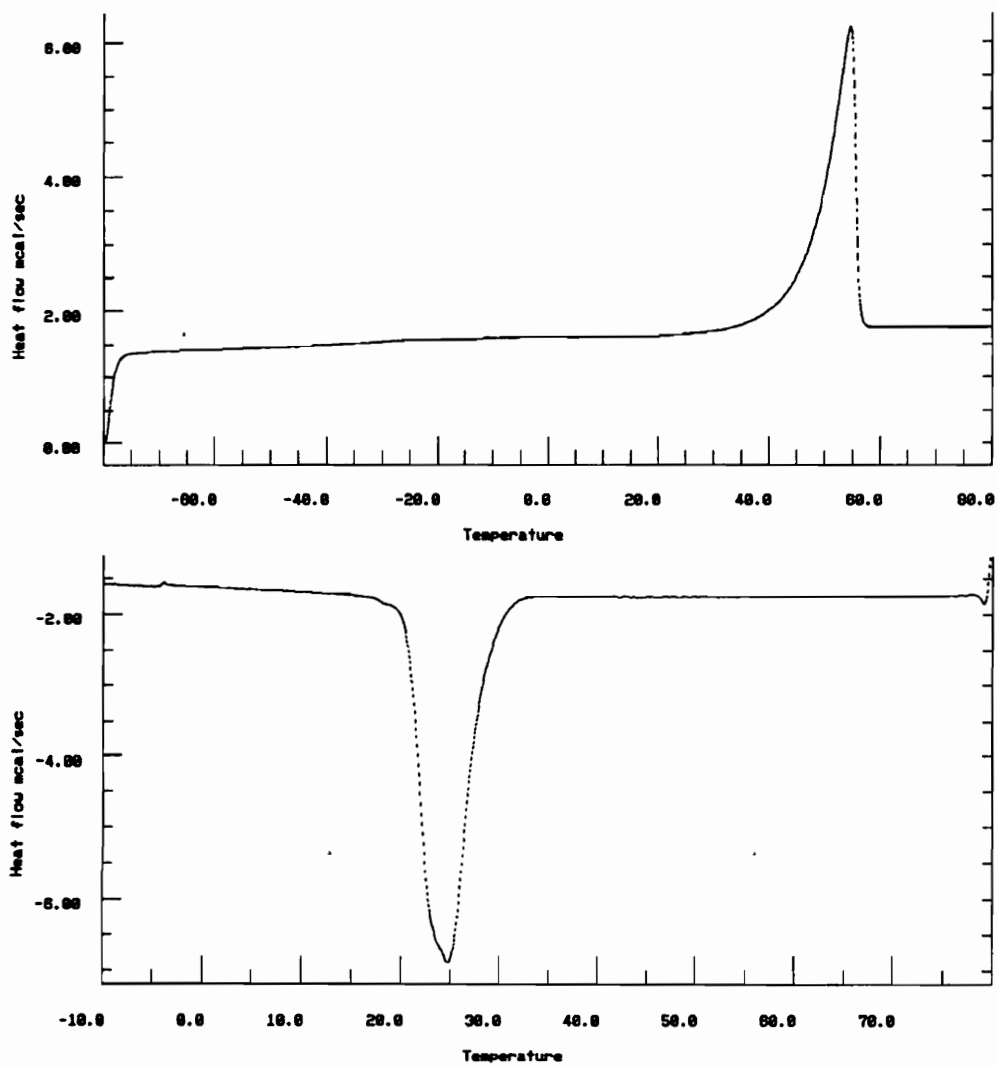


Figure 22. DSC traces for 48-crown-16 (7): a) second heating (top); b) second cooling, 10 °C/min.

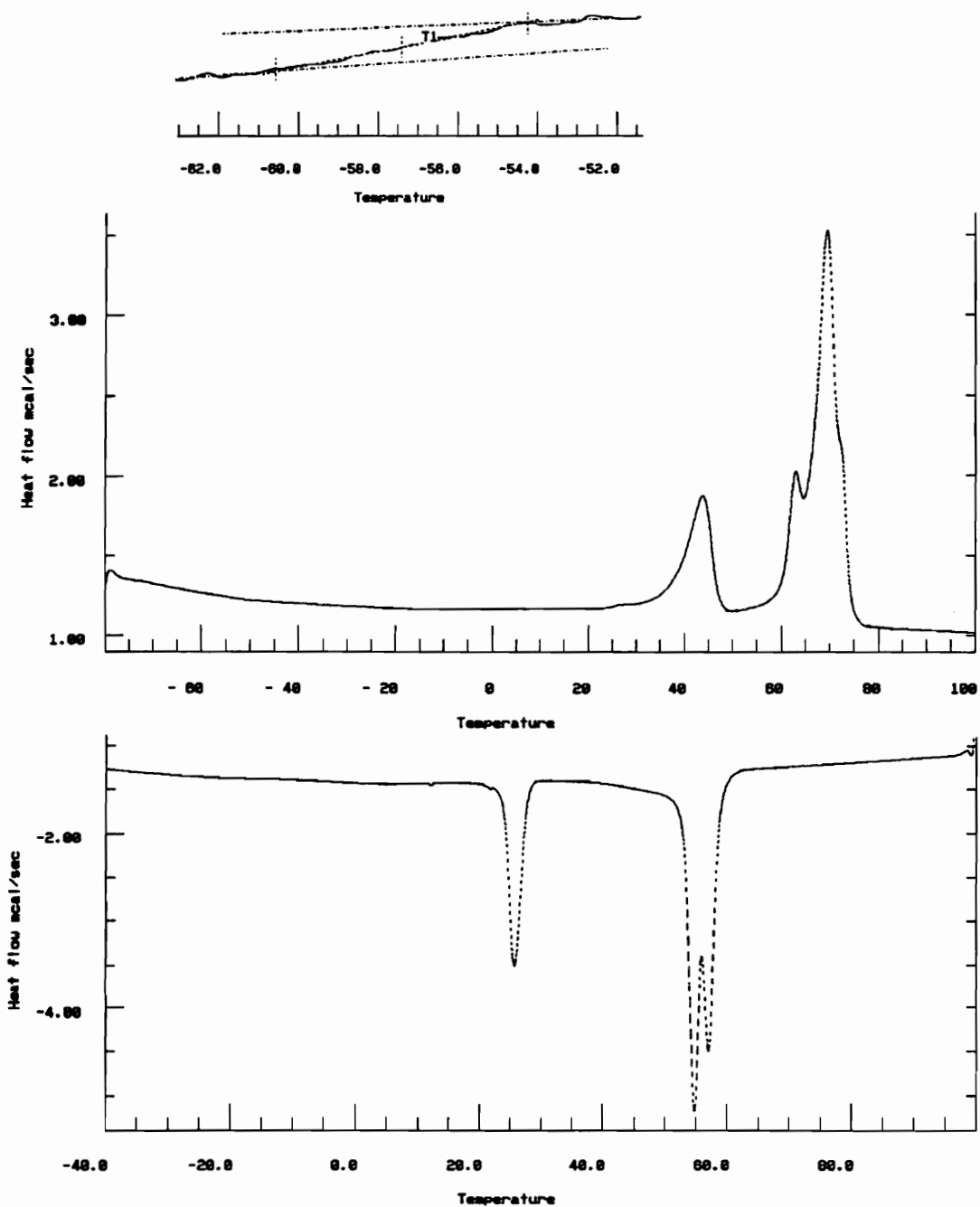


Figure 23. DSC traces for poly[(decamethylene sebacate)-rotaxa-(60-crown-20)] (**16**): a) second heating scan (top), b) second cooling scan (bottom); 10 °C/min.

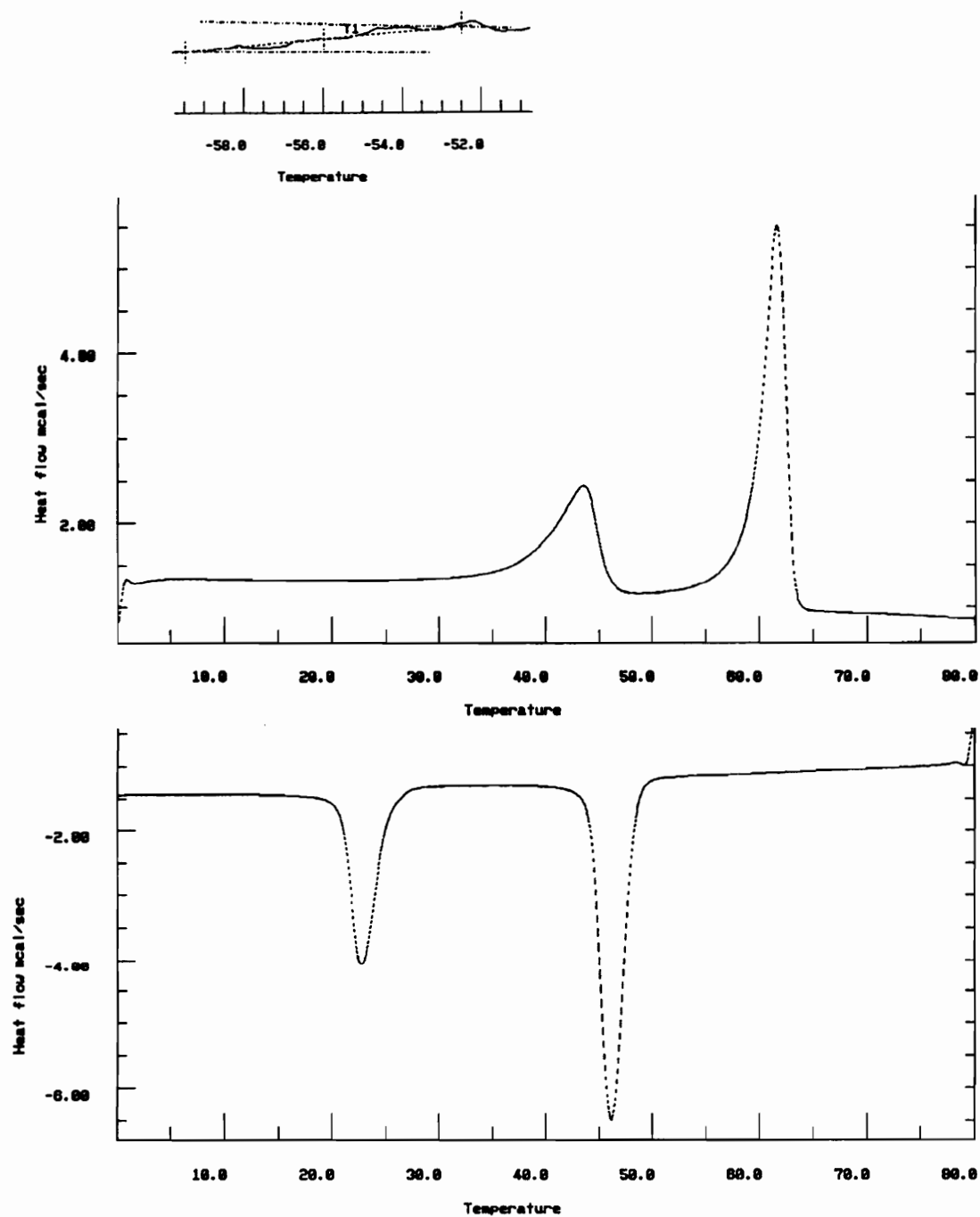


Figure 24. DSC trace for poly[(butylene sebacate)-rotaxa-(42-crown-14)] (10):  
 a) third heating scan (top), b) second cooling scan (bottom), 10 °C/min.

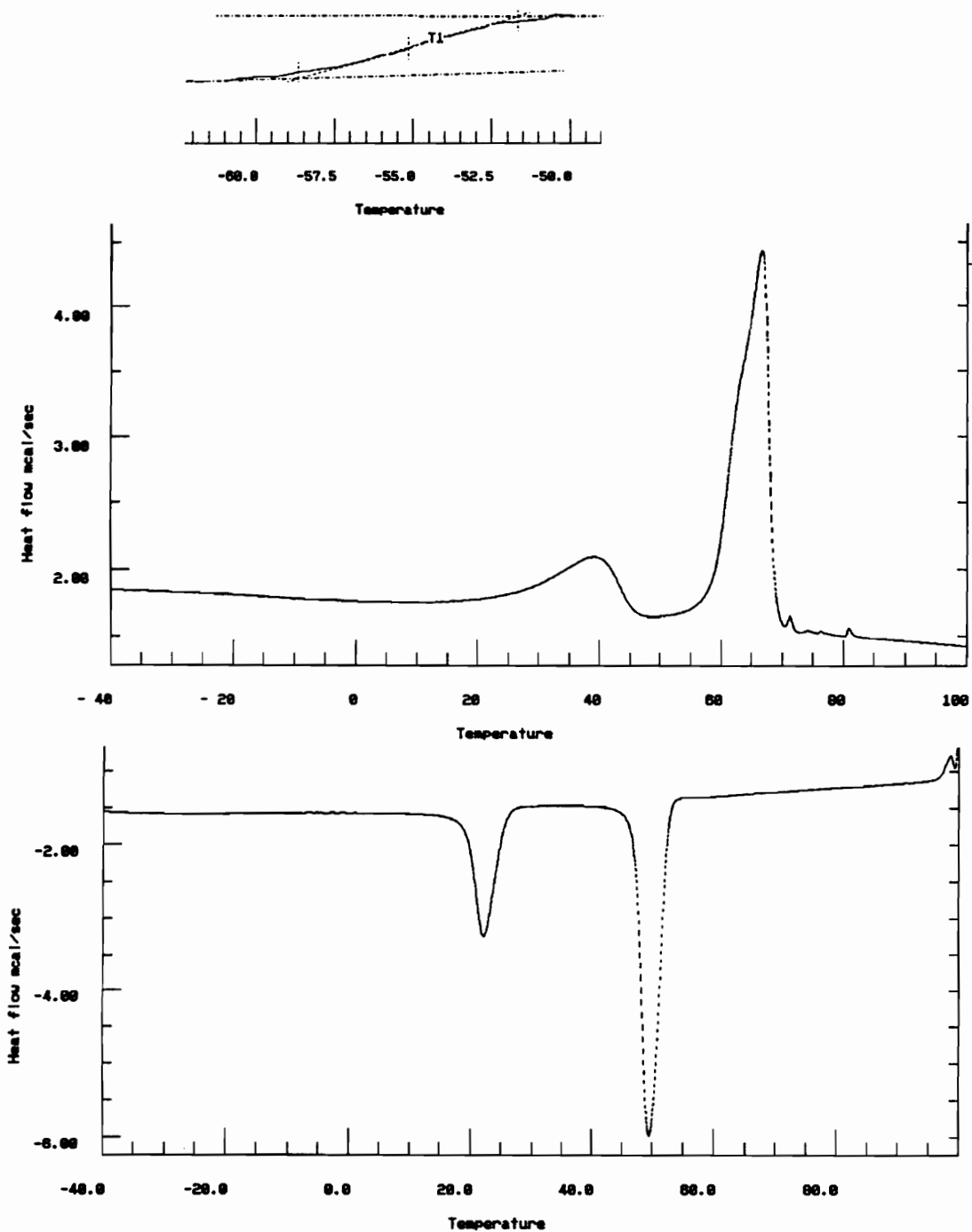


Figure 25. DSC traces for poly[(hexamethylene sebacate)-rotaxa-(42-crown-14)] (11): a) second heating scan (top), b) second cooling scan (bottom); 10 °C/min.

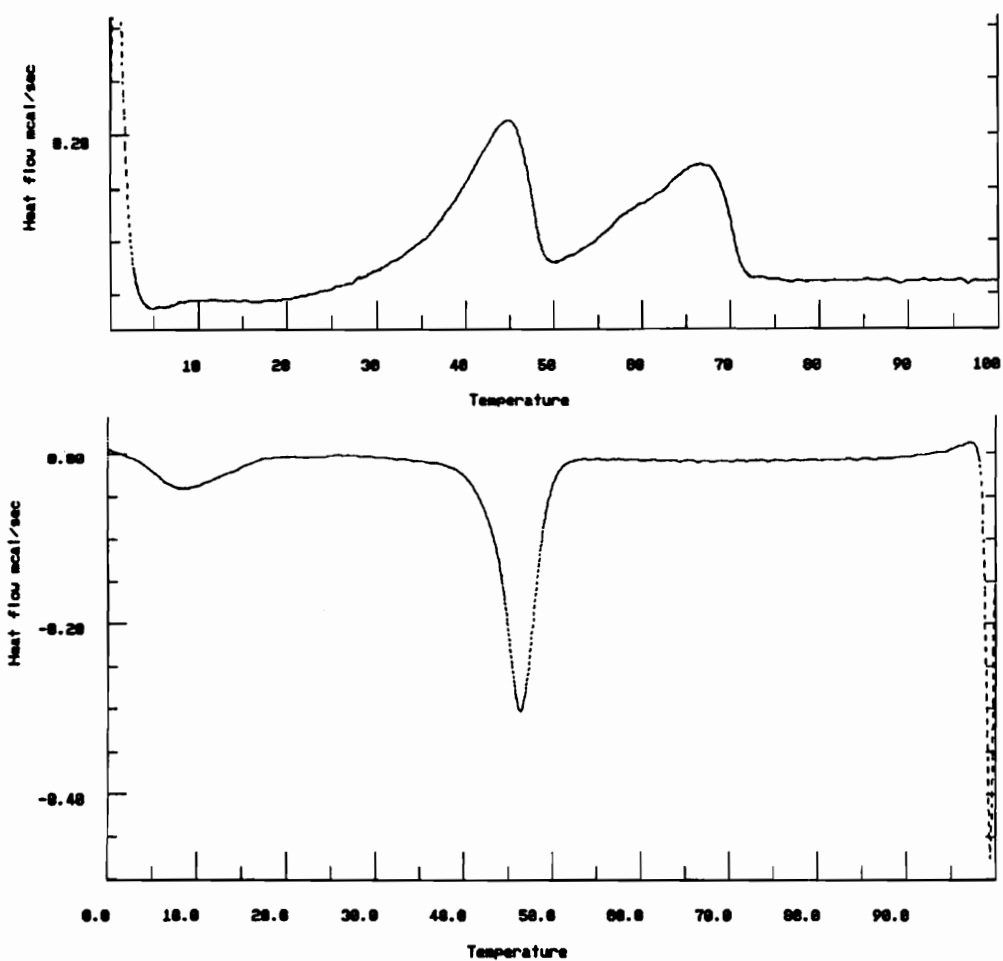


Figure 26. DSC traces for polyrotaxane **18**: a) second heating scan (top); b) second cooling scan (bottom), 10 °C/min.



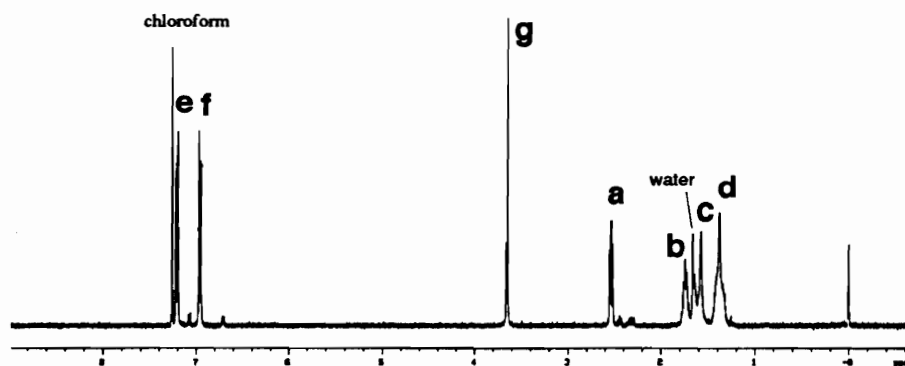
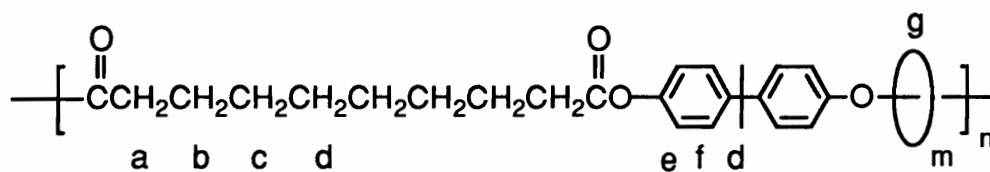


Figure 27. 400 MHz  $^1\text{H}$  NMR spectrum of poly[(bisphenol A sebacate)-rotaxa-(42-crown-14)] (**20**) in  $\text{CDCl}_3$

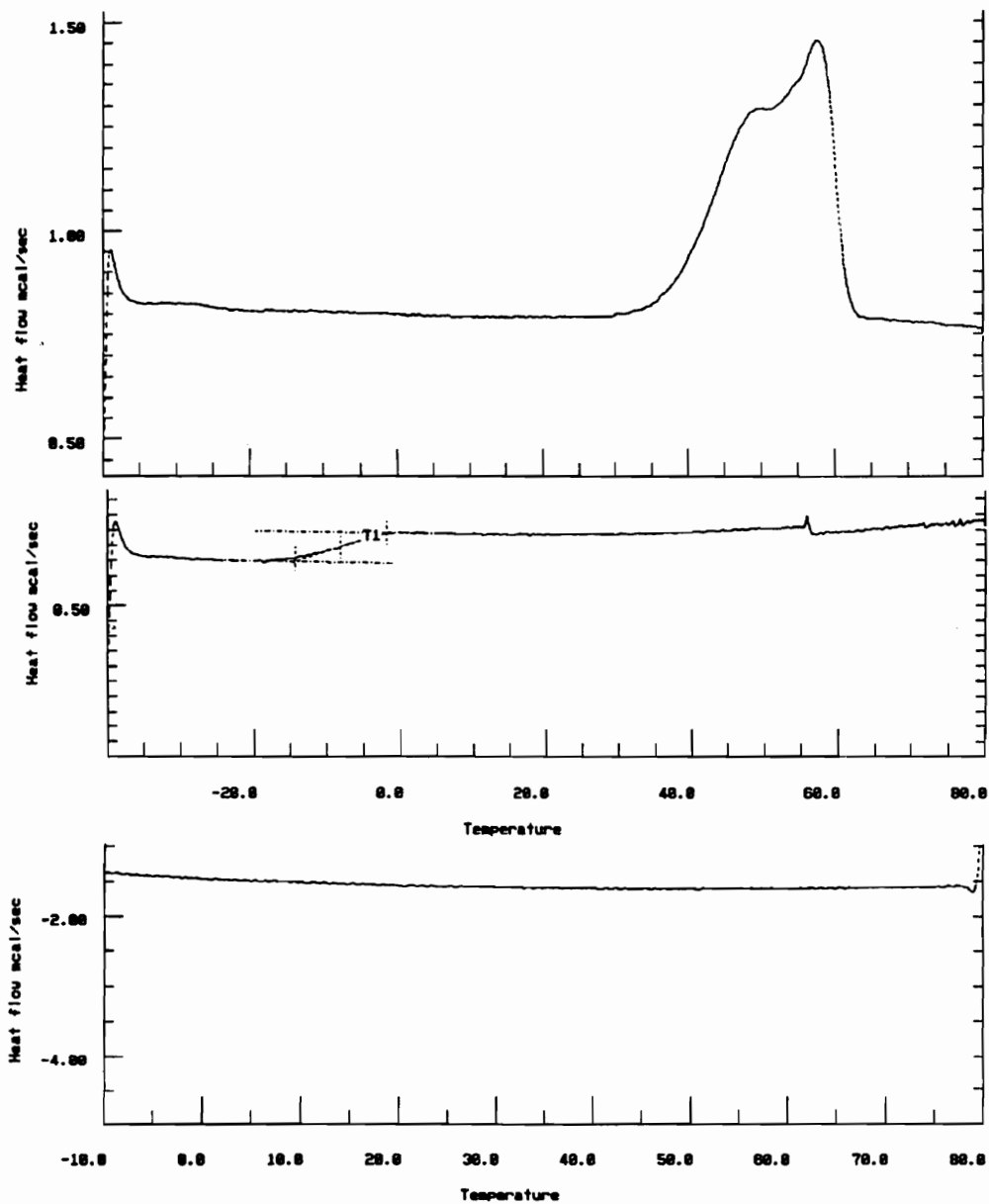


Figure 28. DSC traces for poly[(bisphenol A sebacate)-rotaxa-(42-crown-14)] (20): a) first heating scan (top); b) second heating scan (middle); c) second cooling scan (bottom), 10 °C/min.

## CHAPTER IX

### OVERALL CONCLUSIONS AND FUTURE WORK

#### I. OVERALL CONCLUSIONS

Polyrotaxanes comprised of polysebacate backbones and crown ethers were synthesized by transesterification polymerization and the acid chloride method. Some special properties of polyrotaxanes in solution and in solid state were found by comparison of the characterization results of polyrotaxanes with those of the corresponding linear macromolecules.

30- to 60-Membered crown ethers were prepared in large scale from low molecular mass oligo(ethylene glycol)s. The crown ethers were purified by using poly(methacryloyl chloride) and by crystallizations.

Monofunctional blocking groups based on bulky triarylmethanes were produced via a synthetic route including a Grignard reaction, a Friedel-Crafts alkylation reaction, and a Williamson ether synthesis. Using the same strategy on a diester generated phenolic and alcoholic difunctional blocking groups. Other difunctional blocking groups were also synthesized.

Poly(triethyleneoxy sebacate) and poly(butylene sebacate) rotaxanes containing crown ether macrocycles were prepared by transesterification polymerization of dimethyl sebacate and diols using macrocycles as solvents. The threading of macrocycles onto the backbone leads to enhanced solubilities

in polar solvents. The incorporation of macrocycles reduces  $T_g$  in the tri(ethyleneoxy) system and causes a glass transition in butylene system. Because of the free movement of macrocycles along the backbones, both cyclic and linear components of polyrotaxanes can aggregate and crystallize independently.

The threading process of macrocycles onto diol monomers was studied using the di(acid chloride)-diol polymerization method in unblocked polysebacate-crown ether rotaxane systems. The hydrogen bonding between diol monomers and crown macrocycles plays an important role in the threading process. The formation of polyrotaxanes follows Le Chatelier's principle. Complete constraint of the macrocycles was attained by the copolymerization of a difunctional blocking groups into polymer chains. Polyrotaxanes display glass transitions due to threaded macrocycles. Independent crystallization of cyclic and linear species of polyrotaxanes was also observed.

## II. FUTURE WORK

As a frontier science, polyrotaxane chemistry has a bright prospect from both theoretical and practical points of view. In addition to the development of new types of polyrotaxanes such as side chain polyrotaxanes and dendrimeric rotaxanes [1], it is necessary to increase understanding of the nature of the threading process and the effects of structure and composition on physical properties. The following are some specific suggestions for the polyester rotaxane systems.

## A. Study of the Threading Equilibria

The success in the syntheses of difunctional blocking groups now allows us to study the equilibria of the threading processes. Parameters that needed to be investigated are:

### a. Solvent or Medium Effects

Changes of solvents or medium result in conformational changes for both linear and cyclic species. While it is still not clear which conformational change is more significant with respect to the prethreading process at this time, it is likely that the conformational change of the macrocycles is more important. Two reasons may be involved. First, the molecular weights of crown ethers are higher than those of alkyene diols. Second, the hydrogen bonding between crown ether and diol molecules occurs at the center of crown ether molecules but at the chain ends of diol molecules.

### b. Temperature

Because of the complete constraint of the macrocycles on the polymer chains by the blocking groups, temperature dependence of the threading may be observed. How the percentage of threadable conformations of the macrocycles changes with temperature depends on the energy of different conformations. That is, if the energy of an opened conformation is higher than that the a

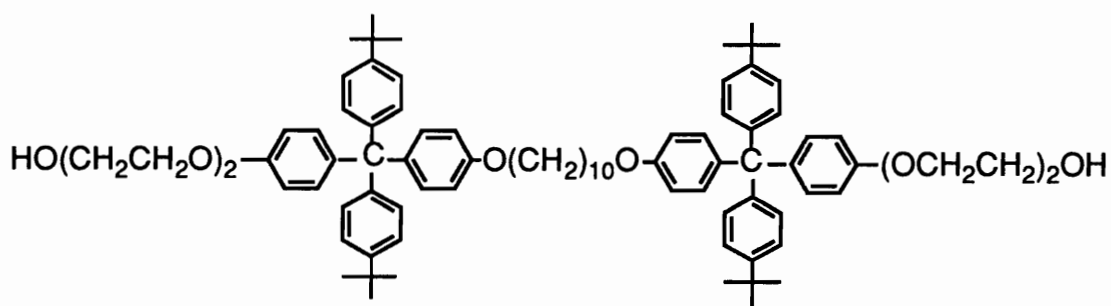
collapsed conformation, the percentage of threadable conformations will increase with temperature and vice versa.

### c. Compatibility of Linear and Cyclic Species

The effect of the compatibility of linear and cyclic species can be studied with systems containing different linear and cyclic components.

### d. Controlling Macrocycle Distribution Along the Polymer Chains

Polyrotaxane **4** with "knots" occurring in long sequences can be synthesized by using the difunctional blocking group **2** (Scheme 1). This polymer showed an interesting independent crystallization behavior, as discussed above. On the other hand, macrocycles can be randomly separated by "knots" along the polymer chain by using the difunctional blocking group **5**. Because the range of movement of the macrocycles will be more limited as the proportion of **5** increases, independent crystallization of macrocycles and polymer backbones may not be observed.



#### e. Synthesis of New Difunctional Blocking Groups

A new synthetic route for new difunctional blocking groups is proposed here (Scheme 2). This method is simpler both in preparation and in the structures of the products compared to the method for **2** and **4**. The yields will be higher too.

#### B. Quantitative Determination of Metal Complexation of Polyrotaxanes

The metal complexation of polyrotaxanes can be quantitatively studied by UV-Vis spectroscopy, NMR spectroscopy, or conductometry [2]. After the metal complexations the resultant polyrotaxanes should be characterized to find their special thermal and mechanical properties.

Takeda measured the complex formation constants of metals and crown ethers using conductometry [3]. The conductance of the solution containing a metal ion and a crown ether decreased as the molar ratio of the crown ether to the metal ion increased. This is because the crown ether-metal ion complex is less mobile than the free metal ion. The rotaxane-metal ion complexes should be less mobile than the crown ether-metal ion complexes. Therefore, conductometry is a powerful tool not only for proving the rotaxane structure but also for the thermodynamic and kinetic studies of the threading processes.

### C. Study of the Solution Behavior of Polyrotaxanes

It has been known that polymer chains can be stiffened by the incorporation of macrocycles [4]. Therefore, the end-to-end distances of polymer backbones of polyrotaxanes should be larger than those of linear polymers with the same molecular weight. The information concerning the unperturbed state of the polyrotaxane backbones can be obtained by the extrapolation of the intrinsic viscosity/molecular weight data to the  $\theta$ -solvent condition using the Stockmayer-Fixman relation [5]:

$$[\eta]/M_w^{1/2} = K_\theta + 0.51B\Phi_0M_w^{1/2} \quad (1)$$

According to equation (1) the intercept of a plot  $[\eta]/M_w^{1/2}$  against  $M_w^{1/2}$  should yield  $K_\theta$ . Assuming the Stockmayer-Fixman approximation is valid for polyrotaxanes and using  $\Phi_0 = 2.1 \times 10^{23}$  which is recommended for unfractionated polymers with polydispersity equaling about 2 [6], the unperturbed chain root-mean square end-to-end distance ( $r_0$ ) can be calculated from Equation (2) [7]:

$$r_0/M^{1/2} = (K_\theta/\Phi_0)^{1/3} \quad (2)$$

The solution behavior of polyrotaxanes depends on the differential solvation of the cyclic and linear species of the polymers. The differential solvation effect could in the extreme case cause either the macrocycle or the linear backbone to be fully expanded or to collapse into a  $\theta$  state. A good solvent for both the cyclic



and linear species leads to expansion of both components. A good solvent for the linear macromolecule but a poor solvent for the cyclic species leads to an expanded backbone but collapsed macrocycle. A poor solvent for the linear backbone but a good solvent for the macrocycle provides a collapsed state of the linear component and an expanded state for the rings. A poor solvent for both the linear and cyclic components affords collapsed conformations of both. This issue can be primarily studied by measuring the intrinsic viscosity of polyrotaxanes and linear polymers in different solvents.

#### D. Study of the Topological Properties of Polyrotaxanes

Special properties of polyrotaxanes found by the comparison of the properties with those of linear polymers with same chemical structure of the backbones are due to the existence of macrocycles in the polyrotaxanes. These properties are termed component properties. Most component properties of polyester-crown ether rotaxanes can be achieved by copolymerizing oligo(ethylene glycol) which has same molecular weight as crown ethers into polyester chains. On the other hand, polyrotaxanes are expected to have distinguishing features compared to conventional copolymers, due to the physical barriers to dethreading of macrocycles and due to the freedom of macrocycles to move laterally, translationally, and circumferentially relative to the linear unit that penetrates them. These special features are termed topological properties. In order to figure out the topological properties of polyrotaxanes, it is necessary to compare the properties of polyrotaxanes with those of corresponding

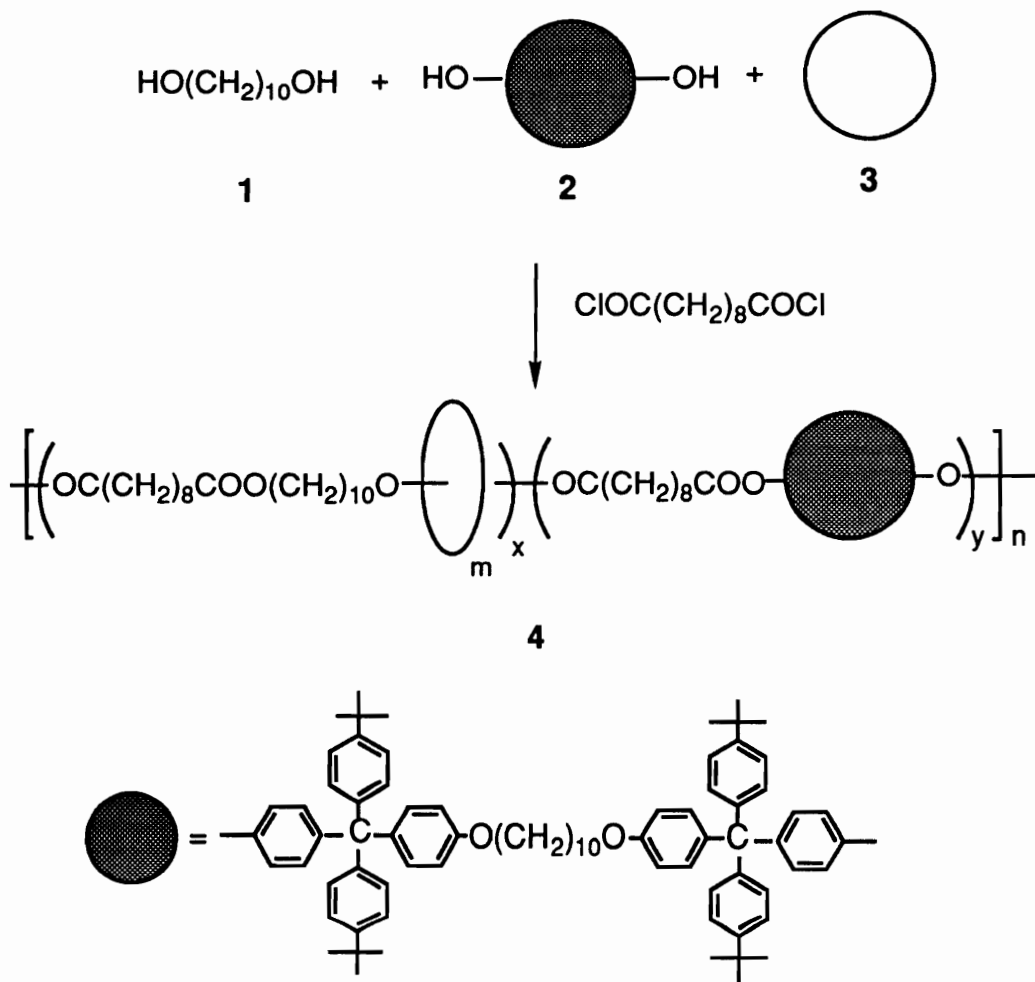
copolymers, e.g., poly[(decamethylene sebacate)-rotaxa-(42-crown-14)] vs. poly[(decamethylene sebacate)-co-(tetradecaethyleneoxy sebacate)].

#### E. Syntheses of Polyrotaxanes by Interfacial Polymerization

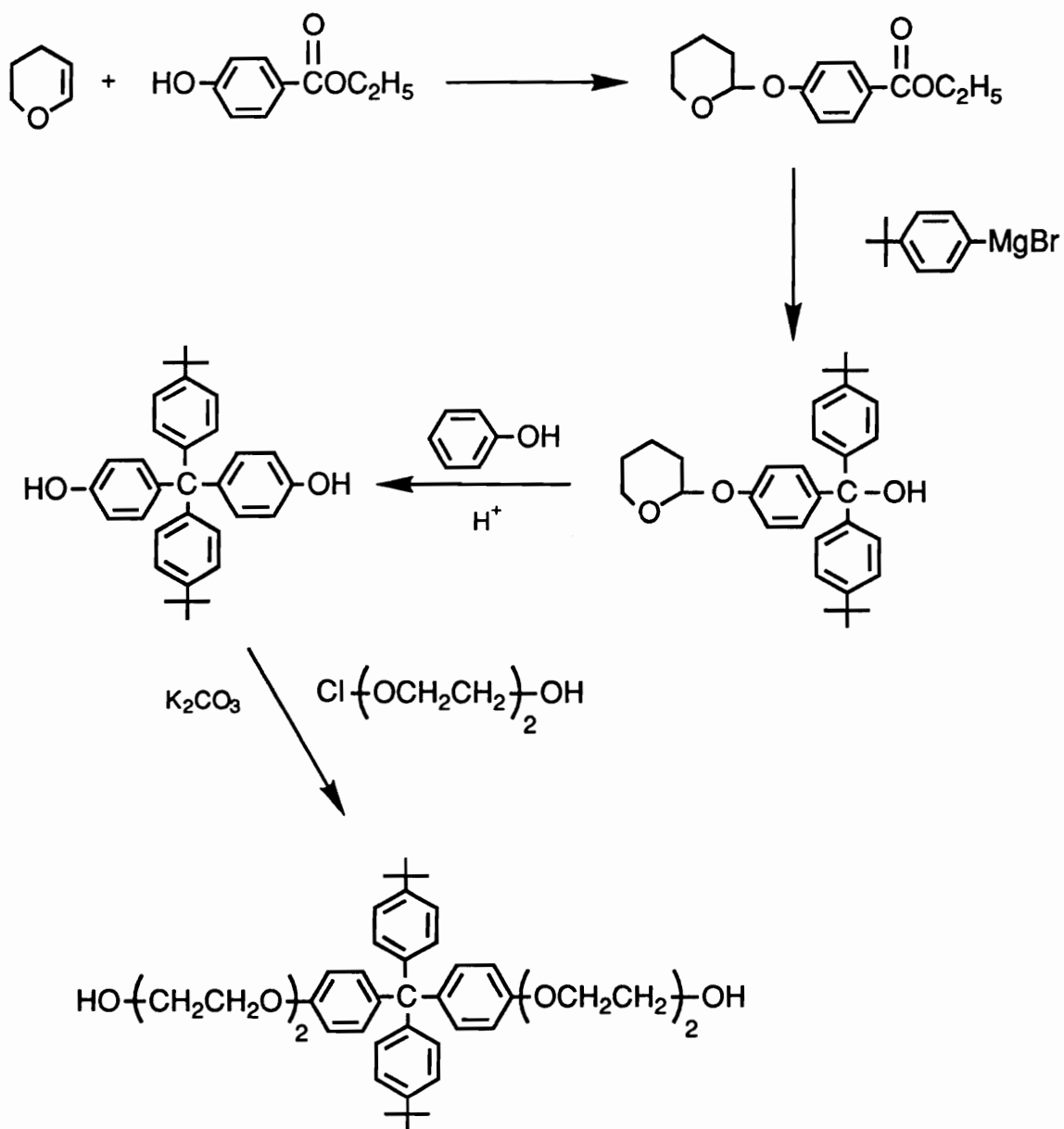
It has been discussed above that polyrotaxanes can be prepared by interfacial polymerizations. The molecular weight of the resultant polyester rotaxane is low due to the hydrolytic instability of the aliphatic acid chloride. Polyamides with relatively high molecular weights were prepared by interfacial polymerizations [8]. While polyamides prepared from primary diamines are virtually not soluble in most organic solvents, those from secondary diamines are quite soluble in many solvents. The solubility of the polyamides may be improved by threaded macrocycles. If the resultant polyamide rotaxanes are still not soluble in organic solvents, we can prepare polyamide rotaxanes from secondary diamines. The good solubility of the resultant polyrotaxanes will allow us to purify and characterize them.

## REFERENCES

1. Gibson, H. W. *Synthesis & Properties of Novel Polymers with Rotaxane Architectures, NSF Proposal*, Chem. Dept., Virginia Tech., August, **1993**.
2. a). Franke, J.; Vögtle, F. *Top. Curr. Chem.* **1986**, *132*, 135. b). Diederich, F. *Angew. Chem., Int. Ed. Engl.* **1988**, *27*, 363. c). Inoue, Y.; Gokel, G. W. *Cation Binding by Macrocycles, Complexation of Cationic Species by Crown Ethers*, Marcel Dekker, New York, **1990**. d). Izatt, R. M.; Pawlak, K.; Bradshaw, J. S. *Chem. Rev.* **1991**, *91*, 1721. e). Izatt, R. M.; Bradshaw, J. S.; Pawlak, K.; Bruening, R. L.; Tarbet, B. J. *Chem. Rev.* **1992**, *92*, 1261.
3. Takeda, Y. in ref.2 c), pp. 133-178.
4. See Chapter VII.
5. Stockmayer, W. H.; Fixman, M. *J. Polym. Sci.* **1963**, *C1*, 137.
6. Kurata, M.; Tsunashima, Y. in *Polymer Handbook, 3rd ed.*, Ed. by Brandrup, J.; Immergut, E. H., eds. John Wiley & Sons, Inc., New York, **1989**, p. VII/4.
7. Flory, P. J.; Fox Jr., T. G. *J. Polym. Sci.* **1950**, *5*, 745. Flory, P. J.; Fox Jr., T. G. *J. Am. Chem. Soc.*, **1951**, *73*, 1904.
8. Beaman, R. G.; Morgan, P. W.; Koller, C. R.; Wittbecker, E. L. *J. Polym. Sci.* **1959**, *XL*, 329. Katz, M. *J. Polym. Sci.* **1959**, *XL*, 337. Shashoua, V. E.; Eareckson, W. M. *J. Polym. Sci.* **1959**, *XL*, 343. Stephens, C. W. *J. Polym. Sci.* **1959**, *XL*, 359.



Scheme 1. Synthesis of molecular string of beads with knots



Scheme 2. A new synthetic route for difunctional blocking groups

## **VITA**

Shu Liu was born in Fuzhou, a southern city in China. After he had obtained his Bachelor degree in Chemical Engineering from Jiangxi Polytechnic University in China in 1982, he worked for eight years as a polymer engineer at Yizheng Joint Corporation of Chemical Fiber Industry in Jiangsu, China. He began his graduate career at Indiana university of Pennsylvania (IUP) in January 1990. After receiving his M.S. degree in Chemistry from IUP in August 1991, he jointed Dr. Harry W. Gibson's group at Virginia Polytechnic Institute and State University.